Impact of human filarial infections on the metabolic and immunological profile and characterization of filariae-induced tropical pulmonary eosinophilia using a newly established mouse model

Dissertation

zur Erlangung des Doktorgrades (Dr. rer. nat.)

der Mathematisch-Naturwissenschaftlichen Fakultät

der Rheinischen Friedrich-Wilhelms-Universität Bonn

vorgelegt von

Benjamin Lenz

aus

Bonn

Bonn 2023

Angefertigt mit Genehmigung der Mathematisch-Naturwissenschaftlichen Fakultät

der Rheinischen Friedrich-Wilhelms-Universität Bonn

Erstgutachter

Prof. Dr. Marc Hübner

Zweitgutachter

Prof. Dr. Walter Witke

Tag der Promotion: 25.01.24

Erscheinungsjahr: 2024

Erklärung

Die hier vorgelegte Dissertation habe ich eigenständig und ohne unerlaubte Hilfsmittel angefertigt. Die Dissertation wurde in der vorgelegten oder in ähnlicher Form noch bei keiner anderen Institution eingereicht.
Es wurden keine vorherigen oder erfolglosen Promotionsversuche unternommen.

Bonn,

Teile dieser Arbeit wurden vorab veröffentlicht oder sind aktuell "under review".

Lenz B*, Andrew BA*, Ritter M, Karunakaran I, Gandjui NVT, Nchang LC, Surendar J, Ebob AOB, Ehrens A, Klarmann-Schulz U, Ricchiuto A, Kuehlwein JM, Fombad FF, Ngwa AM, Katcho TD, Hoerauf A, Wanji S*, Hübner MP*. The design and development of a study protocol to investigate *Onchocerca volvulus, Loa loa* and *Mansonella perstans*-mediated modulation of the metabolic and immunological profile in lean and obese individuals in Cameroon. PLoS One. 2023;18(6) e0285689. doi:10.1371/journal.pone.0285689. PMID: 37267236; PMCID: PMC10237473.

* Authors contributed equally.

Lenz B, Ehrens A, Ajendra J, Risch F, Gal J, Neumann AL, Reichwald JJ, Strutz W, McSorley HJ, Martin C, Hoerauf A, Hübner MP. Repeated sensitization of mice with microfilariae of *Litomosoides sigmodontis* induces pulmonary eosinophilia in an IL-33-dependent manner. *Under review.*

Table of Contents

Summary

Parasitic filarial infections occur in tropical areas and cause debilitating diseases. The interactions between the immune system and parasitic filarial infections are a complex and intricate microcosm that can be divided into host-immune modulation on one side and severe pathology on the other side. Successful immunomodulation during filarial infections can improve parasite longevity and potentially alleviate allergic symptoms, as well as prevent autoimmune and metabolic diseases. In contrast, symptoms of filarial diseases include severe dermatitis and blindness during onchocerciasis or pulmonary eosinophilia, lymphedema and hydrocele formation in patients with lymphatic filariasis but are often asymptomatic or clinically silent. In this thesis, two aspects were investigated: I) The development of tropical pulmonary eosinophilia in a novel mouse model and II) beneficial effects of filarial infections on the metabolic and immunological profile in an open-label pilot trial that was conducted in the rural Northwest of Cameroon.

During tropical pulmonary eosinophilia, microfilariae of *Wuchereria bancrofti* or *Brugia spp.* are retained in the lung tissue of infected patients. Thereby, trapped microfilariae cause local inflammation and induce a hyper-responsive pulmonary syndrome, eosinophilic infiltrates, mast cell recruitment as well as an IgE class switch. Additional symptoms include fever, nocturnal cough, dyspnea, wheezing and pulmonary fibrosis that can lead to severe lung damage and death. In this thesis, a mouse model for tropical pulmonary eosinophilia (TPE) was established using the rodent filarial nematode *Litomosoides sigmodontis*. The mouse model demonstrated immunological and histopathological features that are closely associated with human TPE, i.e., lung eosinophilia, increased microfilariae clearance from the blood and increased microfilariae retention in the lung tissue. Moreover, TPE mice displayed increased total and parasite-specific IgE as well as serum IL-5.

This newly established TPE model was used to further elucidate the role of eosinophils. Eosinophil-deficient dblGATA mice displayed decreased retention of microfilariae in the lung and impaired development of a type 2 immune response, indicating an essential role of eosinophils in microfilariae clearance from the blood and the initiation of a type 2 immune response, with significantly increased IL-33 levels, in the context of TPE.

Interestingly, blocking IL-33 signaling during TPE development, decreased the type 2 shift, eosinophilia, eosinophil activation and alleviated lung lacunarity. In conclusion, this part of the thesis demonstrates that eosinophils and IL-33 signaling are essentially involved in the development of TPE and inhibiting IL-33 signaling might be a potent target to intervene in microfilariae- and potentially eosinophil-derived lung pathology.

Severe pathology and loss of disability-adjusted life years associated with filarial diseases are the main reason for continuous efforts to eliminate tropical filarial diseases. Mass drug administration (MDA) and further global efforts are undertaken to intervene the disease transmission of onchocerciasis and lymphatic filariasis. At the same time, research from animal and observational human studies suggests a connection between the decline in human helminth infections and the rise of lifestyle-associated metabolic diseases in developing regions. Lifestyle-associated metabolic diseases are steadily rising in developed countries but also in low- and middle-income countries, presenting a global health problem. Metabolic disorders like type 2 diabetes and cardiovascular diseases are among the ten leading causes of death as identified by the WHO in 2019 with the prognosis that type 2 diabetes prevalence will increase the strongest in Africa reaching a 134% increase by 2045.

An open-label pilot trial was designed to investigate filarial infections and their impact on metabolic diseases in Cameroon. Two hypotheses were investigated: 1) The induction of regulatory immune responses during filarial infection reduces obesity-induced low-grade inflammatory immune responses, thereby improving metabolic parameters. 2) Anthelmintic treatment abolishes this protective effect and worsens metabolic parameters. Lean (BMI<25), overweight (BMI >25 and <30) and clinically obese (BMI ≥30) participants infected with *Mansonella perstans, Onchocerca volvulus* or *Loa loa* from Littoral regions of Cameroon were evaluated for their parasitological, immunological, metabolic and biochemical profile before and after treatment of their parasitic infections. Anthropomorphic measurements and a detailed questionnaire completed the analysis. As this is an ongoing trial, this thesis assessed the preliminary data of the anthropomorphic measurements, circulating liver and kidney markers, circulating lipids and white blood cell profile at baseline, before anthelmintic treatment.

The results suggest that certain filarial infections improve clinical parameters compared to uninfected endemic individuals, e.g., circulating enzymes that predict liver function and markers for kidney associated diseases were partly decreased. Participants with filarial infections showed significantly decreased serum levels of C-reactive protein and glycated hemoglobin, indicating a decrease of systemic inflammation, metabolic inflammation and improved lipid hemostasis. Moreover, prevalence of type 2 diabetes was 2.3 times higher amongst the endemic normal population compared to the filarial infected participants. Taken together, the data presented here suggests that filarial infections may positively impact low-grade inflammation and metabolic parameters and therefore protect against the development of type 2 diabetes.

Zusammenfassung

Parasitäre Filarieninfektionen treten vorwiegend in tropischen Klimaregionen auf und können schwere Krankheiten auslösen. Die Wechselwirkungen zwischen dem Immunsystem und parasitären Filarieninfektionen sind dabei komplex. Bei erfolgreicher Immunmodulation des Wirts durch den Parasiten verlaufen die Infektionen meist symptomlos. Ist dies nicht der Fall, so kann es jedoch zu schwerwiegenden Pathologien kommen. Eine erfolgreiche Immunmodulation bei Filarieninfektionen bedeutet eine erhöhte Lebensdauer der Parasiten und mildert potenziell zusätzlich Allergien, Autoimmunerkrankungen und Stoffwechselkrankheiten des Wirts. Die Manifestationen dieser Erkrankungen umfassen unter anderem schwere Dermatitis und Erblindung bei der Onchozerkose oder pulmonale Eosinophilie, Lymphödeme und Hydrozelenbildung bei lymphatischer Filariose. Allerdings sind viele Krankheitsverläufe symptomlos und vor allem Infektionen mit *Mansonella perstans* und *Loa loa* zeigen oft keine eindeutigen klinischen Merkmale. In dieser Arbeit wurden sowohl negative als auch mögliche positive Effekte der Parasiten auf den Menschen untersucht. Hierbei standen I) die Entwicklung der Pathologie während der tropischen pulmonalen Eosinophilie in einem neu etablierten Mausmodell und II) die positiven Auswirkungen auf das metabolische und immunologische Profil von Patienten mit Filarieninfektionen im Vordergrund.

Bei der tropischen pulmonalen Eosinophilie werden Mikrofilarien von *Wuchereria bancrofti* oder *Brugia spp.* im Lungengewebe infizierter Patienten zurückgehalten. Dies führt zu einer lokalen Entzündung in der Lunge. Dadurch kann es zu einem pulmonalen Syndrom, Infiltration von Eosinophilen, Mastzellenrekrutierung sowie einem IgE-Klassenwechsel kommen. Die Symptome sind Fieber, nächtlicher Husten, Dyspnoe, Keuchen und Lungenfibrose, die zu schweren Lungenschäden und zum Tod führen können. In dieser Arbeit wurde ein Mausmodell für die tropische pulmonale Eosinophilie (TPE) unter Verwendung der Nagetier-Filarie *Litomosoides sigmodontis* entwickelt. Das Mausmodell wies immunologische und histopathologische Merkmale auf, die eng mit der TPE beim Menschen verbunden sind. Eosinophilie in der Lunge, erhöhte Reduktion von Mikrofilarien aus dem Blut und erhöhte Mikrofilarien-Retention im Lungengewebe wurden dabei beobachtet. Darüber hinaus wiesen TPE-Mäuse erhöhte gesamt- und parasitenspezifisches Konzentrationen an IgE sowie IL-5 im Serum auf.

Des Weiteren wurde dieses neu etablierte Modell verwendet, um die Rolle der Eosinophilen bei der Entstehung der TPE weiter zu erforschen. Dazu wurden dblGATA-Mäuse, die keine eosinophilen Granulozyten besitzen, verwendet. DblGATA-Mäuse zeigten dabei eine verminderte Retention von Mikrofilarien in der Lunge und eine beeinträchtigte Entwicklung einer Typ 2 Immunreaktion. Darüber hinaus verringerte die Blockade der IL-33-Signalkaskade die Entwicklung einer Typ 2 Immunantwort, einer Eosinophilie in der Lunge und verbesserte die Integrität der Lungenstruktur. Zusammenfassend zeigte dieser Teil der Arbeit, dass Eosinophile und die IL-33-Signalkaskade wesentlich an der Entwicklung von TPE beteiligt sind. Darüber hinaus wurde gezeigt, dass eben diese Hemmung der IL-33-Signalkaskade ein wirksames Ziel sein könnte, um in die durch Mikrofilarien hervorgerufene Lungenpathologie einzugreifen.

Schwere Krankheitsverläufe und der Verlust an uneingeschränkten und gesunden Lebensjahren (disability-adjusted life years) sind ausschlaggebend für die ständigen Bemühungen, die Krankheitslast in den betroffenen Ländern zu verringern. Dazu werden in der so genannten „mass drug administration“ (MDA) großflächig Medikamente gegen Infektionen mit Helminthen verabreicht. Interessanterweise deuten Forschungsergebnisse im Tier und Beobachtungen am Menschen auf einen Zusammenhang zwischen dem Rückgang menschlicher Helmintheninfektionen und dem Anstieg lebensstilbedingter Stoffwechselkrankheiten in Entwicklungsregionen hin. Stoffwechselkrankheiten wie Typ 2 Diabetes nehmen in den Industrieländern, aber auch in Ländern mit niedrigem und mittlerem Einkommen stetig zu und stellen ein globales Gesundheitsproblem dar. Typ 2 Diabetes und Herz-Kreislauf-Erkrankungen gehören laut der WHO zu den zehn häufigsten Todesursachen des Jahres 2019. Eine Einschätzung der internationalen Diabetesförderation (IDF) prognostiziert einen Anstieg der Diabetesprävalenz in Afrika um 134% bis zum Jahr 2045. Die hier präsentierte Studie wurde konzipiert, um Filarieninfektionen und ihre Auswirkungen auf Stoffwechselkrankheiten in Kamerun zu untersuchen.

In Folge dessen wurde untersucht, ob die Induktion regulatorischer Immunantworten während einer Filarieninfektion die durch Fettleibigkeit verursachten entzündlichen Immunantworten reduziert und dadurch die Stoffwechselparameter verbessert. Zusätzlich wurde untersucht, ob eine Behandlung mit Anthelmintika diesen Schutzeffekt aufhebt.

Für die Studie wurden Teilnehmer mit *Mansonella perstans*, *Onchocerca volvulus* oder *Loa loa* Infektionen aus ländlichen Teilen Kameruns, mit Normalgewicht (BMI <25), Übergewicht (BMI >25 und <30) oder klinischer Fettleibigkeit (BMI ≥30) auf ihr parasitologisches, immunologisches, metabolisches und biochemisches Profil vor und nach der Behandlung ihrer parasitären Infektionen untersucht. Anthropomorphe Messungen und ein detaillierter Fragebogen ergänzten die Analyse. Da es sich hier um ein laufendes Projekt handelt, wurden in dieser Promotionsarbeit vorläufige Resultate der Untersuchungen der anthropomorphen Daten, zirkulierenden Leber- und Nierenmarker, zirkulierenden Lipide und das Profil der weißen Blutkörperchen der jeweiligen Infektionen vor der Behandlung mit Anthelmintika verglichen. Dieser zweite Teil der Promotionsarbeit zeigte, dass bestimmte Filarieninfektionen Leber- und Nierenwerte positiv beeinflussten. Filarieninfizierte Teilnehmer wiesen zudem signifikant niedrigere Serumspiegel des C-reaktiven Proteins und des glykosylierten Hämoglobins auf. Diese Messwerte deuten auf eine Reduktion der entzündlichen Stoffwechselvorgänge hin. Darüber hinaus war die Prävalenz von Typ 2 Diabetes bei den endemischen nicht-filarieninfizierten Teilnehmern 2,3-mal höher als bei den mit Filarien infizierten Teilnehmern. Insgesamt deuten die hier dargestellten Daten darauf hin, dass sich Filarieninfektionen potenziell positiv auf eine kontinuierliche metabolische Entzündung auswirken und somit schützend gegen die Entwicklung von Typ 2 Diabetes sein könnten.

List of Abbreviations

AAM	Alternatively activated macrophages
ALP	Alkaline phosphatase
ALT	Alanine transaminase
AST	Aspartate transaminase
BAL	Broncho-alveolar lavage
BAT	Brown adipose tissue, beige adipose tissue
B. malayi	*Brugia malayi*
BMI	Body mass index
BP	Blood pressure
CRP	C-reactive protein
CD	Cluster of differentiation
d	Days
DAG	1,2-Diacylglycerol
D. dendriticum	*Dicrocoelium dendriticum*
DI	Downwards incorporation
ECG	Electrocardiogram
EDTA	2,2',2'',2'''-(Ethane-1,2-diyldinitrilo) tetra acetic acid
EDN	Endemic normal
E. multilocularis	*Echinococcus mulitlocularis*
FCS	Fetal calf serum
FI	Filarial infected
FLT3L	FMS-like tyrosine kinase 3 ligand
y-GT	Gamma-glutamyl-transferase
GLUT	Glucose transporter
h	Hours
Hb	Hemoglobin
HbA1c	Glycated hemoglobin
HDL	High-density lipoprotein
HEPES	4-(2-hydroxyethyl) -1-piperazineethanesulfonic acid

HpARI	*Heligmosoides polygyrus* Alarmin Release Inhibitor
HRP	Horseradish peroxidase
IBD	Inflammatory bowel disease
IDF	International diabetes federation
IFNy	Interferon gamma
IgE/G	Immunoglobulin E, G
IL	Interleukin
ILC2	Group 2 innate lymphoid cells
LAMP	Loop-mediated isothermal amplification
LDL	Low-density lipoprotein
LF	Lymphatic filariasis
L.l.	*Loa loa*
L. loa	*Loa loa*
M	Molar
MBP	Major basic protein
MF	Microfilariae
MHC2	Major histocompatibility complex
Min	Minute
ml	Milliliter
M.p.	*Mansonella perstans*
M. perstans	*Mansonella perstans*
MUC5AC	Mucin 5AC, oligomeric mucus/gel-forming protein
NFκB	Nuclear factor 'kappa-light-chain-enhancer' of activated B-cells
ng	Nanogram
NLRp3	NOD-, LRR- and pyrin domain-containing protein 3
nm	Nanometer
NTD	neglected tropical disease
OD_{600}	Optical density at 600 nm wavelength
O.v.	*Onchocerca volvulus*
O. volvulus	*Onchocerca volvulus*
PBS	Phosphate buffer saline

Pen	Penicillin
PFA	Paraformaldehyde
RANTES	Regulated on activation, normal T cell expressed and secreted
RBP4	Retinol-binding protein-4
RPMI	Roswell Park Memorial Institute Medium
RT	Room temperature
SCF	Stem cell factor
S. haematobium	*Schistosoma haematobium*
ST2	Interleukin-1-like receptor 1, IL-33 receptor
S. stercoralis	*Strongyloides stercoralis*
Strep	Streptomycin
T2D	Type 2 diabetes
TAG	Triacylglycerol
TGF-β	Transforming growth factor beta
Th1	T helper cells of the type 1 immune subset
Th2	T helper cells of the type 2 immune subset
Th17	T helper cells of the type 17 immune subset
TLR	Toll-like receptor
TNF	Tumor necrosis factor
TPE	Tropical pulmonary eosinophilia
Treg	Regulatory T cells
TSLP	Thymic stromal lymphopoietin
UI	Upwards incorporation
µg	Microgram
T. gondii	*Toxoplasma gondii*
µl	Microliter
WAT	White adipose tissue
W. bancrofti	*Wuchereria bancrofti*
WT	Wild type

List of Figures

List of Tables

1. Introduction

1.1 Parasitism

Parasitic life forms are estimated to be involved in approximately 75% of all food web structures and could represent up to 5% of larger animal groups [1]. Endoparasitism, i.e., the presence of parasites within a host´s body, tissue or cell, is conducted by diverse organisms, ranging from viruses and bacteriophages to single-cell bacteria, protozoa and large, multicellular organisms like parasitic helminths. Independent of their size and cellular composition, the parasite´s complex lifestyle requires adaptation and co-evolution to the host to ensure parasite and host survival [2, 3]. A prolonged survival of the parasite within the host means continuous interactions with the environment, i.e., the immune system or cellular defense mechanisms for intracellular parasites, which aim to expulse or kill the parasite at all times, sometimes without the needed restraint to prevent damage to the host. This adaptation often needs to be performed not only in a single host species but oftentimes in two or three different host species.

Two potential mechanisms that drive evolutionary ecology of parasites towards complex life cycles are downwards incorporation (DI) and upwards incorporation (UI) [4, 5]. DI resembles a circumstance where a second host, which is lower down the food chain, is added to a parasite´s life cycle. This occurs by the ingestion of parasite progenies, which usually infect the original host. If the parasite survives the new host and does not reproduce, it may become an intermediate or a paratenic host, which increases transmission to the definitive host. In the case of UI, the original definitive host is prey to a common predator. Parasites that survive digestion and reproduce within the new host, acquire a new definitive host [4-6].

Host acquisition marks the starting point for a co-evolutionary arms race [3]. Evolution of parasites will be selected by optimized host exploitation, improving reproduction and transmission. On the contrary, the host's evolution is centered around minimizing the parasite-derived loss of fitness, so called virulence [2, 7, 8]. This virulence, being normally beneficial for neither parasite nor host, was originally attributed to the parasite within these interactions, with parasites being traditionally defined as damage-producing organisms [3, 8]. However, Ebert and Hamilton claimed that it is a product of the host-parasite interaction rather than the parasite [3].

In many cases, parasite and host survival co-evolved over millions of years and are tightly knitted together, subsequently reducing virulence and host pathology. That said, genetic recombination due to sexual reproduction of both the host and the parasite was suggested to play a key role in altering the "status quo" either reducing or increasing virulence [3, 7]. In addition, in some cases, parasite infections promote pathology during their infection to improve reproductive fitness of the parasite.

In some cases, parasites actively influence the host's behavior to improve their own reproductive fitness [9]. Interestingly, this occurs predominantly in intermediate hosts. A famous example for a parasite modifying the behavior or impairing predator evasion of an intermediate host is *Toxoplasma gondii.* This protozoan parasite was shown to modulate mouse behavior, making infected mice less prone to avoid cat urine [10, 11]. Poirotte et al. provided evidence that this might also be the case for chimpanzees as *T. gondii*-infected animals no longer evaded the urine of leopards [12]. Furthermore, human T. *gondii* infections might be associated with enhanced risk-taking, drug consumption, car accidents, and entrepreneurship [13-16]. Gaskell et al. provided insight into a potential modification of the dopamine balance through *T. gondii* with amino-acid hydrolases [17]. That said, differentiating causation and correlation in the context of human *T. gondii* infection is complicated as individuals with higher risk-taking might be more likely to be exposed to *T. gondii* by eating undercooked meat or unwashed vegetables.

A fundamentally more drastic impact on host survival and behavior can be observed in ants infected with the lancet liver fluke, *Dicrocoelium dendriticum*. Here, infected snails release cercariae that are eaten by ants. After digestion, the cercariae develop into metacercariae that migrate to the brain of the ant, ultimately changing the behavior of the ant into climbing to the top of blades of grass, biting down into the grass and waiting until they are taken up by grazing cows, the definitive host of *D. dendriticum*, thereby directly impacting the chance of transmission [18, 19]. In this case, humans are an accidental host of *D. dendriticum* due to the incidental ingestion of infected ants, which causes cholecystitis, liver abscesses and gastrointestinal distress [20, 21].

Further, *Echinococcus multilocularis,* a tapeworm of foxes*,* causes tumor-like growth in its intermediate host, rodents and accidental hosts, including humans [22-24].

In rodents, this severely impacts the ability to escape predators, thereby improving transmission. In humans, intrahepatic growth of metacestode tissue can be observed. Here, *E. multilocularis* and *E. granulosum* are zoonotic diseases causing alveolar and cystic echinococcosis, respectively. Both diseases, especially alveolar echinococcosis, are severe diseases with high fatality rates [25]. Alveolar echinococcosis can be difficult to diagnose as the first phase of primary infection is clinically silent and may last ten or more years after infection [26], leading to a delayed diagnosis of the disease. As a result, invasive tumor-like growth of metacestode tissue can often be observed in the liver and other organs during late stages of the infection. This in turn leaves limited treatment options. In most cases, lifelong chemotherapy with albendazole, which acts parasitostatic in combination with surgery, can improve disease outcomes [27]. Taken together, the instances of parasite-host interactions mentioned above illustrate that parasites severely impact the fitness and behavior of the intermediate or accidental host.

In contrast, in some instances, parasites might benefit from improved health and reproductive fitness of the definitive host, ensuring circumstances where reproduction and continuous release of progeny is possible for the entire life span of the parasite. Here, a relationship leaning towards clinically silent and modulatory effects on the immune system and other parameters might even be beneficial. This circumstance becomes more evident when focusing on large multicellular organisms that reside inside humans for an extended period of time.

1.2 Parasitic filarial nematodes

"Parasitic helminths" is the collective term for worm-shaped multicellular organisms that are distinguished into flatworms (trematodes), tapeworms (cestodes) and roundworms (nematodes). According to the WHO, helminths infected approximately two billion humans in 2020 [28]. Several helminth infections, including some parasitic filariae, are included in the umbrella term neglected tropical diseases (NTD), predominantly impacting the lives of the poorest people in low- and middle-income countries in sub-Saharan Africa. These filamentous worms, which are vector-born parasites, can cause a multitude of diseases in humans.

The most abundant ones being the infective agents *Ochocerca volvulus* (*O. volvulus*), *Brugia malayi* (*B. malayi*), *Wuchereria bancrofti* (*W. bancrofti*), *Loa loa* (*L. loa*) and *Mansonella perstans* (*M. perstans*), with the latter two not being included in the list of NTDs as of now. Filariae are large several centimeter-long, moving worms that can induce severe pathology or clinically silent infections.

The life cycle of human-pathogenic parasitic filarial nematodes shares many common features and the general life cycle is shown in Fig. 1. The arthropod vector transmits the infective third larval stage (L3 larvae) via its bite into the skin/blood vessels of the host. The species of the vector, the migration route of the L3 larvae and the location of the adult worms differ among the respective species. The L3 larvae of *O. volvulus* are transmitted by *Simulium spp.* and migrate into the subcutaneous tissue, where they molt into adult worms that reside in nodules and have a reproductive lifespan of 9-11 years in the human body [29, 30]. The male worms roam between the nodules, mating with the female worms, which then release microfilariae (MF) into the skin. Another bite of the vector takes up MF, the first larval stage of filarial parasites, which penetrate the midgut of the vector and develop into infective L3 larvae, in turn, migrating to the proboscis of the vector completing the life cycle. In 2017, 21 million people were estimated to be infected with *O. volvulus* [31]. Onchocerciasis, also called river blindness, can lead to severe dermatitis, visual impairment and ultimately result in vision loss. Thereby leading to approximately 205 million disability-adjusted life years (DALY´s) [32].

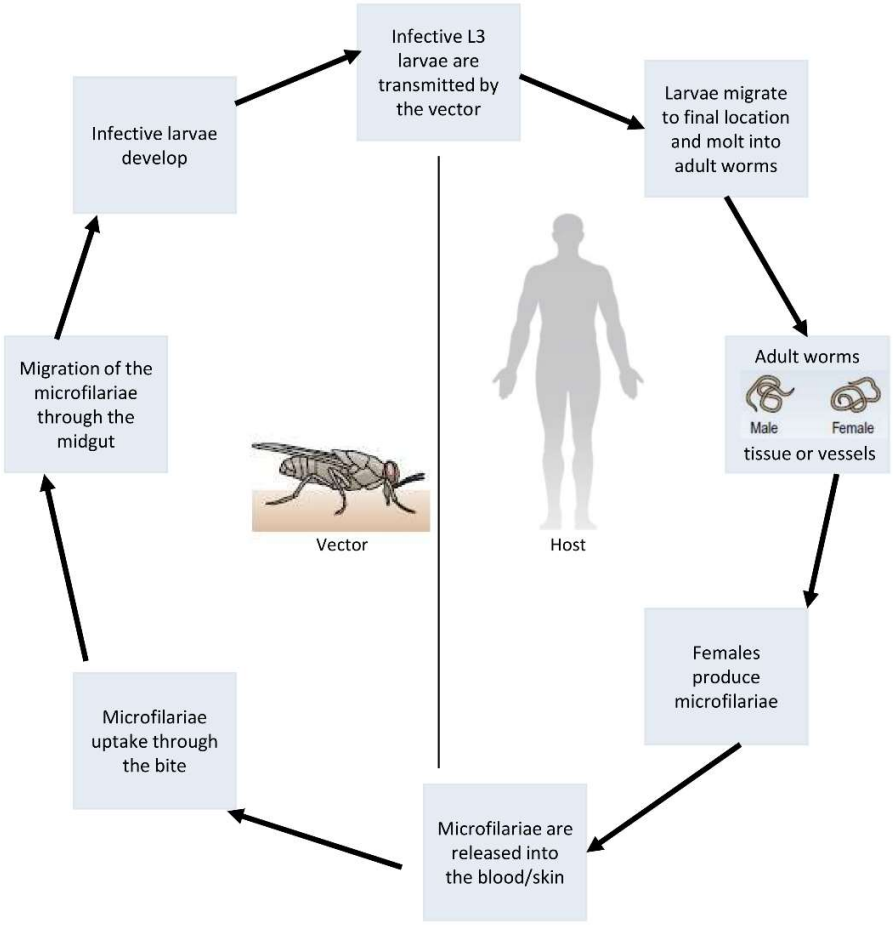

Figure 1. Life cycle of human filariasis. Infective L3 larvae are transmitted by the bite of the vector and migrate through the subcutaneous tissue (*Onchocerca volvulus, Mansonella streptocerca)* connective tissue (*Loa loa*), serous membranes of body cavities (*Mansonella perstans, Mansonella* ozzardi) or lymphatic vessels (*Brugia spp., Wuchereria bancrofti)*, where they molt into adult worms. After mating, female worms release sheathed or un-sheathed MF into the subcutaneous tissue or blood. MF are taken up by the bite of the vector. The MF penetrate the midgut of the vector, develop to L3-larvae and migrate to the proboscis of the vector. Image adapted from Mansons 24th edition, 2023.

M. perstans is transmitted by *Culicoides spp.* The location of adult worms can vary from serous body cavities like the peritoneum to the skin, with the latter being only rarely described. *M. perstans*, with estimated 120 million people infected is the most common human filarial infection. Interestingly, in contrast to *O. volvulus, M. perstans,* is generally not associated with apparent clinical symptoms [33]. Of note, *M. perstans* and *O. volvulus* contain symbiotic *Wolbachia* bacteria*,* which are essential for filarial development, fertility and survival of the adult worms.

The presence of *Wolbachia* gained attention as a potential target for treatment approaches with antibiotics such as doxycycline. However, not all filariae harbor *Wolbachia*. *L. loa*, the causative agent of loiasis, does not contain *Wolbachia* [34-41]. *L. loa* is transmitted via horse flies of the genus *Chrysops. L. loa* adult worms reside in the subcutaneous and connective tissue releasing MF into the blood, which are present during the day. *L. loa* is predominantly endemic in sub-Saharan Africa and approximately 10 million people were infected in 2011 [42-49]. Further, *L. loa* was recently shown to significantly impact the mortality of its infected individuals [50]. *L. loa* infected individuals displayed a median survival time of 39.2 years while MF negative individuals lived for approximately 58.5 years.

Finally, lymphatic filariasis (LF), caused by *Brugia spp.* and *W. bancrofti*, with an estimated 51.4 million cases in 2018, is transmitted by mosquitos [51, 52]. Here the adult worms reside in the lymphatic vessels and MF are found in the blood at night. The presence of adult worms within the lymphatic vessels can lead to various disease outcomes. Like all other filarial infections, asymptomatic infections are predominant [53]. The distinctive features of this disease are hydrocele formation, lymphedema and elephantiasis [54].

Distribution of human filariasis is species dependent but mostly centered in sub-Saharan Africa especially for onchocerciasis, loiasis and mansonellosis. LF has a broader distribution with active transmission in South America and South-East Asia [42, 51, 55, 56].

1.3 Clinical manifestation of filarial infections

Unsuccessful or incomplete immunomodulation by the filarial parasite are often accompanied by severe pathology. During onchocerciasis, severe dermatitis can occur [57]. The severity of dermatitis can be modeled by a grading system established by Murdoch et al. in 1993. The disease spectrum ranges from acute papular onchodermatitis to lichenfield onchodermatitis and depigmentation and hanging groin [58-60]. Similarly, *L. loa* is capable of inducing pathology, i.e., pruritus, edema, Calabar swelling and the transient migration of adult worms through the subcutaneous tissue and sometimes the eye. The latter, giving it its common name, African eye worm. In contrast, *M. perstans* infections do not induce distinct clinical symptoms [61].

However, multiple clinical manifestations have been reported and symptoms are most common during the first exposure to the parasite. For instance, pruritus, fever, joint pain, severe abdominal pain, local swelling, formation of nodules, and exophthalmus have been reported for *M. perstans* infections [62-64]. Finally, LF can lead to severe lymphadenitis and lymphangitis in response to the larvae and adult worms residing in the lymphatic vessels. In some patients, the disease can induce progressive pathology of the lymphatic system that can lead to lymphedema and hydroceles [65].

Tropical pulmonary eosinophilia is a rare but severe complication that occurs in approximately 1% of human LF cases [66-68]. The disease was originally labelled as "pseudotuberculosis with eosinophilia" [69, 70] in 1940. In 1943, Weingarten et al., termed the disease tropical pulmonary eosinophilia and the disease was initially thought to be self-limiting with no fatal outcome but strong scaring of the lung tissue [71]. The pathogenesis was quickly linked to antigens of *Brugia spp.* and *W. bancrofti* and sheathed MF were discovered in the lung, liver and lymph nodes of TPE patients [66]. The symptoms are now known to include fever, malaise, fatigue, nocturnal cough, dyspnea, wheezing and pulmonary fibrosis. If untreated, pulmonary fibrosis can progress over time and lead to lung failure and death. With the exception of some extra-pulmonary manifestations, i.e., hepatosplenomegaly and lymphadenopathy, the majority of the disease progression is centered around the lung tissue [72].

The disease is classified as a hyper-responsive pulmonary syndrome and the condition is shaped by a strong infiltration of eosinophils into the lung tissue, expansion of mast cells and parasite-specific immunoglobulin E (IgE) as a response to trapped MF [66-68, 73] (Fig. 2). The standard of care treatment is diethylcarbamazine (DEC) (6 mg/kg) for 21 days, which eliminates the MF and clears up the pulmonary infiltrates [73, 74]. However, 20% of treated patients relapse within 5 years. Therefore, understanding the underlying mechanisms of TPE development is crucial to improve treatment outcomes and elucidate the role of eosinophils in the context of MF-associated lung pathology. In 1990, Egwang and Kazura showed that sensitizing BALB/c mice with *B. malayi* MF subcutaneously, followed by an intravenous MF challenge induces TPE-like symptoms in mice, including amicrofilaremia, elevated levels of serum IgE as well as blood and pulmonary eosinophilia.

Thereby mimicking the immune response observed in human TPE patients [75]. Further research with this model by Sharma and Srivastava showed that TPE mice develop a type 2 immune response [76], eosinophil presence in the lung [77] and they identified independent phospholipase A2 [78] as fundamental factor for the development of lung pathology. IL-12 was shown to impair TPE development by Mehlotra et al. [79].

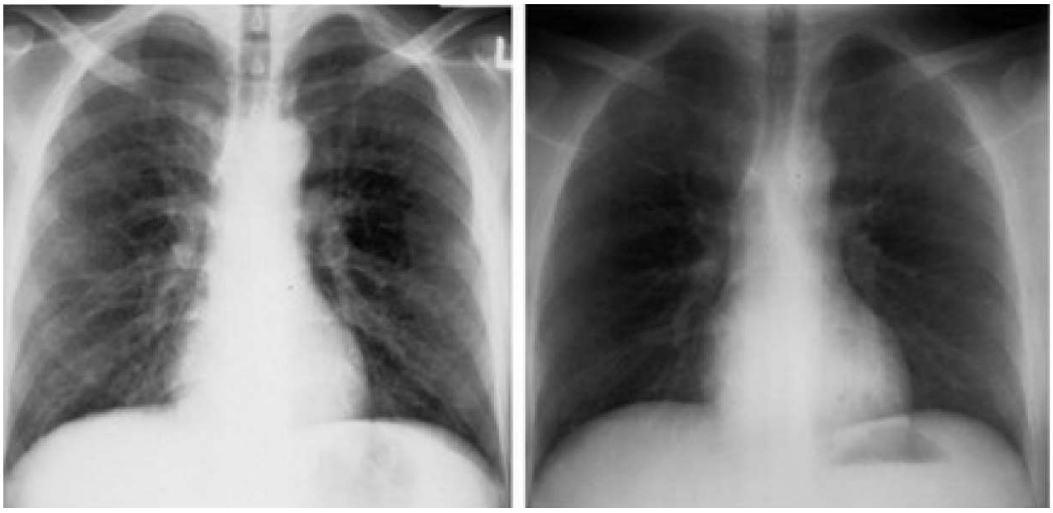

Figure 2. Tropical pulmonary eosinophilia patient chest X-ray image. X-ray image of a tropical pulmonary eosinophilia patient before (A) and after (B) 21 days of diethylcarbamazine treatment [80].

1.4 Filarial immunomodulation and implications for co-infections and co-morbidities

Despite their size, longevity and potential to release high numbers of potentially immunogenic progeny, the majority of filarial infections present with low or no signs of disease [81]. Escaping the protective immune responses of the host and suppressing the development of host pathology is essential for filarial long-term survival within humans. In general, this is achieved by a sophisticated modulation of the host's immune response by the parasite [81-90]. Parasitic filariae shift the host's immune system towards a type 2 immune response, showing the increased release of type 2 cytokines like IL-4 and IL-5, induction of eosinophilia, expansion of Th2 cells and alternatively activated macrophages (AAM) [81, 91, 92]. In addition, during chronic infections, filariae establish a regulatory milieu with increased levels of anti-inflammatory cytokines like IL-10 and TGFβ as well as increased numbers of regulatory T cells [83, 88, 93-97].

Especially T cells were found to be a major target of immunomodulation during human filariasis. Babu et al. demonstrated in 2005 that pro-inflammatory Th1 cells are impaired in LF patients by suppression of the hallmark transcription factor T-bet. Similarly, T cells from individuals with LF were found to have lower levels of TLR1, 2 and 4, indicating that T cells from filarial infected patients might be impaired in reacting to pathogen-associated molecular patterns and inducing pro-inflammatory immune responses [98, 99]. In addition to the suppression of Th1 cells, filarial infections can induce Th2 cells that are essentially involved in the type 2 immune response that are thought to mediate protection against helminth infections, but also support tissue repair and homeostasis [100]. Further, filariae are able to induce regulatory T cells that can actively suppress both type 1 and type 2 immune responses and are usually characterized by IL-10 and TGF-β production [101].

Accordingly, T cells from LF patients displayed significantly higher RNA expression of IL-4, IL-5 and IL-10, indicating not only a reduced Th1 profile but a shift to a type 2 immune response (IL-4, IL-5) and promotion of regulatory responses (IL-10) [99]. Similarly, T cells from *L. loa*-infected individuals displayed a decreased ability to proliferate and express IL-2, which is involved in T cell expansion and proliferation, in response to unspecific mitogens [102]. Furthermore, monocytes from LF-infected patients displayed diminished nitric oxide synthase 2, a second messenger molecule for pro-inflammatory immune responses and increased arginase-1, IL-10 and TGF-β expression after stimulation with *B. malayi* antigen [103]. *M. perstans* MF-positive individuals displayed reduced serum IL-4, IL-6, IL-12p70, IL-8 and RANTES levels, indicating a suppressed immune state complemented by an increase of regulatory B and T cell subsets [104]. After stimulation of the whole blood with filarial antigen, however, IFNγ, IL-10, IL-13 and IL-17A secretion was increased in comparison to uninfected controls [104].

The significant influence on the immune system is further seen in children of mothers carrying filarial infections. *In utero* priming leads to reduced T cell proliferation, higher IL-10 production and increased IgG4 levels as well as decreased inflammatory responses to filarial antigen in the affected children up to 4 years after birth [81, 105-108]. In onchocerciasis, LF and mansonellosis, IgG4 and IgE levels are elevated, again indicating a shift towards type 2 immune responses with IgE but also an anti-inflammatory and tolerance-inducing response by IgG4 [104, 109-112].

Interactions between parasitic helminths and their host are multifaceted and, as a result, bystander immune responses can be impacted by filarial infections as well. Accordingly, filarial infections can alter the immune response and the course of malaria, bacterial and viral infections as well as decrease vaccination efficacy [104, 113-120]. In the case of malaria, co-infections with *W. bancrofti* or *M. perstans* and *Plasmodium falciparum* reduced the parasite-specific production of IL-12p70, CXCL10 and IFNγ in an IL-10-dependent manner [116, 121]. Further, malaria-specific Th1, Th17 and TNF producing CD4 T cell frequencies were reduced [121, 122]. Likewise, bacterial infections can be impacted in their severity and incidence in filarial co-endemic regions.

For instance, *Mycobacterium leprae* disease outcome was significantly worse in regions that are co-endemic for *O. volvulus,* with lepromatous leprosy, the most severe form of leprosy, being twice as common as in non-endemic regions [123]. In the case of *Mycobacterium tuberculosis,* no direct increase of active pulmonary tuberculosis in helminth-infected patients was found [124], but an expanded population of IL-4 producing memory T cells was found [125]. Intriguingly, parameters that are associated with increased bacterial burdens and are necessary for a protective immune response against tuberculosis, i.e., mono- and multifunctional Th1 cells expressing IL-2, TNF/IFNγ or IL-2/IFNγ were significantly decreased in *W. bancrofti*-infected tuberculosis patients [126]. In a similar fashion to findings from co-infections of malaria and filarial parasites, parasite-specific Th1 and Th17 frequencies were decreased [126]. A direct association of the filarial *W. bancrofti* infection and HIV co-infections was observed by Kroidl et al. in 2016, showing that the incidence of HIV was 2.17 times higher in infected individuals compared to the endemic control [115, 127].

In a similar vein, vaccination efficacy, which relies heavily on the induction of a fierce immune response to build sufficient memory effects and immunoglobulin titers to prevent infections, can be influenced by filarial infections. Dampened immune responses during filarial infections were associated with decreased vaccine responses. In one study by Cooper et al., it was described that tetanus-specific cellular and humoral immune responses were decreased in patients suffering from *O. volvulus* [114]. In line, a study by Nookala et al. demonstrated a similar impaired tetanus-specific humoral and cellular response after tetanus vaccination of LF patients [128].

Despite the mentioned negative connotations of filarial infections on co-infection with bacteria, viruses, protozoa and vaccine efficacy, there are also potential beneficial effects of filarial infections. E.g. maladjusted immune responses resulting in autoimmune diseases can be reduced by filarial infection. For instance, the incidence of type 1 diabetes was significantly reduced in individuals infected with LF compared to endemic normals [129, 130]. Accordingly, two observational studies in India and China showed that the prevalence of lymphatic filarial infections is lower in type 2 diabetes patients than in healthy individuals [129, 131]. Further, a negative association between a history of *Schistosoma spp.* infections and glycemic parameters like glycated hemoglobin (HbA1C), fasting blood glucose and homeostatic model assessment of insulin resistance (HOMA-IR) was seen [132].

Another study showed a negative correlation between diabetes prevalence and infection with the intestinal helminth *Strongyloides stercoralis* in indigenous inhabitants of Australia [133]. Similarly, results from South India demonstrate that *S. stercoralis* infections are associated with an improvement of diabetes-associated and anti-inflammatory parameters that are in part reversed after anthelmintic treatment [134-141]. Additional indications were provided by a survey in Flores Island, Indonesia, where individuals infected with soil-transmitted helminths displayed a reduction of insulin and fasting blood glucose, assessed by HOMA-IR, indicating an improved insulin sensitivity [142]. Finally, *S. haematobium*-infected overweight/obese individuals in Lambaréné, Gabun, displayed improved circulating lipids (HDL).

1.5 *Litomosoides sigmodontis* mouse model

Supplementing the expensive and labor-intensive human clinical research with mouse models is a standard method to investigate and further elucidate mechanisms of diseases, as well as immunological and cellular processes. In the case of filarial infections, information about immunomodulation during co-infections, co-morbidities and vaccine efficacies was obtained using the *Litomosoides sigmodontis* (*L. sigmodontis*) mouse model. The natural host of the rodent filaria *L. sigmodontis* is the cotton rat of the species *Sigmodon hispidus* [143, 144]. The life cycle of *L. sigmodontis* in BALB/c mice is depicted in Fig. 3 and resembles human-pathogenic filariae. The infective L3 larvae are transmitted through the bite of the arthropod vector, the tropical rat mite *Ornithonyssus bacoti*.

The larvae migrate through the lymphatic system to the pleural cavity after penetrating the lung between day 2 and 6 post infection [143, 145]. At day 8, the larvae molt into L4 larvae and by day 28, they molt into adult worms, mate and release MF starting as early as day 52 [146, 147]. BALB/c mice develop a chronic infection with *L. sigmodontis* adult worms producing MF in approximately 50% of mice and adult worms are cleared around day 100 post infection. In contrast, C57BL/6 mice do not develop microfilaremia and clear the infection around 45 days post infection [148, 149].

Immunological investigations have been conducted thoroughly using this model. Marechal et al. showed in 1997 that infected BALB/c mice displayed a type 2 immune response, releasing cytokines like IL-4, IL-5 and IL-10. Resistant B10D2 mice lacked this response and developed a quicker antibody response, indicating that a type 2 response might be necessary to establish a patent infection. A similar picture is shown for the cytokine IL-10, where overexpression by macrophages overcomes resistance to murine filariasis [150, 151]. Further characterization of the *L. sigmodontis*-specific immune response showed that regulatory T cells are essential for infection and if missing, lead to clearance of the filarial parasites [152, 153]. Martin et al. demonstrated in 2000 that transgenic mice over-expressing IL-5 reduce the number and size of adult worms. Interestingly, IL-4 was crucial to mediate resistance in C57BL/6 mice and has implications on the MF burden of BALB/c mice, while IL-5 knockout mice had more adult worms [154, 155]. Frohberger et al. recently showed that mice lacking eosinophils (dblGATA mice) or lacking the IL-4 receptor and IL-5 have an increased worm burden, worm length and MF burden [156]. They concluded that IL-4 and IL-5 are associated with *L. sigmodontis* infections and, on one hand, are important for worm clearance but, on the other hand, also necessary to establish the milieu required for a chronic infection. Subsequently, they identified eosinophils, which are producers and recipients of IL-4 and IL-5, as critical cells in shaping anti-filarial immune responses. For instance, lack of eosinophil granular protein, i.e., eosinophil peroxidase and major basic protein impaired the resistance of Sv129j mice and eosinophils respond to MF of *L. sigmodontis* with extracellular DNA traps [157, 158].

Overall, many lessons were taken from this mouse model benefitting from the fact that the observed immune response closely resemble many aspects of the immune responses found in human filariasis [159-161]. Subsequently, the *L. sigmodontis* mouse model essentially helped to get a better understanding on not only the immune responses during filarial infection, but was also used to elaborate on the impact on co-infections, non-communicable diseases, protective immune responses and vaccination efficacy.

Especially protective immune responses for a variety of diseases and co-infections were induced in the *L. sigmodontis* mouse model. It was shown that infections with this parasite or, to a lesser degree, treatment with antigen derived from adult worms has a protective effect against type 1 diabetes by inducing regulatory T cells in the spleen and shifting the immune response towards a type 2 immune response [162-164]. Likewise, during experimental diet-induced type 2 diabetes, *L. sigmodontis* infection and antigen treatment improved glucose tolerance by enhancing insulin signaling, e.g. by increased expression of the glucose transporter-4 (GLUT4) [165]. Further, inflammatory immune responses were again decreased while a type 2 immune response including eosinophils, AAM and ILC2s in the epididymal adipose tissue was promoted [165]. More recently, it was shown that treatment with an *L. sigmodontis* extract also increases adiponectin levels, suppressing the generation of pro-inflammatory Th1 and Th17 cells, which are associated with the development of diet-induced insulin resistance [166]. In the context of cardiovascular disease, a protective effect of *L. sigmodontis* antigen treatment was also observed in atherosclerosis. Here, the infection decreased plaque formation [167]. Strikingly, improved outcomes, i.e., decreased morbidity and improved clearance of bacteria from the blood, were described in *L. sigmodontis* infected mice using a model for bacterial sepsis [168].

On the flipside of these protective mechanisms are implications of vaccination efficacy. Thus, filarial infections compromised the vaccination efficacy against influenza by inducing IL-10 and regulatory T cells and interfered with a thymus-dependent model antigen vaccination by suppressing antigen-producing B cells directly [169-171].

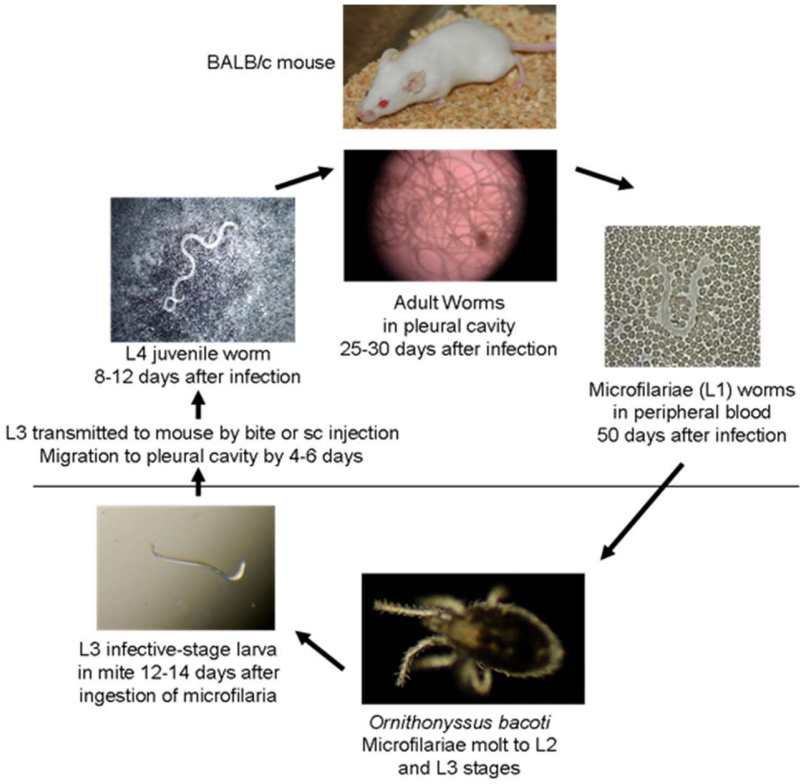

Figure 3. Life cycle of the rodent parasitic filaria *Litomosoides sigmodontis*. The infective L3 larvae are transmitted into the skin of the rodent host by the tropical rat mite *Ornithonyssus bacoti*. The larvae migrate into the pleural cavity 2-6 days post infection. 8 dpi, the L3 larvae within the pleural cavity molt into the L4 larval stage (~10 dpi) which develop to adult worms after 28-30 days post infection. The adult worms mate and the female worms release sheeted MF (L1 larvae) which migrate out of the pleural cavity into the peripheral blood of the host after 52 dpi. The MF are taken up by the rat mite during another blood meal and develop into L3 larvae, completing the life cycle. Image taken from Hübner et al. 2009.

1.6 Eosinophils

Granulocytes, namely, basophils, neutrophils, mast cells and eosinophils, are cells of the innate immune system that contain large quantities of granules. One of the earliest descriptions of granulocytes was given by the Belgium clinician Gottlieb Gluge. He described “inflammatory globules” in inflammatory exudates in 1843 [172]. Gluge´s work was expanded by Julius Vogel. The German pathologist depicted different granular cells, believing that the granules consisted of fat as they dissolved in organic solvents [173]. In 1847, the British physiologist Thomas Wharton Jones, presented fine and coarse granular blood cells [174]. A few years later, Max Johann Sigmund Schultze performed functional experiments on fine and coarse granular blood cells using a heated microscope stage and observed movement and phagocytosis of small objects.

Consequently, dividing blood cells into four different types of leukocytes which were later recognized as lymphocytes, monocytes, neutrophils and eosinophils [175]. Finally, Paul Ehrlich achieved differentiation of granulocytes within the blood using fabric dyes and writing ink on blood films in 1879 [176, 177]. Here, Paul Ehrlich distinguished granulocytes into eosinophils, neutrophils and basophils and defined lymphocytes. He described eosinophils as “the most important of these granulations by far” and stated that they were characteristically stained by acidic coal dyes. Later he further characterized their signature multi-lobed nucleus, primary and secondary granules and suggested the bone marrow to be the site of formation [178].

Almost 150 years later, our understanding of eosinophils has improved significantly. They originate, as correctly proposed by Paul Ehrlich, from hematopoietic stem cells in bone marrow and differentiate into common myeloid progenitors that can also differentiate into monocytes, basophils and neutrophils [179]. The expression of the transcription factor GATA-1 and 2 is essential to drive eosinophil differentiation in mice [180, 181]. In a similar vein, IL-3, IL-5 and granulocyte-macrophage colony stimulating factor (GM-CSF) support eosinophil maturation as reviewed by Dougan et al. in 2019 [182]. Under healthy conditions, low frequencies of eosinophils can be observed circulating in the blood [183, 184].

Further, resident eosinophils are observed in the gastro-intestinal tract, bone marrow, uterus, adipose tissue, thymus and lymphatic tissue [176, 185, 186]. Under these circumstances, eosinophils are associated with maintaining tissue homeostasis and repair [187]. In response to epithelial damage and the release of damage-associated molecular patterns, e.g., alarmins like IL-25, IL-33 and TSLP, eosinophils, Th2 cells, ILC2s, basophils, mast cells and AAMs are recruited. In this context, eosinophils are capable of inducing mucus production and support epithelial growth via MUC5AC, transforming growth factor beta (TGF-β), vascular endothelium growth factor and IL-8 [188]. Furthermore, IL-4 secreted by eosinophils facilitates liver and muscle regeneration in mice [189, 190]. The secreted IL-4 was shown to be capable of recruiting myofibroblasts which respond to injury and mediate wound closure by contraction [191-193]. On the flip side, continuous induction of these tissue repair processes can lead to obstructive tissue remodeling, fibrosis and induce pathology [194].

Furthermore, eosinophil activation can induce the release of inflammatory cytokines, toxic granules and extracellular DNA traps exacerbating eosinophilic inflammation [193].

In a pathological setting, eosinophils are associated with a considerable number of allergies, autoimmune diseases, and infectious diseases, particularly helminth infections. In the context of helminth infections, the role of eosinophils is subject to continuous debates about whether eosinophils are mainly protective or pathogenic. The protective aspect is mainly supported by mouse research using eosinophil deficient mice. For example, absence of eosinophils in mice infected with the helminth model organisms *Heligmosomoides polygyrus, Nippostrongylus brasiliensis, Trichinella spiralis* and the previously mentioned *L. sigmodontis* led to decreased worm clearance and improved the reproduction of the worms [156, 195-199]. In contrast, eosinophil absence was shown to decrease the worm viability and life span of *Trichinella spiralis* infections [200, 201].

During human filarial diseases, eosinophils are closely associated with disease pathology in response to the MF, the filarial progenitor. For instance, the MF numbers have been associated with eosinophils and eosinophil-derived serum proteins in onchocerciasis patients and eosinophils are found in onchocercomata that display an active MF production [110, 202]. Further, patients that had no prior contact with *L. loa* (travelers, expatriates) displayed eosinophilia and worse disease outcome compared to infected patients from endemic countries that are routinely exposed and develop immune tolerance, resulting in less eosinophils and improved disease outcome [203, 204]. Accordingly, treatment of LF using DEC, which predominantly targets MF, can lead to fever, headache and lethargy, which is accompanied by an increase in eosinophils and IL-5 [205, 206]. Taken together, especially MF trigger an eosinophil response which could be responsible for subsequent pathology.

In the context of asthma, eosinophils were identified as early as 1922 to be a crucial part in mediating airway inflammation [207]. Moreover, Humbles et al. demonstrated in 2004 that blocking IL-5 in mild-asthma patients alleviated collagen production and smooth muscle changes, which usually contributes to restriction of airways [208]. In addition, blood and sputum eosinophils are important predictors of asthma exacerbation [209-212].

Interestingly, eosinophils were shown to be closely associated with parasympathetic nerves within the lung tissue and the eosinophil-specific major basic protein (MBP) was shown to directly bind to type 2 muscarinic receptors, thereby potentially promoting lung constriction and airway hyper-responsiveness [213].

Eosinophils were also found in circumstances beyond pulmonary diseases. For instance, inflammatory bowel diseases (IBD) such as ulcerative colitis, a severe inflammation of the colon and Crohn´s disease, an chronic inflammation of the large and small intestine, are closely associated with eosinophils [214]. Here, eosinophils are highly activated during the remission phase of ulcerative colitis and were shown to activate fibroblasts inducing either tissue repair or promote the formation of fibrotic structures in Crohn´s disease [215-217]. Further involvements of eosinophils in a plethora of diseases and autoimmune processes, as reviewed by Lee et al. include hyper-eosinophilic syndromes, autoimmune diseases (pancreatitis, neuromyelitis), endometriosis, cystic fibrosis, transplant rejection, atherosclerosis and many more [176]. In conclusion, eosinophils seem to actively partake in tissue damage in response to pathogens and autoimmune reaction. However, existing damage might induce tissue repair function of eosinophils, while excessive tissue repair in turn might lead to obstructions and complications, i.e., fibrotic tissue and airway obstruction.

The complexity of eosinophils in pathology and tissue hemostasis can be highlighted once more when focusing on the adipose tissue and the metabolic processes in human obesity. Adipose tissue can be differentiated into white (WAT) and beige or brown adipose tissue (BAT). WAT can be swarmed by pro-inflammatory macrophages in obese people and is prone to inflammatory processes [218, 219]. In contrast, BAT, whose original function was thought to be thermogenesis and mediating hibernation, does not show an increase of pro-inflammatory cytokines. Furthermore, BAT increases energy expenditure and metabolic activity via the production of heat, and thus, is generally regarded as the “healthy” fat tissue [218]. In addition to increased energy expenditure which can counteract obesity, BAT improves lipid and glucose homeostasis [220]. It was demonstrated that IL-4, IL-13, AAM and eosinophils are essential to convert WAT to BAT in a process that is called tissue browning in mice. Here, absence of IL-4 and IL-13 abolished BAT biogenesis, whereas administering IL-4 increased BAT formation and ameliorated obesity [221].

Accordingly, absence of ILC2s, AAM and eosinophils in the adipose tissue promotes inflammation [222]. This indicates that eosinophils, alongside ILC2s and AAM, maintain an anti-inflammatory milieu in the adipose tissue and mediate tissue browning.

1.7 Obesity and metabolic inflammation

Obesity and its associated metabolic diseases are a major public health problem on the global scale and an increasing challenge in low- and middle-income countries due to life-style alterations, cultural and social changes, aging populations, increasing urbanization, dietary changes, reduced physical activity, unhealthy behavior and lack of awareness [223-227]. In Africa, around 67% of diabetic subjects are undiagnosed and it is predicted that by 2045, the number of diabetes patients will more than double (134%). For instance, in Cameroon, over half a million people suffer from diabetes totaling in an age-adjusted prevalence of 5.5%, according to the international diabetes federation (IDF) diabetes atlas in 2021 (Fig. 4). Obesity is a primary etiological factor for the development of type 2 diabetes (T2D), which accounts for approximately 90% of all diabetes cases [228, 229]. T2D is predominantly caused by continuous low-grade inflammatory processes in multiple organs (=meta-inflammation), which results from a combination of nutrient-energy stress and immune-metabolic dysfunction [230, 231]. Long-time insulin resistance and elevated fasting blood glucose, i.e., a pre-diabetic state was shown to raise risks for cardiovascular diseases such as hypertension, atherosclerosis, ischemic stroke, myocardial infarction and can lead to the development of T2D [232-234].

Diabetes is commonly diagnosed by measuring the concentration of glycated hemoglobin (HbA1c) within the blood, representing a reliable measuring tool for long-term dietary habits and metabolic dysfunction [235]. HbA1c values below 42 mmol/mol hemoglobin (Hb), which corresponds to 6.0% of hemoglobin being glycated, represent the normal range. Values between 42 and 44 mmol/mol Hb indicate a pre-diabetic (6.0-6.4%) state and values exceeding 48 mmol/mol Hb result in a diabetes diagnosis [235, 236].

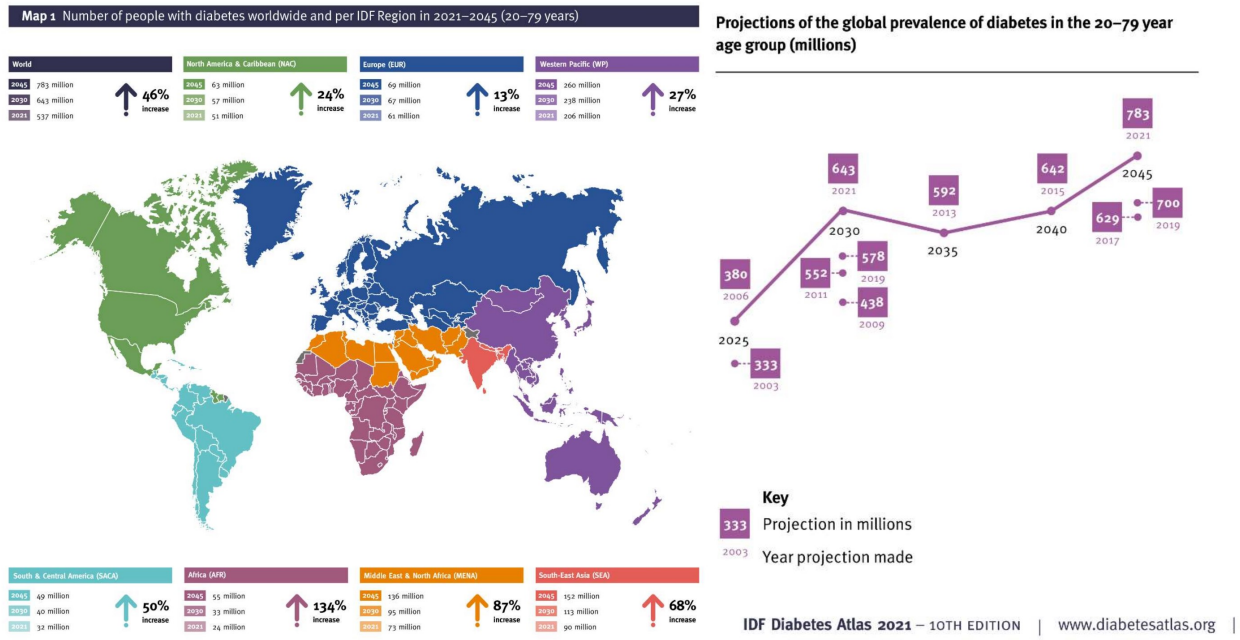

Figure 4. International diabetes federation (IDF) diabetes atlas in 2021 and projection of Type 2 diabetes cases. T2D is severe autoimmune disease with an increasing prevalence. Cases are projected to reach 783 million cases world wide by 2045 and increase by 134% in Africa. Images modified from IDF Diabetes Atlas 2021 [237]

Excess intake of macronutrients, e.g., fat, carbohydrates and proteins, can influence a cornucopia of fine-adjusted tissue and cell communications. Continuously elevated uptake of sugar and lipids stimulates the adipose tissue to release less adiponectin [238-240]. Here, adiponectin release was negatively correlated with adipocyte diameter, which increased during obesity [241, 242]. Loss of adiponectin decreases glucose uptake by the skeletal muscle and increases hepatic glucose output, contributing to increased blood glucose levels (=hyperglycemia) [243]. Hyperglycemia promotes circulating polymorphonuclear immune cells to secret pro-inflammatory cytokines like IL-6 and TNF and promotes oxidative stress [244].

Under normal circumstances, free fatty acids are taken up and stored as low-toxic triacylglycerol (TAG). However, if the concentration of fatty acids increases, diacylglycerol (DAG) is no longer converted to TAG. It accumulates together with sphingolipids and activates protein kinase C which drives TLR-2, TLR-4 and NFκB signaling, again driving the release of pro-inflammatory mediators TNF and IL-1β [245]. In addition, increased fatty acid uptake decreases blood glucose uptake and promotes insulin resistance [246].

Cellular lipid accumulation enhances extracellular recognition of saturated fatty acids through TLR signaling in a high lipid environment which cascades additional inflammation [247, 248]. Moreover, high lipid content results in endoplasmic reticulum stress and activates NFκB and NLRP3-inflammasome (NOD-, LRR- and pyrin domain-containing protein 3) signaling. This induces apoptosis as a mechanism against lipotoxicity via the initiation of oxidative stress and the release of IL-1β, IL-6 and TNF [249]. These mediators were shown to promote the synthesis and exocytosis of C-reactive protein (CRP) in liver hepatocytes [250]. CRP, usually an indicator of acute infection, primes the immune system and regulates energy expenditure, apolipoproteins, gut microbiome and thyroid hormones [251]. Accordingly, continuous elevated levels of CRP are a predictor of metabolic diseases and were shown to be closely associated with the risk of developing type 2 diabetes in a cohort study in South Korea [252, 253].

In a healthy metabolism, increased blood sugar leads to the immediate release of insulin, counteracting the accumulation of glucose in the blood by increasing insulin-mediated glucose transport via the glucose transporter-1 (GLUT-1) and GLUT-4 [254]. Subsequently glucose uptake of liver, muscles and adipose tissue cells is increased, with 75% of postprandial glucose taken up by the skeletal muscle cells [246, 254]. Impairment of the insulin function and production, namely insulin resistance, and the resulting hyperglycemia and hyperlipidemia are crucial focal points in metabolic disease development. Cytokines and adipokines can heavily modify insulin-mediated glucose and lipid uptake.

Adipokines, like the aforementioned adiponectin, are circulating hormones that mediate tissue communication, modulate glucose hemostasis and maintain a tight balance between uptake and release of glucose and lipids. For instance, the knockout of leptin in mice was shown to lead to severe obesity and insulin resistance by Pelleymounter et al. in 1995. In addition, administration of leptin to humans with severe lipodystrophy, a syndrome characterized by the loss of fat tissue, reverses insulin resistance and hyperlipidemia [255, 256]. Therefore, adiponectin and leptin were categorized as “anti-diabetogenic” because of their ability to decrease triglyceride synthesis, increase fatty acid oxidation and insulin sensitivity in the liver and skeletal muscle cells [257, 258].

In contrast, resistin ("resistance to insulin") was shown to antagonize insulin activity [259, 260]. Similarly, TNF and retinol-binding protein-4 (RBP4) were demonstrated to have insulin-desensitizing effects. For instance, TNF and RBP4 were shown to be closely associated with the expression of GLUT-4 (glucose transporter 4), one of the two transmembrane transporters that mediate the majority of glucose uptake [261, 262]. Intriguingly, a fasting state was shown to promote insulin resistance [263]. Muoio et al. suggested that these mechanisms might be able to mediate insulin resistance in diabetes due to excessive availability of nutrients but originally protected against hypoglycemia and loss of cognitive function in an environment that did not allow continuous food intake [257, 264]. Taken together, hyperlipidemia and hyperglycemia, in a continuous state of excess nutrient consumption, were shown to increase the aforementioned pro-inflammatory cytokines IL-1β, IL-6, TNF and obesity-induced adipokines in part to mediate the development of insulin resistance.

The effects of filarial infections on the human body originating from the close relationship that is formed during parasite infections are numerous. On the one side are debilitating pathologies that severely interfere with the lives of the poorest people on earth. Here, it is imperative that efficacious treatment options are developed for the respective filarial diseases and their complications. On the other side potential beneficial effects of filarial parasites could ease disease burdens caused by autoimmune and metabolic diseases, which should be meticulously assessed before filarial parasites are eventually eliminated.

1.8 Aim of the thesis

This thesis aimed to decipher the immunological processes leading to tropical pulmonary eosinophilia in a newly established mouse model and investigate the impact of filarial infections on the metabolic profile of lean, overweight and obese participants.

First, a mouse model for tropical pulmonary eosinophilia was adapted from the established *B. malayi* mouse model to the *L. sigmodontis* mouse model to investigate the underlying mechanisms. This newly established model was characterized and validated in its immune phenotype and used to investigate the role of eosinophils and IL-33 signaling in the context of MF-derived lung pathology using eosinophil-deficient dblGATA mice and the IL-33 antagonist *Heligmosoides polygyrus* Alarmin Release Inhibitor (HpARI).

Secondly, an open label pilot trial in rural Cameroon was conducted to investigate the impact of filarial infections, i.e., *L loa, M. perstans, O. volvulus*, onto the metabolic and immunological profile. Here an in-depth analysis of the anthropomorphic and blood biochemistry data was performed and parameters were compared between lean, overweight and obese participants between each respective infection to elucidate filarial species and BMI-dependent differences. Given that this is an ongoing trial, the analysis was restricted to the baseline data before treatment and concentrated on the anthropomorphic measurements, initial metabolic markers, i.e., circulating lipid profile, liver enzymes and markers for kidney function as well as white blood analysis.

2. Material & Methods

2.1 Tropical pulmonary eosinophilia mouse model

2.1.1 Mouse keeping and animal ethics

Experiments were performed with 6-8 week old female BALB/c WT or dblGATA knock-out mice. WT mice were obtained from Janvier (Saint-Berthevin, France) and kept in individually ventilated cages within the animal facility of the Institute for Medical Microbiology, Immunology and Parasitology (IMMIP). BALB/c dblGATA mice were bred at the Haus für Experimentelle Therapie, University Hospital Bonn. Animal experiments were performed according to the EU Directive 2010/63/EU and were approved by the state authorities (Landesamt für Natur-, Umwelt- und Verbraucherschutz, Recklinghausen, Germany). Water and food were provided *ad libitum*. Animals were checked daily for wellbeing and weighed once a week during the experiments to additionally monitor health conditions.

2.1.2 Microfilariae purification

Cotton rats (*Sigmodon hispidus)* were naturally infected with *Litomosoides sigmodontis*. Blood was isolated and diluted 1:2 in pre-warmed RPMI-1640 media (Gibco™, Thermofisher Scientific, California, USA) and layered on top of a 25% and 30% sucrose gradient (Carl Roth, Karlsruhe, Germany) of 0.25 M in iso-osmotic percoll (Merck, Darmstadt, Germany). The gradient was centrifuged at 1300 g for 30 min without brakes. The MF were contained in a white layer which was taken up and washed 3 times with pre-warmed RPMI-1640. MF were counted in a Neubauer counting chamber (Laboroptik GmbH., Friedrichsdorf, Germany) MF were adjusted to $1x10^5$ in 150 µl PBS (Gibco™, Thermofisher Scientific, California, USA).

2.1.3 Sensitization and induction of TPE mice

Mice were injected once a week for three weeks with $1x10^5$ dead (killed by freezing) microfilariae in 100 µl PBS, subcutaneously into the neck fold. The MF were checked for viability or lack thereof with bright field microscopy. One week after the third MF injection, mice were injected intravenously with $1x10^5$ living motile MF in 150 µl PBS (Gibco™, Thermofisher Scientific, California, USA). Control mice received 150 µl PBS in all instances.

2.1.4 Inhibitor treatment of TPE mice

Full length HpARI with a 6-His tag was expressed in Expi293 cells, and purified by nickel affinity chromatography, as previously described [265]. HpARI was provided by Dr. Henry McSorley. 10 µg HpARI was administered intranasally under light anesthesia induced with 2% isoflurane (Piramal Critical Care, New-Delhi, India) into the right nostrils in 10µl PBS (Gibco™, Thermofisher Scientific, California, USA). Treatment with 100 µg anti-IL-17a (clone 17F3, Biomol GmBH, Hamburg, Germany) blocking antibody was performed intraperitoneally with 100 µl PBS. TPE was induced as described above. Control mice received 10 µl PBS for intranasal and 100 µl PBS for intraperitoneal treatment.

2.1.5 Treatment of TPE mice

Starting one day after TPE induction, the mice were treated with the respective drugs for 5-7 days. DEC was administered orally for a total of 5 days at 50 mg/kg dissolved in 1% Tween in H_2O (10 ml/kg) once a day. Oxfendazole was administered twice daily for 5 days at 12.5 mg/kg dissolved in 100% corn oil. Corallopyronin A was administered intraperitoneally (i.p.) at a concentration of 18 mg/kg in polyethylene glycol (PEG400) for 5 days, once daily. Polyethylene glycol was administered as vehicle control i.p. at 10 ml/kg. Mice were opened at day 38 post MF challenge.

2.1.6 Bronchio-alveolar lavage (BAL)

Mice were sacrificed with an isoflurane overdose. The ribcage was opened carefully to allow the lungs to dilate completely. The throat of the animals was cut open to expose the trachea. A 20G Vasofix® (B. Braun Melsungen, Melsungen, Germany) intravenous vein catheter was inserted into the trachea and the lung was flushed with 1 ml PBS. The first ml was centrifuged at 400g for 10 min at 4°C and the supernatant was used for the analysis of cytokines. The lung was flushed with additional 4 ml PBS (Gibco™, Thermofisher Scientific, California, USA). Finally, 1 ml of PBS was injected into the lung to dilate the lobes before paraffin (Carl Roth, Karlsruhe, Germany) fixation. Flushed out BAL cells were centrifuged at 400g for 10 min at 4°C. Cells were used for flow cytometry.

2.1.7 Perfusion of the lung for microfilariae recovery

Following the necropsy, lung and heart were isolated from the mice and placed into a glass petri dish. 20 g needles (B. Braun Melsungen, Melsungen, Germany) were placed into the left and right atrium. An additional needle was placed into the right atrium and attached to a 10 ml syringe (B.

Braun Melsungen, Melsungen, Germany) containing PBS (Gibco™, Thermofisher Scientific, California, USA). The lungs were flushed with 10 ml PBS. The flow-through was collected in a 15 ml falcon tube and centrifuged for 10 min at 400g at room temperature (RT). The supernatant was discarded and 1 ml of red blood cell lysis buffer (Thermofisher Scientific, California, USA) was added to the pellet and the cells were resuspended. After 5 min, the samples were centrifuged again at 400g for 10 min at RT. 950 µl of the supernatant was carefully removed. The pellet was resuspended in the remaining 50 µl and transferred to a microscopy slide. All recovered microfilariae contained under the coverslip (Paul Marienfeld GmbH & Co. KG, Lauda-Königshofen, Germany) were counted.

2.1.8 Lung tissue dissociation

The lung tissue was dissociated using the gentleMACS in combination with the tissue dissociation kit (Miltenyi Biotec, Bergisch Gladbach, Germany). The protocol was performed according to the manufacturer's protocol. Briefly, the lung was cut into the respective lobes and added into the dissociation tube with 2.4 mL of 1× buffer S, 100 µL of enzyme D, and 15 µL of enzyme A. The lung lobes were dissociated at 37°C for 30 min under rotation of the tube (program: 37C_m_LDK_1) in the gentleMACS (Miltenyi Biotec, Bergisch Gladbach, Germany). Single cells were collected via centrifugation (400g, 10 min at 4°C) and red blood cells were lysed (eBioscience™, Thermofisher Scientific, California, USA). Finally, cells were washed and filtered through a 70 µm MACS SmartStrainer (Miltenyi Biotec, Bergisch Gladbach, Germany) and used for flow cytometry.

2.1.9 Spleen dissociation

Spleens were isolated from the sacrificed mice and dissociated using syringe stamp and pressing the organ through a 70 µm MACS SmartStrainer (Miltenyi Biotec, Bergisch Gladbach, Germany). Splenocytes were collected by centrifugation at 400g RT for 5 min and red blood cells were lysed (eBioscience™, Thermofisher Scientific, California, USA). Cells were washed with RPMI1640 media (Gibco™, ThermoFisher Scientific, California), counted and used for flow cytometry.

2.1.10 Serum preparation

Mice were bled from the facial veins. Blood was collected in EDTA Tubes (Sarstedt AG & Co. KG, Nümbrecht, Germany). 50 µl of blood was transferred to a 1.5 ml Eppendorf tube (Eppendorf SE, Hamburg, Germany) to determine the number of blood microfilariae. Therefore, 1 ml of red-blood cell lysis (Thermofisher Scientific, California, USA) was added to the 50 µl of blood and incubated

for 5 min at RT. The lysis was stopped by centrifugation at 400g for 10 min at RT. 1 ml supernatant was removed from the tube and all MF contained in the 50 µl pellet were counted under a microscope.

2.1.11 Bone marrow eosinophil culture

Bone marrow from BALB/c WT mice was isolated from the two hind legs using a 20-gauge needle and 5 ml RPMI-1640 for each bone. Flushed out cells were collected by centrifugation (400g, 10 min, 4°C) and red blood cells contained in the pellet were lysed by adding 1 ml of red blood cell lysis buffer (eBioscience™ ,Thermofisher Scientific, California, USA) for 5 min at RT. Cells were washed with 9 ml PBS (Gibco™, Thermofisher Scientific, California, USA) and centrifuged at 400g at RT for 10 min, adjusted to $1x10^6$/ml in RPMI-1640 + 20% fetal calf serum (FCS) + penicillin(10000 U/mg)/streptomycin (100 mg/ml)/glutaMAX™/gentamycin (50 mg/ml) (Gibco™, ThermoFisher Scientific, California, USA for all contents) and incubated with 100 ng/ml Fms-like-tyrosine kinase-3-ligand (FLT3L) and 100 ng/ml stem cell factor (SCF) (PeproTech inc., ThermoFisher Scientific, California, USA) for 4 days. Afterwards, cells were cultured with 20 ng/ml IL-5 (PeproTech inc., ThermoFisher Scientific, California, USA) until day 12 with half of the medium the medium changed on day 2, 6, 10 and the whole medium changed on day 4 and 8 (additional flask change). Cells were adjusted using CASY automated cell counter (OLS OMNI Life Science GmbH & Co. KG, Bremen, Germany). Cells were centrifuged and adjusted to $1x10^6$ in culture media (RPMI-1640 + 10% fetal calf serum, penicillin /streptomycin /glutaMAX™/gentamycin (ThermoFisher Scientiffic, California, USA). Cell purity was determined using flow cytometry and cell viability was assessed using the Annexin-V-PI staining kit (ThermoFisher Scientiffic, California, USA) (Suppl. Fig. 1).

2.1.12 Enzyme linked immunosorbent assay

Invitrogen ELISAs (IL-2, IL-4, IL-5, IL-6, IL-10) (Invitrogen, Thermofisher Scientific, California, USA) were performed according to the manufacturer's protocol from serum, BAL, pleura wash or lung homogenates. 50 µl serum was diluted 1:2 in assay buffer, 100 µl of either BAL, pleura wash or lung homogenates was transferred onto a plate that was coated with the capture antibody and blocked with assay diluent. Samples were incubated alongside the respective standard for 2 h at RT and 200 rpm. Plates were washed and incubated with the detection antibody for 1 h at RT and 200 rpm. Afterwards, plates were washed and HRP-conjugate was added for 30 min at RT and 200 rpm. After washing of excess HRP-conjugate, colorimetric detection was performed by adding

50 µl TMB into each well. The reaction was stopped using 100 µl of 1 M H_2SO_4 (Carl Roth, Karlsruhe, Germany) to each well. Optical density of the plates was measured in a SpectraMax Molecular Devices LLC, California, USA) at 450 and 570 nm wave length. Concentration calculations were performed in the Softmax Pro software.

2.1.13 Detection of IgE

Parasite-specific serum IgE was detected by coating a high binding ELISA plate (Sigma-Aldrich, MERCK, Darmstadt, Germany) with 1 mg/ml adult worm crude extract of female *Litomosoides sigmodontis*, diluted in PBS (Gibco™, Thermofisher Scientific, California, USA) for 24 h at 4°C. The crude extract was discarded and plates were washed and subsequently blocked for 1 h with 5% BSA/PBS (MERCK, Darmstadt, Germany) at RT. The biotinylated anti-mouse IgE antibody was diluted 1:200 in PBS, added to each well and incubated for 1 h at RT, shaking at 200 rpm. The detection antibody was removed by washing and the plates were incubated with the conjugated HRP for 30 min at RT, shaking at 200 rpm. Colorimetric detection was performed by adding 50 µl TMB into each well. The reaction was stopped using 100 µl of 1 M H_2SO_4 (Carl Roth, Karlsruhe, Germany) to each well. Optical density of the plates was measured in a SpectraMax (Molecular Devices LLC, California, USA) at 450 and 570 nm wave length.

2.1.4 DNA quant

DNA quantification was performed as described previously [158]. In brief, The Invitrogen Quant-iT™ dsDNA Assay Kit, high sensitivity (ThermoFisher Scientific, California, USA) was used for DNA quantification of bone marrow-derived eosinophils. Eosinophils were cultured in 96-well plates with medium containing IL-5 (20ng/ml PeproTech inc., ThermoFisher Scientific, California, USA). After the incubation time (24 h) the exo-nuclease from micrococcus (PeproTech inc., ThermoFisher Scientific, California, USA) (2.5 U/well) was added to all samples to prevent DNA sticking to the bottom of the wells. The culture plates (Sigma-Aldrich, MERCK, Darmstadt, Germany) were incubated at 37°C for 15 min. The micrococcal nuclease reaction was stopped with 10 µl 1 mM EDTA. Culture plates were centrifuged at 400 g for 8 min at 4°C and the supernatant was removed and transferred to a new 96-well plate (Sigma-Aldrich, MERCK, Darmstadt, Germany). The quantification was done with 100 µl Quant-iT™ dsDNA HS buffer after a 1:200 dilution. The diluted DNA Quant-iT™ solution was added to 20 µl of the supernatant.

For quantification, a standard was used. The standard ranged from 0 to 10 ng/µL (0, 0.5, 1, 2, 4, 6, 8, and 10 ng/µL) and 10 µl of the standard was used in duplicates. The absorption of sample and standard was measured using the Tecan infinity M200 (Tecan Group, Männedorf, Switzerland) at 525 nm.

2.1.14 Lung histology

Mice were sacrificed and the lung lobes were inflated with 1 ml PBS (Gibco™, Thermofisher Scientific, California, USA) via the trachea using a 20G Vasofix® intravenous vein catheter (B. Braun, Melsungen, Germany). To contain the inflated status of the lung tissue, the trachea was closed with yarn tied into a knot. The lung was cut out together with the heart and placed into 2% methanol free formalin (ThermoFisher Scientific, California, USA) for 24 h at RT. The lung tissue was washed twice with PBS (PBS, Gibco™, Thermofisher Scientific, California, USA) and dehydrated by being submerged in ascending ethanol baths (50, 70, 80, 96, 100%) and finally 100% xylene for 30 min (STP-120 automated sample processor, Especialidades Médicas Myr, S.L., Tarragona, Spain). The tissue was embedded in paraffin (Merck, Darmstadt, Germany) (modular tissue embedding center, Especialidades Médicas Myr, S.L., Tarragona, Spain). Hardened paraffin blocks were cut into 4 µm sections and paraffin was removed with alcohol baths. Sections were stained with Mayer´s hematoxylin and eosin (Merck, Darmstadt, Germany) and mounted with entellan (Merck, Darmstadt, Germany). Stitched histology images were taken on the Axio-observer 5 (Zeiss, Oberkochen, Germany) using Zen V3.6 (Zen Blue edition V3.6, Zeiss, Oberkochen, Germany). 50 10x10 µm Random regions of interests (ROI) were generated using KNIME (https://www.knime.com/ [266]) and lacunarity analysis was performed using the Image J [267] plugin FracLac (Karperien, A., FracLac for ImageJ. http://rsb.info.nih.gov/ij/plugins/fracla c/FLHelp/Introduction.htm).

2.1.15 Flow cytometry

Cells were blocked in 1 µg/ml rat IgG/PBS (Sigma-Aldrich, MERCK, Darmstadt, Germany) for 1 h at 4°C. The blocking buffer was removed by centrifugation (400g, 8 min, 4°C) and the cell pellet was dissolved in 100 µl fixation buffer (BioLegend, California, USA). Cells were fixated at RT for 15 min and washed with PBS (Gibco™, Thermofisher Scientific, California, USA), centrifuged at 400g for 10 min at RT and stained in 20 µl surface marker antibody mix (Tab. 1) and stained for 30 min at 4°C.

Stained cells were washed twice with PBS and subsequently centrifuged at 400g for 10 min at RT each time. For additional intracellular staining, cells were centrifuged twice in 100 µl permeabilization buffer (BioLegend, California, USA) and stained for 30 min at 4°C. Finally, cells were washed twice with PBS and measured using a CytoflexS (Beckman Coulter, California, USA).

Table. 1. Flow cytometry antibodies, manufacturer, dilutions and clones.

Antigen	Fluorophore	Manufacturer	Clone	Dilution
CD11b	Bv510	BioLegend	M1/70	1:400
CD11c	Bv605	BioLegend	N418	1:400
CD45	FITC	BioLegend	30-F11	1:400
CD101	AL700	BioLegend	BB27	1:400
Ly6C	PE-Cy5.5	BioLegend	HK1.4	1:400
Ly6G	Bv421	BioLegend	1A8	1:400
MHC2	PE-Cy7/FITC	BioLegend	30-F11	1:100
CD107a	APC-Cy7	BioLegend	H4A3	1:400
CD86	AL700	BioLegend	GL-1	1:400
Realm-α	APC	BioLegend	D58RELM	1:200
GATA3	PE-Cy7	BioLegend	L50-823	1:200
Siglec-F	PE/ APC-Cy7	BD	E-50-2440	1:400
CD206	PE	BioLegend	CD068DC2	1:400
Linage cocktail	Bv421	BioLegend	Cat. 133310	1:400
Sca-1	Bv510	BioLegend	D7	1:200
CD54	FITC	BioLegend	YN1/1.7.4	1:400
ST2	APC	BioLegend	DIH9	1:200
CD90.2	PE	BioLegend	53-2.1	1:400
TCRβ	AL700	BioLegend	H57-597	1:400

2.1.16 Statistical analysis for TPE

Statistical analysis was performed using Kruskal-wallis or Mann-Whitney-U-Tests. Significance between multiple groups was tested by Dunn´s multiple comparison. A p value < 0.05 was considered significant. Statistical calculations were performed in GraphPad PRISM v.9 (GraphPad Software, San Diego, California USA).

2.2 Implementation of the ”FIMMIP” trial

The trial described in the following is part of a German-African collaboration project funded by the DFG. The objective during this PhD thesis was the implementation of the trial in rural Cameroon. The laboratory used in Manjo, Cameroon, for this trial was constructed during this project (Fig. 5, 6). Thus, my responsibilities in this project included the design of the assays for flow cytometry and whole blood stimulation and trial document revisions and adjustments (case report form and informed consent form) as well as re-application of ethical consent. Further, I wrote and established the standard operating protocols for white blood cell analysis, clinical biochemistry, anthropomorphic measurements, storage of patient samples, sample sequencing and coding for bio-banking.

During this thesis, I was able to visit Cameroon, the Manjo laboratory as well as a field center four times. Here, I gave workshops and training on blood pressure and pulse measurement (Fig. 7A), ECG measurements (Fig. 7B), body-fat analyzer (Fig. 7C), waist circumference (Fig. 7D), clinical biochemistry (Fig. 8A), whole blood stimulation for ELISA and flow cytometry (Fig. 8B, C) as well as white blood cell analysis (Fig. 8D). Moreover, I organized and co-supervised a training on clinical biochemistry that was performed by the company LeviSarl (Douala, Cameroon) in Cameroon. Finally, I organized the purchase and shipment of laboratory equipment, e.g., consumables, plastics and medical instruments.

For this thesis, I analyzed the anthropomorphic, biochemistry, parasitology and white blood cell analysis data obtained during baseline, before the anthelmintic treatment. As this is an ongoing trial, additional analysis (e.g. flow cytometric analyses, cytokine/chemokine data) will follow after the completion of the trial and are not part of this thesis.

Figure 5. Manjo research center in rural Cameroon. A+C) Images taken from the laboratory during the early stage of the FIMMIP trial (2019). B) Manjo research center during the FIMMIP trial in 2022. D) Manjo laboratory 2020 (D) and 2022 (E).

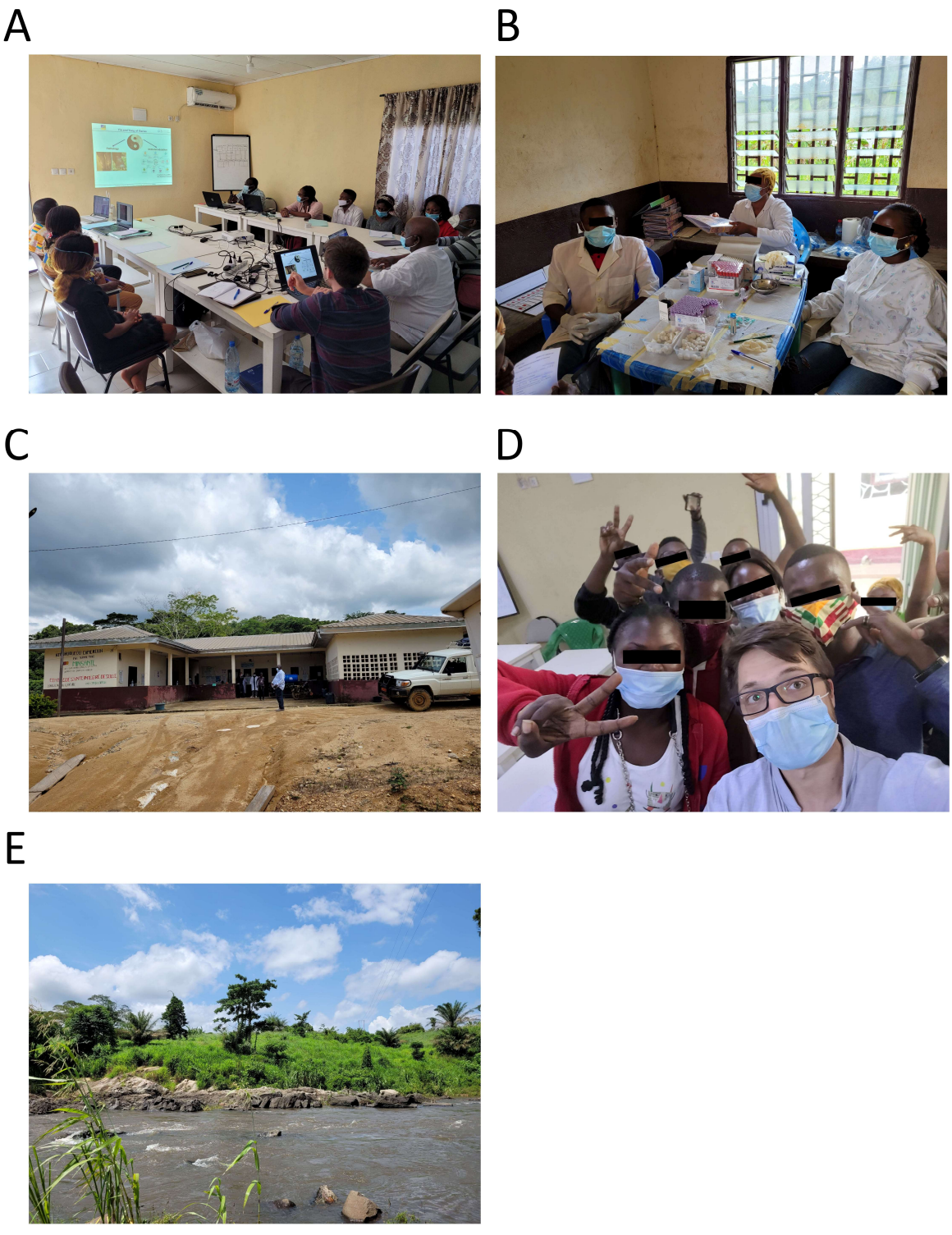

Figure 6. Trial sites and field team of FIMMIP. A) Introduction of the trial and background information in Cameroon. B) FIMMIP nurse team in the health center for blood draw and skin snipping. C) Example health center as a study site in the rural Yabassi area. D) FIMMIP field nurses and parasitologists after the training session for anthropomorphic assessment. E) Ideal breeding spot for *Simulium spp.* near fast flowing rivers in the Yabassi health district with *Culicoides* spp. present.

Figure 7. Anthropomorphic assessment training for the FIMMIP study. A) Blood pressure measurement and pulse training. B) Body fat analyzer training for BMI, weight, visceral adipose tissue, body fat and muscle mass. C) Training of electrode placement and ECG measurement. D) Training for the assessment of waist circumference.

Figure 8. Laboratory training session in the Manjo laboratory. A) Humastar200 serum analyzer training session for clinical biochemistry assessment. B) Training on whole blood stimulation and cryopreservation of flow cytometry samples. C) Whole blood stimulation workshop for ELISA assessment. D) Workshop for the white blood cell analyzer Yumizen H500. E) Demonstration of the parasitological assessment for the FIMMIP trial.

2.2.1 Trial setting

Participants of both sexes that consented to partake in the study (age 18-65) were recruited from several scouted sites in the rural areas around the Littoral region of Cameroon. Mapping of the filarial infections showed an incidence of the respective parasites *O. volvulus* (4.9-21.9%)*, L. loa* (1.4-22.5%) and *M. perstans* (0.2-16.9%) (Tab. 2) within the study regions. The rural communities are close to the field medical research station in Manjo to ensure a quick transfer of the samples from the field to the site of sample storage and analysis. Half of the samples were stored in Cameroon and the other half will be stored in Bonn, Germany. Storage and use of theses samples was specifically addressed to the participants in combination with the informed consent form.

Table 2. Prevalence of *O. volvulus*, *M. perstans* and *L. loa* infections in the study area

Health district	*M. perstans* prevalence	*O. volvulus* prevalence	*L. loa* prevalence	Screened persons (total)
Yabassi	16.9%	21.9%	22.5%	1225
Manjo	0.2%	4.9%	1.4%	2429
Loum	13.9%	17.3%	18.2%	583
Melong	1.4%	4.9%	2.9%	1748

2.2.2 Trial governance

Ethics approval to perform this study was obtained from the Cameroon National Ethics Committee for Human Health Research (No 2019/03/CE/CNERSH/SP). In Germany, ethical approval was obtained by the Ethic committee for clinical human research (No. 046/18). Protocol amendment were re-submitted to the ethics boards for approval. The clinical trial was registered under ISRCTN43845142 (doi.org/10.1186/ISRCTN43845142). Written informed consent was obtained from respondents after ensuring that the participant understood and accepted their role in the study. This study was funded by the DFG German-African Cooperation Projects in Infectiology (HU-2144/3-1). The funder did not impact the study design and had no impact on the study execution nor the analysis.

2.2.3 Study population

The first phase was comprised of a cross sectional study containing four main study groups (Fig. 23). All participants were evaluated according to the inclusion and exclusion criteria listed in table 3. Group 1 consists of *M. perstans*-infected participants which tested positive for microfilariae in the prick blood smear and/or the *M. perstans*-specific loop-mediated isothermal amplification (LAMP) [268].

Group 2 includes *O. volvulus*-infected individuals that showed at least one palpable onchocercoma and were tested positive in a diagnostic Ov150 (*Onchocerca volvulus* antigen 150) LAMP [269] or PCR and/or are skin snip positive for MF. Group 3 consists of non-filarial-infected endemic (normal) individuals that have lived in the endemic study area for at least five years, have normal eosinophil frequencies (<4%), and are negative for microfilariae by microscopy and PCR. Group 4 includes *L. loa*-infected participants that had detectable microfilariae by microscopy and/or are LAMP positive. Co-infections with mentioned filariae are included in were analyzed separately. Stool samples from each participant were also tested for intestinal helminth parasites. Presence of intestinal helminths in Kato-Katz was no exclusion criteria for groups 1, 2, 3 and 4. Upon recruitment, anthropomorphic measurements and the immunological and metabolic profile of each participant was analyzed.

The next phase of the study, although not analyzed in this thesis, was an intervention study that focuses on analyzing the changes in the metabolic and immunological profiles after anthelmintic treatment. The goal was to provide direct evidence of the filariae-mediated protective effect and to investigate the causal relationship between absence/clearance of filarial infection and a disadvantageous metabolic profile and increased inflammation. In this regard, all *M. perstans*- as well as *O. volvulus*-infected lean, overweight and obese participants (including *L. loa* co-infected individuals) were recruited in the cross-sectional study for anti-filarial therapy with 200 mg doxycycline for 42 days (for individuals with >50 kg body weight; individuals with 40-50 kg body weight were treated with 100 mg doxycycline for 42 days). Participants from all groups were treated with a single dose of 400 mg albendazole every three months with four treatments in total to eliminate intestinal helminth infections.

All participants were followed up at 12 and 18 months after treatment and a selection of immunological and metabolic parameters that were determined in the first part of this study will be analyzed. Patients were screened for filarial and intestinal helminth infections and the impact of possible re-infections following albendazole and doxycycline treatment was analyzed. Compliance to the treatment was confirmed by collecting empty drug containers during the visit of the study subjects. Subjects were monitored throughout the study for any adverse effects.

Table 3. Inclusion and exclusion criteria

Inclusion criteria	▪ Males and females between 18-60 years old ▪ Body weight > 40kg ▪ Resident in the endemic area for at least 5 years ▪ Good general health without any clinical condition requiring long-term medication ▪ Willingness to participate in the study as evidenced by signing the Informed Consent Form ▪ Negative pregnancy test
Inclusion in *O. volvulus* positive	▪ *O. volvulus* patients with at least one palpable onchocercoma, microfilariae skin snip positive and/or LAMP/PCR positive for *O. volvulus*
Inclusion in *M. perstans* positive	▪ *M. perstans* patients positive for microfilariae and/or LAMP/PCR
Inclusion in *L. loa* positive	▪ *L. loa* patients positive for microfilariae and/or LAMP/PCR
Inclusion in endemic normal	▪ Endemic controls, judged by absence of microfilariae, palpable onchocercoma, LAMP/PCR negative for *M. perstans, O. volvulus* and *L. loa*. Possess normal eosinophil frequencies (0.5-4%).

Exclusion criteria	▪ Positive pregnancy test ▪ Lactating mothers ▪ Last intake of ivermectin (IVM) less than 4 months ago ▪ Intake of anti-filarial antibiotics (tetracycline) less than 12 months ago ▪ Evidence of tuberculosis (clinical aspects) ▪ Evidence of clinical aspects of HIV infection ▪ Evidence/previous diagnosis of chronic diseases (urolithiasis, liver cirrhosis, congestive heart failure, chronic lung diseases, chronic infections other than filariae, viral hepatitis) ▪ Evidence of autoimmune diseases and allergies ▪ Evidence of acute infection (haematuria, cough, fever). Evidence of clinically significant neurological, cardiac, pulmonary, metabolic, malaria, rheumatologic or renal disease as far as can be assessed by history of individuals, physical examination, and/or laboratory examinations ▪ Childbearing potential and not willing or able to use methods to prevent a pregnancy for the entire treatment duration in addition to hormonal contraception (e.g. condoms) unless surgically sterilized/ hysterectomized or any other criteria considered sufficiently reliable by the investigator ▪ Behavioural, cognitive or psychiatric disease that in the opinion of the trial clinician affects the ability of the participant to understand and cooperate with the study protocol
Laboratory exclusion values	▪ Hemoglobin < 8 g/dL ▪ Neutrophil count < 500/µl ▪ Platelet count < 100 000/µl ▪ Creatinine > 2 times upper limit of normal ▪ AST (GOT) > 2 times upper limit of normal ▪ ALT (GPT) > 2 times upper limit of normal ▪ γ-GT > 2 times upper limit of normal ▪ HbA1c above 44 mmol/mol Hb (6%) ▪ Abnormal white blood cell counts below or above (3.5-11.3 x 10^3/µl)

2.2.4 Referral System

All newly diagnosed diabetic subjects were not treated in the study and were referred to a local public health center or to a private practitioner specialized in diabetes care, whose details were provided by field investigators on request. Anthropometric measurements, blood pressure readings, and capillary glucose values were immediately conveyed to study subjects and instructions to seek medical attention or adopt life-style measures were provided when results deviate from the normal range. Biochemical parameters and electrocardiogram (ECG) results and if needed instructions to seek medical attention, were mailed to the subjects later.

2.2.5 Definitions/Evaluation criteria for metabolic abnormalities

Diabetes

Diabetes was defined by prior diagnosis and current use of medications for diabetes (insulin or oral hypoglycemic agents) or fulfillment of criteria laid down by the WHO-IDF Consultation Group Report (2006) [270], i.e., fasting capillary blood glucose ≥126 mg/dl or 2 h capillary post-glucose value ≥200 mg/dl. **Hemoglobin A_{1C} ≥ 6.5% were considered as diabetes** according to the American Diabetes Association criteria (2014) guidelines [271].

BP/ hypertension

Hypertension was diagnosed based on past medical history and drug treatment and/or if the subjects had systolic blood pressure (SBP) of 140 mmHg or greater and/or diastolic blood pressure (DBP) of ≥ 90 mmHg [270].

General obesity

BMI was calculated as weight/(height)^2[kg/m^2]. Over-weight was defined as BMI ≥25.0–29.9 kg/m^{2}and obesity as BMI ≥ 30.0 kg/m^2.

Abdominal obesity

Abdominal/central obesity was defined as waist circumference (WC) ≥ 90 cm in men and ≥ 80 cm in women according to the IDF criteria (2006) [270].

Dyslipidemia

National Cholesterol Education Programme (NCEP-ATP) guidelines were used for definitions of dyslipidemia [272].

- *Hypercholesterolemia:* Serum cholesterol levels ≥ 200 mg/dl (≥ 5.2 mmol/liter) or drug treatment for hypercholesterolemia
- *Hypertriglyceridemia:* Serum triglyceride levels ≥ 150 mg/dl (≥ 1.7 mmol/liter) or drug treatment for hypertriglyceridemia
- *Low High-Density Lipoprotein (LDL) cholesterol:* High-density lipoprotein cholesterol levels < 40 mg/dl (< 1.04 mmol/liter) for men and < 50 mg/dl (< 1.3 mmol/liter) for women
- *High Low-Density Lipoprotein (HDL) cholesterol:* Low-density lipoprotein cholesterol levels ≥ 130 mg/dl

Metabolic syndrome

Metabolic syndrome was diagnosed according to the IDF criteria (2006) [270]. For a person to be defined as having the metabolic syndrome they must have central obesity (defined as WC ≥90 cm for males and ≥80 cm for females) and any two of the following four factors:

- Triglycerides ≥ 150 mg/dL (1.7 mmol/L) or specific treatment for this lipid abnormality
- HDL cholesterol < 40 mg/dL (1.03 mmol/L) in males < 50 mg/dL (1.29 mmol/L) in females or specific treatment for this lipid abnormality
- Blood pressure systolic BP ≥ 130 or diastolic BP ≥85 mm Hg or treatment of previously diagnosed hypertension
- Fasting plasma glucose (FPG) ≥ 100 mg/dL (5.6 mmol/L) or previously diagnosed type 2 diabetes.

2.2.6 Questionnaire and anthropometric measurements

A structured questionnaire was used to obtain data on demographic and socioeconomic parameters like education, family status, occupation, family history of metabolic diseases and income. In addition, the participants were asked to describe their dietary habits, extent of daily physical activities and sport in depth to closely observe and evaluate the living conditions.

The diet questionnaire was designed to gather information on the carbohydrate, fat and protein intake, fruit and vegetable consumption as well as the number of sugared drinks and candy. Further, the complete medical history and family history of diabetes and cardio-vascular disease was gathered. Anthropometric measurements complemented the questionnaire. The participant´s age, gender and waist circumference measure was taken. The weight, body fat, muscle mass, visceral fat and calorie intake were measured using a body analyzer (Body analyzer HBF-511B-E Omron, Mannheim, Germany). Blood pressure was recorded from the right arm of each participant. In addition, platelet count and density, white blood cell counts for eosinophils, neutrophils, basophils, monocytes and lymphocytes as well as HbA1c and hemoglobin were assessed for each participant. Capillary blood glucose was assessed using Accu-Check-Aviva glucometer and test strips (Roche, Basel, Switzerland). Finally, 12-channel resting ECG (IG ECG series 12 Channel ECG machine, International Group medical technology and electronics GmbH, Bremen, Germany) was performed.

2.2.7 Intestinal helminth infections

Intestinal helminth and protozoa infections were detected using Kato-Katz from stool samples. In detail, a single fresh stool sample was taken from each patient before treatment and 12 and 18 months after treatment. A small amount of stool sample was placed on a newspaper and covered with a small piece of nylon. Using a spatula, the sample was pressed through the nylon. The sieved stool was distributed evenly using a calibrated template for egg quantification. A methylene blue glycerol-soaked cellophane piece was placed over the stool sample. Finally, a glass slide was placed on top of the stool sample and pressed down until the writing of the newspaper can be seen through. The glass slide was removed carefully and placed under a microscope.

2.2.8 Detection of filarial infections

O. volvulus infections were assessed via two skin biopsies of 2 mm diameter at the posterior iliac crest, which were placed in a 96-well plate containing PBS. MF contained in the skin snip leaving the biopsy tissue were counted. Skin biopsies from the left and right side were taken for each participant. *M. perstans, L. loa* and other filarial infections were detected via blood prick test followed by staining and microscopy. Due to *Wuchereria bancrofti* not being endemic in the study region, a collection of blood at night was not performed.

An additional LAMP test of the skin snips and whole blood was used as a validation for skin and blood dwelling filarial infections and to determine possible co-infection [273, 274].

2.2.9 Determination of the metabolic and immunological profile

Serum was obtained from blood drawn into 5 ml serum clot activator tubes (BD Vacutainer®, Franklin lakes, NJ, USA), incubated for 20 min and centrifuged at 2000g for 10 min (Human Biochemica und Diagnostica GmbH, Wiesbaden, Germany). Participant´s serum and urine were collected at the study site and analyzed at the study coordinating center using a HumaStar200 auto-analyzer (Human Biochemica und Diagnostica GmbH, Wiesbaden, Germany). The lipid profile (cholesterol (liquicolor CHOD PAP), triglyceride (liquicolor, GPO POD), HDL (homogenous enzymatic assay) and LDL (homogenous enzymatic assay)), liver enzymes (aspartate aminotransferase (IFCC), alanine-aminotransferase (IFCC), alkaline phosphatase (IFCC), y-glutamyltransferase (IFCC, gamma glutamly-3-4-nitroanilide)), kidney function (creatinine (Jáffe), urea (Urease UV) and microalbumin (Immunoturbidimetry)), C-reactive protein (immunoturbidimetry) and glucose (GOD) was assessed using the HumaStar200 serum analyzer (Human Biochemica und Diagnostica GmbH, Wiesbaden, Germany).

Further serum analysis will be performed using custom designed Luminex ProcartaPlex assays (Thermo Fisher Scientific, Waltham, Massachusetts, USA) to investigate the cytokine and chemokine profile and metabolic status between groups and time points, e.g., upon study inclusion, 12 and 18 months after the treatment. The focus will be on an analysis and comparison of a broad range of chemokines and cytokines: Pro- and anti-inflammatory cytokines (IL-1β, IL-2, IL-5, IL-13, IFNγ, IL-9, IL-17, IL18) as well as eosinophil specific parameters like Eotaxin 1 and 2, and RANTES.

The following metabolic parameters will be assessed with ProcartaPlex (Thermo Fisher Scientific, Waltham, Massachusetts, USA): adiponectin, leptin, visfatin, resistin, plasminogen activator factor (PAI-1), pancreatic hormones (glucagon, insulin, C-peptide), gut hormones (ghrelin, gastric inhibitory polypeptide (GIP), glucagon like peptide 1 (GLP-1)) and acute-phase proteins (SAA). Multiplex assays will be performed according to the manufactures protocol.

Cytokines and chemokines will be additionally measured in the supernatant upon whole blood stimulation.

Therefore, all samples were stimulated with anti-CD28/CD49 antibodies (Biolegend®, San Diego, CA, USA, Ultra-LEAF™ purified anti-human antibody), as well as the corresponding stimuli Pam3Cys (100 ng/ml Roche, Basel, Switzerland), lipopolysaccharide from *Salmonella minnesota* (100 ng/ml, Merck, Darmstadt, Germany) or *Onchocerca ochengi* antigen (provided by Prof. Wanji, Buea, Cameroon) with and without palmitic acid (Sigma-Aldrich, ST. Louis, MI, USA) for 18 h at 37 °C and 5% CO_2. Cells were separated from the supernatant by centrifugation at 1500 g for 5 min. The supernatant was carefully removed and transferred into microdilution tubes (STARLAB International GmbH, Hamburg, Germany) and stored at -20°C. The ELISA and/or Luminex assays will be performed according to the manufacturer's protocol.

2.2.10 Human whole blood stimulation for flow cytometry

In accordance to the investigations mentioned before, flow cytometry analysis was performed for 50 participants of each group to assess and phenotype the blood immune cells and investigate prior priming due to infections or obesity. For this, a whole blood re-stimulation assay was designed during this thesis and used in Cameroon. Here, blood was collected in S-Monovette® Li-heparin tubes (Sarstedt AG & Co KG, Nürnbrecht, Germany). 100 µl whole blood was plated according to the scheme in Fig. 9. The whole blood was subsequently stimulated with anti-CD28 and anti-CD49d (1 µg/ml, Ultra-LEAF™, Biolegend, San Diego, California, USA) and additionally, either 2.5% BSA, 100 mM phytohemagglutinin (Sigma-Aldrich, Merck, Darmstadt, Germany), 100 mM palmitic acid (Sigma-Aldrich, Merck, Darmstadt, Germany) or *Onchocerca ochengi* antigen. Cells were stimulated at 37°C and 5% CO_2 for 2 hours before the addition of 0.5 mg/ml brefeldin A (Sigma-Aldrich, Merck, Darmstadt, Germany). Cells were incubated additional 14 h at the same conditions. After the incubation, cells were centrifuged at 600g for 5 min and a red blood cell lysis (Roche, Basel, Switzerland) was performed by discarding the supernatant and adding 100 µl RBC lysis to each well. The lysis was stopped after 10 min at RT by centrifugation at 600g for 5 min. The supernatant was discarded and the RBC lysis and centrifugation was repeated. Finally, the supernatant was removed, cells were washed with 180 µl PBS and again centrifuged at 600g for 5 min.

The pellet was resupended in freezing media (90% FBS and 10% DMSO) and stored at -20°C. The flow cytometry analysis has not been performed up to this point, but a proposed gating strategy for the panels was established (Fig. 24-28).

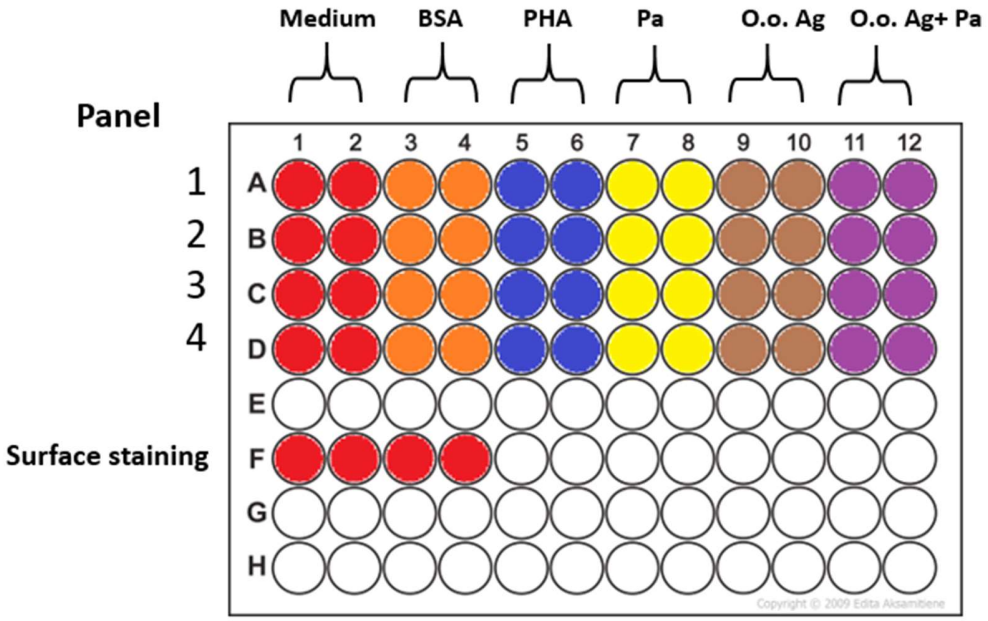

Figure 9. Flow-cytometry stimulation overview. BSA: Bovine serum albumin, PHA: phytohemagglutinin, Pa: palmitic acid. O.o Ag: *Onchocerca ochengi* antigen.

2.2.11 Human whole blood stimulation protocol for ELISA and multiplex assays

Serum samples and whole blood stimulation for ELISA were planned for all participants included in the study. The stimulation of the whole blood should determine the cytokine, chemokine and adipokine profiles after stimulation with parasite antigen, fatty acids and pro-inflammatory molecules to assess the metabolic and immunological profile of the participants. For this, a whole blood re-stimulation assay was designed during this thesis and used in Cameroon. Here, blood was collected in S-Monovette® Li-heparin tubes (Sarstedt AG & Co KG, Nürnbrecht, Germany). 100 µl whole blood was plated according to the scheme in Fig. 10. The whole blood was subsequently stimulated with anti-CD28 and anti-CD49d (1 µg/ml, Ultra-LEAF™, Biolegend, San Diego, California, USA) and additionally, either LPS (100 ng/ml, Sigma-Aldrich, Merck, Darmstadt, Germany), Pam-3-Cys (100 ng/ml, Sigma-Aldrich, Merck, Darmstadt, Germany), 100 mM palmitic

acid (Sigma-Aldrich, Merck, Darmstadt, Germany) or *Onchocerca ochengi* antigen. Cells were stimulated at 37°C and 5% CO_2 for 16 hours. After the incubation, cells were centrifuged at 600g for 5 min and the supernatant was transferred into microdilution tubes (StarLab, Hamburg, Germany) and stored at -20°C. The proof of concept was performed by stimulating human whole blood with LPS and Pam-3-Cys and TNF, IL-6 and IL-12p70 were measured after freezing using a multiplex assay (Fig. 29). In addition, the detection of adipokines in the serum was tested by detecting adiponectin and serum amyloid A in unstimulated serum samples after storage at -20°C.

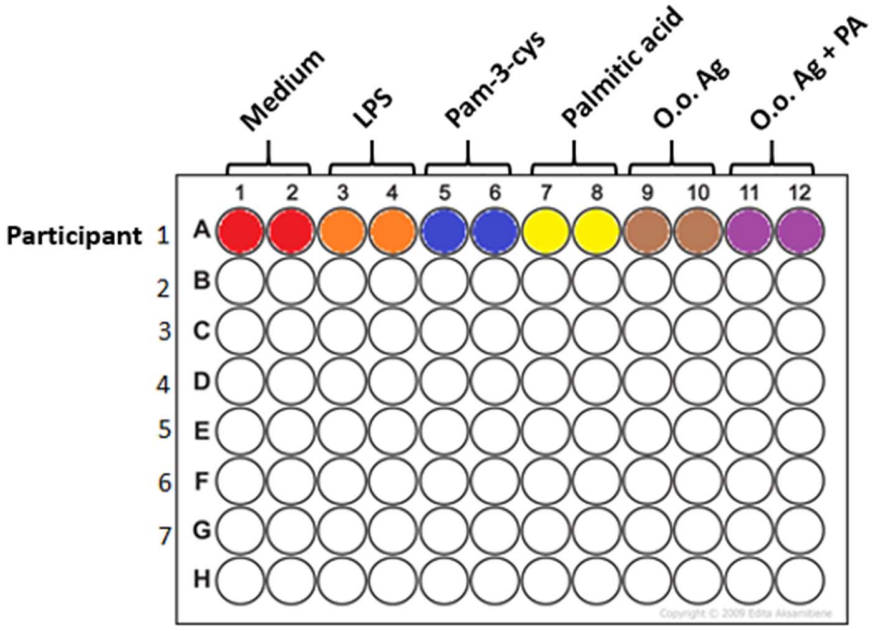

Figure 10. ELISA stimulation overview. LPS: lipopolysaccharides, Pam-3-cys: (S)-[2,3-Bis(palmitoyloxy)-(2-RS)-propyl]-N-palmitoyl-(R)-Cys-(S)-Ser-(S)-Lys_4-OH, Pa: palmitic acid. O.o Ag: *Onchocerca ochengi* antigen.

2.2.12 White blood cell analysis

The peripheral blood cell composition of all patients was investigated using the Horiba Yumizen H500 white blood cell analyzer (Horiba Europe GmbH, Wiesbaden, Germany). The device was used to measure frequencies and numbers of eosinophils, neutrophils, basophils and lymphocytes. Furthermore, platelet count and volume as well as red blood cell count and volume were analyzed.

2.2.13 Intervention protocol

Doxycycline: Individuals infected with *M. perstans* and *O. volvulus* were treated with a daily dose of 200 mg doxycycline for six weeks. Individuals with less than 50 kg body weight received 100 mg doxycycline for six weeks. Pregnancy tests were done before starting the treatment and every two weeks during the doxycycline treatment to prevent doxycycline treatment in pregnant women. Participating women were advised to use contraception measures and willingness to comply was an inclusion criterion. In case of pregnancy during doxycycline treatment, treatment was immediately to be stopped and women were to be referred to a local clinic and monitored till the end of pregnancy for potential side effects of prior doxycycline treatment.

Albendazole: All participants in this study were treated with albendazole (before the first doxycycline treatment in the respective group) to remove intestinal helminths and to complement anti-filarial therapies. Therefore, individuals received a single dose of 400 mg albendazole every three months with four treatments total.

2.2.14 Treatment efficacy

The treatment efficacy at 12 months and a potential reinfection was monitored at 18 months after treatment using skin snips, diagnostic PCR, thick blood smears and Kato-Katz.

2.2.15 Choice of comparator

Doxycycline is a macrofilaricidal drug for *Wolbachia*-containing filariae such as *O. volvulus* and *M. perstans*. Ivermectin, which is used for MDA, has no prominent macrofilaricidal efficacy. Albendazole, is the standard drug used for intestinal helminths. Therefore, doxycycline and albendazole are justified as comparators.

2.2.16 Recruitment

The study site population was familiarized with the study by social scientists before the screening started. The sensitization included study advertisement and clear depiction of the participation benefits and risks as well as the location of the study centers. A comprehensive pre-screening of the study sites was performed. 4000 participants were screened for their infection status to ensure sufficient numbers of filariasis patients. Participants were allocated into their respective groups using the measured BMI and infection status. Sensitization, screening, enrollment and follow-up was performed by the field team from Prof. Wanji, which includes social scientists, parasitologists, nurses, medical doctors and drivers.

2.2.17 Retention plan

Participant retention was promoted by providing albendazole treatments every three months and connecting the 12 months albendazole treatment with the 12-months follow-up and therefore giving increased incentive to participate. In addition, the free medical examination, ECG, white blood cell counts, fasting blood glucose and biochemistry test were provided as an additional incentive. Further, a free meal was provided for all attending participants, due to the fasting requirement. Potential outcomes for the participants are listed in the table 4.

Table 4. Trial variables and predicted outcomes.

Variable/Outcome	Hypothesis	Parameters measured
Primary Outcome	Quantitative change in insulin resistance (HOMA-IR) in lean, overweight and obese participants before and after treatment of *O. volvulus, M. perstans* and *L. loa* infection	HOMA-IR (blood glucose, insulin)
Secondary Outcome	• Infection with *O. volvulus, L. loa* or *M. perstans* reduce risk factors to develop type 2 diabetes • Type 2 diabetes is negatively associated with filarial infection • Co-infections have additional effects on the metabolic and immunological parameters • There is an adverse impact on the metabolic and immunological profile 12 and 18 months after treatment of filarial infection • Reinfection changes the metabolic and immunological profile	Microfilariae counts, HbA1c, waist circumferences, fasting blood glucose, LDL, HDL, ALP, AST, yGT, ALP, GOP, GTP, CRP, triglyceride, cholesterol, creatinine, HbA1c, adipokines and cytokines, treatment success, white blood cells, blood pressure, egg count in stool, risk factors according to questionnaire

	• Clearance of the adult filariae (*O. volvulus, M. perstans*) by doxycycline treatment abolishes the protective effects of *O. volvulus* and *M. perstans* infection	
Sub-Group Analysis	Sex and age, food intake, living condition, income, physical activity significantly impact the metabolic profile	Demographic data, participant data obtained via the questionnaire

2.2.18 Data management and statistical analysis

High level of confidentiality was ensured to safeguard the personal information of the study participants and other data. Such information is made accessible only to authorized personnel and the study's principal investigators. All data collected in the paper CRF is stored under strict confidentiality and entered electronically in the data collection program REDCap (https://www.project-redcap.org/, REDCap Consortium Emory University, Atlanta, USA) [275, 276] and verified by double data entry. The paper CRF are stored in locked rooms in the central laboratory at the study site. All statistical analysis was performed using SPSS version 16.0 software. Hard copies like questionnaires and ECG results are stored for 15 years and password-protected electronic databases for 35 years. Missing data was excluded from the primary evaluation. The study's principal investigators as well as the data management team are able to access the collected trial data.

2.2.19 Primary outcome assessment

The primary outcome of this study is the quantitative change in insulin resistance (HOMA-IR) in lean, overweight and obese participants before and after treatment of their respective filarial infection. Comparisons will be made using two-sided hypotheses with $\alpha = 0.05$ under the assumption that filarial infection improves insulin resistance and treatment of filarial infections will reduce their protective effect and increase the risk to develop insulin resistance. The statistical test used is the two-sided Fisher's Exact Test or Chi-squared test. Additionally, 95% confidence intervals will be calculated using the recommended method by Altman [277].

2.2.20 Statistics for secondary outcome measures

Descriptive statistics such as median, 95% confidence intervals and interquartile range were calculated for all continuous variables and percentages for all categorical variables from all participants. Multiple comparisons were performed using Kruskal-Wallis followed by Dunn´s posthoc test. Two groups were compared using the Mann-Whitney-U test. For assessments of differences over time in one group (i.e. comparison to baseline values) either a paired t-test (normally distributed variables) or a Wilcoxon-signed-rank test will be used for continuous variables and the McNemar-test for related variables. 95% confidence intervals for mean, median or proportions will be calculated where appropriate. Categorical variables will be analyzed for differences between infected and uninfected individuals utilizing Fisher's Exact tests.

2.2.21 Model to analyze pre-post change

To evaluate if treatment of filarial infections reduces a potential effect on HOMA-IR, the pre-post change of the respective groups will be analyzed. Therefore, the individual change will be assessed for each treated participant at 12 and 18 months post treatment and will be aggregated for each group as reliable individual change. The reliable individual change will be reported together with standard effect size calculations [278]. The sample size calculation will be evaluated using a pre-post-control design [279].

3. Results

3.1 Establishing a mouse model for tropical pulmonary eosinophilia

3.1.1 Microfilariae are rapidly cleared from peripheral blood and retained in the lung tissue of TPE mice in an eosinophil-dependent manner

TPE is a rare but fatal complication of LF that occurs in approximately 1% of cases. MF are trapped within the lung tissue of patients, leading to eosinophilia and subsequent eosinophilic infiltration and tissue damage. The disease is classified as a type 2 hyper-sensitivity reaction with increased total and parasite-specific IgE and the formation of a type 2 associated immune response including the cytokines IL-4 and IL-5. The first aim of this thesis was establishing a mouse model for TPE using *L. sigmodontis* and using said model to investigate immunological processes and mechanisms of MF-derived lung pathology with a focus on the role of eosinophils. The capacity of *L. sigmodontis* MF to induce TPE like symptoms, i.e., amicrofilaremia, eosinophilia, increased total and parasite-specific IgE, a concomitant type 2 immune response, was assessed in WT BALB/c and an eosinophil-deficient mouse strain with BALB/c background (dblGATA).

Adapting the protocol from Egwang and Kazura et al. for the *B. malayi* TPE mouse model, 10^5 dead MF (killed by freezing) were injected subcutaneously three times in weekly intervals into the neck fold of WT BALB/c or dblGATA mice (sensitization phase) [75]. After a gap week, mice were challenged intravenously with 10^5 living and motile MF. Mice were sacrificed 24 h after the challenge and MF clearance from the blood, retention in the lung, lung cell count and immune cell composition of the lung was analyzed using flow cytometry (Fig. 11, Fig. 12A).

Sensitized and challenged mice (TPE group) displayed similar blood MF numbers 1 h after injection (Suppl. Fig. 2) and significantly lower blood MF numbers after 24 h than control mice with no prior sensitization (MF group) (Fig. 12B). Fittingly, fully sensitized mice displayed increased retention of MF within the lung tissue (Fig. 12C) compared to mice only receiving the final MF challenge without prior sensitization. Interestingly, absence of eosinophils impaired the MF clearance from the blood and partly abolished the MF retention in the lung (Fig. 12B-C). Accordingly, TPE mice showed increased cell counts in the dissociated lung tissue compared to naïve, MF challenged and eosinophil-deficient dblGATA TPE mice (Fig. 12D). Flow cytometry analysis of the lung cell composition showed no differences in ILC2s 24 h after the injection (Fig. 12E).

The frequency of AAMs was significantly increased in TPE mice compared to dblGATA TPE mice (Fig. 12F). Further, eosinophil frequencies were significantly increased in mice receiving only MF once as well as in TPE mice (Fig. 12G). In contrast, neutrophil and alveolar macrophage frequency was only increased in dblGATA TPE mice compared to TPE mice (Fig. 12H-I). Finally, monocytes increased in both TPE and dblGATA TPE mice (Fig. 12J). Analysis of the serum revealed increased IL-5 levels in TPE mice compared to naïve, MF- challenged and dblGATA TPE mice (Fig. 12K). In contrast, IFNγ levels were highest in MF-challenged mice (Fig. 12L). Furthermore, TPE mice and dblGATA TPE mice to a lesser extent, showed high levels of total and parasite-specific IgE compared to naïve and MF-challenged mice (Fig. 12M-N). Taken together, retention of MF in the lung tissue was observed in TPE mice. This was dependent on eosinophils and was accompanied by increased serum IL-5 as well as total and *L. sigmodontis*-specific IgE levels 24 h after MF challenge.

These findings suggest that repeated sensitization with MF of *L. sigmodontis* leads to enhanced retention of MF within the lung tissue, lung eosinophilia and increased serum IgE and IL-5. Further, eosinophil-deficient dblGATA mice showed impaired retention of the MF in the lung, indicating that MF-retention might be partially dependent on eosinophils.

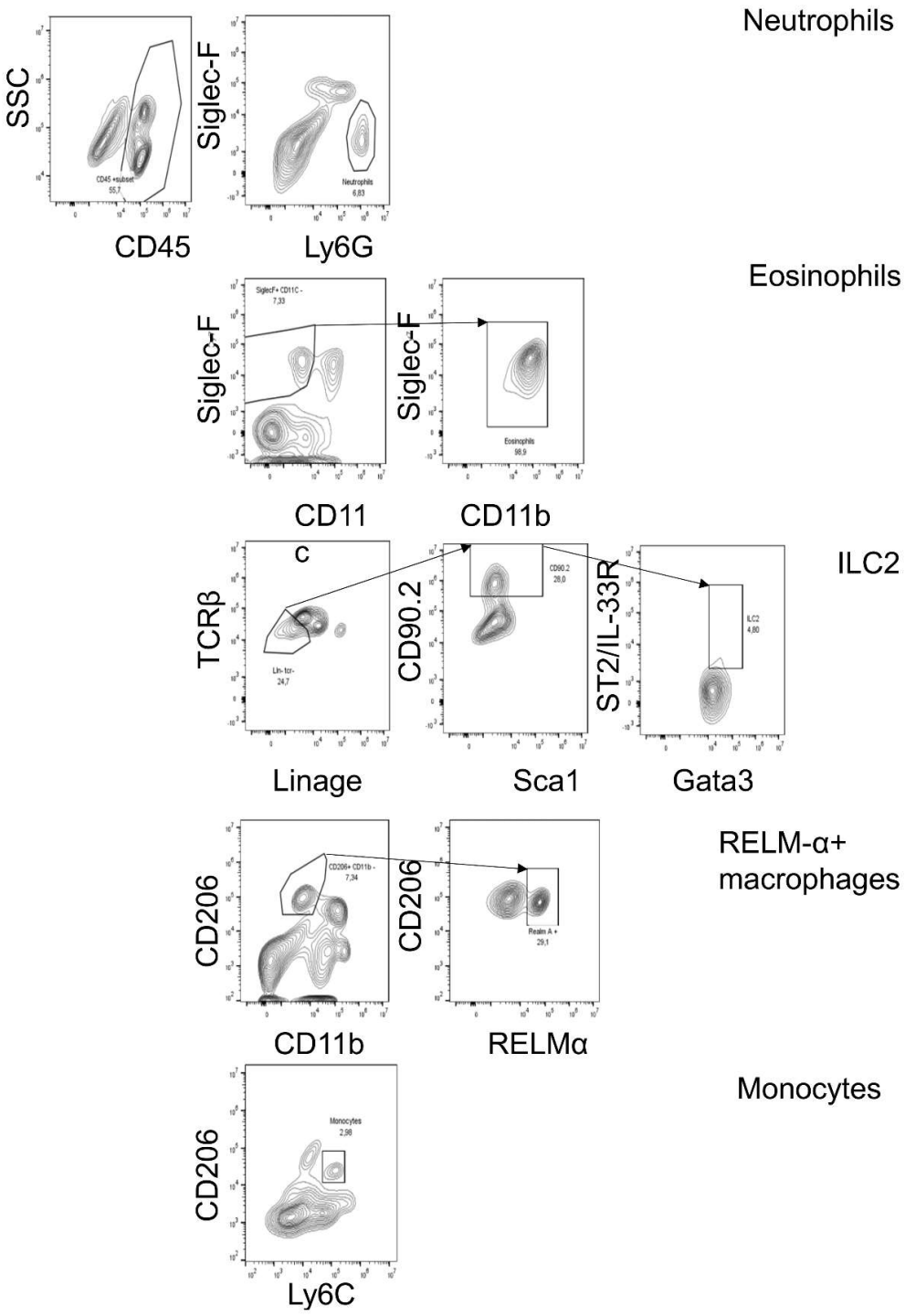

Figure 11. Gating strategy of lung cells. Neutrophils ($CD45^+$, $Ly6G^+$), eosinophils ($CD45^+$, $CD11c^-$, $Siglec\text{-}F^+$, $CD11b^+$), ILC2s ($CD45^+$, $linage^-$, $TCRb^-$, $CD90.2^+$, $GATA3^+$, $ST2^+$) and macrophages, i.e., AAM ($CD45^+$, $CD11b^-$, $CD206^+$, $RELM\text{-}\alpha^+$), alveolar macrophages ($CD45^+$, $CD11c^+$, $CD206^+$, $Siglec\text{-}F^+$) and monocytes ($CD45^+$, $Ly6C^+$, $CD206^{low}$, $Siglec\text{-}F^-$) were gated as shown in dissociated lung tissue of naïve, MF-challenged, TPE and dblGATA TPE mice.

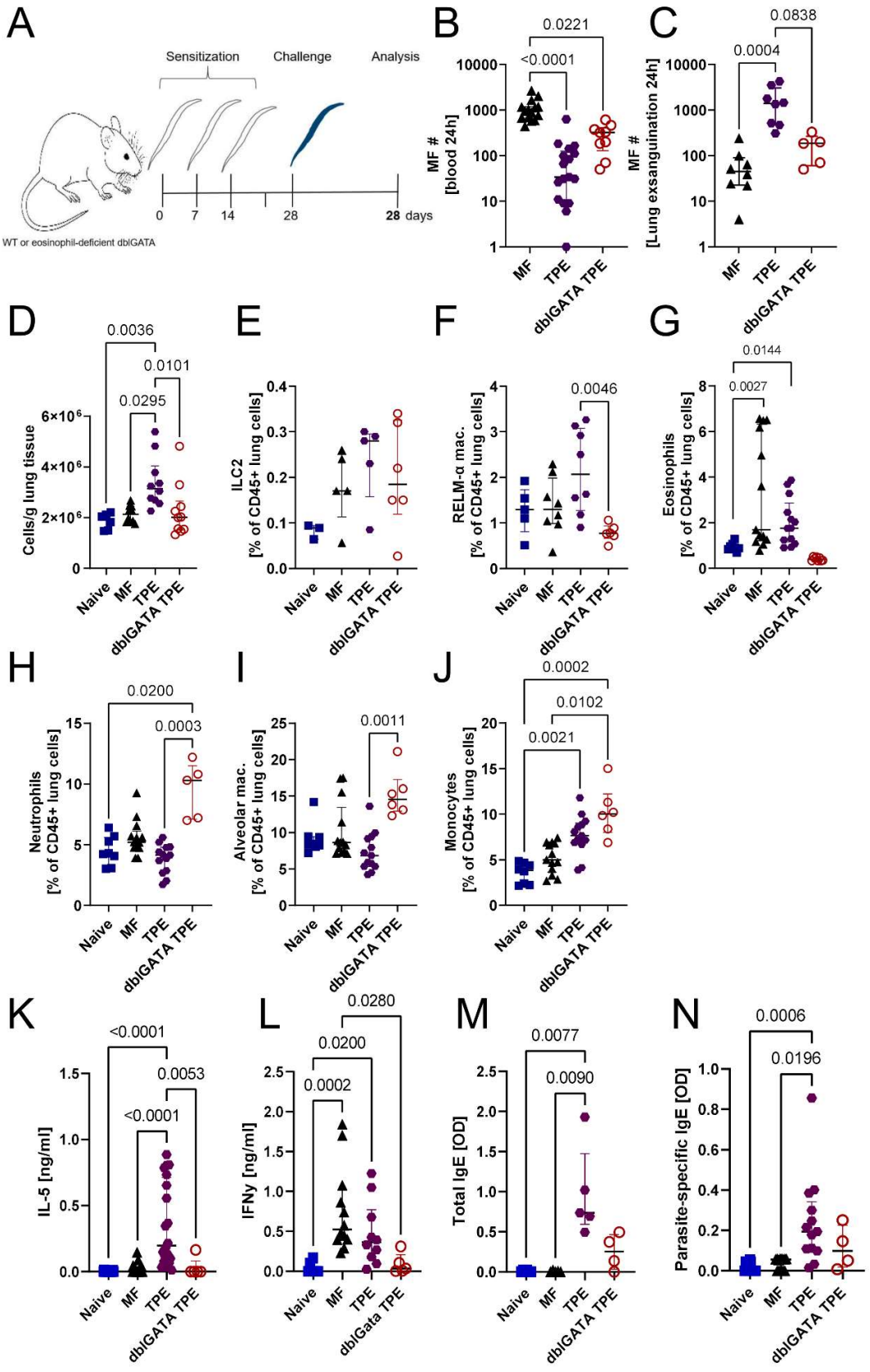
A
Sensitization
Challenge
Analysis
0
7
14
28
28 days
WT or eosinophil-deficient dblGATA
B
MF # [blood 24h]
0.0221
<0.0001
C
MF # [Lung exsanguination 24h]
0.0838
0.0004
MF
TPE
dblGATA TPE
D
Cells/g lung tissue
0.0036
0.0101
0.0295
E
ILC2 [% of CD45+ lung cells]
F
RELM-α mac. [% of CD45+ lung cells]
0.0046
G
Eosinophils [% of CD45+ lung cells]
0.0144
0.0027
Naive
H
Neutrophils [% of CD45+ lung cells]
0.0200
0.0003
I
Alveolar mac. [% of CD45+ lung cells]
0.0011
J
Monocytes [% of CD45+ lung cells]
0.0002
0.0102
0.0021
K
IL-5 [ng/ml]
<0.0001
0.0053
<0.0001
L
IFNγ [ng/ml]
0.0280
0.0200
0.0002
dblGata TPE
M
Total IgE [OD]
0.0077
0.0090
N
Parasite-specific IgE [OD]
0.0006
0.0196

Figure 12. Sensitized mice display eosinophilia as well as increased MF retention in the lung and decreased blood MF numbers. (A) Experimental design. Wild-type TPE and eosinophil-deficient dblGATA TPE mice were sensitized with dead MF and challenged with viable MF two weeks later. Controls received solely the MF challenge (MF) or remained naïve. Analyses were performed one day after MF challenge. (B) Number of microfilariae (MF) in 50 µl of peripheral blood 24 h after challenge injection and (C) exsanguinated from the lung of TPE WT and eosinophil-deficient dblGATA mice as well as MF only challenged mice (MF). (D) Total cell count/g lung tissue. Cell frequencies of (E) ILC2s ($CD45^+$, $linage^-$, $TCRb^-$, $CD90.2^+$, $ST2^+$, $GATA3^+$), (F) RELM-α positive macrophages ($CD45^+$, $CD206^+$, $Siglec\text{-}F^+$, $RELM\text{-}\alpha^+$), (G) eosinophils ($CD45^+$, $CD11c^-$, $Siglec\text{-}F^+$, $CD11b^+$), (H) neutrophils ($CD45^+$, $Ly6G^+$), (I) alveolar macrophages ($CD45^+$, $CD206^+$, $Siglec\text{-}F^+$), (J) monocytes ($CD45^+$, $Siglec\text{-}F^-$, $CD11c^+$, $ly6C^+$) in the $CD45^+$ lung cell fraction. Serum (K) IL-5, (L) IFNy, (M) total IgE and (N) parasite-specific IgE levels. Data is pooled from 1-3 independent experiments with a total of n=5-18 animals per group and shown as median with interquartile range. Statistical analysis was performed with Kruskal-Wallis followed by Dunn´s multiple comparison test. P values ≤ 0.05 are shown.

3.1.2 TPE induction leads to an increased type 2 immune response and eosinophil activation

Due to the eosinophil-dependent MF retention within the lung tissue 24 h after the MF challenge, a later time point (10 days post challenge) was analyzed to monitor the development of the immune response in the lung, broncho-alveolar lavage (BAL) and spleen (Fig. 13A). TPE WT mice had significantly increased cells in the lung compared to naïve and MF challenged mice (Fig. 13B). The frequency of ILC2s was significantly increased only in TPE but not dblGATA TPE mice compared to naïve controls and MF-challenged mice (Fig. 13C). Similarly, TPE mice had increased AAM frequencies compared to naïve and dblGATA TPE mice (Fig. 13D), indicating that eosinophils, which were significantly increased in TPE mice 10 days after challenge (Fig. 13E), might play a role in maintaining or inducing ILC2s and AAM within the lung. In contrast, neutrophil frequencies increased in both TPE and dblGATA TPE mice compared to naïve mice (Fig. 13F). Finally, alveolar macrophages were not altered 10 days after the challenge and monocytes were only increased by trend ($p = 0.0507$) in TPE mice (Fig. 13G-H).

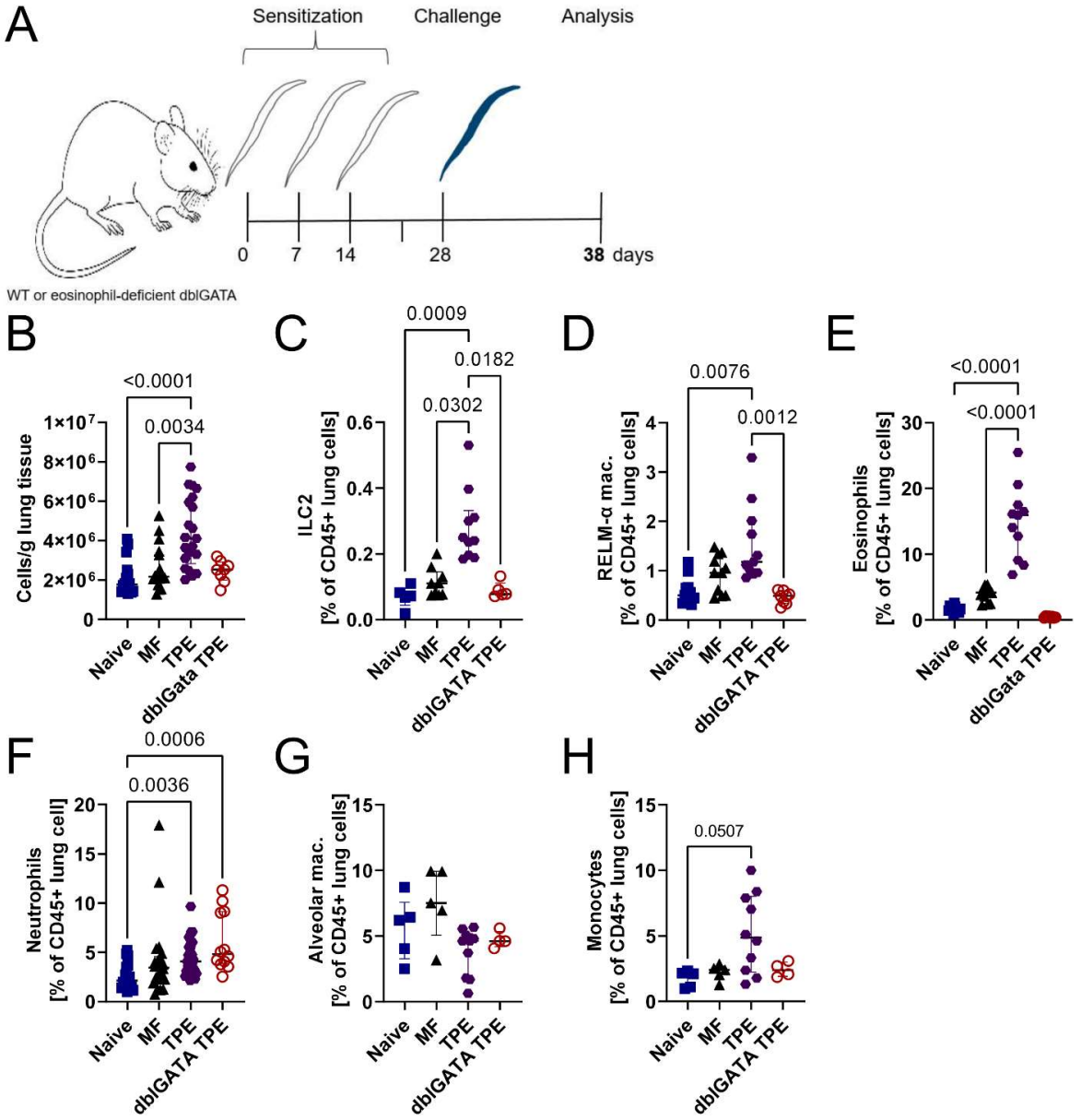

Figure 13. TPE mice display a strong type 2 immune response and eosinophilia in the lung. (A) Experimental design. WT TPE and eosinophil-deficient dblGATA TPE mice were sensitized with dead MF and challenged with viable MF two weeks later. Controls received the MF challenge (MF) or remained naïve. Analyses were performed ten days after MF challenge. (B) Total cell count per g of lung tissue for naïve, MF only challenged, as well as WT TPE and dblGATA TPE mice. Frequencies of (C) ILC2s ($CD45^+$, $linage^-$, $TCRb^-$, $CD90.2^+$, $ST2^+$, $GATA3^+$), (D) RELM-α positive macrophages ($CD45^+$, $CD206^+$, $Siglec\text{-}F^+$, $RELM\text{-}\alpha^+$), (E) eosinophils ($CD45^+$, $CD11c^-$, $Siglec\text{-}F^+$, $CD11b^+$), (F) neutrophils ($CD45^+$, $Ly6G^+$), (G) alveolar macrophages ($CD45^+$, $CD206^+$, $Siglec\text{-}F^+$), and (H) monocytes ($CD45^+$, $Siglec\text{-}F^-$, $CD11c^+$, $ly6C^+$) in the $CD45^+$ lung cell fraction. Data is pooled from 1-3 independent experiments with a total of n=6-18 animals per group. Data is shown as median with interquartile range. Statistical analysis was performed with Kruskal-Wallis followed by Dunn´s multiple comparison test. P values ≤ 0.06 are shown.

Lung eosinophils from TPE mice were characterized by a significantly elevated expression of CD11b, Siglec-F and CD86 as well as the ST2/IL-33 receptor (Fig. 14A-H). Spleen and BAL analysis revealed increased splenocyte numbers (Fig. 15A) and increased eosinophil frequencies in the spleen and BAL (Fig. 15B-C). In addition, AAM frequency increased in the BAL and eosinophils expressed significantly higher levels of CD11b and CD86 (Fig. 15D-F).

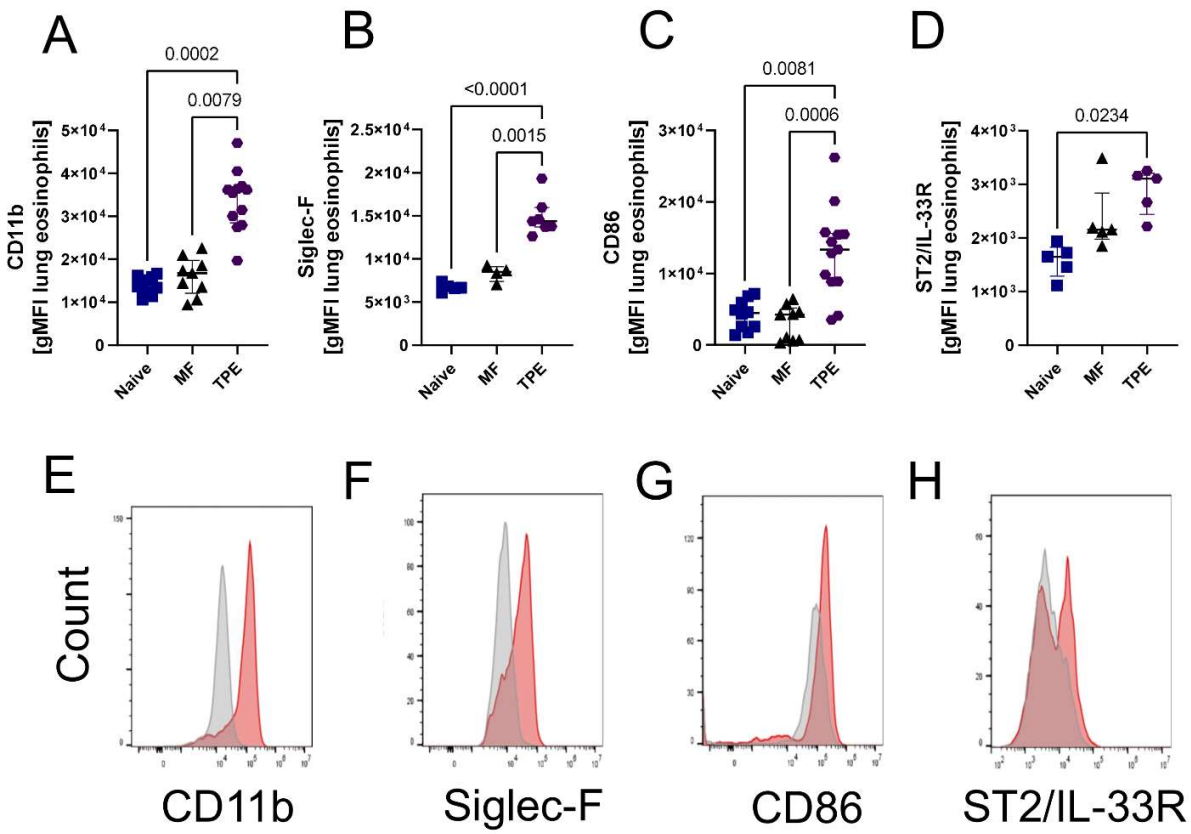

Figure 14. Lung eosinophils are highly activated during TPE. Geometric mean of the fluorescence intensity (gMFI) of (A) CD11b, (B) Siglec-F, (C) CD86 and (D) ST2/IL-33R of lung eosinophils isolated from WT TPE mice, mice solely challenged with MF (MF) or naïve animals. (E-H) Representative histograms comparing eosinophils from naïve (grey) and TPE mice (red). (A-D) Data is pooled from 1-3 independent experiments with a total of n=5-13 mice per group. Data is shown as median with interquartile range. Statistical analysis was performed with Kruskal-Wallis followed by Dunn´s multiple comparison test. P values ≤ 0.05 are shown.

Serum and BAL fluid analysis by ELISA showed elevated serum IL-33 and IL-4 in TPE mice compared to naïve mice (Fig. 16A-B). In contrast to 24 h after the challenge, serum IL-5 and IFNγ were below the detection limit in TPE mice (Fig. 16C-D).

However, total and parasite-specific IgE were still significantly increased in TPE mice and dblGATA TPE mice albeit to a lesser extent (Fig. 16E-F). Interestingly, extracellular DNA measured in the BAL fluid and the pleura wash was significantly elevated in TPE but not dblGATA TPE mice (Fig. 16G-H).

The level of IL-9 in the BAL was increased in all mice receiving the MF challenge, but did not statistically significantly differ in TPE and dblGATA TPE mice compared to naïve controls or animals receiving only the MF challenge (Fig. 16I). BAL IL-4 was elevated in mice challenged with MF and TPE mice but not dblGATA TPE mice while IL-17A was below the detection limit in all cases except for half of the TPE mice (Fig. 16J, K).

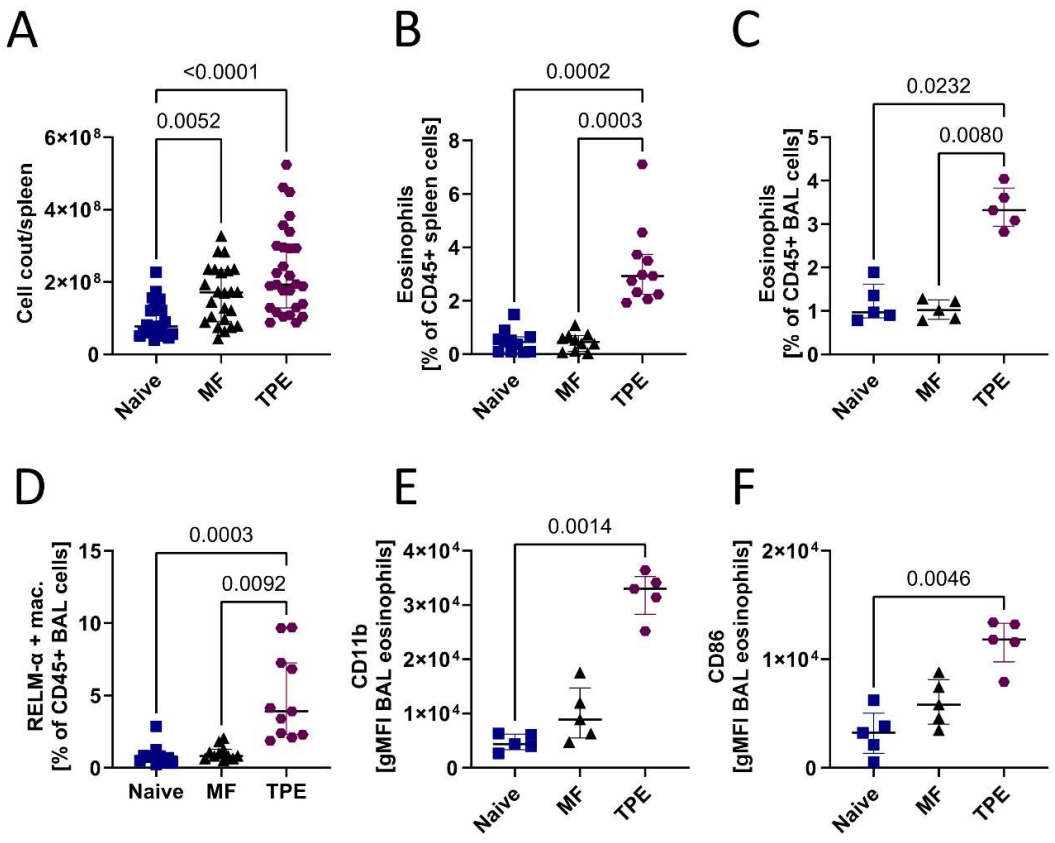

Figure 15. TPE induces eosinophil accumulation in the spleen and BAL. (A) Spleen cell count for naïve, MF only challenged and TPE mice. Frequency of (B) spleen and (C) BAL eosinophils ($CD45^+$, $CD11c^-$, $Siglec\text{-}F^+$, $CD11b^+$) and (D) BAL RELM-α positive macrophages ($CD45^+$, $CD206^+$, $Siglec\text{-}F^+$, $RELM\text{-}\alpha^+$), frequencies in naïve, challenged or TPE mice. (E-F) Geometric mean fluorescence intensity of (E) CD11b and(F) CD86 of BAL eosinophils. Data is pooled from 1-3 independent experiments with a total of n=4-25 mice. Median with interquartile range and Kruskal-Wallis test followed by Dunn´s multiple comparison. P values ≤ 0.05 are shown.

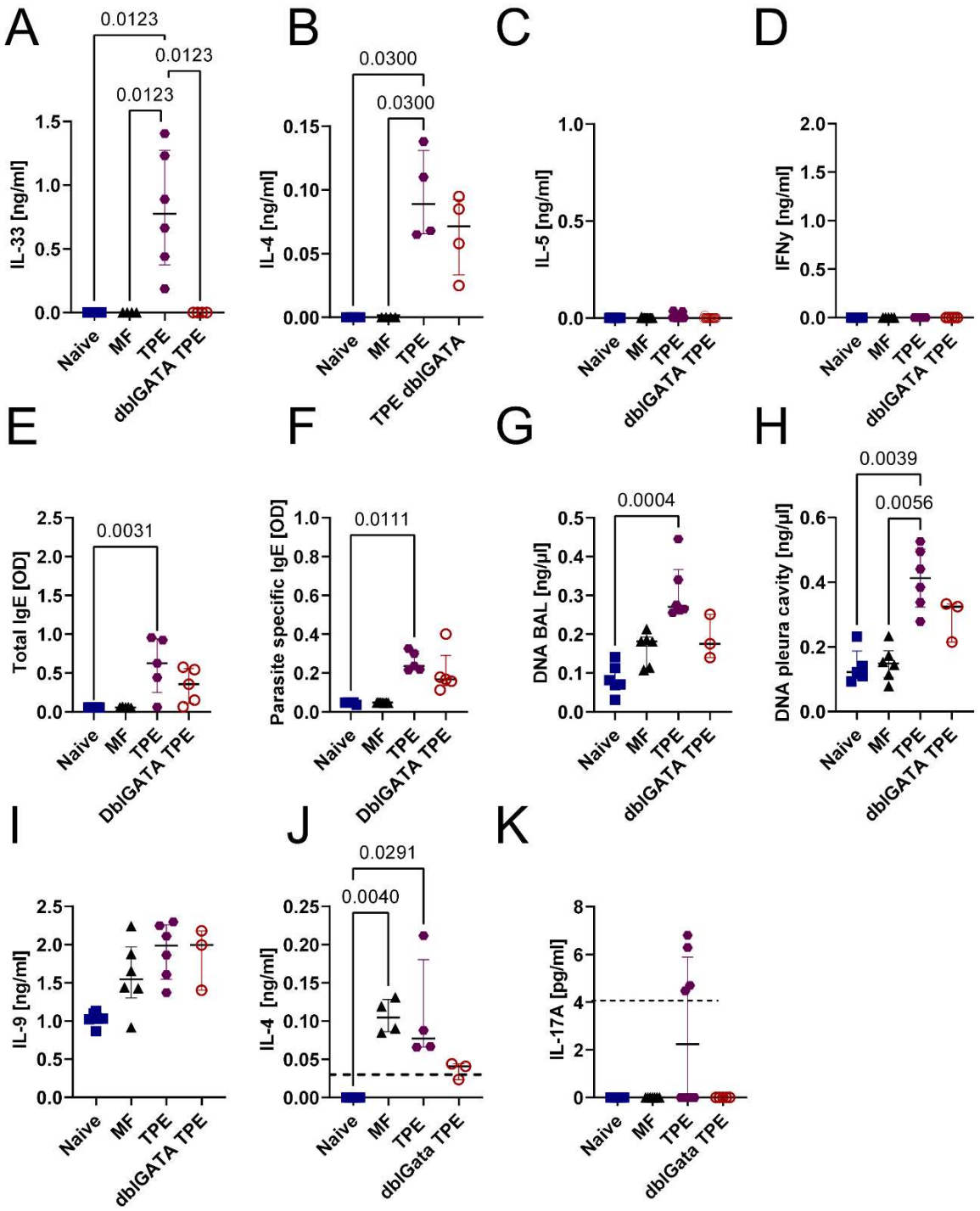

Figure 16. TPE mice display increased serum IL-33 and IL-4. Serum (A) IL-33 and (B) IL-4, (C) IL-5, (D) IFNγ, (E) total and (F) parasite-specific IgE and (G) BAL DNA, (H) pleura DNA, BAL (I) IL-9, (J) IL-4 and (I) IL-17A of naïve, MF only challenge (MF), sensitized and challenged WT (TPE) and eosinophil deficient dblGATA mice (dblGATA TPE) 10 days after the final challenge. Data from 1 experiment with n=4-6 mice, data shown as median with interquartile range. Statistical analysis with Kruskal-Wallis test followed by Dunn´s multiple comparison test. P values ≤ 0.05 are shown.

Interestingly, mice showed hemorrhages in the lung tissue in some cases after 10 days of MF challenge (Fig. 17). Naïve mice had no hemorrhages while 3/15 MF challenged mice (20%), 8/20 TPE mice (40%) and 3/8 dblGATA TPE mice (37.5%) displayed bloody spots at the inferior part of the lung (Fig. 17A-D). These hemorrhages increased in visibility after lung perfusion (Fig. 17E-F). Taken together, 10 days after the challenge, TPE mice displayed eosinophilia in the lung tissue, spleen and BAL. Further, lung and BAL eosinophils were highly activated. The immune response consisting of ILC2s, AAM together with IL-4 indicates a type 2 immune response. AAM and ILC2s were significantly decreased in frequency in eosinophil deficient dblGATA mice. Interestingly, serum IL-33 was significantly elevated in TPE but not dblGATA TPE mice, indicating eosinophils might play a role in IL-33 signaling and release. In line, eosinophils from dblGATA mice displayed significantly higher expression of the IL-33 receptor ST2.

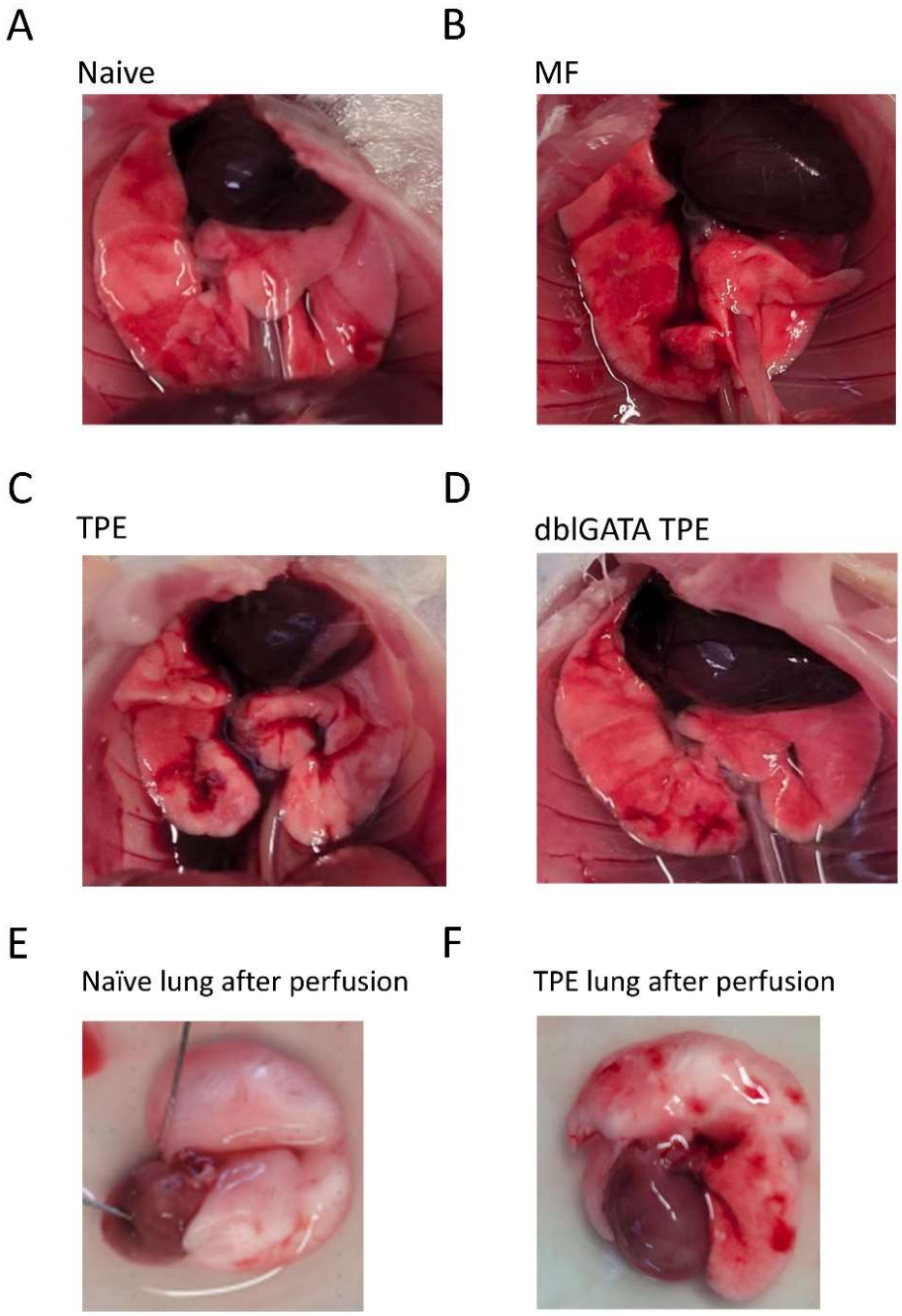

Figure 17. TPE mice develop lung hemorrhages. Lungs of (A) naïve, (B) MF only challenged (MF), (C) TPE and (D) dblGATA TPE mice 10 days after the challenge. (E-F) Images of lungs from (E) naïve and (F) TPE mice after perfusion.

3.1.3 Treatment of TPE mice

Diethylcarbamazine (DEC) is the standard treatment for TPE. To further verify the *L. sigmodontis* TPE model and assess the capability to test new treatment options of human TPE, TPE mice were treated with either 50 mg/kg DEC (once a day, QD), 36 mg/kg corallopyronin A (CorA) (QD), 12.5 mg/kg oxfendazole (OXF) (twice a day, BID) or a vehicle (QD) for 5 days starting 3 days after the final MF challenge.

Lung cell counts decreased significantly after CorA ($p = 0.0014$) and DEC treatment by trend ($p=0.0556$) but not after OXF treatment (Fig. 18A). Further, DEC treated animals had significantly decreased lung ILC2 and slightly reduced AAM frequencies when compared to TPE mice receiving only the vehicle. This reduction was not as prominent when mice were treated with OXF or CorA (Fig. 18B-C). Furthermore, the frequency of alveolar macrophages decreased only upon DEC treatment (Fig. 18D). All TPE mice displayed significantly increased frequencies of eosinophils in comparison to the MF-only control (Fig. 18E). TPE mice that were treated with CorA had the highest frequency of eosinophils while TPE mice treated with the vehicle and DEC showed comparable elevation of eosinophil frequencies and OXF treated mice displayed a minor but not statistical significant decrease of eosinophils in the lung tissue compared to the MF-only control (Fig. 18E). Neutrophil frequencies were not significantly different between the respective treatments (Fig. 1.8F). Lastly, lung eosinophils of vehicle treated animals expressed significantly higher levels of CD54 (Fig. 18G) and elevated expression of CD86 ($p=0.0505$, Fig. 18H) when compared to MF challenged animals. A similar trend was observed for eosinophils of mice that received DEC, OXF and CorA. These results suggest that treatment of TPE mice with DEC reduces lung ILC2 frequencies which could indicate a decrease of TPE-like immune responses after treatment.

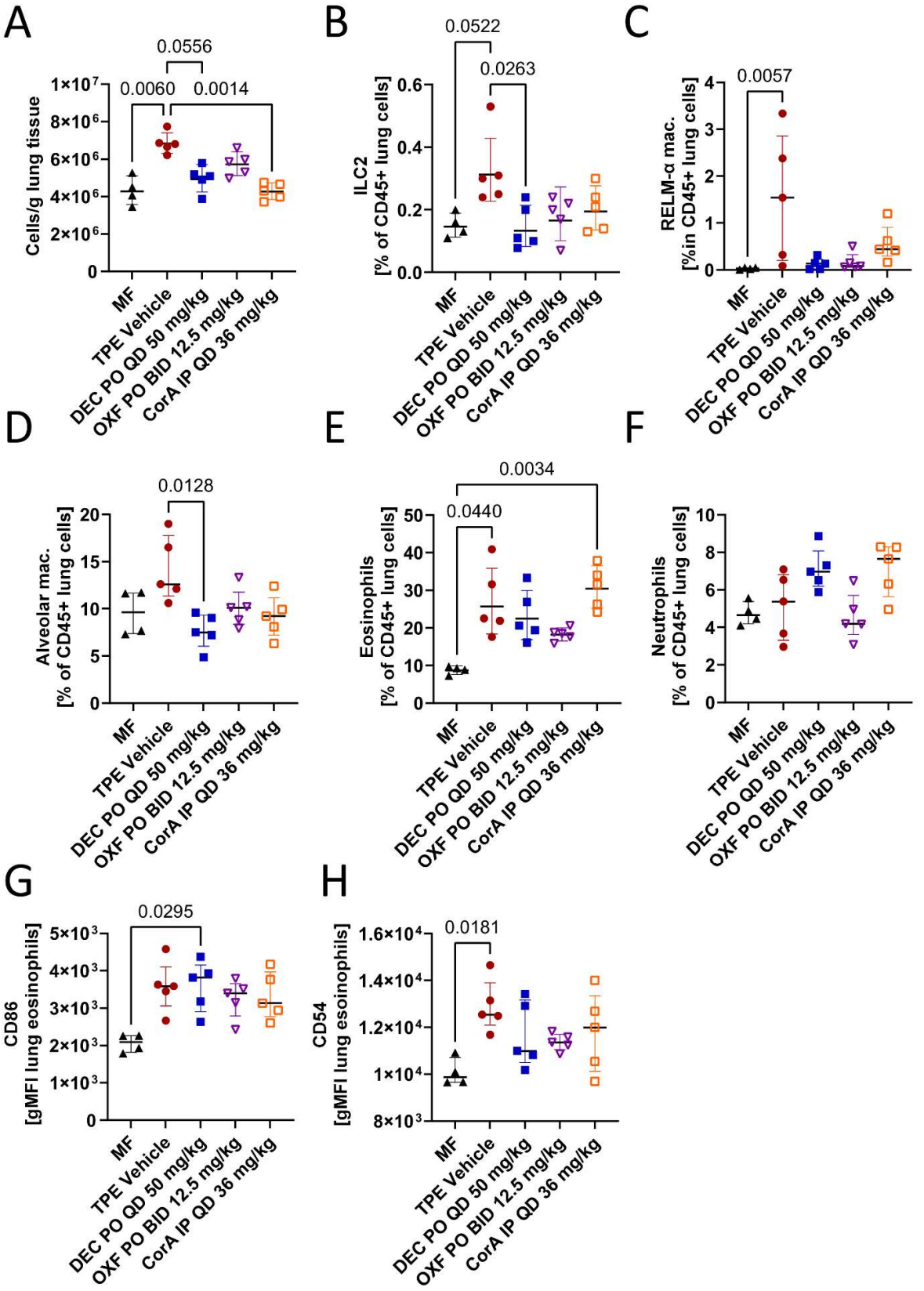
A
0.0556
0.0060
0.0014
Cells/g lung tissue
1×10^7
8×10^6
6×10^6
4×10^6
2×10^6
0
B
0.0522
0.0263
ILC2
[% of CD45+ lung cells]
0.6
0.4
0.2
0.0
C
0.0057
RELM-α mac.
[%in CD45+ lung cells]
4
3
2
1
0
D
0.0128
Alveolar mac.
[% of CD45+ lung cells]
20
15
10
5
0
E
0.0034
0.0440
Eosinophils
[% of CD45+ lung cells]
50
40
30
20
10
0
F
Neutrophils
[% of CD45+ lung cells]
10
8
6
4
2
0
G
0.0295
CD86
[gMFI lung eosinophils]
5×10^3
4×10^3
3×10^3
2×10^3
1×10^3
0
H
0.0181
CD54
[gMFI lung esoinophils]
1.6×10^4
1.4×10^4
1.2×10^4
1×10^4
8×10^3
MF
TPE Vehicle
DEC PO QD 50 mg/kg
OXF PO BID 12.5 mg/kg
CorA IP QD 36 mg/kg

Figure 18. Treatment of TPE mice with DEC, oxfendazole and corallopyronin A. (A) Lung cell count of mice receiving the MF challenge (MF) as well as TPE mice receiving 50 mg/kg DEC (QD), 36 mg/kg CorA (QD), 12.5 mg/kg OXF (BID) or a vehicle (QD) for 5 days in the morning (QD) or morning and 8 h later (BID). Frequencies of lung (B) ILC2s ($CD45^+$, $linage^-$, $TCRb^-$, $CD90.2^+$, $ST2^+$, $GATA3^+$), (C) RELM-α positive macrophages ($CD45^+$, $CD206^+$, $Siglec\text{-}F^+$, $RELM\text{-}\alpha^+$), (D) alveolar macrophages ($CD45^+$, $CD206^+$, $Siglec\text{-}F^+$), (E) eosinophils ($CD45^+$, $CD11c^-$, $Siglec\text{-}F^+$, $CD11b^+$), (F) neutrophils ($CD45^+$, $Ly6G^+$, $Ly6C^+$) of mice receiving the MF challenge (MF) as well as TPE mice receiving 50 mg/kg DEC (QD), 36 mg/kg CorA (QD), 12.5 mg/kg OXF (BID) or a vehicle (QD). (G-H) Geometric mean fluorescence intensity of CD86 (G) and CD54 (H) of lung eosinophils. Data from 1 experiment with n=5-6 mice. Statistical analysis with Kruskal-Wallis test followed by Dunn´s multiple comparison test. P values ≤ 0.06 are shown.

3.1.4 IL-33 activates eosinophils *in vitro* in a concentration-dependent manner

Lung eosinophils from TPE mice displayed increased expression of the IL-33 receptor ST2 (Fig. 14D) and TPE mice had significantly elevated IL-33 serum levels (Fig. 16A). Thus, in a first step, a potential impact of IL-33 on eosinophils was investigated by stimulating 10^5 bone marrow-derived eosinophils with different concentrations of IL-33 (0.1, 0.01 and 0.001 µg/ml).

The activation status of eosinophils after 24 h of culture with the respective IL-33 concentrations was measured using flow cytometry (Fig. 19). Eosinophils stimulated with 0.1 µg/ml IL-33 displayed significantly increased expression of CD11b, CD54, CD86, CD107a, MHC2, and ST2 in comparison to unstimulated cells (Fig. 19A-C, E-F, H). The expression of the aforementioned markers increased in a concentration dependent manner. In contrast, Siglec-F and CD101 showed only a minor increase when eosinophils were stimulated with 0.1 µg/ml that was, however, not statistically significant (Fig. 19D, G). Further, eosinophils stimulated with 0.1 µg/ml IL-33 released significantly more DNA compared to unstimulated eosinophils (Fig. 19I). These findings indicate that IL-33 induces the expression of CD11b, CD54, CD86, CD107a, MHC2 and ST2 *in vitro* and increases DNA release of eosinophils in a concentration-dependent manner. These findings imply that IL-33 can directly activate eosinophils *in vitro* and might promote adhesion (CD11b, CD54), antigen presentation (MHC2) and the release of DNA.

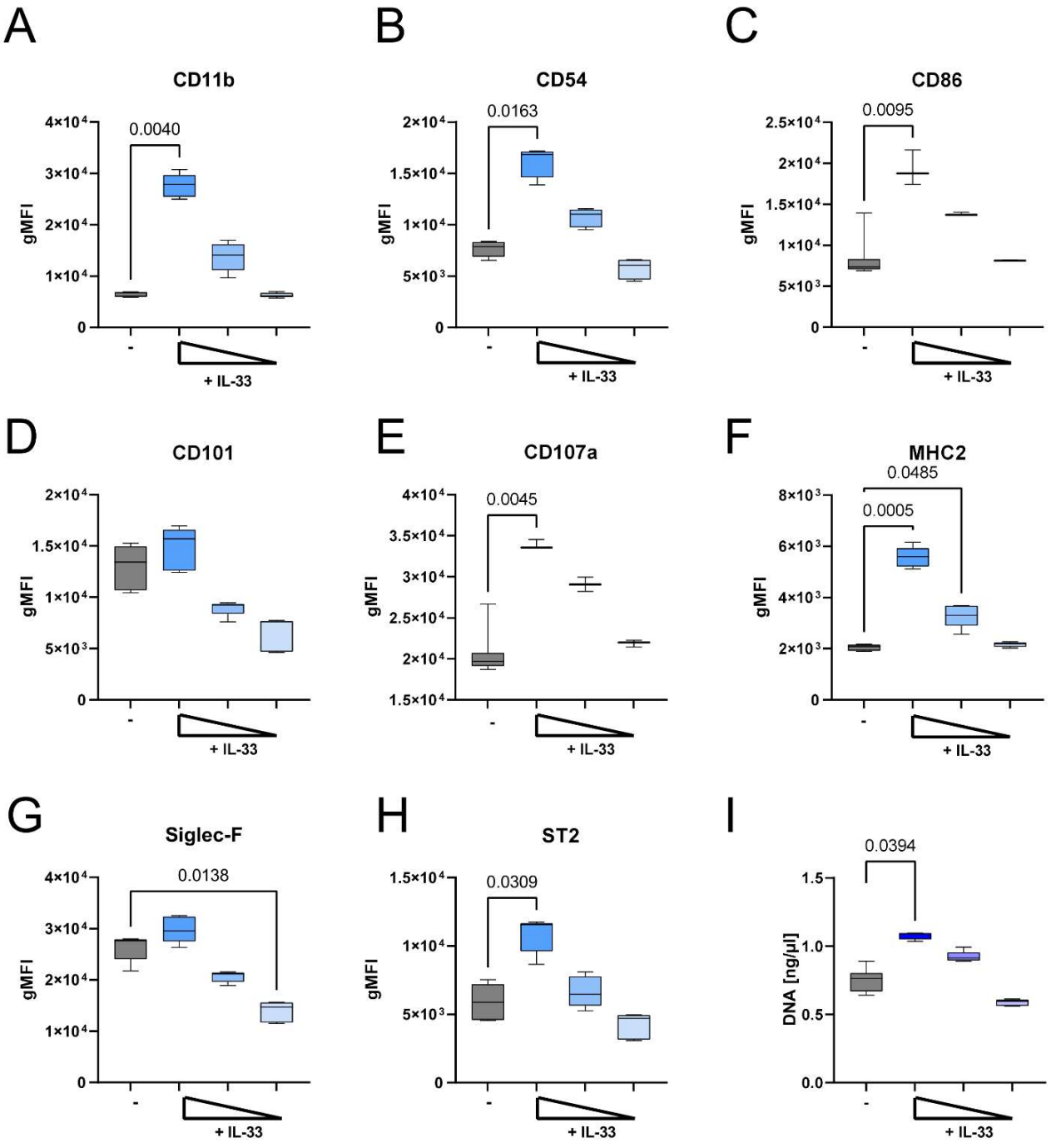

Figure 19. IL-33 activates bone marrow-derived eosinophils in a concentration-dependent manner. Bone marrow-derived eosinophils were stimulated with 0.1, 0.01, 0.001 µg/ml recombinant IL-33 and cultured for 24 h. (A) CD11b, (B) CD54, (C) CD86, (D) CD101, (E) CD107, (F) MHC2, (G) Siglec-F and (H) ST2 geometric mean fluorescence intensity (gMFI). (I) DNA release of eosinophils after 24 h. Data pooled from 2 independent experiments with a total of n=3 mice per group. Data is shown as median with interquartile range. Statistical analysis with Kruskal-Wallis test followed by Dunn´s multiple comparison. P values ≤ 0.05 are shown.

3.1.5 IL-33 signaling is essential for TPE-induced type 2 immune responses

Having shown that eosinophils are essential for TPE induction and display highly elevated expression of the IL-33 receptor, the role of said receptor in the development of TPE was investigated *in vivo*. The IL-33 suppressor *Heligmosomoides polygyrus* Alarmin Release Inhibitor (HpARI) [280] was used to sequester IL-33 to the DNA of necrotic cells and thereby inhibit IL-33 signaling. HpARI was administered intranasally (i.n.) to MF-sensitized mice 1 h before the MF challenge as well as 3 and 6 days after the challenge. Again, mice were sacrificed 10 days after the MF challenge (Fig. 20A). Additionally, IL-17a, which was previously shown to be in the BAL fluid of TPE mice, was blocked using an anti-IL-17a blocking antibody (aIL-17). TPE mice were treated with 100 µg IL-17a blocking antibody every three days intraperitoneally in the same interval as the HpARI treatment. TPE mice that were administered HpARI showed significantly decreased total lung cell, ILC2, AAM, eosinophil and neutrophil frequencies in comparison to TPE animals not treated with HpARI (Fig. 20B-F). In contrast, TPE mice treated with aIL-17 did not display significantly altered frequencies for the aforementioned cell subsets.

Alveolar macrophages were not significantly altered in TPE mice regardless of HpARI or aIL-17 treatment and monocytes increased only in TPE mice (Fig 20G-H). IgE and parasite-specific IgE levels were comparable between TPE and HpARI treated TPE mice (Suppl. Fig. 3A-B) while again neither serum IL-5 nor IFNγ reached the detection limit (data not shown). The reduction of eosinophils, ILC2s, AAM and neutrophils in HpARI treated mice indicates that IL-33 drives TPE associated immune responses. Accordingly, eosinophils contained in the lung tissue had a significantly lower expression of Siglec-F, CD11b, CD101 but not CD86 when animals were treated with HpARI in comparison to untreated TPE mice, indicating a decreased activation (Fig. 20I-L). Further, lung B cells were significantly reduced after HpARI treatment, while CD4 and CD8 T cells did not change in TPE mice independent of treatment (Fig. 21A-C).

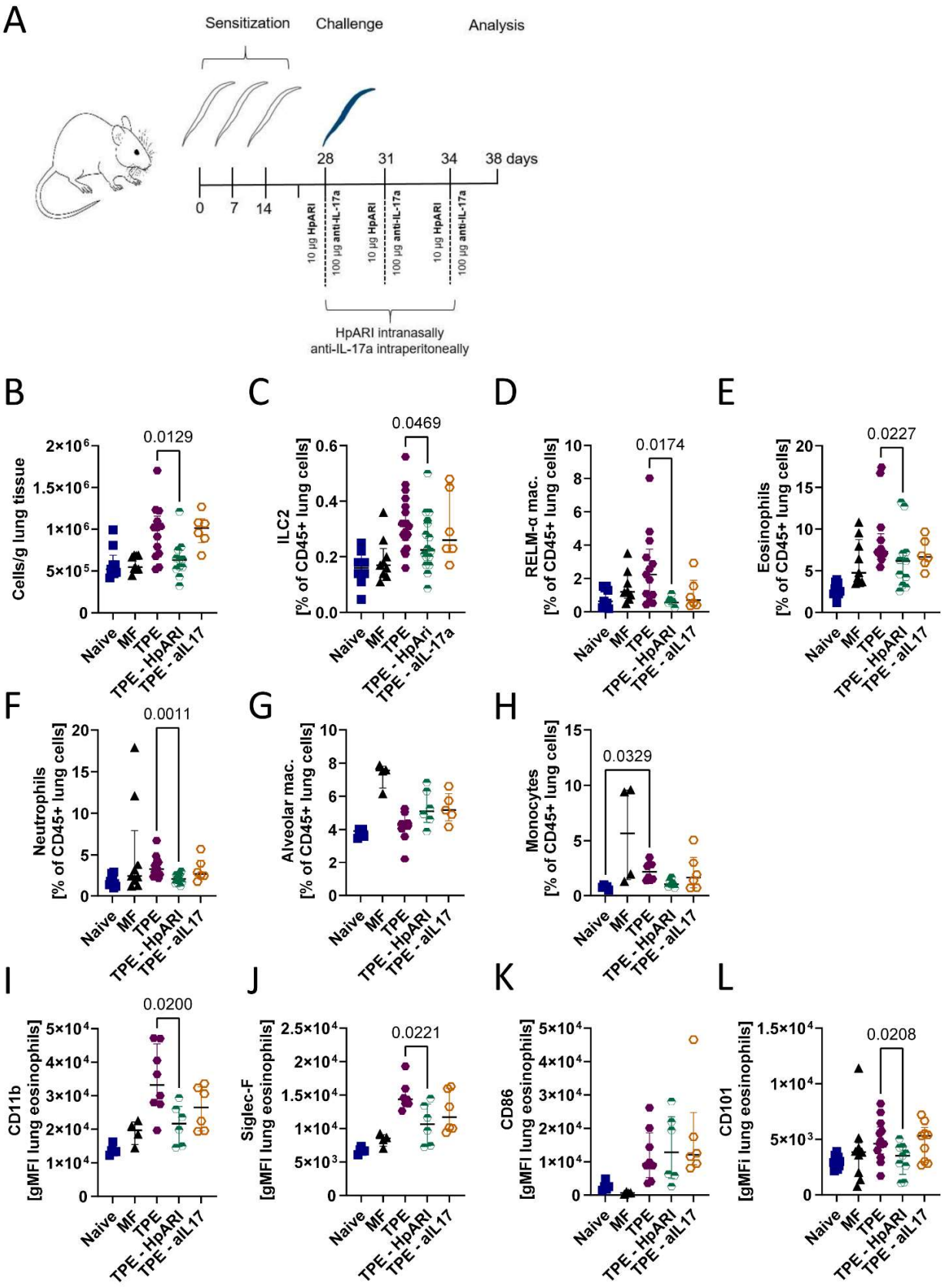
A
Sensitization
Challenge
Analysis
28
31
34
38 days
0
7
14
10 µg HpARI
100 µg anti-IL-17a
HpARI intranasally
anti-IL-17a intraperitoneally
B
Cells/g lung tissue
0.0129
C
ILC2
[% of CD45+ lung cells]
0.0469
D
RELM-α mac.
[% of CD45+ lung cells]
0.0174
E
Eosinophils
[% of CD45+ lung cells]
0.0227
F
Neutrophils
[% of CD45+ lung cells]
0.0011
G
Alveolar mac.
[% of CD45+ lung cells]
H
Monocytes
[% of CD45+ lung cells]
0.0329
I
CD11b
[gMFI lung eosinophils]
0.0200
J
Siglec-F
[gMFI lung eosinophils]
0.0221
K
CD86
[gMFI lung eosinophils]
L
CD101
[gMFi lung eosinophils]
0.0208
Naive
MF
TPE
TPE - HpARI
TPE - aIL17
TPE - HpAri
TPE - aIL-17a

Figure 20. IL-33-signaling inhibitor HpARI decreases lung eosinophil frequency and treated animals display a reduced type 2 immune response. (A) Experimental setup. Sensitized TPE mice were treated with 10 µg HpARI i.n. or 100 µg anti-IL-17a antibody i.p. 1 h before and every three days after the final challenge. (B) Lung cell count of naive mice, mice receiving the MF challenge (MF) as well as sensitized mice receiving PBS (TPE), HpARI (TPE-HpARI) or anti-IL-17a blocking antibody (TPE-aIL-17). Frequencies of (C) ILC2s (CD45$^+$, linage$^-$, TCRb$^-$, CD90.2$^+$, ST2$^+$, GATA3$^+$), (D) RELM-α^+ macrophages (CD45$^+$, CD206$^+$, Siglec-F$^+$, RELM-α^+), (E) eosinophils (CD45$^+$, CD11c$^-$, Siglec-F$^+$, CD11b$^+$), (F) neutrophils (CD45+, Ly6G$^+$), (G) alveolar macrophages (CD45$^+$, CD206$^+$, Siglec-F$^+$), and (H) monocytes (CD45$^+$, Siglec-F$^-$, CD11c$^+$, Ly6C$^+$). (I-L) Geometric mean fluorescence intensity of (I) CD11b, (J) Siglec-F, (K) CD86 and (L) CD101 of lung eosinophils. Data is pooled from 2 independent experiments with a total of n=6-15 mice per group. Data is shown as median with interquartile range and statistical comparison between TPE and HpARI mice was performed using Mann-Whitney-U test. P values ≤ 0.05 are shown.

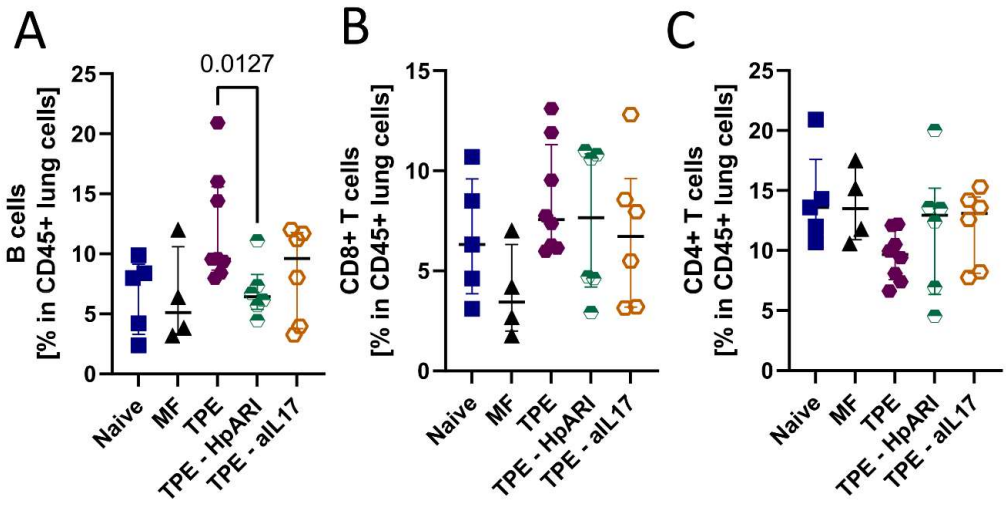

Figure 21. IL-33 signaling inhibitor HpARI decreases B cell frequencies in TPE mice. Sensitized TPE mice were treated with 10 µg HpARI i.n. or 100 µg anti-IL-17a blocking antibody i.p. 1 h before and every three days after the final challenge. (A-C) Frequencies of (A) B cells (CD45$^+$, CD19$^+$), (B) CD8 positive T cells (CD45$^+$, CD3$^+$, CD8$^+$) and (C) CD4 positive T cells (CD45$^+$, CD3$^+$, CD4$^+$). Data from 1 experiment with a total of n=5-8 mice per group. Data is shown as median with interquartile range and statistical comparison between TPE and HpARI mice was performed using Mann-Whitney-U test. P values ≤ 0.05 are shown.

In addition, histological analysis of the lung lacunarity, i.e., disintegration of the lung structure, was compared between TPE and HpARI-treated TPE animals. The lacunarity was significantly increased in TPE mice, indicating damage of the integrity, and was reduced by HpARI treatment (Fig. 22A-B). This implies that TPE associated eosinophil activation, type 2 immune responses and lung tissue damage was improved by blocking IL-33 signaling. In contrast, IL-17a blockage with i.p. injections of a blocking antibody was not sufficient in decreasing the TPE-associated immune response.

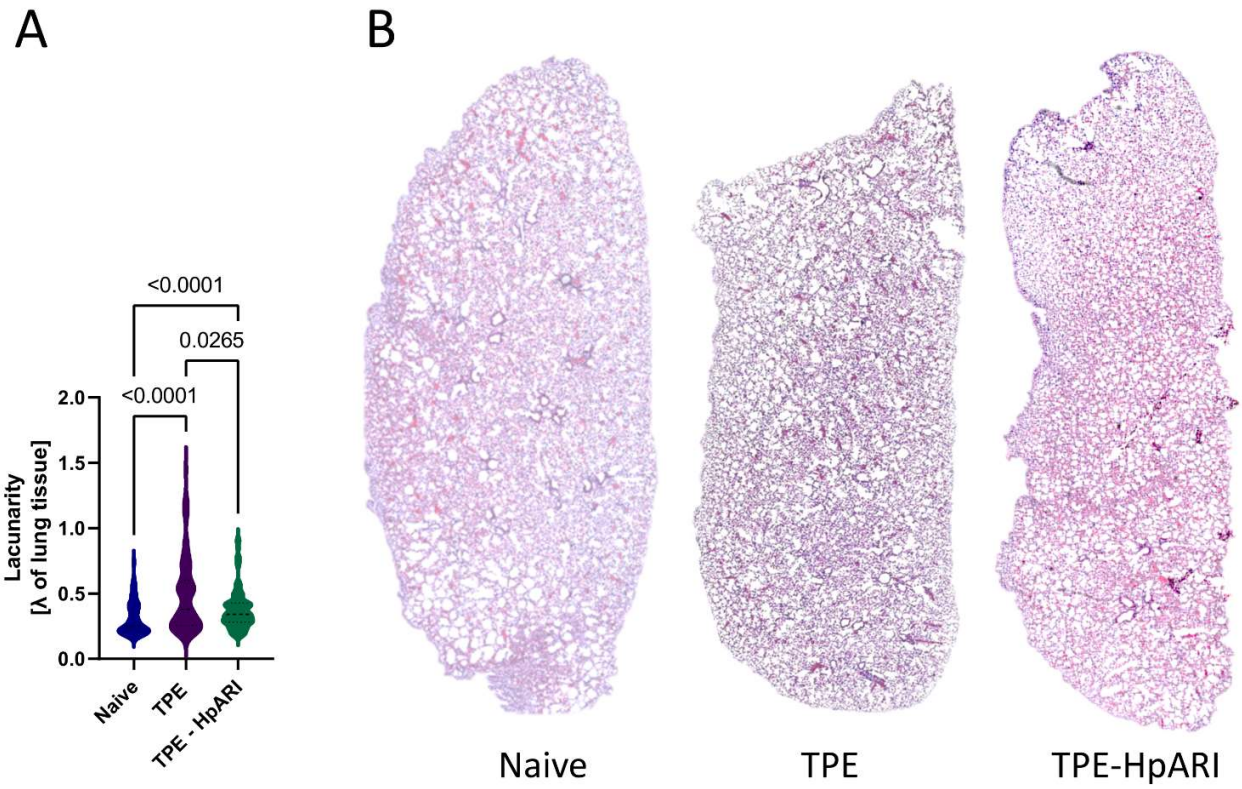

Figure 22. HpARI treatment reduces lung lacunarity. A) Lacunarity of 5 µm lung tissue sections. Lacunarity was assessed in 50 randomly generated regions of interest for naïve, TPE and TPE-HpARI treated animals. B) Representative tissue section for of untreated (Naïve) mice, sensitized mice receiving PBS (TPE) or HpARI (TPE-HpARI) stained with hematoxylin and eosin. Data from one out of three representative experiments with n=50 random generated regions of interest for n=5 mice are shown. Statistical analysis with Kruskal-Wallis test followed by Dunn´s multiple comparison. P values ≤ 0.05 are shown.

3.2 Impact of human filarial infections on the metabolic and immunological profile

3.2.1 Study design

To investigate potential beneficial effects of parasitic filarial infections against metabolic diseases, the open label pilot trial "FIMMIP" (Impact of filarial infections on the metabolic and immunological profile) was planned and started during this thesis. Uninfected participants (endemic control group without a filarial infection, EDN) or people infected with *O. volvulus*, *M. perstans* or *L. loa* (filarial infected, FI) were classified as lean, overweight or obese based on their body mass index (<25, 25-29 and ≥30), were recruited in rural regions of Cameroon (Fig. 23).

At baseline, extensive anthropomorphic measurements, i.e., height, weight, waist circumference, body fat, muscle mass, visceral adipose tissue, electrocardiography (ECG), blood pressure and pulse were done to compare FI and EDN participants. Further, the medical history, concurrent medical conditions and a detailed questionnaire including information about physical activity, income, religion and dietary habits was conducted for all participants. In addition, blood biochemistry was to be performed to investigate circulating lipids and liver enzymes, parameters of kidney function, HbA1c and fasting blood glucose. Finally, whole blood stimulations for flow cytometry and ELISA were performed at baseline as well as 12 and 18 months after anti-filarial chemotherapy to assess the immunological profile of the participants. All participants received 400 mg albendazole every three months with a total of four times to clear potential intestinal helminth infections. *M. perstans* and *O. volvulus* infections were treated with 200 mg doxycycline for 42 days. The aim was to assess potential differences between individuals with filarial infections compared to the uninfected endemic normal control group and elucidate changes in the metabolic and immunological profile after the treatment of the respective filarial infection.

At baseline, biochemistry, anthropomorphic evaluation, white blood cell analysis and whole blood stimulations for flow cytometry and ELISA were already performed. The immunological assessment which includes flow cytometry and multiplex analyses, i.e., the investigation of cytokine production as a response to multiple stimuli, immune cell phenotyping and adipokine measurement will be done after all samples were shipped to Bonn (scheduled for Q4 2023). In this thesis, the baseline characteristics of the cohort after screening are shown. The here presented preliminary data was subjected to double data entry and is therefore verified.

Data exceeding measuring ranges of the medical instruments was excluded from the analysis completely. At the current time (August 2023), the 18 months follow up is still ongoing.

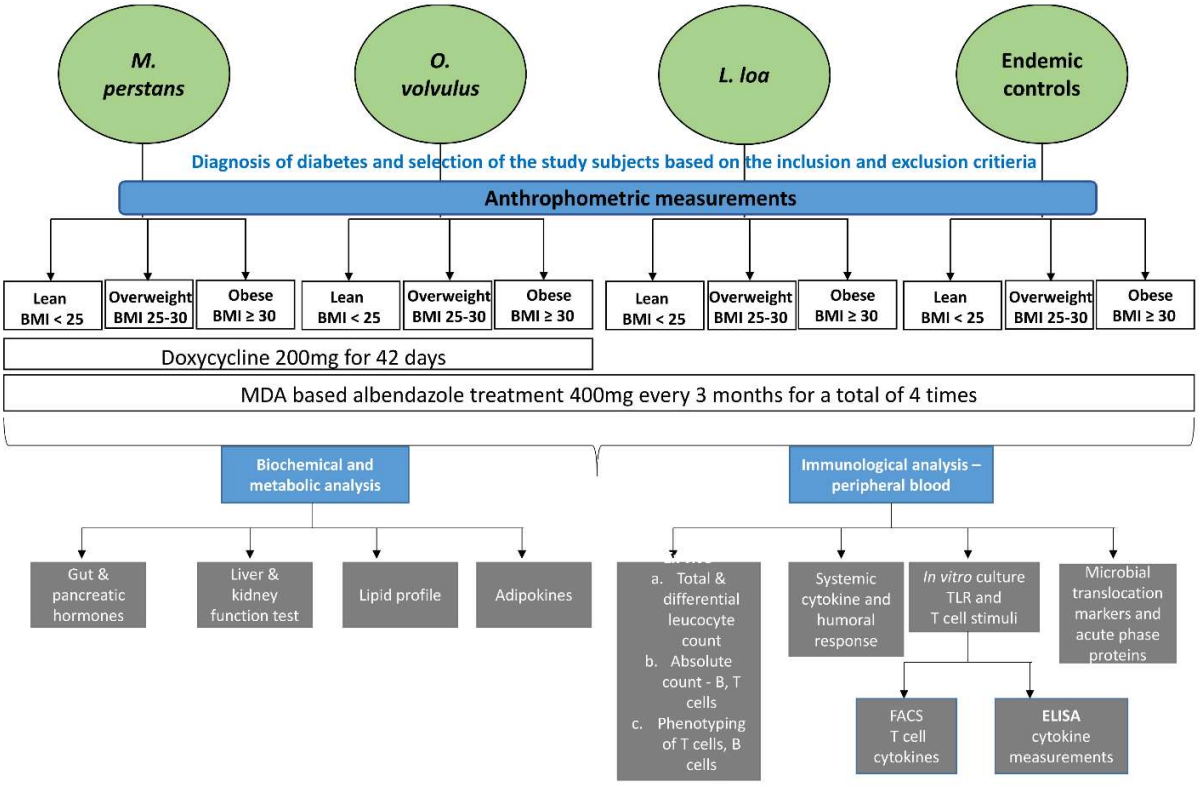

Figure 23. Group assessment and time table of the open label pilot trial "FIMMIP". Overview of the study. *M. perstans*-, *O. volvulus*- and/or *Loa loa*-infected participants and endemic controls were enrolled in this study and grouped according to their BMI as lean (BMI<25), overweight (BMI 25-29) or obese individuals (BMI≥30). *M. perstans* and *O. volvulus* positive participants received 200 mg doxycycline for 42 days. All participants received 400 mg of albendazole every three months to treat intestinal helminth infections. Before, 12 month and 18 months after doxycycline treatment, anthropomorphic, metabolic and immunological measurements will be performed as indicated in the figure. Assessment of the baseline data for anthropomorphic measurements, biochemistry and white blood cell analysis was performed. Cytokine responses, whole blood phenotyping and adipokines will be analyzed in the future. In addition, all aforementioned parameters are assessed for follow up visits after 12 and 18 months and will be analyzed after double data entry is complete.

3.2.2 Implementation of the “FIMMIP” trial

The main objective of this part of the PhD thesis was the implementation of the “FIMMIP” trial. This implementation consisted of establishing the methodology for anthropomorphic assessments, white blood cell analysis, clinical biochemistry, ECG, whole blood stimulations for ELISA and flow cytometry, and flow cytometry staining panels first in Bonn and then the transfer to the field laboratory in Cameroon. Further, during my visits in Cameroon I carried out capacity building by giving workshops for anthropomorphic assessments (blood pressure, waist circumference, ECG, body analyzer), blood glucose measurement, white blood cell analysis and whole blood stimulations for ELISA and flow cytometry and arranging and supporting a training for clinical biochemistry (see Fig. 5-8 in the material and methods section). Subsequently, I was responsible for purchasing and shipping instruments, supplies and consumables to Cameroon during the trial. Finally, I conducted preliminary data analysis and designed and adapted the study documents (case report form, informed consent form, statistical analysis plan, standard operating protocols).

3.2.3 Cell stimulation conditions and flow cytometry panel design

The first task was designing a whole blood stimulation assay for the assessment of the cytokine responses and immune cell phenotyping of the study participants. Whole blood was taken from all study participants at baseline and all included participants at baseline, 12 and 18 months follow up, and stimulated to investigate chemokine and cytokine responses to pro-inflammatory stimuli, fatty acids and filarial antigen. Further, whole blood from fifty enrolled participants per group was stimulated for flow cytometry. Flow cytometry panel were designed to differentiate B cells into naïve, regulatory, plasma, memory and activated memory subtypes and T cells into Th1, Th2, Th17, memory and regulatory T cells. In addition, frequencies of neutrophils, NK cells, monocytes and eosinophils were assessed in whole blood cells. Finally, the intracellular cytokines IFNγ, IL-2, IL-4, IL-5, IL-10, IL-13, IL-17A, IL-17F and CD40L were analyzed in B and T cells after stimulation. For this, I designed 12 flow cytometry panels during my thesis and established these on unstimulated (surface marker only) or stimulated (intracellular markers) human whole blood (Fig. 24-28).

The detection of the T cell, B cell and immune cell subsets as well as intracellular cytokines was accomplished after fixation and freezing of cells, ensuring analysis of participants' samples was feasible after storage of stimulated samples and their shipment. Additionally, to investigate if the serum samples and whole blood stimulated supernatant can be used to detect serum adipokines and cytokines after stimulation, proof of concept multiplex assays after freezing and storage of serum and supernatant were performed for the adipokines adiponectin and serum amyloid A (Fig. 29).

The pro-inflammatory cytokines TNF, IL-6 and IL-12p70 were detected in the whole blood stimulation supernatant and cytokine release was dependent on the concentration of LPS and partially dependent on the Pam3Cys concentration used (Fig. 29A). Serum adiponectin and serum amyloid A were within the detection limit of the multiplex assay (56.12 pg/ml – 230000 pg/ml) for all samples obtained during this test as long as the dilution recommended from the manufacturer of 1:50 was used (Fig. 29B). This indicates that the approach to measure adipokines and cytokines should be a reliable method to evaluate the participants' immunological and metabolic profile during this study.

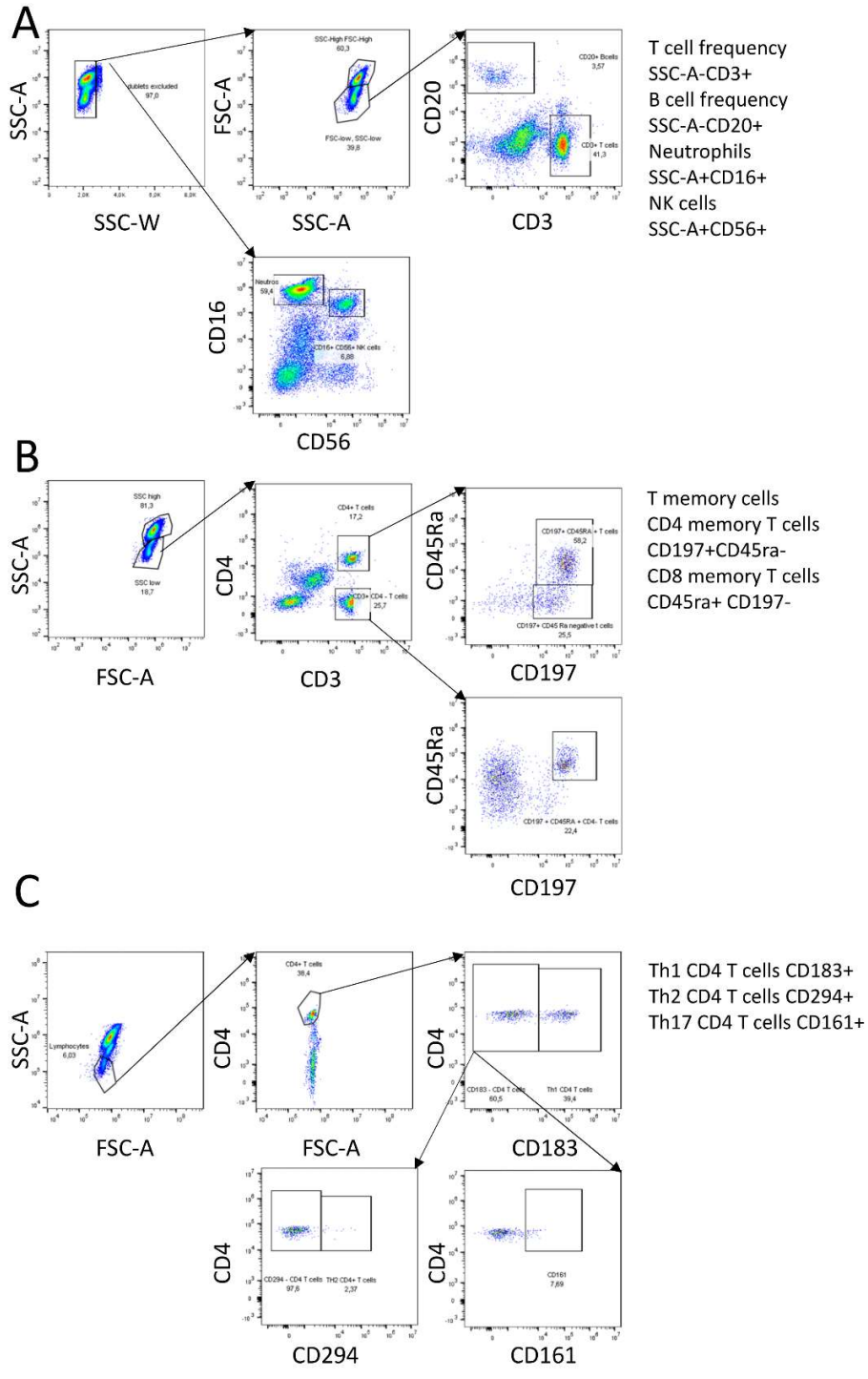

Figure 24. Overview panel for human whole blood and T cell phenotyping strategies for the "FIMMIP" trial. (A) Overview panel: neutrophils (SSC-A^{high}, CD16^{+}), NK cells (SSC-A^{high}, CD16^{+}, CD56^{+}), B cells (SSC-A^{low}, CD20^{+}), and T cells SSC-A^{low}, CD3^{+}). (B) Memory T cells: CD4 and CD8 memory T cells. (C) T helper subtype panel (Th): Th1 cells (SSC-A^{low}, CD4^{+} CD183^{+}), Th2 cells (SSC-A^{low}, CD4^{+}, CD183^{-}, CD294^{+}) and Th17 cells (SSC-A^{low}, CD4^{+}, CD183^{-}, CD183^{+}).

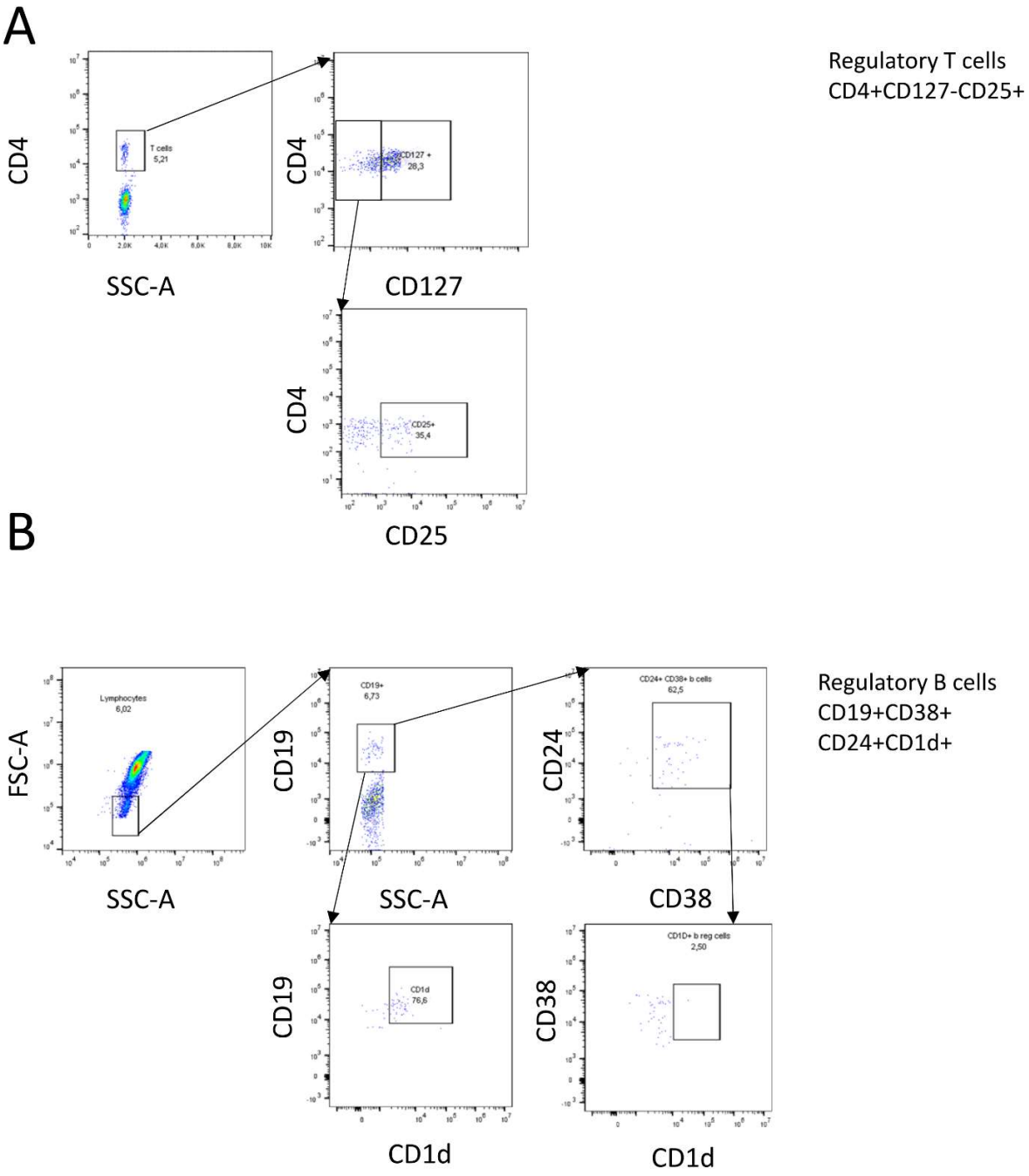

Figure 25. Gating strategies for regulatory B and T cells from human whole blood for the "FIMMIP" trial. (A) regulatory T cells (SSC-A^{low}, CD4^{+}, CD127^{-}, CD25^{+}) and (B) B cell panels (SSC-A^{low}, CD19^{+}, CD38^{+}, CD1d^{+}).

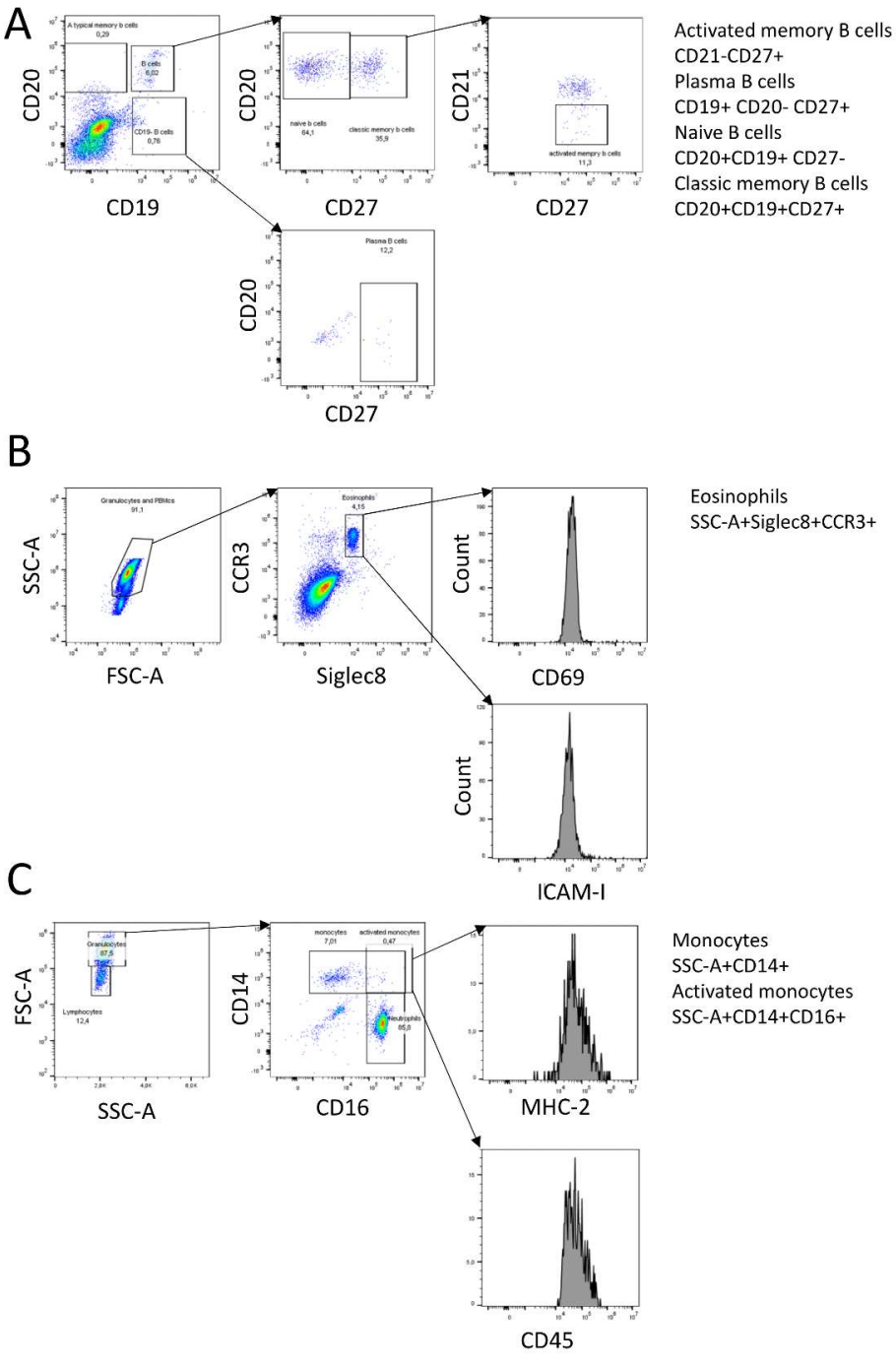

Figure 26. Gating strategies for B cell phenotyping and eosinophil and monocyte activation for the "FIMMIP" trial. (A) B cell subtype panel. Naïve B cells ($CD20^+$, $CD19^+$, $CD27^-$), classic memory B cells ($CD20^+$, $CD19^+$, $CD27^+$), activated memory B cells ($CD20^+$, $CD19^+$, $CD27^+$, $CD24^-$), a-typical memory B cells ($CD20^+$, $CD19^-$), plasma B cells ($CD19^+$, $CD20^-$, $CD27^+$). (B) Eosinophil phenotyping panel. Eosinophils were gated as SSC-A^{high}, $CCR3^+$, Siglec-8^+ and activation was assessed by the mean fluorescence intensity of CD69 and ICAM-1 expression. C) Monocyte phenotyping panel. Monocytes were gated as SSC- A^{high}, $CD14^+$ and activation was assessed by expression of $CD16^+$ and the mean fluorescence intensity of MHC-2 and CD45.

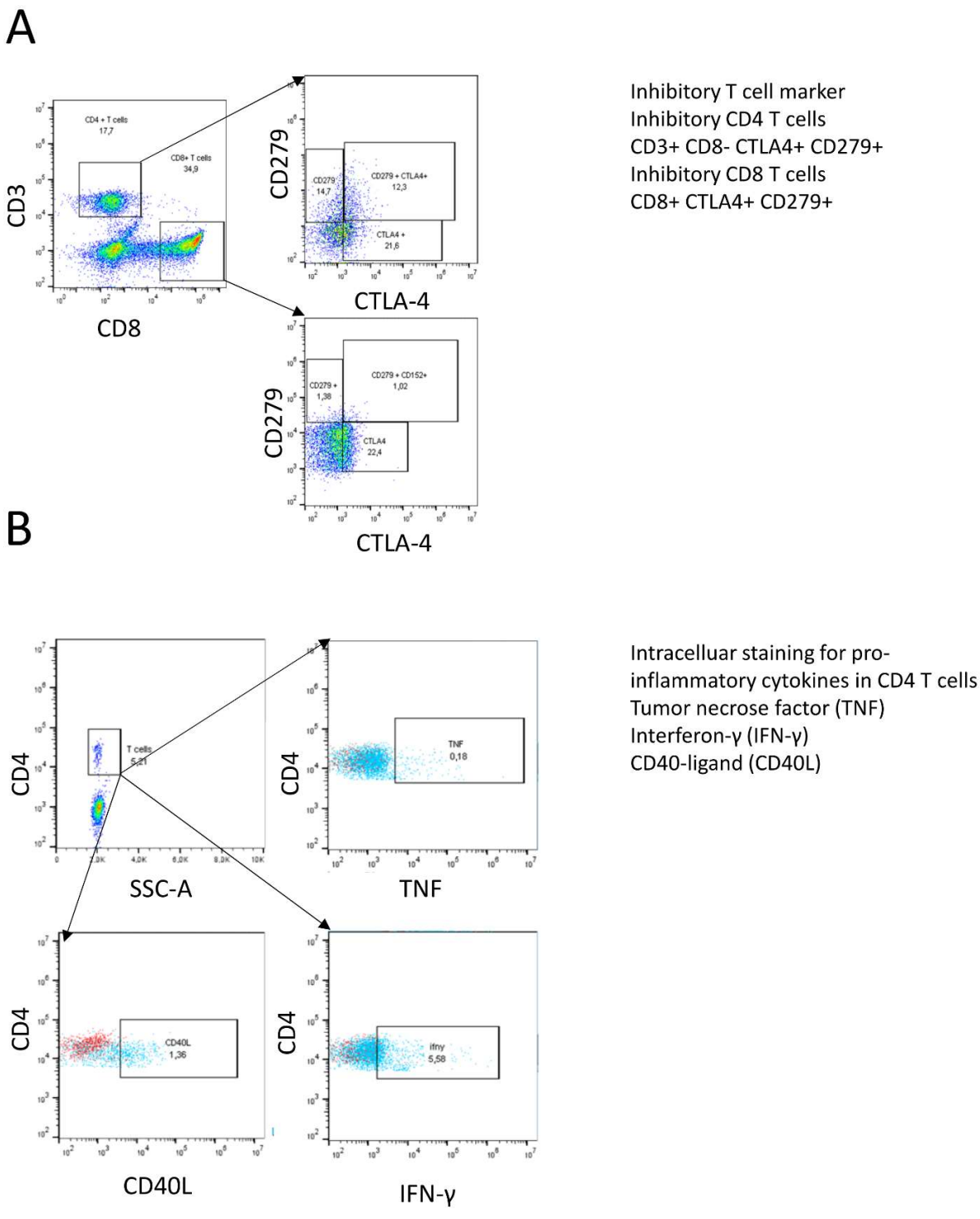

Figure 27. Inhibitory CD4 and CD8 T cell gating and assessment of intracellular IFNγ and TNF in CD4 T cells for the "FIMMIP" trial. (A) Inhibitory markers (CTLA4 and CD279) on CD4+ and CD8 + T cells. (B) Intracellular staining of IFNγ and TNF after stimulation (blue overlay) with phytohemagglutinin, anti-CD28, anti-CD49d and brefeldin A for 16h.

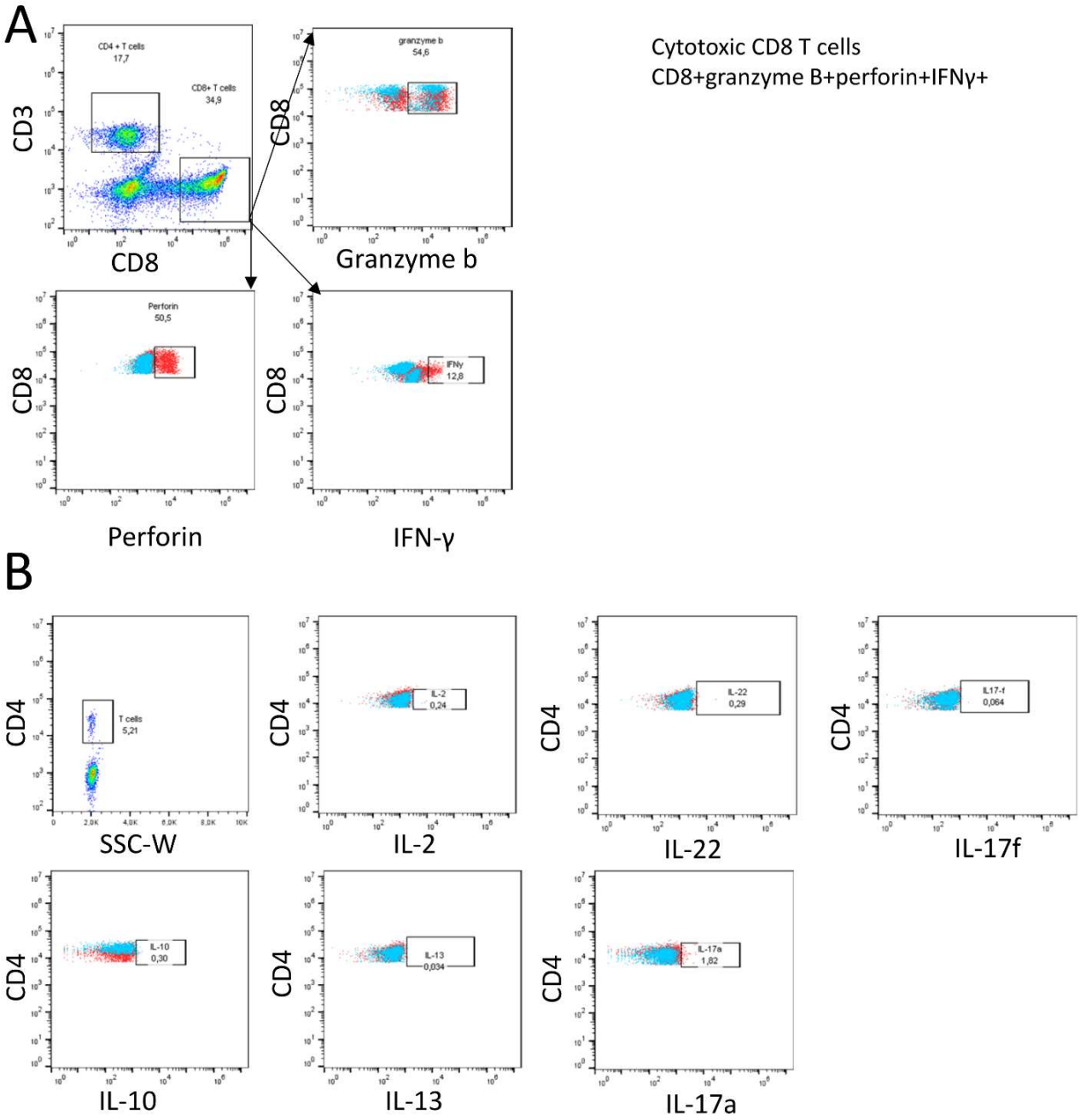

Figure 28. Cytotoxic CD8 T cell gating and intracellular cytokine stainings for the "FIMMIP" trial. (A) Cytotoxic CD8 T cell panel with perforin, granzyme b and IFNγ. (B) Intracellular staining of anti-inflammatory and regulatory cytokines, i.e., IL-2, IL-10, IL-17a, IL-17f and IL-22 in CD4 T cells after stimulation (red overlay) with phytohemagglutinin, anti-CD28, anti-CD49d and brefeldin A for 16h.

A

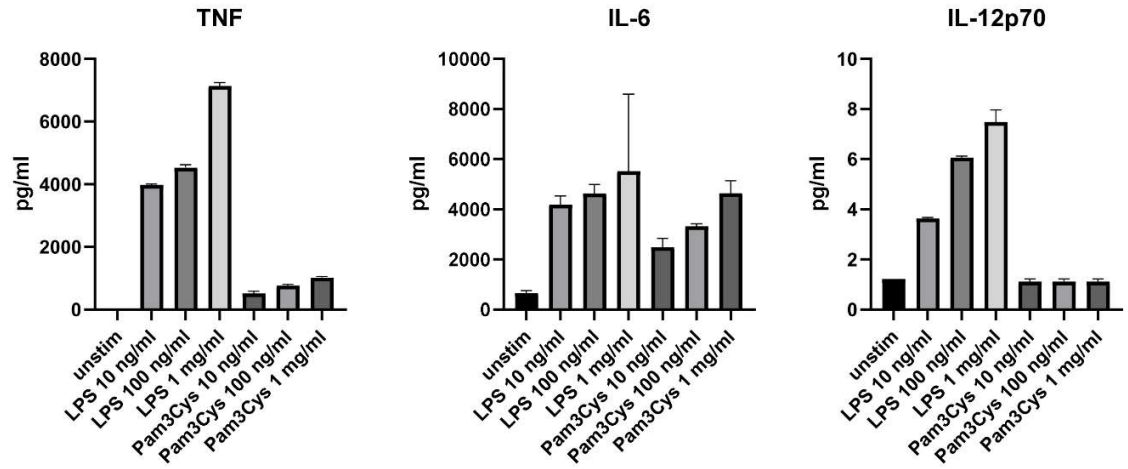

B

Adiponectin

	1	2	3	4	5	6
A	640900.000	640900.000	376275.481	75369.712	27328.582	18261.866
B	160225.000	160225.000	8727.126	14355.639	15599.340	20098.684
C	40056.250	40056.250	28055.415	47126.798	OOR<	29000.784
D	10014.060	10014.060	74133.593	62743.585	10991.323	10557.980
E	2503.510	2503.510	49457.115	25134.317	26909.310	21829.280
F	625.880	625.880	47494.450	140514.816	19970.553	12662.533
G	156.470	156.470	31681.337	22563.857	OOR<	18711.264
H	B	B	79360.713	6377.448	OOR<	19621.731

C

Serum amyloid A

	1	2	3	4	5	6
A	173800.000	173800.000	15209.945	11975.203	7482.373	4765.199
B	43450.000	43450.000	3047.681	4313.702	5286.044	3697.263
C	10862.500	10862.500	5829.042	8125.117	OOR<	6890.124
D	2715.630	2715.630	10943.566	8613.565	4131.008	4067.801
E	678.910	678.910	8460.998	6566.451	7635.982	4894.577
F	169.730	169.730	7185.777	17549.055	5699.785	3341.548
G	42.430	42.430	7130.535	5939.430	OOR<	4063.454
H	B	B	11678.852	2668.871	OOR<	4265.016

Figure 29. Proof of concept for the multiplex analysis of whole blood stimulation supernatant for cytokines and detection of adipokines from human serum after freezing. (A) Multiplex of human whole blood for TNF, IL-6 and IL-12p70 in the supernatant after 16 h stimulation with LPS or Pam3Cys. Shown are median with interquartile range. (B-C) Multiplex assay for the adipokine adiponectin (B) and the acute phase protein serum amyloid A (C) in 4 human serum samples after different freezing cycles (A6 – D6 1:50 diluted frozen once and E6 – H6 1:50 dilution frozen twice) and standard (A1, A2 to H1, H2).

3.2.4 Baseline characteristics of the cohort

Participants that did not provide skin snips, finger prick or stool samples and/or did not consent to BMI measurement were excluded from the analysis. Skin snips were used to identify onchocerciasis patients by investigating the presence and absence of skin MF and PCR. Finger pricks were used to detect peripheral MF and PCR of *L. loa* and *M. perstans*, while stool samples were analyzed with Kato-Katz to identify intestinal helminth infections by searching for larvae or eggs. In total 1619 participants were analyzed for their baseline characteristic (Tab. 5). 695 participants tested PCR positive for *O. volvulus, M. perstans* or *L. loa* including participants that were positive for multiple filarial infections. 924 participants were PCR negative for filarial infection and therefore represent the endemic normal control group. Age ($p = 0.112$), pulse rate ($p = 0.716$) and systolic blood pressure ($p = 0.629$) did not show a statistically significant difference between endemic normal (EDN) and filarial infected (FI) individuals. ECG measurements displayed an increased QT interval in FI by trend ($p = 0.071$). Interestingly, weight, BMI, waist circumference, visceral adipose tissue, body fat, muscle mass and diastolic blood pressure were significantly reduced in the FI group ($p = 0.07$-0.0001). At baseline only minor differences between lean FI and lean EDN were observed when participants were categorized by BMI (Tab. 6). Body fat was decreased in infected individuals with a BMI below 25 ($p < 0.0001$) and between 25 and 29 ($p = 0.0267$) when compared to EDN participants of similar BMI. Overall, both groups presented with anthropomorphic measurements that are within the respective normal ranges for a healthy population.

Table 5. Anthropomorphic baseline characteristics of filariae infected and endemic normal participants in rural Cameroon. Columns were compared with Mann-Whitney-U test. If applicable, normal ranges are added below the respective parameter. Data shown as median and 95% confidence interval (CI). The measurements were performed by the team of Prof. Dr. Samuel Wanji in Cameroon. Preparation of the field team was accomplished by an in-depth workshop (Fig. 7).

Parameter	Filarial infection	Endemic normal	p-value
	n=695	n=924	
Age [y]	50.0	48.0	0.112
	(49.0-52.0)	(47.0-50.0)	
Weight [kg]	**64.0**	**66.7**	<0.0001
	(63.1-64.6)	(65.8-67.6)	
Waist circumference	**82.0**	**84.0**	<0.0001
Male <102 cm	(82.0-83.0)	(84.0-8.05)	
Female <88 cm			
BMI	**23.2**	**24.4**	<0.0001
20-25	(23.0-23.6)	(24.0-24.8)	
Visceral adipose tissue	**6.0**	**7.0**	<0.0001
[%]	(6.0-7.0)	(7.0-8.0)	
Body fat	**20.1**	**26.9**	<0.0001
[%]	(19.6-21.3)	(25.7-28.6)	
Muscle mass	**36.6**	**32.0**	<0.0001
[%]	(35.9-37.2)	(31.1-33.0)	
Pulse rate	72.0	72.0	0.716
60-100 /min	(72.0-74.0)	(71.0-74.0)	
BP systolic	118	117	0.629
<120 mm Hg normal	(116-120)	(115-118)	
120-129 mm Hg elevated			
130-139 mm Hg Hypertension I			
>140 mm Hg Hypertension II			
BP diastolic	**74.0**	**78.0**	0.007
<80 mm Hg normal	(71.0-77.0)	(78.0-80.0)	
80-89 mm Hg Hypertension I			
>90 mm Hg Hypertension II			
QT interval	390	387	0.071
350-450 ms	(387-393)	(385-390)	

Table 6. Anthropomorphic baseline characteristics of filariae infected and endemic normal participants in rural Cameroon separated into lean, overweight and obese by BMI. Pairwise comparison was performed with Kruskal-Wallis and Dunn's multiple comparison test between each infected and endemic normal BMI subgroup and statistically significant differences ($p \leq 0.05$) are expressed by bold letters. If applicable, normal ranges are added below the parameter. Data shown as median and 95% CI. The measurements were performed by the team of Prof. Dr. Samuel Wanji in Cameroon. Preparation of the field team was accomplished by an in-depth workshop (Fig. 7).

	Filarial infection			**Endemic normal**		
BMI range	**Lean**	**Overweight**	**Obese**	**Lean**	**Overweight**	**Obese**
	< 25	**25-29**	**≥ 30**	**< 25**	**25-29**	**≥ 30**
	n=457-472	n=173-175	n=39	n=511-516	n=269-270	n=128-129
Age [y]	50.0	50.0	49.0	48.0	49.0	49.0
	(49.0-50.0)	(47.0-54.0)	(43.0-51.0)	(46.0-50.0)	(47.0-52.0)	(44.0-53.0)
Weight [kg]	60.1	74.4	86.3	60.0	73.3	88.6
	(59.3-61.1)	(72.4-75.5)	(83.1-92.2)	(59.3-61.1)	(72.5-74.2)	(86.0-91.7)
Waist	**80.0**	86.0	97.5	80.0	86.0	92.0
Circumference	**(80.0-82.0)**	(86.0-88.0)	(89.0-101)	(80.0-82.0)	(86.0-89.0)	(90.0-98.0)
Male < 102 cm						
Female < 88 cm						
BMI	22.0	26.7	33.5	22.3	26.7	33.1
20-25	(21.8-22.3)	(26.4-26.9)	(32.2-35.1)	(22.0-22.6)	(26.4-27.1)	(32.4-34.1)
Visceral adipose	5.00	9.00	11.0	5.00	9.00	11.0
tissue [%]	(5.00-6.00)	(9.00-10.0)	(10.0-13.0)	(5.00-6.00)	(9.00-10.0)	(11.0-13.0)
Body fat	**17.5**	**25.8**	45.85	**20.5**	**32.4**	43.8
[%]	(16.9-18.5)	(24.0-29.7)	(39.6-47.6)	(19.5-21.9)	(29.5-35.4)	(42.5-45.1)
Muscle mass	**38.7**	**34.7**	23.8	35.7	30	25.1
[%]	(37.8-39.5)	(32.5-35.7)	(23.4-26.0)	(34.3-36.7)	(28.6-31.8)	(24.1-26.1)
Pulse rate	71.0	72.0	75.0	70.0	73.0	76.0
60-100 /min	(70.0-73.0)	(72.0-76.0)	(72.0-80.0)	(69.0-72.0)	(71.0-75.0)	(73.0-79)
BP systolic	110	120	122	111	120	120
> 120 mm Hg norm.	(110-110)	(120-126)	(110-130)	(110-115)	(120-128)	(120-130)
120-129 mm Hg						
elevated						
130-139 mm Hg						
Hypertension I						
<140 mm Hg						
Hypertension II						

BP diastolic	70.0	80.0	80.0	75.0	78.0	80.0
< 80 mm Hg normal	(70.0-75.0)	(80.0-85.0)	(80.0-86.0)	(73.0-78.0)	(76.0-80.0)	(80.0-84.0)
80-89 mm Hg						
Hypertension I						
> 90 mm Hg						
Hypertension II						
QT interval	392	388	388	389	385	383
350-450 ms	(388-395)	(385-393)	(382-395)	(387-393)	(383-392)	(377-389)

3.2.5 Distribution of filarial infection by species in the cohort

Table 7 shows the distribution of the different filarial infections that are endemic within the study region. Single infections with *O. volvulus* with 359 individuals were the most prominent among the study population (22.2%), followed by *M. perstans* single infections with 117 patients (7.2%). Interestingly, single infections with *L. loa* and co-infections of *L. loa* and *M. perstans* displayed similar prevalence with 54 (3.3%) and 55 (3.4%) infected individuals respectively, indicating that there might be factors that increase the susceptibility or probability of co-infections. Triple infections (2.3%) and the remaining co-infections of *O. volvulus* with either *M. perstans* (2.2%) or *L. loa* (2.3%) showed the lowest prevalence.

Table 7. Prevalence of the respective filarial infections and co-infections within the cohort. Prevalence of filarial infection (number of patients and frequency of population). Assessment and preparation of blood smears and skin punches were performed by the team of Prof. Dr. Samuel Wanji.

Group	Number of patients	Prevalence
Endemic normals	924	57.0%
O. volvulus	359	22.2%
M. perstans	117	7.2%
L. loa	54	3.3%
M. perstans, L. loa	55	3.4%
M. perstans, O. volvulus	35	2.2%
L. loa, O. volvulus	37	2.3%
M. perstans, L. loa, O. volvulus	38	2.3%

3.2.6 Circulating liver enzymes and markers for kidney dysfunction are reduced during filarial infection

To evaluate an effect of filarial infection on liver function and health, biochemical assessments of circulating liver enzymes were performed. Serum levels of the circulating liver enzymes alkaline phosphatase (ALP), alanine-aminotransferase (ALP/GPT), aspartate-aminotransferase (AST/GST), Gamma-glutamyl-transferase (Gamma-GT) and CRP were assessed. ALP, a measure for potential obstructions of the bile duct, was significantly reduced in the FI group compared to EDN participants (Tab. 8, $p < 0.0001$), with strong differences in lean, overweight and obese individuals (Tab. 9, $p < 0.0001$, $p = 0.0328$ and $p = 0.0364$). A similar trend was observed for ALT/GPT, a marker that can point towards liver inflammation when elevated and AST/GST which is usually associated with liver damage or acute infection ($p < 0.0001$), while the strongest differences again were observed in FI participants in comparison to EDN with an BMI below 25 ($p < 0.0001$) with no significant differences between and overweight FI compared to EDN. Gamma-GT, which can be associated with liver damage or alcoholic liver damage, was not significantly altered between infected and uninfected individuals overall (Tab. 8). However, obese FI individuals showed significantly reduced gamma-GT values in comparison to obese individuals from the EDN group (Tab. 9). CRP, a sensitive biomarker for systemic inflammation and predictor of metabolic disease, was significantly reduced in FI individuals in comparison to EDN participants ($p < 0.0001$). When comparing lean EDN individuals against lean FI individuals, CRP was significantly reduced in a similar manner ($p < 0.0001$).

Kidney function was assessed by monitoring levels of urine microalbumin, serum creatinine and serum urea content (Tab. 8). Microalbumin ($p = 0.002$) and creatinine ($p < 0.0001$) were significantly reduced in FI individuals. When compared by BMI, only microalbumin was significantly reduced in overweight (BMI 25-29) infected individuals compared to overweight (Tab. 9, $p = 0.0324$) and lean uninfected participants ($p = 0.035$). Further, serum creatinine was reduced in lean infected individuals when compared to the uninfected controls group ($p = 0.0003$). Differences in serum urea content were not statistically significant throughout the different comparisons.

Taken together, circulating liver enzymes and creatinine in the serum as well as urine microalbumin levels were decreased in the cohort of individuals that were PCR positive for one or multiple filarial infections, indicating a beneficial impact of filarial infections on liver and kidney health.

Table 8. Circulating liver enzymes and kidney function of filariae infected and endemic controls. Columns were compared with Mann-Whitney-U test. If applicable, normal ranges are added below the respective parameter. Data shown as median and 95% CI. Assessment of clinical biochemistry parameters were performed by the team of Prof. Dr. Samuel Wanji in Cameroon. Preparation of the field team was accomplished by an in-depth workshop (Fig 8).

Circulating liver enzymes	Filarial infection	Endemic normal	p-value
	n=671-688	n=909-915	
ALP	**104**	**129**	<0.0001
40-130 U/L	(99.0-109)	(123-136)	
ALT/GPT	**20.3**	**22.9**	<0.0001
<45 U/L	(19.65-21.18)	(22.34-24.49)	
AST/GOT	**25.9**	**27.6**	<0.0001
<35 U/L	(24.78-27.27)	(26.58-29.43)	
γGT	25.0	25.0	0.469
<35 U/L	(25.0-27.0)	(24.0-26.59)	
CRP	**10.7**	**16.32**	<0.0001
≤5 mg/L	(8.98-12.8)	(13.14-21.73)	
Kidney function	n=535-681	n=727-918	
Microalbumin	**39.5**	**50.0**	0.002
<30 mg/L	(36.13-44.2)	(46.2-53.9)	
Creatinine	**0.62**	**0.72**	<0.0001
0.4-1.19 mg/dl	(0.60-0.65)	(0.70-0.76)	
Urea	19.2	18.6	0.168
15-55 mg/dl	(18.8-20.0)	(18.0-19.0)	

Table 9. Circulating liver enzymes and assessment of kidney function of filariae infected and endemic normal participants in rural Cameroon separated into lean, overweight and obese by BMI. Pairwise comparison was performed with Kruskal-Wallis and Dunn's multiple comparison test between each infected and endemic normal BMI subgroup. Statistically significant differences with $p \leq 0.05$ are expressed in bold numbers and all groups were compared to the lean endemic normal group with a BMI <25, *p<0.05, **p<0.01, ***p<0.005 and ****p<0.0001. If applicable, normal ranges are added below the respective parameter. Data shown as median and 95% CI. Assessment of clinical biochemistry parameters were performed by the team of Prof. Dr. Samuel Wanji in Cameroon. Preparation of the field team was accomplished by an in-depth workshop (Fig. 8).

Circulating liver enzymes	**Filarial infection**			**Endemic normal**		
BMI range	**Lean**	**Overweight**	**Obese**	**Lean**	**Overweight**	**Obese**
	< 25	**25-29**	**≥ 30**	**< 25**	**25-29**	**≥ 30**
	n=457-472	n=173-175	n=39	n=511-516	n=269-270	n=128-129
ALP	**104** ****	**107** ****	**94.0** **	**134**	**122**	**125**
40-130 U/L	(99.0-109)	(98.0-113)	(87.0-123)	(126-142)	(108-138)	(110-138)
ALT/GPT	**19.8** ****	21.0	21.9	**22.7**	23.5	23.5
<45 U/L	(19.0-21.0)	(20.0-23.2)	(20.0-28.7)	(21.5-24.8)	(22.3-25.5)	(20.7-27.0)
AST/GOT	**25.9** ****	26.16	**20.1** **	**28.6**	27.2	**25.6**
<35 U/L	(24.6-27.7)	(24.3-29.2)	(18.6-29.2)	(26.6-30.1)	(26.0-29.8)	(23.2-30.0)
γGT	25.0	26.0	**19.0** *	25.35	25.0	**27.0**
<60 U/L	(25.0-27.0)	(23.0-30.0)	(19.0-26.0)	(24.0-27.0)	(23.0-27.0)	(24.0-31.0)
CRP	**9.61****	14.2	14.1	**16.7**	13.1	22.1
≤5 mg/l	(7.81-12.3)	(9.41-18.3)	(6.25-32.3)	(13.1-23.2)	(9.67-22.3)	(11.9-34.3)
Kidney function	n=368-471	n=136-177	n=31-39	n=399-518	n=217-271	n=111-129
Microalbumine	40.8	**36.6***	34.9	50.0	**50.5**	48.7
<30 mg/L	(37.8-49.7)	(28.9-43.2)	(18.3-53.9)	(44.03-54.5)	(45.0-60.0)	(33.3-65.0)
Creatinine	**0.61*****	0.68	0.58	**0.71**	0.74	0.72
0.4-1.19 mg/dl	(0.58-0.65)	(0.64-0.72)	0.51-0.79)	(0.68-0.76)	(0.69-0.78)	(0.67-0.83)
Urea	19.0	19.8	21.25	18.0	19.7	19.2
15-55 mg/dl	(18.4-19.7)	(18.6-20.5)	(17.9-22.8)	(17.4-18.7)	(18.6-20.5)	(17.9-20.3)

3.2.7 Comparison of serum glucose levels and lipid profile during filarial infection

Analyzing glucose and circulating lipids within the serum is crucial to elucidate the ability of human filarial parasites to modulate the metabolic profile. To determine if filarial infections influence the lipid profile, total serum cholesterol, triglycerides as well as high-density (HDL) and low-density lipoprotein (LDL) were assessed in a fasting state (Tab. 10). Total cholesterol ($p = 0.045$) and HDL ($p = 0.023$) were decreased in filarial infected participants while triglycerides were increased ($p = 0.002$). LDL was decreased by trend ($p = 0.057$) in infected individuals. Comparing infected and uninfected participants after BMI categorization (Tab. 11), LDL was elevated in both obese groups (infected $p = 0.0019$ and uninfected $p = 0.0073$), while triglycerides were elevated in overweight FI individuals compared to overweight EDN ($p = 0.0029$).

Table 10. Blood sugar and circulating lipids in filariae infected and endemic controls. Columns were compared with Mann-Whitney-U test. If applicable, normal ranges are added below the respective parameter. Data shown as median and 95% CI. Assessment of clinical biochemistry parameters were performed by the team of Prof. Dr. Samuel Wanji in Cameroon. Preparation of the field team was accomplished by an in-depth workshop (Fig. 8).

	Filarial infection	**Endemic normal**	**p-value**
Blood sugar	n=641-690	n=826-913	
and lipid profile			
Cholesterol	**135**	**139**	0.045
≤190 mg/dl	(131-139)	(135-143)	
HDL	**60.5**	**65.2**	0.023
>60 mg/dl	(58.3-63.8)	(62.5-67.4)	
LDL	110	113	0.057
≤100 mg/dl	(106-115)	(110-117)	
Triglycerides	**37.0**	**35.0**	0.002
≤150 mg/dl	(35.0-40.0)	(33.0-37.0)	
HbA1c	**39.9**	**43.0**	<0.0001
<42 mmol/mol Hb	(38.9-40.3)	(42.3-43.9)	
FB glucose	98.0	99.0	0.45
<99 mg/dl	(98.0-100)	(98.0-101)	

Further, triglycerides were increased in both obese groups as well as overweight FI compared to lean EDN. Strikingly, glycated hemoglobin (HbA1c), a measure for long term blood sugar levels and diagnostic criteria for T2D, was significantly reduced in FI individuals (Tab. 10, $p < 0.0001$) compared to the endemic control group if a BMI independent analysis was done.

A median of 43 for the uninfected participants exceeds the normal range of 42 mmol/mol Hb and might indicate a pre-diabetic state (above 42mmol/mol Hb). Similarly, lean infected participants displayed significantly reduced Hb1Ac levels compared to lean non-infected controls (Tab 11).

Fasting blood glucose was assessed by a finger prick and glucometer. Fasting blood glucose was not significantly different between infected and uninfected individuals ($p = 0.45$) when compared in total. However, overweight ($p = 0.0148$) infected as well as overweight ($p < 0.0001$) and obese ($p < 0.0001$) uninfected but not obese filarial infected participants displayed significantly elevated levels of blood glucose, which could indicate improved glucose uptake of filarial infected individuals.

Table 11. Blood sugar and circulating lipids of filariae infected and endemic normal participants in rural Cameroon separated into lean, overweight and obese by BMI. Pairwise comparison was performed with Kruskal-Wallis and Dunn's multiple comparison between each infected and endemic normal BMI subgroup and statistically significant differences ($p \leq 0.05$) are expressed in bold numbers. All groups were compared to lean endemic normal participants with BMI <25, *p<0.05, **p<0.01, ***p<0.005 and ****p<0.0001. If applicable, normal ranges are added below the respective parameter. Data shown as median and 95% CI. Assessment of clinical biochemistry parameters were performed by the team of Prof. Dr. Samuel Wanji in Cameroon. Preparation of the field team was accomplished by an in-depth workshop (Fig. 8).

Blood sugar and lipid profile	**Filarial infection**			**Endemic normal**		
BMI range	**Lean**	**Overweight**	**Obese**	**Lean**	**Overweight**	**Obese**
	< 25	**25-29**	**≥ 30**	**< 25**	**25-29**	**≥ 30**
	n=445-474	n=162-177	n=34-39	n=479-517	n=231-270	n=116-129
Cholesterol	139	139	144	135	139	149**
≤190 mg/dl	(124-136)	(134-144)	(130-170)	(129-141)	(131-146)	(143-159)
HDL	60.2	62.5	59.4	64.5	65.3	65.8
>60 mg/dl	(56.2-64.5)	(58.6-68.4)	(43.8-68.4)	(61.0-67.6)	(61.5-70.0)	(59.3-70.7)
LDL	105	115.4	149.**	108	118	129**
≤100 mg/dl	(101-111)	(109-123)	(123-174)	(104-114)	(110-129)	(115-145)
Triglycerides	36.0	**42.0****	45.0*	33.0	**35.0**	43.0**
≤150 mg/dl	(33.0-38.0)	(35.0-47.0)	(36.0-73.0)	(29.0-37.0)	(32.0-38.0)	(37.0-50.0)
HbA1c	**38.9****	40.9	40.0	**43.7**	42.7	43.3
<42 mmol/mol Hb	(37.8-40.0)	(40.1-41.8)	(36.1-41.5)	(42.4-44.6)	(41.2-43.9)	(40.3-47.0)
FB glucose	98.0	100*	101	97.0	103****	105****
<99 mg/dl	(97.0-100)	(98.0-103)	(98.0-108)	(96.0-99.0)	(101-105)	(102-108)

3.2.8 White blood cell analysis of filarial infected individuals

Infections as well as obesity can have far-reaching implications within the human body, and amongst other things greatly impact immune cell composition and counts within the blood. Thus, monitoring potential alterations during filarial infections and obesity is crucial to ensure a broader view on potential metabolic and immunomodulatory processes during filarial infections. Therefore, whole blood of the participants was analyzed (Tab. 12). Leukocyte numbers were significantly increased in FI individuals ($p = 0.012$). Similarly, eosinophils were significantly elevated ($p < 0.0001$), while neutrophil ($p = 0.936$) and platelet ($p = 0.226$) counts were not statistically significant between infected and uninfected participants.

Tab. 12: White blood cell analysis and hemoglobin levels of filariae infected and endemic controls. Columns were compared with Mann-Whitney-U test. If applicable, normal ranges are added below the respective parameter. Data shown as median and 95% CI. Statistically significant differences ($p \leq 0.05$) are expressed in bold numbers. The white blood cell analysis was performed by the laboratory team of Prof. Dr. Samuel Wanji in Cameroon. Preparation of the field team was accomplished by an in-depth workshop (Fig. 8).

Hemogram	**Filarial infection**	**Endemic normal**	**p-value**
	n=569-679	n=650-886	
Leukocytes	**4.83**	**4.69**	0.012
5.5-11*10^9/L	(4.74-5.03)	(4.58-4.81)	
Neutrophils	1.65	1.66	0.936
2.5-7*10^6/L	(1.59-1.72)	(1.6-1.73)	
Eosinophils	**0.34**	**0.19**	<0.0001
0.3-0.35*10^6/L	(0.31-0.39)	(0.17-0.21)	
Basophils	0.06	0.06	0.03
0-0.3*10^6/L	(0.06-0.07)	(0.06-0.07)	
Platelets	234	235	0.226
150-450*10^9/L	(227-240)	(231-242)	
Hemoglobin	13.8	13.6	0.078
12.1-17.2 g/L	(13.7-14.0)	(13.5-13.8)	

Interestingly, neutrophil counts with 1.65*10^9/L for FI and 1.66*10^9/L for EDN were below the expected range of 2.5-7*10^9/L. Basophil counts were slightly decreased within the FI group ($p = 0.03$) and hemoglobin was reduced by trend ($p = 0.078$). Comparing leukocytes after separation by BMI groups revealed increased counts for lean ($p = 0.0423$) and obese ($p = 0.0263$) FI individuals compared to their respective endemic control group (Tab. 13). Eosinophils increased significantly in lean ($p < 0.0001$) and overweight ($p < 0.0001$) participants but not in the obese FI cohort compared to the controls. Platelets, neutrophils and hemoglobin content was not significantly different between the different BMI groups and infection status.

Tab. 13: White blood cell analysis and hemoglobin levels of filariae infected and endemic normal participants in rural Cameroon separated into lean, overweight and obese by BMI. Pairwise comparison was performed with Kruskal-Wallis and Dunn's multiple comparison test between each infected and endemic normal BMI subgroup and statistically significant differences ($p \leq 0.05$) are expressed in bold numbers. All groups were compared to lean endemic normal with BMI <25, *p<0.05, **p<0.01, ***p<0.005 and ****p<0.0001. If applicable, normal ranges are added below the respective parameter. Data shown as median and 95% CI. The white blood cell analysis was performed by the laboratory team of Prof. Dr. Samuel Wanji in Cameroon. Preparation of the field team was accomplished by an in-depth workshop (Fig. 8).

Hemogram	**Filarial infection**			**Endemic normal**		
BMI range	**Lean**	**Overweight**	**Obese**	**Lean**	**Overweight**	**Obese**
	< 25	**25-29**	**≥ 30**	**< 25**	**25-29**	**≥ 30**
	n=389-466	n=141-175	n=30-39	n=352-497	n=202-266	n=96-125
Leukocytes	**4.81**	4.80	**5.16****	**4.66**	4,77	**4.69**
5.5-11*10^9/L	(4.70-5.06)	(4.64-5.08)	(4.78-5.97)	(4.54-4.8)	4.55-5.01)	(4.44-5.16)
Neutrophils	1.65	1.62	1.92*	1.6	1.74	1.76
2.5-7*10^6/L	(1.55-1.71)	(1.47-1.81)	(1.65-2.17)	(1.51-1.69)	(1.64-1.9)	(1.56-1.9)
Eosinophils	**0.34****	**0.35****	0.21	**0.19**	**0.16**	0.19
0.3-0.35*10^6/L	(0.31-0.41)	(0.27-0.43)	(0.16-0.42)	(0.17-0.22)	(0.14-0.21)	(0.14-0.22)
Basophils	0.06	0.06	0.06	0.06	0.06	0.07*
0-0.3*10^6/L	(0.06-0.07)	(0.05-0.07)	(0.06-0.07)	(0.06-0.07)	(0.06-0.07)	(0.07-0.08)
Platelets	237	225	233	234	235	236
150-450*10^9/L	(230-244)	(218-243)	(210-263)	(227-242)	(228-248)	(228-255)
Hemoglobin	13.8	13.8	13.4	13.6	13.6	13.5
12.1-17.2 g/L	(13.7-14.0)	(13.6-14.2)	(13.4-14.1)	(13.6-13.8)	(13.3-13.9)	(13.3-14.0)

3.2.9 Intestinal helminth prevalence and concomitant disease

The ability of intestinal helminths to modulate the metabolic profile is well established [131, 132, 281, 282]. Therefore, identifying the prevalence of intestinal helminth infections as well as other highly endemic diseases in the study region is indispensable to decipher the specific impact of intestinal and filarial parasites on the metabolic and immunological profile. In this study, a pre-screening or sensitization step was performed to monitor filarial infection prevalence and intestinal helminth infections. Table 14 displays the prevalence of different co-infections with soil transmitted helminths and the incidence of tuberculosis and HIV within the study cohort. The prevalence of soil transmitted helminths in general is considerably similar for most infections even if the total frequency is slightly elevated for FI participants with approximately 22% and 15% of EDN participants having an ongoing infection. Trematode infections were the most prevalent intestinal helminth infections in this study area with 10.2% of FI and 7.1% of EDN participants being infected. The lancet liver fluke (*Dicrocoelium dendriticum*) was the most common infection in this study population with 5.4% of FI and 4.7% of EDN participants having eggs in their stool. The trematode with the second highest prevalence was the lung fluke (*Paragonimus spp.)* with 3.9% of FI and 1.2% of EDN individuals being infected. The remaining trematodes detected, i.e., *Schistosoma mansoni* (blood fluke), *Fasciola hepatica* (liver fluke) and *Opisthorchis spp.* did not surpass 1% of prevalence.

Nematodes had the second highest prevalence with 9.7% of FI and 5.7% of EDN participants being infected. The highest prevalence of nematode infections was observed for *Capillaria spp.* (hairworm) and *Trichuris spp.* (whipworm) with 4.2% of FI and 2.6% of EDN individuals being infected with *Capillaria spp.* and 3.1% FI and 2.6% of EDN having an active infection with *Trichuris* species*.* 2.3% and 1.2% of FI participants and EDN participants were infected with *Ascaris spp.* (roundworm), respectively. Infections with hookworms (*Ancylostoma duodenale* or *Necator americanus*) and *Enterobius spp.* (pinworm) were below 1% in both groups.

Cestodes (tapeworms) were out of the three classes the least abundant within this study cohort. 2.9% of FI and 2.3% of EDN participants had an cestode infection. *Taenia spp.* displayed the highest prevalence with 2.8% for FI participants and 1.7% for EDN participants. Finally, *Hymenolepis spp.* and *Diphyllobothrium latum* had a prevalence below 1% in the FI and EDN group. Prevalence of all other intestinal parasites was below 0.5%. Incidence of HIV and tuberculosis was 0.6% and 0.3% in the FI and 0.2% and 0.7% in the EDN group, respectively.

For infections with *Capillaria spp.* (FI 4.2%, EDN 2.61%)*, Trichuris spp.* (FI 3.1%, EDN 1.5%)*, Ascaris spp.* (FI 2.3%, EDN 1.2%)*, Dicrocoelium spp.* (FI 5.4%, EDN 4.7%)*, Paragonimus spp.* (FI 3.9%, EDN 1.7%)*, Taenia spp.* (FI 2.8%, EDN 1.7%) FI participants had increased prevalence. A comparison of individuals positive for intestinal helminths and study participants without these infections displayed only a minor impact of intestinal helminths on the here described parameters, i.e., circulating liver enzymes, markers of kidney function, lipid profile and anthropomorphic data. (Suppl. Table 2). Importantly, CRP (positive: 12.28 mg/l, negative: 13.65 mg/l), fasting blood glucose (99 mg/dl for both groups), HbA1c (positive: 40.8 mmol/mol Hb, negative: 41.01 mmol/mol Hb) were comparable between participants when grouped as intestinal helminths positive and negative without separation by into FI and EDN participants.

When split into FI and EDN individuals and additionally positive and negative for intestinal helminths, trends observed in the prior analysis were conserved for most assessed parameters (Suppl. Table 3). Here, CRP was 10.08 mg/dl for FI without ST and 11.36 mg/dl for FI participants that were positive for intestinal helminths. In line, median HbA1c reduction was the strongest in FI individuals (39.85 mmol/mol Hb) that were not infected with STH compared to EDN without STH (43.03 mmol/mol Hb). Due to the minimal differences in CRP and HbA1c and overall similar infection prevalence, the infection status with intestinal helminths was not assessed separately for this analysis, but could be investigated in the future to elucidate on potential effects of the respective intestinal helminths on the aforementioned parameters.

Tab. 14: Prevalence of intestinal parasite infections, HIV and tuberculosis. Intestinal helminth infections were assessed using Kato-Katz. HIV and tuberculosis prevalence was assessed using the medical history provided by the participant. Stool sample analysis was performed by the laboratory team of Prof. Dr. Samuel Wanji. Incidence of HIV and tuberculosis were assessed by a questionnaire.

	Filarial infection	**Endemic normal**
	n=688	n=919
Intestinal helminths	22%	15%
Nematodes	**9.7%**	**5.7%**
Capillaria spp.	29	24
	4.22%	2.61%
Trichuris spp.	21	14
	3.05%	1.52%
Ascaris spp.	16	11
	2.32%	1.19%
Enterobius vermicularis	1	2
	0.15%	0.22%
Hookworm	0	1
	0%	0.11%
Trematodes	**10.2%**	**7.07%**
Dicrocoelium dendriticum	37	43
	5.38%	4.68%
Paragonimus spp.	27	16
	3.93%	1.74%
Schistosoma spp.	5	4
	0.73	0.44%
Fasciola hepatica	1	1
	0.15%	0.11%
Opisthorchis spp.	0	1
	0%	0.11%
Cestodes	**2.9%**	**2.29%**
Taenia spp.	19	16
	2.76%	1.74%
Dipylidium spp.	1	2
	0.15%	0.22%
Hymenolepis spp.	0	2
	0%	0.22%
Diphyllobothrium latum	0	1
	0%	0.11%
Others		

Tuberculosis	2	6
	0.29	0.65
HIV	4	2
	0.58	0.22

3.2.10 Impact of different filarial species on anthropomorphic measurements

In the prior analysis, all filarial infections were pooled and compared to the uninfected control and potential differences in the groups were displayed after categorization by BMI. However, the different infections might modulate the immune system and metabolic profile to different degrees. Therefore, all individuals were sorted by their respective infection with filarial parasites according to table 7. Age was comparable between the different filarial infections and co-infections when compared to the EDN group (Fig. 30A). Male and female individuals were comparable in numbers amongst *O. volvulus* infected, EDN and triple infected, while males were infected more often with *M. perstans, L. loa* or double infected (Fig. 30B). *O. volvulus* infected individuals displayed significantly decreased body weight, waist circumference, BMI, visceral adipose tissue, body fat and increased muscle mass (Fig. 30C-H). Interestingly, while pulse and blood pressure were comparable between all groups, *O. volvulus* infected individuals displayed an increased QT value (Fig. 31A-D). *M. perstans* infected individuals showed decreased waist circumference, BMI, body fat and increased muscle mass. All co-infected individuals displayed decreased body fat, BMI and increased muscle mass except the triple infected group. In contrast, none of the aforementioned anthropomorphic measurements are improved in *L. loa* infected individuals.

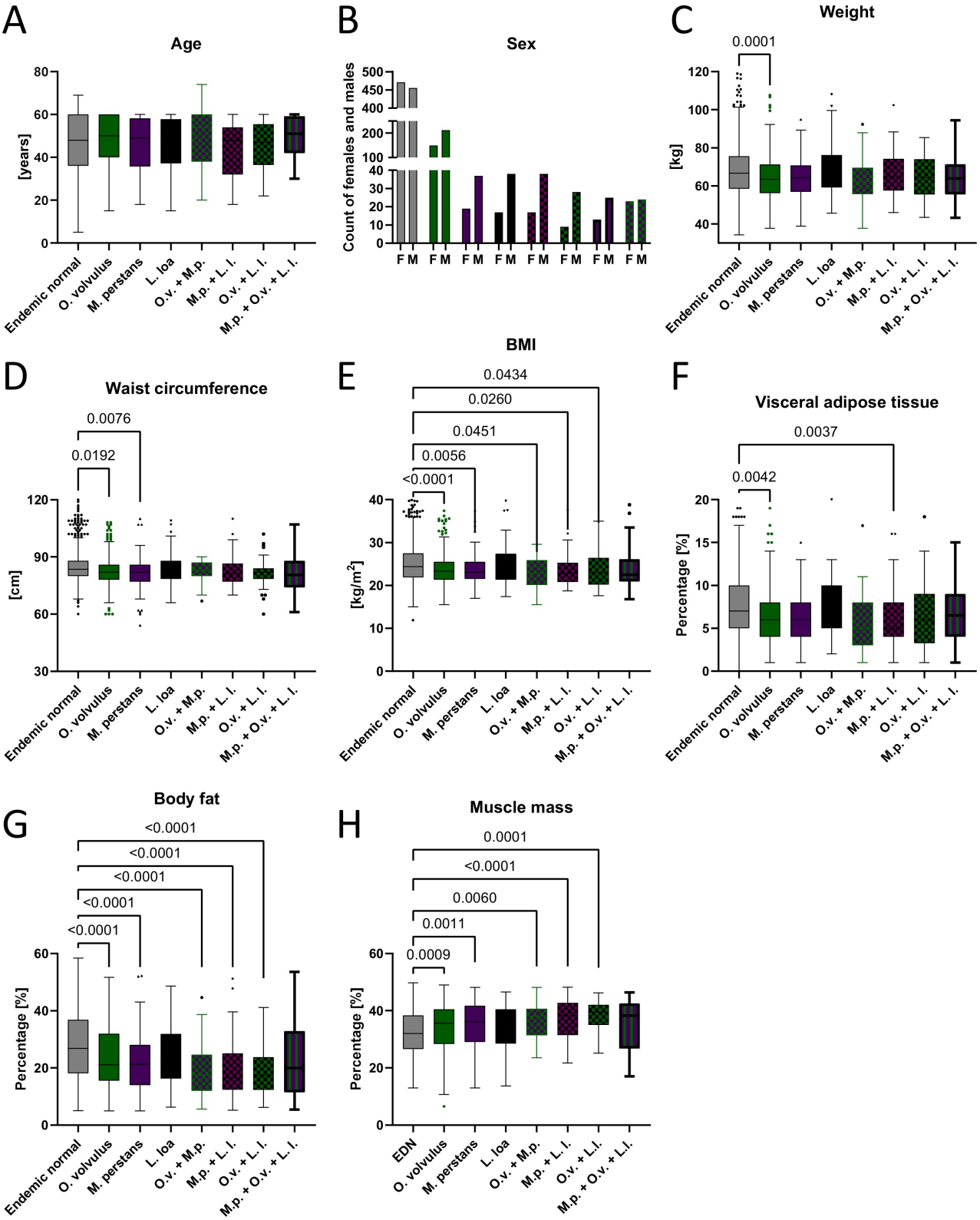
A
Age
[years]
Endemic normal
O. volvulus
M. perstans
L. loa
O.v. + M.p.
M.p. + L. l.
O.v. + L. l.
M.p. + O.v. + L. l.
B
Sex
Count of females and males
F M
C
Weight
0.0001
[kg]
D
Waist circumference
0.0076
0.0192
[cm]
E
BMI
0.0434
0.0260
0.0451
0.0056
<0.0001
[kg/m²]
F
Visceral adipose tissue
0.0037
0.0042
Percentage [%]
G
Body fat
<0.0001
Percentage [%]
H
Muscle mass
0.0001
<0.0001
0.0060
0.0011
0.0009
EDN

Figure 30. Anthropomorphic baseline characteristics of participants grouped according to their filarial infection, co-infection or absence of filarial infection. Age (A), sex (B), body weight (C), waist circumference (D), BMI (E), visceral adipose tissue (F), body fat (G) and muscle mass (H) for endemic normals, *O. volvulus* (O.v.), *M. perstans* (M.v.), *L. loa* (L.l.), *O. volvulus* + *M. perstans*, *M. perstans* + *L. loa, O. volvulus* + *L. loa* double or triple infected. Pairwise comparison was performed with Kruskal-Wallis and Dunn's multiple comparison between each infected and endemic group and significance with p<0.05. Data shown as median and interquartile range.

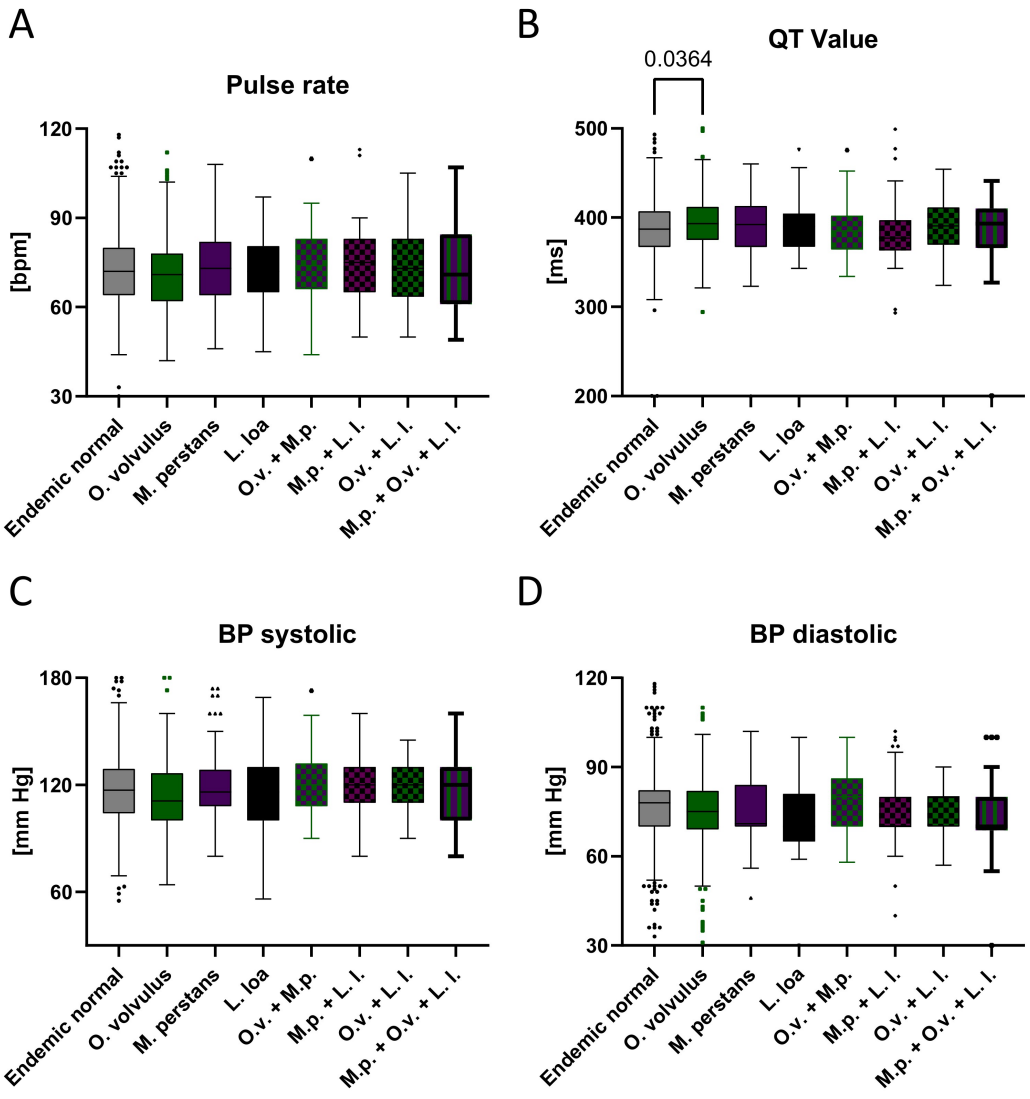

Figure 31. Pulse, QT value and blood pressure assessment of participants grouped according to their filarial infection, co-infection or absence of filarial infection. Pulse rate (A), QT-value (B), systolic (C) and diastolic blood pressure of endemic normals, *O. volvulus* (O.v.), *M. perstans* (M.v.), *L. loa* (L.l.), *O. volvulus* + *M. perstans*, *M. perstans* + *L. loa, O. volvulus* + *L. loa* double or triple infected. Pairwise comparison was performed with Kruskal-Wallis and Dunn's multiple comparison between each infected and endemic group and significance with p<0.05. Data shown as median and interquartile range.

3.2.11 Impact of different filarial infections on the white blood count

When differentiating the cohort into different filarial infections, leukocyte counts were significantly elevated in participants co-infected with *M. perstans* and *L. loa* as well as triple infected compared to EDN (Fig. 32A). Eosinophils but not neutrophils, basophils, platelet counts and hemoglobin were significantly increased in all FI groups when compared to the EDN participants (Fig. 32B-F). The lowest alteration in eosinophils was observed in *O. volvulus* and *L. loa* co-infected individuals (p = 0.049).

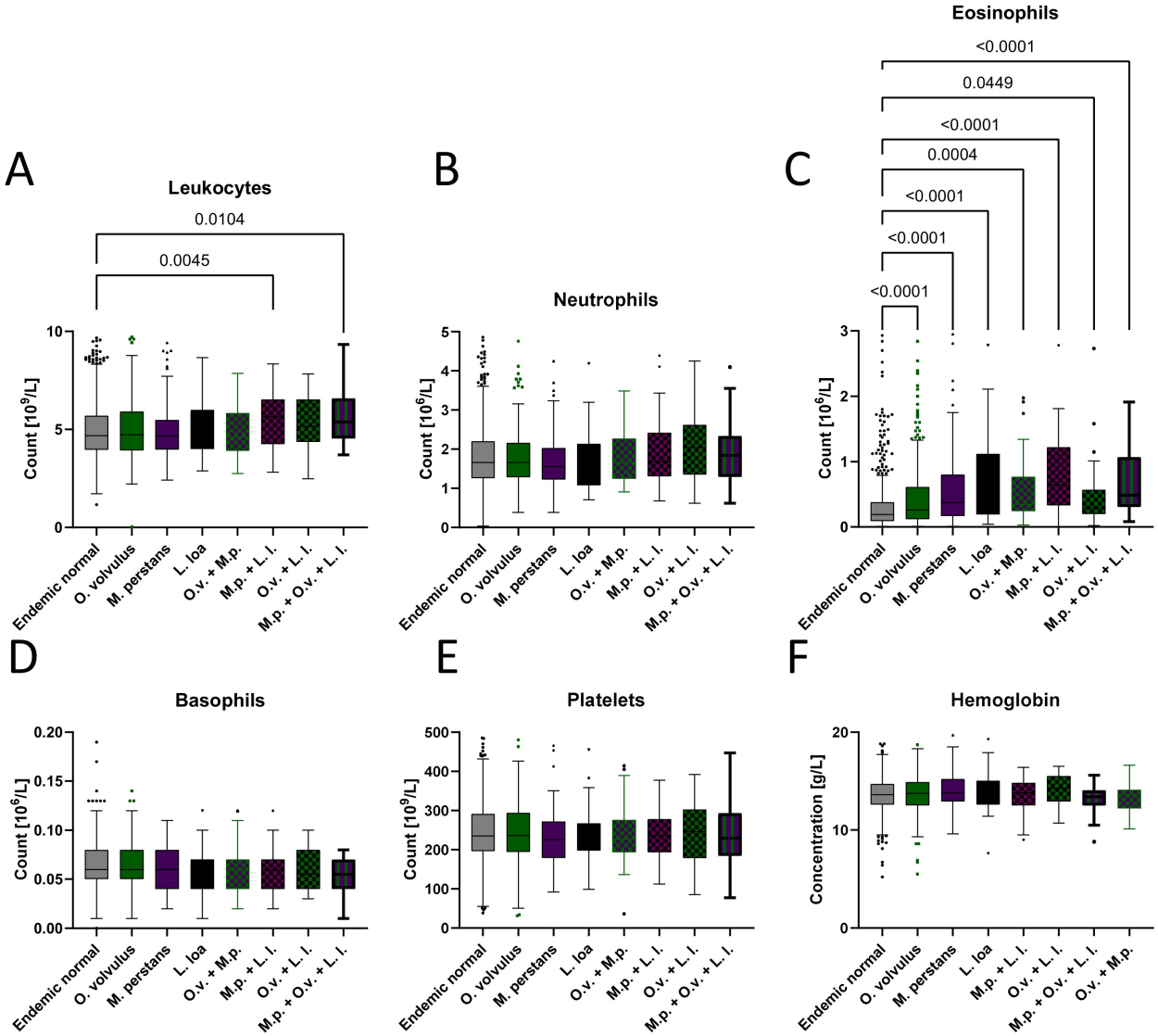

Figure 32. White blood cell analysis of participants grouped according to their filarial infection, co-infection or absence of filarial infection. Leukocyte (A), neutrophil (B), eosinophil (C), basophil (D), platelet count (E) and hemoglobin (F) of endemic normals, *O. volvulus* (O.v.)*, M. perstans* (M.v.)*, L. loa* (L.l.)*, O. volvulus* + *M. perstans*, *M. perstans* + *Loa, O. volvulus* + *Loa* double infected or triple infected. Pairwise comparison was performed with Kruskal-Wallis and Dunn's multiple comparison between each infected and endemic group and significance with $p<0.05$. Data shown as median and interquartile range.

3.2.12 Influence of filarial infections on the circulating enzyme, lipid profile and blood glucose

A potential difference in modulation of the host lipid profile was assessed by comparing LDL, HDL, total cholesterol, fasting blood glucose, triglycerides and HbA1c levels of each filarial infection and their co-infections to the EDN participants (Fig. 33A-F). LDL levels were not significantly different between EDN and FI, while total cholesterol was decreased by trend in patients co-infected with *M. perstans* and *L. loa* (Fig. 33A, C, $p = 0.0635$). HDL was significantly reduced in *M. perstans* single infected and *O. volvulus* + *M. perstans* double infected groups by trend (Fig. 32B, $p = 0.0632$). Fasting blood glucose was not altered in infected individuals (Fig. 33D). Surprisingly, triglycerides were increased in participants with *M. perstans* only (Fig. 33E). Strikingly, apart from *L. loa* single infected individuals, all infection groups displayed significantly reduced levels of serum HbA1c (Fig. 33F).

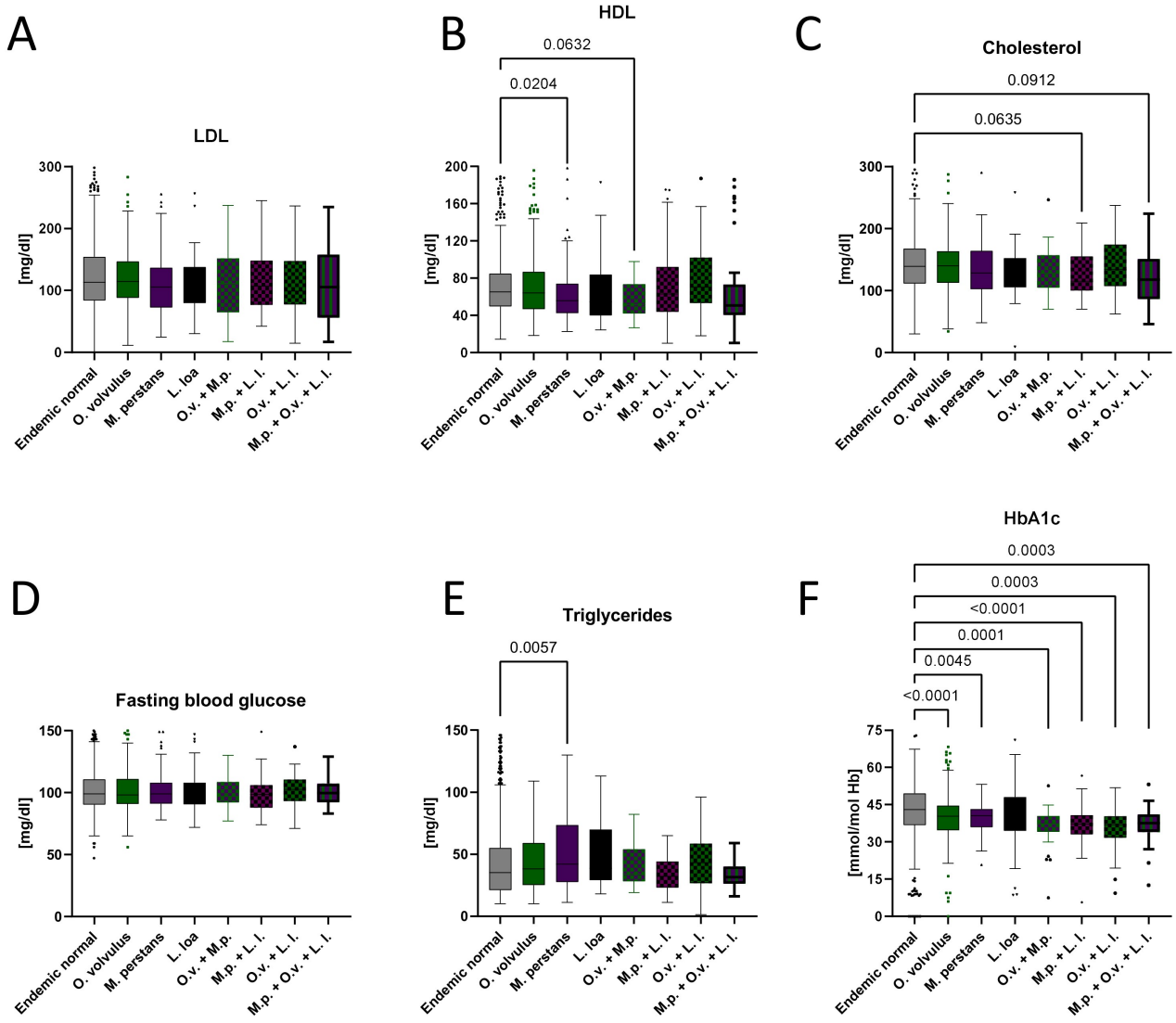

Figure 33. Circulating lipids and HbA1c levels of participants grouped according to their filarial infection, co-infection or absence of filarial infection. Circulating serum lipids: LDL (A), HDL (B), total cholesterol (C), fasting blood glucose (D), triglycerides (E) and HbA1c (F) of endemic normals, *O. volvulus* (O.v.), *M. perstans* (M.v.), *L. loa* (L.l.), *O. volvulus* + *M. perstans*, *M. perstans* + *L. loa*, *O. volvulus* + *L. loa* double infected or triple infected. Pairwise comparison was performed with Kruskal-Wallis and Dunn's multiple comparison between each infected and endemic group and significance with $p<0.05$. Data shown as median and interquartile range.

Due to prior observations that circulating liver enzymes were altered in FI individuals, all infections were again compared to the EDN participants (Fig. 34A-E). Serum ALP levels were significantly reduced in all filarial infected groups except for *L. loa* infected and *L. loa, O. volvulus* co-infected individuals (Fig 34A). ALT/GPT was significantly reduced in *O. volvulus* and *M. perstans* single infected and *O. volvulus, M. perstans* double infected and in *M. perstans, L. loa* double infected patients by trend (Fig. 34B p = 0.0615). AST/GST was only significantly reduced in *M. perstans* single and triple infected patients (Fig. 34C). Notably, all infections in which *M. perstans* was included displayed reduced levels of serum CRP. In case of *O. volvulus* and *M*. *perstans* co-infections this difference was only by trend, while the level of CRP was significantly reduced in all other groups including *M. perstans* infections (Fig. 34D). Interestingly, *L. loa* and *O. volvulus* either as co-infections or single infections did not induce this reduction, indicating that this might be an effect that is specific to *M. perstans*. In contrast, Gamma-GT was not altered (Fig. 34E).

Comparing markers for kidney function showed decreased serum creatinine for participants infected with *O. volvulus, M. perstans* and *O. volvulus* + *M. perstans* co-infected groups in comparison to the EDN participants (Fig 35A). Urine Microalbumine levels were significantly decreased in *M. perstans* and *M. perstans* + *L. loa* double positive groups (Fig 35B). Serum urea was not significantly altered between all infections and the EDN (Fig 35C).

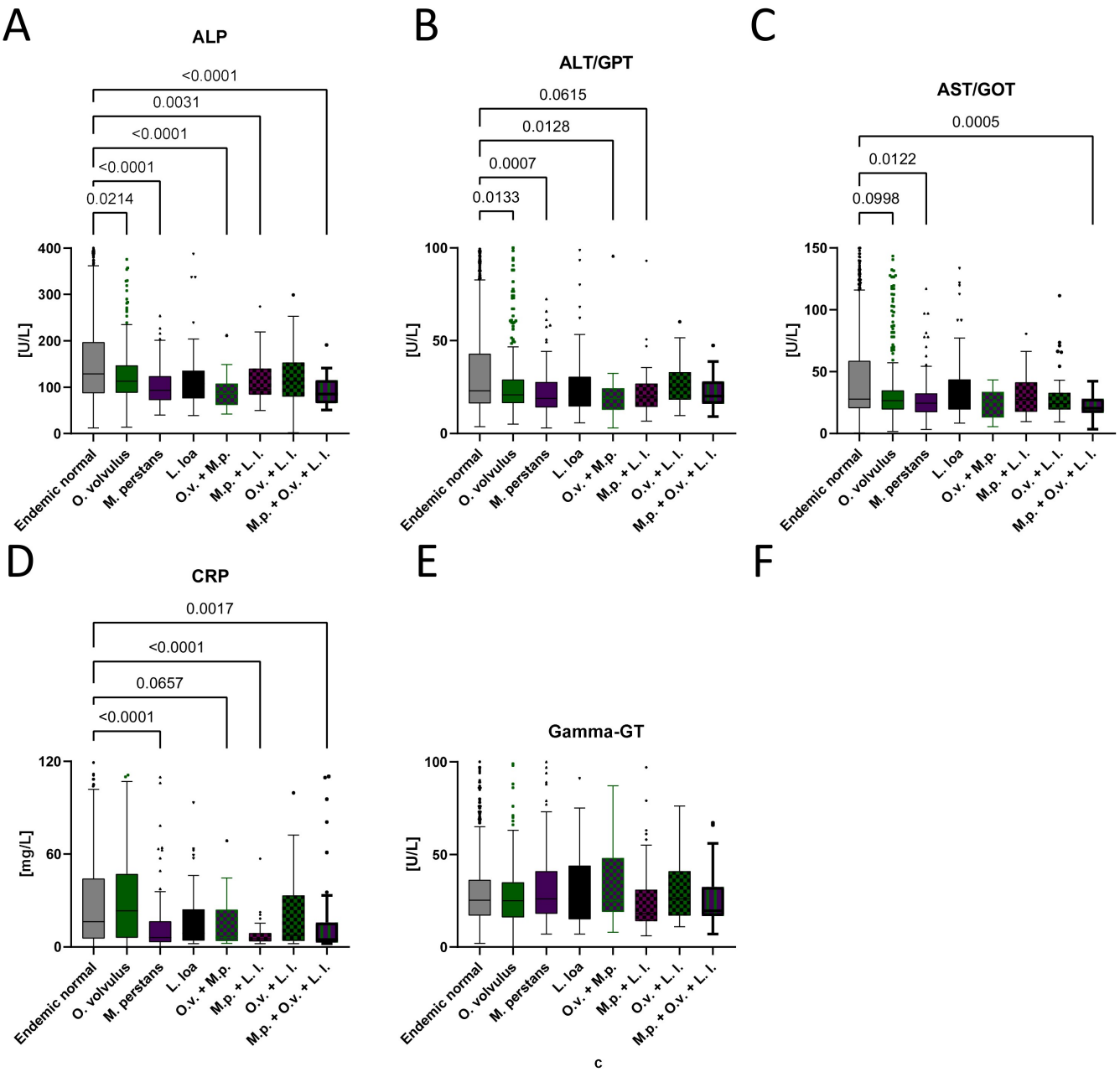

Figure 34. Circulating liver enzymes of participants grouped according to their filarial infection, co-infection or absence of filarial infection. Circulating liver enzymes: ALP (A), ALT/GPT (B), AST/GOT (C), CRP (D), Gamma-GT (E) of endemic normals, *O. volvulus* (O.v.), *M. perstans* (M.v.), *L. loa* (L.l.), *O. volvulus* + *M. perstans*, *M. perstans* + *L. loa*, *O. volvulus* + *L. loa* double infected or triple infected. Pairwise comparison was performed with Kruskal-Wallis and Dunn's multiple comparison between each infected and endemic group and significance with $p<0.05$. Data shown as median and interquartile range.

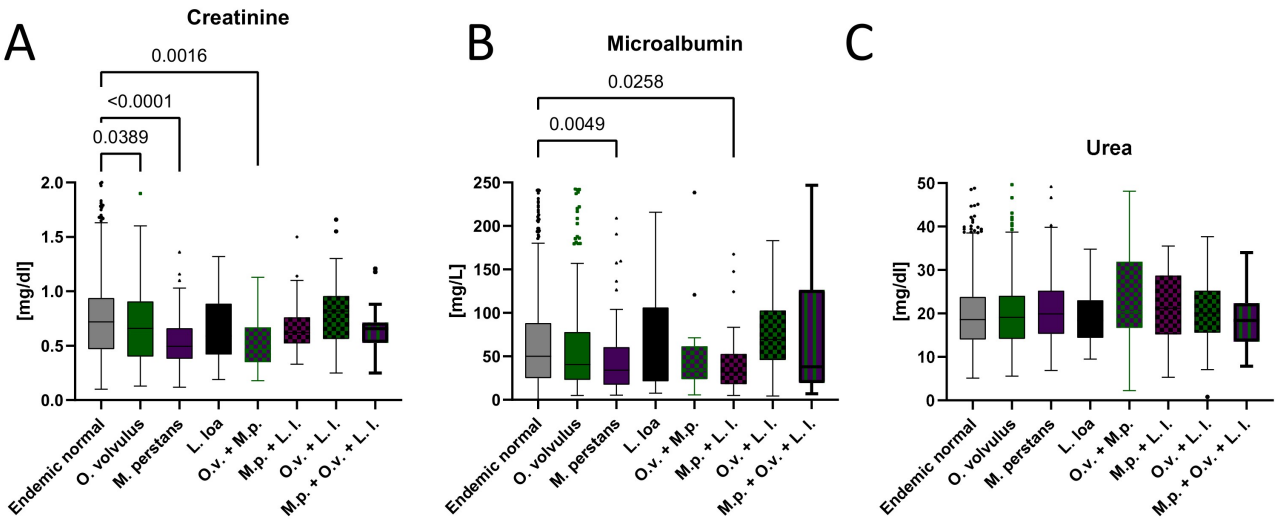

Figure 35. Circulating markers of kidney function of participants grouped according to their filarial infection, co-infection or absence of filarial infection. Kidney function assessment: Serum creatinine (A), urine microalbumine (B), serum urea (C) of endemic normals, *O. volvulus* (O.v.), *M. perstans* (M.v.), *L. loa* (L.l.), *O. volvulus* + *M. perstans*, *M. perstans* + *L. loa, O. volvulus* + *L. loa* double infected or triple infected. Pairwise comparison was performed with Kruskal-Wallis and Dunn's multiple comparison between each infected and endemic group and significance with $p<0.05$. Data shown as median interquartile range.

Lastly, the total and parasite-specific number of participants with an HbA1c level of above 48 mmol/mol Hb (6.5%), which is the main diagnosis criteria for T2D, was determined too (Fig. 36A). All participants that were already diagnosed with diabetes and indicated ongoing treatment were excluded from the analysis. A HbA1c level above 48 mmol/mol Hb was determined for 255 out of 828 EDN (31.0%) and 87 out of 648 filarial infected individuals (13.4%), indicating that filarial infection may indeed protect against T2D. These findings coincide with estimations that two thirds of all diabetes cases in Africa are not diagnosed to this point. When analyzed by BMI (Fig. 36B), filarial infected lean individuals displayed a T2D incidence of 11.2% while 22.8% of overweight and only 17.7% of obese FI participants were diabetic. In contrast, 37.4% of lean, 35.5% of overweight and 45.6% of EDN participants displayed an HbA1c above 48 mmol/mol Hb and were thereby considered diabetic (Fig. 36B).

Interestingly, the respective filarial infections displayed different rates of T2D (Fig. 36C, Tab. 15). Participants with *L. loa* and *O. volvulus* infections displayed a higher prevalence of T2D with 24.1 and 17.9%. Strikingly, T2D incidence in *M. perstans* individuals was only 9.4% and 0% of obese *M. perstans* infected individuals had an HbA1c value of above 48 mmol/mol Hb. Similarly, *L. loa* – *O. volvulus* double infected patients had a prevalence of 8.6% and all other double and triple infections were 4.29%. All in all, in line with improved CRP and HbA1c, incidence of T2D was decreased in filarial infected individuals compared to EDN. *L. loa* infections did not significantly reduce serum HbA1c and CRP levels and did not improve kidney and liver function which is in line with the less prominent protective effect against T2D. Accordingly, *O. volvulus* infected individuals had decreased serum HbA1c but not improved CRP levels and only displayed a decrease in some circulating kidney markers (creatinine but not microalbumin) and liver enzymes (ALP and ALT but not AST). *O. volvulus* infected individuals showed a lower T2D incidence than *L. loa* infected (*O. volvulus:* 17.9%; *L. loa:* 24.1%) but higher than *M. perstans* infected individuals.

In conclusion, *M. perstans* infected individuals displayed the lowest overall incidence of T2D out of the single infections. Taken together with the improved anthropomorphic profile, the decrease of CRP, HbA1c, improved circulating liver enzymes (ALP, AST, ALT) and improved circulating kidney markers (microalbumin, creatinine), *M. perstans* might be the most effective modulator of the metabolic profile and therefore could offer protection against T2D.

Table 15. Incidence of type 2 diabetes in different filarial infections and co-infections. Type 2 diabetes was defined as HbA1c above 48 mmol/mol Hb (6.5%).

Incidence of type 2 diabetes	HbA1c above 48 mmol/mol Hb	Total	%
Endemic normals	255	828	31.0
Filariae infected	87	648	13.4
O. volvulus	56	313	17.9
M. perstans	11	117	9.40
L. loa	13	54	24.1
M. perstans, L. loa	2	55	3.64
M. perstans, O. volvulus	1	35	2.86
L. loa, O. volvulus	3	35	8.60
M. perstans, L. loa, O. volvulus	1	38	2.63
Multiple infections combined	7	163	4.29
Total	342	1476	23.2

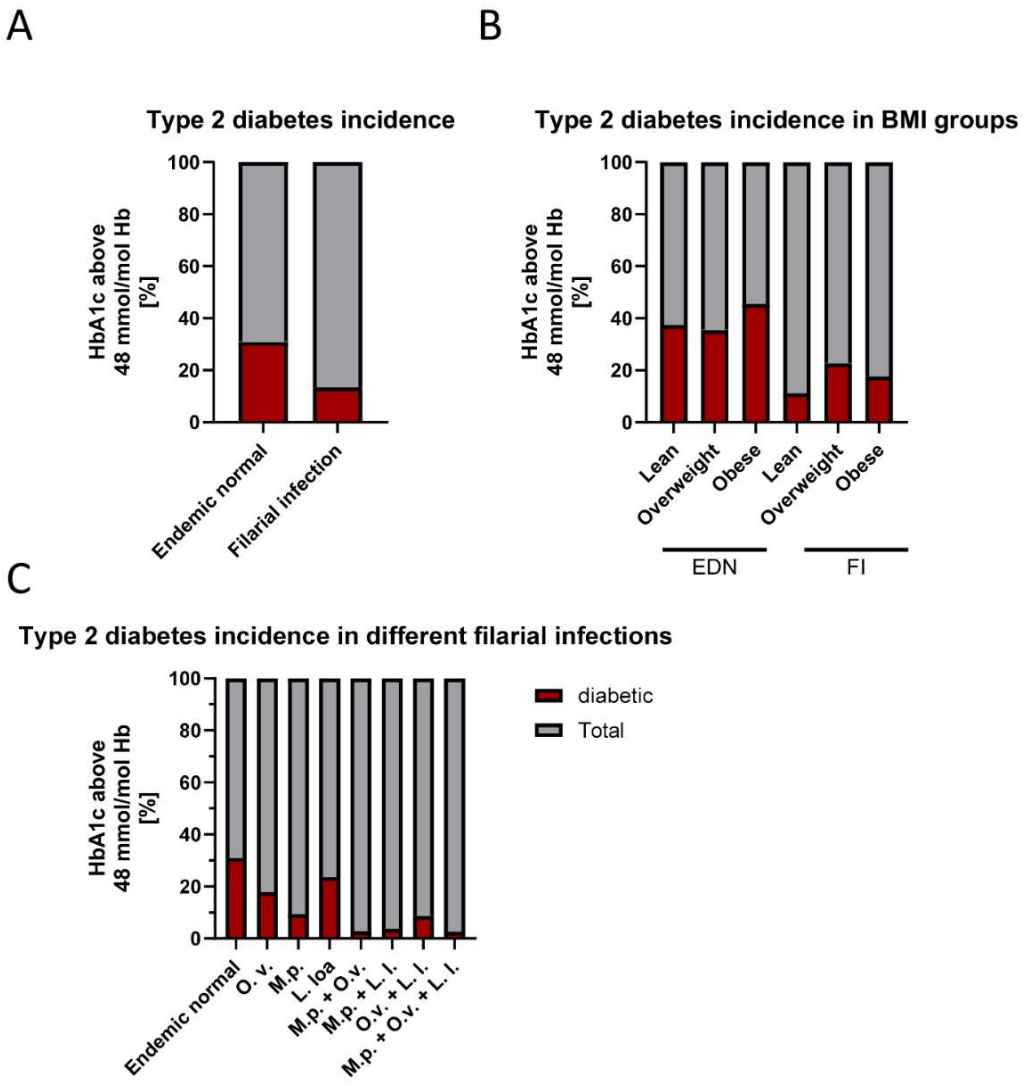

Figure 36. Incidence of diabetes in filarial infected and endemic control group. Percentage of participants with HbA1c levels above 48 mmol/mol hemoglobin with filarial infections (A), divided by BMI and infection status with FI=filarial infected and EDN (endemic normal) and split by infections (C) or endemic normal participants.

4. Discussion

4.1 Mouse model for tropical pulmonary eosinophilia using *L. sigmodontis*

4.1.1 Phenotype of the *L. sigmodontis* TPE model

The first objective of this thesis was establishing a mouse model for tropical pulmonary eosinophilia with the rodent parasite *L. sigmodontis.* The purpose of the model was to investigate the underlying mechanisms of TPE development and explore the role of eosinophils and IL-33 signaling in the context of MF-derived lung pathology using eosinophil-deficient dblGATA mice and the IL-33 antagonist HpARI. To trigger TPE-like symptoms, mice were sensitized with dead MF once a week totaling 3 times and challenged with living motile MF after a gap week. The concomitant immune response was analyzed. 24 hours after the final challenge, sensitized mice displayed increased MF clearance from the blood and a strong retention of MF in the lung. The retention was accompanied by increased cell influx into the lung, including prominent eosinophilia and an influx of monocytes compared to naïve mice (Fig. 12). Absence of eosinophils during TPE induction significantly reduced cell recruitment into the lung tissue and impaired MF retention 24 h after the challenge. Additionally, total and parasite-specific serum IgE was elevated after 24 h and 10 days (Fig. 12, 16). The cytokine response was dominated by IL-5 and IFNγ one day and IL-33 and IL-4 10 days after the challenge, respectively. Interestingly, the increase in lung cells and eosinophilia was still present 10 days after the challenge and was accompanied by an increase of AAM and ILC2s at this time point (Fig. 13). This was not the case in dblGATA mice which displayed significantly reduced AAM and ILC2 numbers, but again displayed elevated neutrophil frequencies. Eosinophilia extended to BAL and spleen at day 10 and eosinophils observed during TPE displayed increased expression of CD11b, Siglec-F, CD86 and the IL-33 receptor ST2 in the lung (Fig. 14). Furthermore, lung structural changes and hemorrhages were observed in 40% of the mice. Finally, inhibition of IL-33 signaling using HpARI reduced eosinophil activation, eosinophil accumulation in the lung tissue, suppressed type 2 immune responses and mitigated the development of structural damage to the lung. In the following discussion, the immune response observed in this model is compared to findings in human TPE patients and the TPE mouse model that uses *B. malayi* MF established by Egwang and Kazura in 1990 to assess the validity of this new model [75].

In the here presented model, we identify IL-33 signaling and eosinophil activation within the lung as main driver of TPE-induced immune responses within the lung that are associated with the retention of MF.

4.1.2 Validity of the tropical pulmonary eosinophilia mouse model

The evaluation criteria for a newly established mouse model in the context of infectious diseases is, as of now, not well defined. However, McKinney and Bunny suggested several criteria for validating a mouse model specifically for depression but broadened the criteria for mouse models in research [283]. Firstly, the newly established mouse model should be validated for its "Construct Validity". Construct validity describes the similarities and differences in the induction of the mouse model compared to the disease etiology of the human condition. TPE induction in the model is achieved by repeated sensitization of BALB/c mice using dead MF of *L. sigmodontis* and a final challenge with living and motile MF. Through the process of sensitization, an immune response is formed that leads to the trapping of MF within the lung of these mice and subsequently initiates a local immune response. First and foremost, retention of MF in the lung is accompanied by eosinophilia and morphological changes of the lung tissue. Further, parasite-specific IgE is present in both the murine model and human TPE and IgE is crucial for hypersensitivity reactions [284, 285], indicating that in both cases MF-derived hypersensitivity originate from a mechanistically similar foundation.

That said, in human TPE, there are some differences in the induction that could potentially impact the validity of the mouse model or should be considered to be adjusted depending on the research hypothesis investigated. First, MF are released by the adult worms, recognized by the immune system and retained within the lung tissue and not injected intravenously [66, 67, 286]. Here the main difference is that the adult worms recently existed or are still alive within human TPE patients and the immune response could be influenced by the prior infection. Adaptations of the model could be performed using naturally infected mice and injecting MF intravenously before the adult worms release MF or treat MF-positive infected animals with microfilaricidal drugs like DEC or ivermectin and inject MF afterwards. Another option could be the usage of MF negative animals infected with *L. sigmodontis.*

This occurs in approximately 50% of the infected animals. The usage of these animals that are not suited for some research questions for the TPE experiments would additionally follow the 3R-principle.

Additionally, only a minority of lymphatic filariasis patients develop TPE [72]. This circumstance could be attributed to genetic differences, co-morbidities, interspecies differences and other environmental factors between individuals, as it is the case for other filarial pathologies like the occurrence of lymphedema. For instance, some TPE symptoms predominantly occur at night (nocturnal cough). Thus, nocturnal movement of the MF that are retained within the lung could induce nocturnal cough. Due to the absence of epidemiological data for TPE, identifying the factors that might lead to the different disease outcomes is difficult. In the literature, no difference in incidence of TPE originating from *Brugia spp.* or *Wuchereria bacrofti* could be found. However, it would be possible that one of the parasites is more likely to induce TPE. Further, depending on the region of transmission, different vectors can transmit lymphatic filariasis. Investigating the impact of different strains and species as well as integrating potential genetic differences of both the host or parasite and alternative environmental factors is a key strength of mouse models. Accordingly, it was demonstrated that in addition to *B. malayi* MF, MF of *L. sigmodontis* can induce TPE-associated immune responses.

The second aspect to validate mouse models is the “Face Validity”. This parameter describes how well the model replicates the disease phenotype in humans. In human TPE, MF are rapidly cleared from the blood and are retained in the lung tissue, liver and lymph nodes [66, 69, 287]. Further, Nutman et al. demonstrated a strong increase of parasite-specific IgE, IgG and IgM and total serum IgE [286]. Interestingly, IL-4 is associated with the induction of MF-derived pulmonary hypersensitivity [288]. Characteristics of the herein described mouse model are MF-clearance from the blood, development of eosinophilia in the lung, as well as elevated levels of IgE and IL-4 in the serum (Fig. 12B-D, M, N) and IL-4 in the BAL (Fig. 16B, J). Accordingly, induction of a type 2 immune response including ILC2s and AAM was observed (Fig. 13E-J). These aspects match the immunological phenotype observed in human [69].

In the model presented here, liver and lymph nodes were not investigated in-depth, however results from an ongoing cooperation indicate that lymph node weight increases in this TPE model.

Accordingly, liver and spleen were already demonstrated to harbor MF during active *L. sigmodontis* infections [289]. Thus, it is very likely that a similar retention is possible in this TPE model. Localization of MF in the above mentioned tissues as well as other organs could be assessed using whole tissue lysis and by performing PCR to detect filarial-specific *actin* and *Wolbachia ftsz*. Additional localizations of MF could be identified by labelling MF with a stable fluorescent tag (cell tracer) that survives the fixation process of organs. Injected, labelled MF could be identified within cleared whole organs by locating the fluorescence *ex vivo* using a laser scanning microscope.

TPE commonly presents with eosinophilic infiltrates within the lung tissue, fibrosis, fever and cough [67, 72, 286]. These parameters were only partially addressed in the here presented experiments. Mouse lungs did display hemorrhages in approximately 40% of animals and TPE mice showed decreased integrity of the lung tissue structure measured by the lacunarity (Fig. 17, Fig. 22). However, evidence from the performed experiments might not be sufficient to elucidate whether or not fibrosis and eosinophilic infiltrates are present within the lung tissue of these mice. Literature on *L. sigmodontis*-derived lung pathology highlights that it is likely that these hemorrhages originate from either eosinophils or neutrophils or a combination of both. Fercoq et al. demonstrated that MF-dependent thoracic pathology was associated with eosinophilic and fibrotic polyps [290]. Karadjian et al. described L3 larvae of *L. sigmodontis* induce pulmonary lesions that are associated with neutrophils [291]. To investigate the state of the lung tissue further, a micro-CT and additional histological investigations could be done to investigate the presence of infiltrates and fibrosis in the lung and the immune cells responsible. Masson's Trichrome staining for instance could be a simple way to detect fibrosis within the lung tissue [292]. Thus, lung sections were preserved from the presented experiments for histological analysis to further investigate if tissue damage and fibrosis are occurring in this model. In regards to fever, cough, fatigue, malaise and wheezing, assessment becomes increasingly more difficult. Fever in mice is often represented by hypothermia instead of hyperthermia and could be measured using a surface infrared thermometer [168, 293].

Cough and wheezing during TPE could be summarized into general restrictions in breathing and lung function. Here a lung function test could further validate the murine TPE model. Of note, a methodology for this analysis is already established and its use was prevented so far by not getting the approval from the local authorities (LANUV) [294].

The final assessment suggested by McKinney and Bunny is the “Predictive Validity”. This parameter describes how well a model can be used to predict unknown aspects of the disease it represents. This read-out is by far the most difficult to assess, because only time and future knowledge will prove or disprove advances made with the model. In the context of this murine TPE model, two results obtained indicate the potential for a predictive validity of this model. First, usage of the drug DEC which is used to treat human TPE but not OXF, a benzimidazole that does not act on MF, reduced TPE-like immune responses, i.e., ILC2s, in this model. This finding indicates that treatment that doesn’t target MF directly does not decrease TPE-like immune responses.

Secondly, the here presented results suggest that eosinophils and IL-33 signaling are fundamental in the development of TPE and absence of eosinophils as well as inhibition of IL-33 signaling impairs the formation of TPE-like immune responses. Furthermore, the presence of ILC2s in TPE is – to the best of my knowledge – described here for the first time. As the combination of IL-33, eosinophils and ILC2s are already associated with asthma and lung pathology, it seems likely that these findings could withstand the test of time and provide insight into the development of human TPE.

Taken together, the herein described novel mouse model mirrors many of the characteristics that are known from human TPE. Even though the induction of the model is different from the human disease, immunological features observed are predominantly similar between mice and humans. Moreover, further adjustments and additional measures that are specific to mouse models can significantly improve the informative value obtained from the model. Furthermore, extension of the already known mechanisms and potential treatment options like the intervention of the IL-33 signaling may already be useful details gathered from this work.

4.1.3 Comparison to the *B. malayi* mouse model

In addition to the observations made in humans during TPE, a mouse model using *B. malayi* MF was established by Egwang and Kazura in 1990 [75]. The *B. malayi* TPE mouse model shares many of the immunological processes observed in human TPE and the *L. sigmodontis* TPE model. *B. malayi* TPE presents with lung and blood eosinophilia as well as parasite-specific IgE. Using this model Sharma and Srivastava et al. showed that TPE mice develop a type 2 immune response [76] including the presence of eosinophils in the lung [77] and they reported that the independent phospholipase A2 [78] was essential for the development of lung pathology. IL-12 was shown to antagonize TPE development by Mehlotra et al. [79]. The type 2 immune response could also be observed as TPE mice in this study displayed, next to the eosinophilia and increased total and parasite-specific IgE, increased frequencies of AAMs and ILC2s as well as increased serum IL-4. The effects of IL-12 and the role of the independent phospholipase A2 were not investigated in the presented study here. Finally, Gang et al., observed eosinophils in the lung of B. *malayi* TPE mice that were phenotypically similar to the ones observed in this thesis, as they expressed high levels of Siglec-F and CD101.

A significant drawback of the *B. malayi* mouse model concerns the acquisition of the parasite. Obtaining *B. malayi* MF to study the underlying mechanisms and potential therapeutic approaches in non-endemic countries is a challenging task, particularly if experiments are to be performed on a routine basis. Moreover, the size difference of MF between *B. malayi* and *L. sigmodontis* is substantial. *B. malayi* MF are approximately 260 x 8 µm in size, while *L. sigmodontis* MF approximately are one third of the size with 78-85 x 3.5 µm [49, 295]. This circumstance might be relevant when deciding on which of the two model is more “physiological”. The *B. malayi* mouse model might suffer from amplified immune responses and artificial clogging of capillaries by MF as human microvessels are double the size compared to mice [296]. However, in some instances, elevated immune responses might be beneficial to highlight minuscule changes that lead to disease development. That said, a key advantage of the *L. sigmodontis* TPE mouse model is the potential to incorporate the presence of adult worms. This project focused on the contribution of eosinophils in recognition, lung pathology development and formation of an immune response against MF.

Adapting the model in a way that includes adult worms in the system would integrate the immunomodulatory effects of a patent infection and therefore greatly extend similarities to the human TPE immune responses. Comparing the observed immune responses in the respective mouse model allows to elucidate on many similarities. For instance, alternatively activated macrophages, parasite-specific IgE and eosinophilia increase similar to the published model as well as the human condition [67, 75, 76, 297].

4.1.4 The role of eosinophils and IL-33 during tropical pulmonary eosinophilia

The distinct role of eosinophils during helminth infections and allergic disease is difficult to define. On one hand, eosinophils are an essential part of the protective immune response against MF in filarial infections of mice and humans [91, 203, 298, 299]. On the other hand, eosinophils actively partake in airway remodeling, hyper-responsiveness and can cause tissue damage and fibrosis [300]. During TPE seemingly both types of responses combine for the disease development.

This thesis shows that IL-33 mediates the presence of highly active eosinophils during murine pulmonary eosinophilia induced by MF sensitization and challenge. These eosinophils are characterized as Siglec-F^{high}, CD11b^{high}, CD86^{high}, ST2^{high} and CD101^{high}. In the literature, a separation of eosinophils into regulatory eosinophils (CD101^{low} Siglec-F^{int}) and inflammatory eosinophils (CD101^{high} Siglec-F^{high}) during experimental murine asthma was made by Mesnil et al. in 2016 [301]. Similarly, Gang et al. recently demonstrated that an increase in inflammatory eosinophils occurs in the *B. malayi* TPE model [302], which could indicate that these eosinophils might be associated with lung hyper-responsiveness, MF clearance and potentially lung pathology.

Interestingly, CD101 expression on eosinophils was not significantly increased after treatment with IL-33 in the *L. sigmodontis* TPE model (Fig. 19D). It has been reported that CD101 expression on eosinophils is induced by amphiregulin, an additional alarmin-like molecule that is produced by mast cells upon IgE cross-linkage, pathogenic Th2 T cells, γð-T cells, eosinophils themselves as well as ILC2s [193, 303-306]. Pathogenic Th2 T cells and ILC2s in the lung which express high levels of the ST2 receptor were shown to respond to IL-33 with the release of amphiregulin and thereby inducing the release of osteopontin by eosinophils. This process has been shown to contribute to airway fibrosis in house-dust-mite sensitization of mice [305].

Similar mechanisms might be at play during TPE development as *in vitro* stimulation with IL-33/IL-5 did not significantly increase CD101 expression on bone marrow-derived eosinophils. Measuring amphiregulin in the serum or BAL fluid of TPE mice using ELISA could provide more insight into mechanistic similarities.

Further differentiations in eosinophil subtypes were recently demonstrated by the work of Gurtner et al. that introduced immature B-eosinophils and active A-eosinophils in the gut which could be induced by an IFNγ and IL-33 treatment [307]. Ongoing research trying to replicate these findings in other organs, i.e. in the lung tissue, were not able to locate this eosinophil subtype. In their study active eosinophils were associated with regulatory functions and bactericidal efficacy. In the here presented experiments, eosinophils were cultured with IL-33 in combination with culture media containing IL-5, which might be an important detail to outline the phenotypical differences, due to IL-5 inducing eosinophil maturation and activation. That said, in the context of this TPE model, experiments using dblGATA mice showed that eosinophils mediated entrapment of MF, formation of a type 2 immune response and potentially contributed to pathological alterations in the lung tissue.

It was described previously that IL-33 is activating eosinophils and driving eosinophilia [308, 309]. For example, IL-33 increased expression of CD11b on eosinophils in this study which was described previously to promote cell adhesion by Suzukawa et al. [310]. Results obtained in this thesis further highlight the role of IL-33 signaling during the development of MF-induced pulmonary eosinophilia. Inhibition of IL-33 signaling during TPE development reduced eosinophil frequency and activation, further fortifying the role of IL-33 in controlling eosinophilia and eosinophil activation in the lung. The origin of IL-33 in this TPE model was not assessed in this study. That said, it is likely that lung epithelial cells are the main source of IL-33 release [311] but it could also be released by immune cells directly [312]. This hypothesis could be tested by using a conditional knock in of report IL-33 mice that express a GFP-labelled version of IL-33 in epithelia cells. Serum IL-33 originating from epithelia cells would be detectable in a plate reader, tracing back if the IL-33 is indeed released by these cells.

The factors responsible for the damage to the lung architecture are not clearly defined as of now. The movement of MF through the blood vessels by itself might be enough to cause damage to the lung tissue, thereby inducing the release of IL-33 and recruitment of immune cells. The recruited immune cells in turn could cause additional damage and amplify the effects. However, up to now very little is known about the interactions of MF with epithelial cells. MF have been found in close proximity to epithelial cells and the occasional adherence of MF to the epithelial barrier has been reported for some species of filariae [313].

This work indicates that the IL-33 release could be part of immunopathology. In fact, eosinophil-deficient dblGATA mice did not show elevated frequencies of lung ILC2s, AAM and had reduced serum IL-33 levels compared to wild type mice, which indicates a role of eosinophils in the release or production of IL-33 and the subsequent formation of a type 2 immune response. Thus, it seems likely that eosinophils recognize MF directly, as it was shown *in vitro* [158]. This recognition may then lead to the degranulation of eosinophils and cause damage to the epithelial cell barrier, recruiting AAM and inducing IL-33 release either directly or indirectly which in turn induces ILC2 proliferation, creating a feedback loop.

Further, ILC2s were detected within the lung of BALB/c mice in this TPE model. This has not been described in the *B. malayi* model yet, but their presence is very likely. ILC2s were not the main focus of this work, however, due to the high serum levels of IL-5, it is expected that ILC2s support the development of pulmonary inflammation by triggering the IL-5 mediated recruitment of eosinophils, controlling AAM differentiation by the release of IL-13 and thus exacerbating the disease progression in a similar manner as it was described in airway inflammatory processes [314-316]. The ILC2 frequency decreased when IL-33 signaling was blocked which is in line with prior studies that showed that IL-33 directly induces ILC2 expansion [317].

Interestingly, our *in vitro* experiments indicate that IL-33 stimulation triggers extracellular DNA trap formation (ETosis) from eosinophils (Fig. 19I). Ehrens et al. previously showed that eosinophil ETosis traps MF and supports MF removal [158]. Moreover, TPE mice displayed significantly increased DNA levels in the BAL and pleura wash, indicating either increased cell death or DNA expulsion from cells. This DNA release was slightly decreased when eosinophils were absent in dblGATA mice (Fig. 16G, H).

These findings suggest that increased DNA release and increased clearance of MF from the blood in TPE might be closely related and extracellular DNA-traps, high cell influx and cell-antibody-MF interactions might further tighten the small blood vessels surrounding the alveoli, shrinking the already tight diameter of~20-30 µm and thereby retaining MF within the lung tissue [158, 318].

4.1.5 Additional immune cell phenotyping

The analysis of the immune response honed in on the changing populations of specific myeloid cells, i.e., monocytes, alveolar macrophages, AAM, eosinophils and neutrophils within the lung tissue. However, there is merit in investigating the role of other immune cells in the context of MF-derived pathology. For instance, basophils and mast cells are highly relevant in pulmonary pathology and asthma [319]. Especially the high serum levels of IL-4 could be caused by basophils or mast cells [320, 321]. Moreover, substantial levels of IgE were measured in this murine TPE model. In mice, mast cells and basophils but not eosinophils are the primary responders to IgE as they utilize the high affinity IgE receptor FCεR1 [322, 323]. In contrast to murine eosinophils, human eosinophils express the high affinity IgE receptor [176, 324]. Nevertheless, mast cells and basophils should be investigated in the context of this murine TPE model in subsequent research.

In addition to myeloid cells, lymphoid cells are crucial to mount and maintain immune responses and are capable of contributing to pulmonary hyper-responsiveness. They are fundamentally involved in disease progression of chronic obstructive pulmonary disorder [325]. Especially in the context of TPE, B cells might essentially contribute to the immune response, due to IgE being present in all animal models as well as the human disease. In this thesis, B cell frequency was elevated in TPE mice and this increase was dependent on IL-33 signaling (Fig. 21A). In terms of understanding TPE immune responses, phenotyping B cells and their antibody profile could prove useful to further investigate the mechanisms of TPE development. Moreover, using µMT mice that have impaired B cell development and lack antibody production could assess whether or not the presence of B cells is necessary for the formation of TPE. A similar case can be made for T cells, however experiments did not depict alterations in lung T cell frequencies (Figure 21C, D). That said, phenotyping T cells into Th1, Th2, regulatory T cells and analyzing the intracellular cytokine profile is likely to reveal changes in the occurrence of Th2 populations.

Similarly, to basophils and mast cells, T cells could be a source of IL-4 and additionally produce IL-5 leading to the recruitment of eosinophils [326].

Interestingly, asthma-like symptoms and eosinophil inflammation were still inducible in $RAG^{-/-}$ knockout mice that lack B and T cells using IL-33 [327, 328]. This suggests that B and T cells might be important albeit redundant contributors to IL-33-mediated airway inflammation.

4.1.6 Hypothesis of TPE development

Based on information received from the experiments performed in this PhD thesis in combination with existing literature, the following immunological mechanisms are proposed to be involved in the development of TPE: The presence of eosinophils in the lung tissue and parasite-specific IgE, due to prior sensitization in mice or presence of adult worms in humans mark the starting point of TPE development. Addition of MF in this primed system potentially leads to the recognition of MF by immune cells with eosinophils playing a major role as it was demonstrated using dblGATA mice. Here, MF are most likely coated with immunoglobulins, particularly IgE, but they might also be recognized directly by the immune cells via pattern recognition receptors like the C-type lectin receptor dectin-1 as it was shown by Ehrens et al. 2021 [158]. The recognition of MF induces cytokine release (IL-5, IL-4), degranulation and extracellular trap formation by eosinophils.

In addition, extracellular DNA might contribute to platelet adhesion, further promoting the clogging process. If this process occurs in the thin blood vessels surrounding the alveoli, MF-cell complexes might get stuck and induce local inflammation due to the release of inflammatory mediators and cytotoxic granules. Subsequently, granulocytes degranulate, release IL-4 and recruit the tissue repair machinery, e.g. AAM and myofibroblasts. However, released granules and the movement of MF may damage the epithelial cell barrier of the blood vessels and lead to the subsequent release of IL- 33 and associated mediators like amphiregulin. IL-33 recruits ILC2s to the site of MF retention and induces IL-5 production, which in turn together with IL-5, IL-33 and factors like amphiregulin drive eosinophil maturation, inducing a pathogenic eosinophil phenotype leading to fibrosis which would ultimately facilitate clinical symptoms of tropical pulmonary eosinophilia.

4.2 Impact of filarial infections on the metabolic profile

4.2.1 Impact of filarial infections on the metabolic profile

The preliminary data presented in this thesis originates from the trial with the ISRCTN registry 43845142 which was set up for a six-year period and started in 2021. The trial is currently running and the 18 months follow up is still ongoing as of the writing of this thesis. As part of this thesis the baseline data describing the cohort was analyzed to elucidate differences and similarities between filarial infected and uninfected participants.

4.2.2 Anthropomorphic comparison of the cohort

Pulse rate, blood pressure and QT interval were not significantly different between EDN and FI participants. In contrast, weight, BMI, waist circumference, body fat and visceral adipose tissue were decreased in FI individuals. In order to determine if those differences are caused by the respective filarial infections, potential other causes have to be considered and are discussed below.

First and foremost, sex differences have major implications on the metabolic profile. Here, male and female participants were distributed equally in the EDN group. In contrast, among FI patients male participants dominated with 63.2%, while only 36.8% of participants were female. Besides the sex of the participants, age is a known risk factor for the development of T2D [329-331]. A similar age of FI (50.0) and EDN individuals (48.0) as observed in this study facilitates the comparison of the potential impact of filarial infections on the development of T2D (Tab. 5). Pre-menopausal women display higher skeletal and hepatic insulin sensitivity and secretion upon stimulation, resulting in lower fasting blood glucose and HbA1c values than age-matched men [332-334]. Further, in middle-aged populations, men show a higher prevalence of T2D than women [237]. However, after menopause, these differences are mitigated and differences in glucose tolerance are no longer apparent, leading to a similar cardiovascular risk [333, 335].

At this point, woman have higher changes in BMI, BP, lipids and fasting blood glucose [334, 336, 337]. The median age of the cohort is around the age of menopause, metabolic difference should be decreasing between men and women, but a potential bias due to sex differences between the FI group has to be considered.

Due to potential differences in the cohort that could be caused by sex-bias, a table containing all parameters investigated split by sex is provided in the supplementary information (Suppl. Table 1). Here, decreased weight, waist circumference, visceral adipose tissue and body fat was observed in males and females in the FI group compared to EDN participants. Interestingly, the median BMI of female FI individuals was 6% lower than the BMI of EDN females (FI: 23.6, EDN: 25.1), while males only displayed 3% reduced median BMI (FI: 23.0, EDN: 23.7). Taking a reduced group size into consideration after differentiation of male and female participants, this data suggests that observed differences were most likely not significantly altered by the imbalance of male and female participants in the FI group.

The reason for the difference in female to male ratio between FI and EDN participants in this study is open for speculation. In general, males are more susceptible for many parasitic infections [338, 339]. For filarial parasites, a review by Brabin from 1990 found that out of 7 studies, 6 study cohorts displayed an decreased prevalence for lymphatic filariasis in female participants in Africa [338]. 12 out of 14 studies from India and in 17 out of 22 studies conducted in South-East Asia reported similar findings [338]. Further, a study in Southwest Ethiopia found an *O. volvulus* prevalence of 10% in males and 2.5% in females [340]. These findings suggest that a decreased prevalence of filarial infections amongst female participants in this study is not an artifact of the recruitment process. There are several potential reasons for a sex specific difference in prevalence, i.e., immunological, behavioral and hormonal differences. For example, adult women exhibit a stronger adaptive and innate immune response than men, which might improve pathogen clearance and is primed towards a pro-inflammatory type 1 immune response [341, 342]. That said, lymphatic filariasis is associated with a severe stigmatization and psychosocial burden [343, 344]. This might allude to another contributing factor, if filarial infected males with pathology are more willing to exit social isolation compared to females.

Finally, occupational and cultural differences between men and women could add to the discrepancy in prevalence of filarial infections as both sexes might spend a different amount of time within areas of high transmission, such as farming fields and rivers.

The anthropomorphic data was mostly similar between male and female filariae-infected individuals, i.e., reduction of weight, waist circumference, body fat and BMI in comparison to the EDN participants were present and could indicate an altered anthropomorphic profile of FI individuals. Thus, this data provides indications that FI individuals might be leaner than EDN individuals. The cause of this reduced BMI, waist circumference and body fat could be attributed to numerous causes other than the filarial infection itself. For instance, increased physical labor and time spent outside of the house during the biting times of the respective vector could correlate with increased risk for infection [345]. In addition, dietary habits in different regions that might align with hot spots of increased transmission could further influence the physical fitness of the FI participants. For instance, regions which are highly endemic for filarial infections could demonstrate isolated dietary habits, i.e., low amounts of processed food due to being strongly secluded from markets and urban areas. That said, EDN and FI participants were recruited from the same study area, which suggests that dietary habits are comparable.

To analyze whether the differences between FI and EDN participants at baseline originate from dietary habits, physical labor or exposure, or are caused by the filarial infection itself, a detailed questionnaire was answered from each participant and will be evaluated once the study is completed. This questionnaire, which included physical exercise, income, standard of living, labor intensity, sport, region of origin and dietary habits will put these findings into perspective.

It is crucial to mention that the observed differences in anthropomorphic data were abolished when obese FI and EDN individuals were compared (Tab. 6), which allows a thorough analysis of the clinical, metabolic and immunological profile of these groups. Interestingly, prevalence of a clinical obese BMI (BMI ≥ 30) was doubled in EDN (13.0%) when compared to FI participants (5.6%). Hence, FI participants were less likely to be obese, however once obesity was reached, anthropomorphic measurements were comparable in both FI and EDN participants.

To further elucidate on the underlying causality, which most likely is not rooted in differences of female and male participants, for the reduced incidence of obesity and general leaner BMI of filarial infected participants, behavioral and dietary habits, the standard of living, occupation and the living environment of the respective groups will be assessed, using the data generated from the questionnaire that will be available in the near future.

4.2.3 Liver function assessment

Loss of liver function and pathology are a hallmark of T2D. Approximately 70% of T2D patients develop non-alcoholic fatty liver disease (NAFLD) [346]. NAFLD is characterized by hepatic steatosis or “fatty liver” in the absence of excessive alcohol consumption and can lead to non-alcoholic steatohepatitis, fibrosis and cirrhosis [347]. Liver cirrhosis in turn can increase the risk of hepatocellular carcinoma development [348]. Therefore, assessing liver function in the cohort and comparing FI and EDN groups as a whole and in the respective BMI groups might allude to potential effects of the filarial infections on T2D development and associated liver disease. Here, the circulating liver enzymes alkaline phosphatase (ALP), alanine-aminotransferase (ALT/GPT), aspartate-aminotransferase (AST/GST), gamma-glutamyl-transferase (GGT) and C-reactive protein (CRP) were assessed in the serum of the participants.

Strikingly, in this baseline data set, FI participants displayed significantly decreased ALP, ALT, AST and CRP levels compared to EDN individuals (19%, 11%, 6%, 34%, Tab. 8). In contrast, GGT levels were not significantly different between FI and EDN participants. However, it needs to be considered that the aforementioned parameters are closely associated with obesity and as mentioned above, the FI individuals displayed a slightly reduced BMI.

When the groups are divided by BMI, lean FI participants still displayed decreased ALP, ALT, AST and CRP serum levels compared to lean EDN participants. Interestingly, obese FI individuals displayed decreased GGT levels in addition to reduced ALP and AST. Especially the reduction of GGT, ALP and AST in obese FI compared to obese EDN participants and the reduction of CRP in lean individuals is of interest and future studies should investigate this in more detail.

Intriguingly, not all filarial infections investigated displayed the same capacity in reducing circulating liver enzymes (Fig. 34). For instance, *L. loa* infected individuals did not display a decrease in ALP, ALT, AST or CRP, while *O. volvulus* infected individuals displayed decreased ALP and ALT levels. In contrast, *M. perstans* infected individuals displayed significantly reduced levels of all four parameters. Furthermore, CRP levels for all co-infections including *M. perstans* displayed at minimum a decrease by trend (*O. volvulus* + *M. perstans*). This could indicate that *M. perstans* could be the most potent modulator of liver enzymes.

As mentioned before, CRP levels are closely associated with chronic inflammation and directly correlate with the risk of T2D and this decrease at baseline between infected and uninfected individuals could potentially indicate a protective effect of *M. perstans* in the context of continuous low-grade inflammation and thereby imply a similar effect on the development of T2D [252, 349]. Interestingly, CRP release often is triggered by IL-6 secretion. Serum IL-6 was previously described to be significantly decreased in the serum of *M. perstans* MF positive individuals, thus potentially being one of the mechanisms by which *M. perstans* infections modulate CRP levels [104, 350]. Thus, IL-6 will be assessed in the cohort serum and the levels between the respective filarial infections will be compared within the planned immunological analysis. Decrease of IL-6 levels and regulation of CRP gene expression could be a potential mechanism occurring in *M. perstans* infections, which might modulate continuous low-grade inflammation.

In summary, FI individuals displayed significantly reduced amounts of the circulating serum liver enzymes ALP, ALT, AST and CRP, indicating an improved liver function. Nevertheless, the medians of the respective parameters are close to normal ranges for a healthy population in most cases, often including all FI and EDN individuals even if obese. Lean EDN participants only slightly surpassed the normal range for ALP (134 U/lL, normal range: 130 U/L) and strongly surpassed the normal range of below 5 mg/ml CRP with 16.7 mg/ml. That said, these ranges are used for the clinical assessment of a European population, which is in terms of living conditions, difficult to compare to rural regions with ongoing transmission of multiple infectious diseases and non-comparable hygiene standards. Of note, all other circulating liver enzymes were within the normal ranges even for obese participants.

The parameters assessed here were determined to be important predictors of T2D incidence. For instance, a study with 132.677 adults showed that the increase in the circulating serum enzymes ALP, ALT, AST and GGT are associated with an increased risk of T2D development [351]. Similarly, CRP has been closely associated with increased risk for T2D and adult-onset obesity [251, 252]. A decrease in CRP and other circulating liver enzymes in FI participants could indicate improved liver function and a reduced risk of developing T2D.

Such a decrease of circulating liver enzymes and potential improvement of liver function in filarial infections was not found in the literature. Even soil-transmitted helminth trials, which are considerably more common than filarial studies, could not be found for the subject matter. Subsequently, no data was found linking ALP, ALT and AST to human helminth infections in a protective context. This indicates that the here obtained results are the first description of a beneficial effect of filarial infections on liver health and function.

On the other hand, some helminth infections were described to induce liver pathology. Stettler et al. suggested in 2001 that increased ALP levels might predict metacestode damage of the liver associated in *E. multilocularis* infections [352]. Further, infections with *Schistosoma spp.* can lead to severe liver pathology [353, 354]. In case of lymphatic filariasis, some case reports about liver pathology were published [355, 356]. Extending the scope from human filarial infections to animal infections provides some implications for the impact of filarial infections on circulating liver enzymes. One example of reduced liver enzyme function as a consequence of helminth infections was provided by Thamsborg and Hauge in 2001 in sheep. Here grazing lambs displayed decreased serum ALP and osteopenia when infected with *Ostertagia circumcincta* and *Trichostrongylus vitrinus.* Unpublished data from our group suggests that *L. sigmodontis* could have a similar impact on the bone structure of infected mice. This circumstance and the reduction of ALP within the human FI cohort could indicate that a process might be ongoing during human filarial infections.

Studies of human helminth infections that investigated CRP have found levels of CRP to be increased during intestinal helminth infections and in chronic lymphedema patients but not asymptomatic infections with *W. bancrofti* [357, 358].

The majority of studies conducted with soil-transmitted helminths did not detect a signifcant influence of said infections on serum CRP [359, 360].

Studies that support or contradict the decrease of CRP, AST and ALT could not be identified in the literature, indicating that this is the first discription of a reduction of circulating liver enzymes by filarial infections. Interestingly, splitting the different mono-infections into BMI subgroups (Suppl. Table 4) suggests that this improvement of circulating liver enzymes and potentially reduced inflammation as assessed by CRP is not only due to the fact that FI participants are of leaner BMI. However, it needs to be taken into account that the group sizes are strongly reduced in this procedure (obese EDN: 131, *O. volvulus*: 19, *M. perstans*: 5, *L. loa*: 8). Nonetheless, obese *M. perstans* and *L. loa* infected participants displayed a strikingly decreased median for CRP (obese EDN: 22.1 mg/L, *O. volvulus*: 26.8 mg/L, *M. perstans*: 13.7 mg/L and *L. loa*: 4.13 mg/L). Similarly, ALP, ALT and AST were reduced in obese *M. perstans* infected participants. Especially the differences in the obese groups but also the general reduction of circulating liver enzymes suggest a potential effect of especially *M. perstans* infections in promoting liver health, which in turn could have positive implications for T2D and obesity-associated liver disease like NAFLD.

4.2.4 Kidney function assessment

Continuous uptake of excessive macronutrients and metabolic obesity can not only lead to severe liver dysfunction, but also cause chronic kidney disease [361, 362]. Urine microalbumin, serum creatinine and serum urea were used as markers for kidney function in this trial. Microalbuminuria, i.e., urine microalbumin levels above 30 mg/L is closely associated with vascular damage of the glomeruli, small renal blood vessels that filter waste and water out of the blood [363, 364]. Glomeruli damage and the subsequent leakage of proteins into the urine are predictive of cardiovascular morbidity and mortality [363]. Furthermore, in T2D patients, a relationship between microalbuminuria and myocardial infarct and stroke was established and 20-40% of T2D patients with microalbuminuria progress to overt nephropathy and end-stage-renal disease [365-368].

At baseline, FI participants displayed a reduction of 21% in urine microalbumin levels in comparison to EDN participants (Tab. 8). After BMI matching, the differences were the strongest when comparing overweight FI and overweight EDN individuals, while lean and obese FI individuals compared to lean and obese EDN participants did not display a significant reduction. However, the median reduction was 18.4% (FI: 40.8 mg/L, 37.8-49.7 mg/L CI; EDN: 50.0 mg/L, 44.03-54.5 mg/L CI) for lean FI and 28.3% for obese FI individuals when compared to the respective EDN groups (FI: 34.9 mg/L, 18.3-53.9 mg/L CI; EDN: 48.7 mg/L, 33.3-65.0 mg/L CI). This could indicate that filarial infections have a beneficial effect on the maintenance of renal function. Similar to the striking reduction of CRP, microalbumin levels were the lowest in *M. perstans* infected individuals (Fig. 35). This might suggest that *M. perstans* infections have a positive effect on glomeruli filtration rate and subsequently kidney health. That said, honing in on potential beneficial effects and mechanisms of improved kidney health would need further investigations. For instance, measuring glomerular filtration rates in real time could be done using fluorescent markers [369]. This would allow future studies to assess if the decreased urine microalbumin is in fact due to increased filtration or is originating from dietary differences. That said, assessing glomerular filtration rates in the field is a difficult task and would require additional visits for the patients which in turn needs an additional ethics application, field activities and funding and is therefore challenging.

Another more feasible but more indirect assessment of glomerular filtration rate and kidney function is the accumulation of waste products within the blood. Default parameters to evaluate waste accumulation are serum creatinine, a product of muscular creatine catabolism, and serum urea, the primary metabolite from dietary and tissue protein turnover [370]. In this trial, serum urea was not statistically different between FI and EDN individuals. This neither changed when the cohort was evaluated after BMI matching nor after dividing the participants by their respective filarial infection. In contrast, serum creatinine was significantly reduced in FI compared to EDN individuals. Similarly, lean FI participants displayed decreased creatinine compared to lean EDN participants. Furthermore, *O. volvulus* infected and *M. perstans* infected as well as the *M. p.* – *O. v.* double infected participants displayed reduced serum creatinine. Elevated serum creatinine levels are associated with increased cardiovascular risk [371, 372].

However, recent publications suggest that in the context of T2D, low serum creatinine is a risk factor for the development of T2D in Japan and Korea [373, 374]. In contrast, glomerular filtration rate was impaired within 40% of patients in a cross-sectional study in Thailand [375].

Estimating the glomerular filtration rate can be done by using sex, age and creatinine values [376]. Using the median age and creatinine for the study population results in a glomerular filtration rate that is within the normal range of above 60 ml/min/1.73m^2 for FI participants (116 ml/min/1.73m^2 for male FI, 108 ml/min/1.73m^2 for females) and EDN participants (113 ml/min/1.73m^2 for males, 103 ml/min/1.73m^2 for females). Importantly, even though high creatinine levels are a predictor of kidney disease and cardiovascular risks, creatinine levels assed here were within the normal range, indicating a general good health in the study population independent on the filarial infection status and BMI. Due to the BMI difference between FI and EDN participants at baseline, obese individuals of the respective filarial infections were compared (Suppl. Table 4). Amongst obese individuals in this cohort, the median creatinine (0.38 mg/dl) and microalbumin (21.8 mg/L) was the lowest in *M. perstans* infected individuals. Obese EDN participants had the highest creatinine (0.72 mg/dl) and microalbumin (48.7 mg/L) levels. Although the group sizes are small for the obese infected participants, this further indicates that the differences are not only due to a reduced BMI of FI individuals and especially *M. perstans* infected participants displayed improved circulating kidney markers even if obese.

Taken together, the reduction in urine microalbumin and decreased serum creatinine could hint towards improved kidney function during filarial infection. Mechanisms that could improve kidney health as a side effect of the filarial infections are hard to pinpoint with the data collected to this point. As of writing, literature regarding parasites improving kidney function is limited. On the contrary, parasitic infections, including filariasis, can induce renal pathology, e.g., glomerulonephritis or glomerulonephropathy [377]. For example, secondary collapsing glomerulopathy of a 56 year old woman was associated with a *L. loa* infection in Congo [378]. In Brazil, some MF positive *B. malayi* infected individuals displayed proteinuria and hematuria before treatment. After the treatment almost all MF positive displayed these symptoms transiently [379]. In line, *B. malayi* infected patients in India displayed renal abnormalities [380, 381].

In case of onchocerciasis, one study has implied that among patients with renal failure in an *O. volvulus* endemic region of unknown prevalence, 9 out of 63 were infected with *O. volvulus* [382]. Due to missing data about the baseline prevalence of onchocerciasis, it is not clear if this incidence is significant. For *M. perstans* infections, no literature was found. When comparing these findings to the data depicted here, *L. loa* single infected individuals displayed the highest microalbumin level within the urine (median: 47.49 mg/L) compared to all other single infections. *L. loa – O. volvulus* double infected individuals displayed the highest median compared to all other groups (median: 69.25 mg/L) (Fig. 35). While the literature provides some insight into effects of filarial infections on the kidney, all listed instances were associated with pathology.

Values of microalbumin and creatinine obtained for *M. perstans* positive individuals were in contrast to these findings. The observed reductions indicate a potential beneficial effect of *M. perstans* on these parameters. A more in-depth analysis would be required to depict the actual state of the kidney to compare the physiological relevance in this circumstance. The best assessment would be a combination of the assessment of the globular filtration rate together with a tissue biopsy. Such invasive investigations are unadvisable for field studies with limited medical equipment and are ethically questionable when taking patient risk into account and weighing the potential scientific benefit. Non-invasive strategies like ultrasound could be used to observe potential fibrosis and scaring of kidney and liver in a follow-up investigation.

There could be several mechanisms triggered by filarial infections that could potentially improve kidney function. Immune responses are crucially involved in the development of kidney disease in the context of diabetes [383]. Interestingly, in human diabetics, reduced IL-6 levels among diabetics was associated with a 14% decreased risk for kidney disease after one year [384]. Taking again into consideration that *M. perstans* MF positive individuals were previously described to have decreased serum IL-6 levels, infections with *M. perstans* could have positive effects on long-term kidney function [104]. Further support for this hypothesis is provided by a study that showed a negative correlation between IL-6 and glomerular filtration rates in patients with chronic renal failure [385].

Another mechanism that could explain a potential beneficial effect on kidney function could be the suppression of auto-reactive IgG3 antibodies together with Th1 cells which are crucially involved in injury and outcomes of several forms of human glomerulonephritis, i.e., crescent glomerulonephritis, anti-glomerular basement membrane glomerulonephritis and more [386-389]. Importantly, human filarial infections are often characterized by increased frequencies of regulatory T cells and enhanced levels of IgG_4 [84, 109, 110, 390, 391]. Both IgG4 class-switch and induction of regulatory T cells were demonstrated to promote immune tolerance [96, 392, 393].

4.2.5 White blood cell analysis

White blood cell counts are standard assessments during clinical trials and may serve as indicators for the health status of recruited individuals. In this trial, the FI group displayed increased eosinophils and white blood cells (Tab. 12). Eosinophilia is a central feature of helminth infections and was expected for FI participants [49]. However, obese FI participants did not display a significant increase of eosinophils compared to lean EDN individuals. Here, data from high-fat diet mice experiments suggests that eosinophils are reduced in the adipose tissue [394], which could indicate a similar mechanism in human obesity. It was shown that in a mouse model of diet-induced diabetes, blood eosinophils do not correlate negatively with obesity under non-helminth-infected conditions, however, excess eosinophils during filarial infections could be recruited to the adipose tissue from the blood, due to an increased activation and cell migration.

4.2.6 Impact of filarial infections on the lipid profile and blood glucose

Blood glucose and lipid profile are main parameters to assess metabolic health and disease. High amounts of lipids and glucose in the blood are fundamentally connected to lipid toxicity and hyperglycemia, which in turn can cause metabolic inflammation, so called meta-inflammation [395]. To assess the lipid and blood sugar profile of the cohort, fasting blood glucose, circulating cholesterol, high- and low-density lipoprotein (HDL, LDL), triglycerides and HbA1c were measured for each participant at baseline before treatment as well as 12 and 18 months after treatment.

High serum total cholesterol and LDL levels are associated with increased risk for cardiovascular mortality and the development of T2D [396]. Bhowmik et al. demonstrated that the risk for T2D was 12.75 times higher for participants that displayed increased combined LDL and total serum cholesterol [397]. In contrast, HDL was negatively associated with cardiovascular mortality [396]. In the present study, total serum cholesterol was slightly decreased in FI individuals (135, 131-139 mg/dl) compared to EDN participants (139, 135-143 mg/dl). Obese EDN participants displayed significantly higher serum cholesterol levels compared to lean EDN participants while, in contrast, obese FI participants displayed similar cholesterol values as lean EDN individuals. LDL levels were, by trend ($p = 0.057$) reduced in FI compared to EDN participants. However, FI obese participants displayed the highest median for LDL (149, 123-174 mg/dl). HDL and triglyceride levels were not statistically different between FI and EDN individuals. That said, *M. perstans* infected individuals displayed decreased HDL levels and an increase in triglycerides ($p = 0.0057$) (Fig. 33). Interestingly, if *M. perstans* infected individuals were split by BMI, obese *M. perstans* infected participants displayed high median serum cholesterol (184 mg/dl), LDL (166.5 mg/dl) and HDL (72.46 mg/dl) levels (Suppl. Table 4), thereby having the highest serum lipid content out of all groups. This is of importance, as high LDL and cholesterol are significant risk factors for cardiovascular disease while HDL is negatively correlated with it [396]. Due to the low group size of 5 individual, it is difficult to set these findings into perspective. However, even with this high lipid profile, circulating liver enzymes, kidney health markers and HbA1c were all improved in *M. perstans* infected individuals in comparison to obese EDN participants.

Taken together, filarial infections appear to have limited effect on the here assessed parameters investigating the lipid profile. Interestingly, triglycerides were very low in the obese groups of this trial. It would be expected that obesity significantly increased serum triglyceride levels. That said, Yu et al., described in 2012 that there is a triglyceride paradox in the individuals of African descent [398]. These findings suggest that in contrast to people of European and Asian origin, triglycerides are usually not associated with insulin resistance, cardiovascular disease and T2D in the African population. Moreover, obese people of African descent usually have normal triglyceride levels.

FI and EDN participants displayed no significant differences in fasting blood glucose (Tab. 10). However, when split by BMI, fasting blood glucose was significantly increased in overweight and obese EDN individuals (103 and 105 mg/dl) when compared to lean EDN participants (97 mg/dl). In contrast, obese FI individuals (101 mg/dl) did not display this increase when compared to lean EDN individuals. Although the measured fasting blood glucose levels were within the normal range for non-diabetics of below 120 mg/dl, this could indicate that blood glucose uptake is increased slightly in obese FI.

HbA1c is a predictor for long term blood glucose and is a predictor and diagnostic parameter for diabetes [399]. Diabetes is defined by prior diagnosis and current use of medications for diabetes (insulin or oral hypoglycemic agents) as well as/or fulfillment of criteria laid down by the WHO-IDF Consultation Group Report from 2006 [270], i.e., fasting capillary blood glucose ≥126 mg/dl or 2 h capillary post-glucose value ≥200 mg/dl. An alternative definition by the American Diabetes Association criteria (2014) guidelines requires HbA1c to be ≥6.5% or 48 mmol/mol Hb for the diagnosis of diabetes [271].

HbA1c reflects the average plasma level of glucose of the last eight to twelve weeks reliably and is therefore a solid measure for long term hyperglycemia [400]. In the study cohort, FI individuals (39.9 mmol/mol Hb) displayed a significant reduction of HbA1c compared to EDN participants (43.0 mmol/mol Hb). This difference was strongest between lean FI and lean EDN participants (38.9 and 43.7 mmol/mol Hb). Similarly, obese FI participants (40.0 mmol/mol Hb) displayed reduced median HbA1c levels compared to obese EDN participants (43.3 mmol/mol Hb), although this difference was not statistically significant. This difference is important to highlight, due to the characterization of a prediabetes state of above 43 mmol/mol Hb in EDN participants in comparison to a normal range of 40 mmol/mol Hb in FI ones. The reduction of 3.3 mmol/mol Hb in median HbA1c within obese FI compared to obese EDN individuals is within a similar range as a lifestyle change that includes a limit of 2 meals a day and additional exercise, achieving a reduction of HbA1c by 3.4 mmol/mol Hb within 3 months [401]. In comparison, in a 5-year trial oral anti-diabetic drugs reduced HbA1c levels by 3-12 mmol/mol Hb [402]. Interestingly, when split by their respective infections, *L. loa*-infected individuals where the sole group not displaying a significant reduction of HbA1c compared to EDN individuals (Fig. 33 F).

This discrepancy could be due to an imbalance in cohort size, due to the *L. loa* group only being 54 individuals which is only half of the *M. perstans* group. An increase in *L. loa* patients could result in a statistical significance as the median with 40.54 mmol/mol Hb for *M. perstans* infected is comparable to the median of 40.69 mmol/mol Hb for *L. loa* infected participants. This is even more obvious after splitting *L. loa* infected individuals by BMI (Suppl. Table 4). Obese *L. loa* infected individuals displayed a median HbA1c value of 40.5 mmol/mol Hb compared to the obese EDN participants with 43.3 mmol/mol Hb.

The provided data suggests that FI individuals have decreased HbA1c levels. This indicates decreased long-term blood glucose levels and could indicate improved insulin sensitivity. Importantly, prevalence of diabetes assessed by HbA1c was 31% in the EDN and 13.4% in the FI group. This prevalence strongly exceeds the expected percentage of 5-7% for Cameroon [403]. One reason for this discrepancy could be that HbA1c cut-offs for diabetes might be inadequate for individuals of African descent or the dietary habits in the rural Cameroonian study region and may need to be adjusted. However, Khosla et al. found that a diagnoses of T2D using the European normal range of above 48 mmol/mol Hb even lead to an underdiagnosis of T2D arguing for a stricter range for African Americans in four studies, while three studies stated that this normal range lead to an overdiagnosis of T2D [404]. Alarmingly, according to the WHO analytical fact sheet “Diabetes, a silent killer in Africa” approximately 54% of diabetes cases in Africa are undiagnosed [405].

4.2.7 Species dependent differences in filarial infection

Throughout the analysis performed, the various filarial infections influenced the here presented parameters to a different degree. For instance, *M. perstans*-infected individuals showed decreased BMI, waist circumference, visceral adipose tissue, body fat, BMI, ALP, ALT, AST, CRP, creatinine, urine microalbumin and HbA1c. As mentioned before, *L. loa*-infected individuals did not display any of these significant reductions, which could be simply due to the decreased group size and therefore a statistical artifact. In case of HbA1c, this circumstance becomes more prominent when *L. loa* positive individuals were compared after categorization by BMI.

Here, obese *L. loa* infected individuals displayed improved HbA1c compared to obese EDN participants (40.5 mmol/mol Hb compared to the obese EDN participants with 43.3 mmol/mol Hb). However, *L. loa* patient microalbumin levels for example are close to the median of EDN individuals (*M. perstans:* 34.0 mg/L, *L. loa:* 47.5 mg/L, EDN: 50.0 mg/L). These findings imply that *M. perstans*, the filarial parasite that produces the least disease specific symptoms, might also have the strongest immunomodulatory capacities. It is important to note that *M. perstans*-infected individuals were all positive for MF in this trial, which is not the case for the other filarial infections. In contrast, infections with *O. volvulus* and *L. loa* were assessed by PCR, many of which were MF negative. *M. perstans* infections are so far only detectable by PCR or microscopy when the individual is MF positive [61, 104].

This limitation should be taken into consideration when ranking the different filarial parasites by their capacity to modulate the metabolic profile, as the presence of MF influences the degree of immunomodulation present in *O. volvulus* [110]. MF positive onchocerciasis patients were shown to respond with higher IL-5, IL-10 and IL-13 levels after *ex vivo* stimulation and displayed increased serum IL-5 levels and eosinophil numbers, indicating an increased type 2 immune phenotype. Further, individuals that are positive for *O. volvulus* but MF negative could have I) received mass drug administration treatment beforehand, as for instance ivermectin can reduce the MF burden of *onchocerciasis* patients but does not affect *M. perstans* [49] or II) have an old infection were MF are no longer produced and potentially provide less immunomodulation. Additional evaluation based on MF load and presence for *O. volvulus* and *L. loa* will be performed at later time point to elaborate on the species specific differences. It is important to consider, that if there are MF negative *M. perstans*-infected individuals, which is not known yet, they would not be detected by the diagnostic tools used in this study and could be present in other groups of this study.

4.2.8 Do filarial infections provide a protective effect against type 2 diabetes?

The hypothesis of the trial was that filarial infection provides a protective effect against T2D and treatment of those filarial infections abolishes the protective effect. The preliminary baseline data was evaluated for differences and similarities between the FI and EDN individuals. In the following, the differences will be condensed and potential implications for the hypothesis but also for the following part of the trial will be presented.

The observed anthropomorphic differences between the two groups could be due the decreased percentage of females in the EDN group. However, separating FI and EDN participants displayed similar trends between male FI and EDN individuals as well as female FI and EDN participants (Suppl. Table 1). Nevertheless, an analysis for sex-biases and assessment of physical activity, income, diet and occupation will be performed within this data set, after the data is validated completely. That said, liver enzymes, kidney function assessment and the lipid profile are less likely to be influenced by sex. If the here described differences sustain after correction for socio-economic differences between the groups, it can be concluded that filariae influence body fat and body weight.

To further investigate this circumstance, the potential impact on energy consumption, adipose tissue browning and glucose hemostasis should be considered as an additional route of investigation. As of now, these measures are generally difficult to assess in humans using non-invasive methods, especially in rural areas of developing countries.

Browning of adipose tissue can so far only be monitored by detecting the expression of genes like *ucp1*, *cidea* or *pgc1a*, none of which are soluble and detectable in the serum [406]. Energy consumption, on the other hand, could be assessed by detecting metabolites that are associated with energy consumption and physical activity like *N*-lactoyl-phenylalanine, which is associated with supressed hunger and obesity and is a product of exercise [407]. Accordingly, long-term changes in glucose uptake as indicated by HbA1c would additionally benefit from the assessment of adipokines like adiponectin, visfatin, resisting, grehelin, leptin etc. These molecules could explain how sugar uptake may be modified in FI participants.

Finally, assessing insulin resistance by HOMA-IR within the respective groups is indispensable to elucidate on the impact of filarial infections on the metabolic profile. These measures alongside the investigation of the immunological profile of the participants are planned within the project and should help to further narrow down on potential mechanisms in which filariae are able to modulate the here presented parameters, i.e., HbA1c, CRP and circulating markers of liver and kidney health.

The medical significance of the reduction in liver enzymes, slightly improved kidney function and HbA1c need to be critically assessed. In general, the population investigated is within the normal range of most parameters for both populations. However, especially HbA1c and CRP are reliable risk factors that directly correlate with the likelihood of developing cardiovascular disease and T2D. The following treatment of doxycycline against *O. volvulus* and *M. perstans* and albendazole against *L. loa,* together with the follow-up visits at 12 and 18 months should further clarify the impact of filarial infection. Thus, the treatment of the filarial infections should abolish some of the differences found between FI and EDN individuals. A subsequent increase in CRP, HbA1c and insulin resistance, which will be assessed once the trial is completed, would provide compelling evidence for a protective effect of (some) filarial infections against T2D. This would further support the hypothesis of the trial conducted. However, metabolic changes and abolishing the established filarial immunomodulation potentially takes a long time. Therefore, a follow up proposal with a five year's follow up after the clearance of the infections is planned for this cohort. This long term follow up should be used to re-analyze the cohort and to elucidate on the consequences for the metabolic and immunological profile of clearing the filarial infections in the long term.

The main parameters indicating a potential role of filarial infections on the metabolic profile in this trial are HbA1c, CRP as well as liver and kidney function assessments. Especially CRP, liver and kidney enzymes are closely associated with inflammatory processes and auto-immune pathology that is closely associated with a type 1 immune response. Therefore, it is likely that suppression of pro-inflammatory immune responses by filaria-induced regulatory T cells and immunoglobulin class-switches to IgG4 and IgE could have a dampening effect on immunological processes that could lead to kidney, liver and general metabolic disease in obesity.

Based on this interim conclusion, an assessment of the immunological profile, i.e., phenotyping of the whole blood and assessment of serum cytokines will be performed as soon as all samples are obtained to further investigate the mechanism of the respective filarial infections to potentially modulate kidney and liver function and the metabolic profile with HbA1c and CRP in the focus.

In essence, FI individuals in this study displayed a decreased BMI, body fat and visceral adipose tissue. Further, FI participants displayed decreased circulating serum ALP, ALT, AST and CRP values, which could indicate a reduction of systemic inflammation and improved liver function. In addition, parameters assessing kidney functions might indicate decreased urine microalbumin and creatinine and thus improved kidney function. Furthermore, the lipid profile showed only minor differences between FI and EDN participants, while HbA1c was significantly reduced in FI, which was still consistent after BMI matching. Obesity induced kidney and liver dysfunction, metabolic inflammation assessed by CRP and long term lipid and sugar exposure measured by HbA1c are all potent predictors of metabolic disease and T2D. In this study, all these parameters were improved in the filarial infected cohort, especially in *M. perstans* infected individuals. These results, as of now, strongly support the hypothesis that filarial infections have a protective effect on T2D.

4.2.9 Helminth infections and T2D

Helminth infections have been associated with a protective effect against metabolic diseases and T2D in the past. Nazligul et al. reported an inverse relationship between soil-transmitted helminth infections and the prevalence of diabetes in 2001 [408]. Since then, several studies were published describing a positive impact of helminth infections, but not filariae on insulin sensitivity and a decreased risk to develop metabolic syndromes as well as a reduced diabetes incidence [129, 130, 281, 409-414]. A reduction of HbA1c, as demonstrated here, was also found in patients previously infected with *Schistosoma spp.* in China or actively infected with *Opisthorchis viverrini* in Thailand. Interestingly, *Strongyloides stercoralis* infections displayed contradictory findings.

Hays et al. demonstrated a potential protective effect of *S. stercoralis* on the development of T2D in infected indigenous inhabitants of Australia and that failure of treatment increases the risk of T2D development. In contrast, Rajamanickam et al. did not detect a decrease of HbA1c [137, 281, 282, 415]. Evidence of potential effects by filarial parasites was provided by trials conducted by Babu, Nutman and Aravindham et al., depicting a decreased incidence of lymphatic filariasis amongst type 1 diabetics [129, 130].

Taken together, evidence for potential protective effects against T2D by helminths are present, but filarial parasites are so far only linked to a protective effect in an experimental mouse model [163]. The here presented findings are in line with the literature and indicate a connection between filarial species and a reduction in CRP and HbA1c which are known predictors and risk factors for T2D and a pre-diabetic state. Furthermore, a potential beneficial effect on liver and kidney function is suggested by the findings of the baseline analysis. This improvement of circulating liver and kidney markers could not be found in the literature not only for filariae but helminths in general. This analysis supports the hypothesis that filarial infections provide protection against low-grade continuous inflammation that can lead to T2D and its associated pathologies by modulating CRP, HbA1c as well as circulating liver and kidney enzymes. The latter two being novel implications on improved kidney and liver function during (some) filarial infections.

4.2.10 Closing remarks

On the one hand, filarial infections can cause debilitating diseases that put a physical and socio-economic strain on the inhabitants of low- and middle-income countries. In consequence, treatment, prevention of transmission and education about the diseases is essential to alleviate this burden from some of the poorest regions in the Global South and facilitate disease free growth and development [416]. On the other hand, filarial immunomodulation and filaria-derived products might be a promising perspective in decreasing exacerbated and auto-reactive immune responses in the future. These two contradicting viewpoints underscore the significance of understanding the processes of disease development and immunomodulation between host and parasite and are required so that the best of both worlds may be obtained.

Curing filarial diseases and retaining some if not all of the immunomodulatory functions of parasitic infections by isolating active compounds from the lipidome, proteome, transcriptome and excretory secretory products of the filariae may be a promising way to combat the rise of lifestyle-derived and autoimmune diseases without the need of an active infection.

Supplementary information

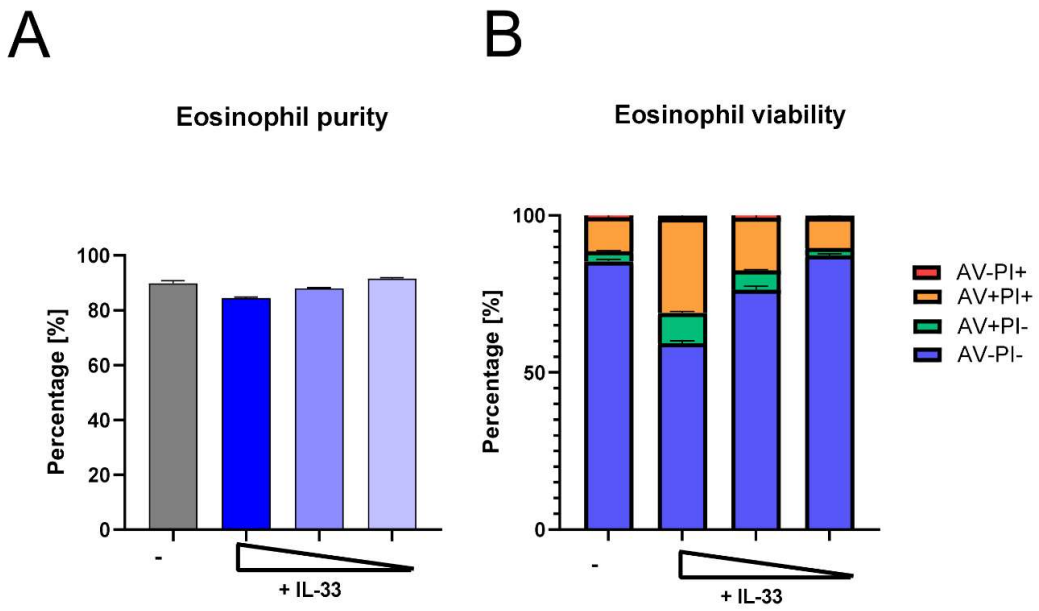

Supplement figure 1. (A) Purity and (B) viability of bone marrow-derived eosinophils after 24 h of *in vitro* culture. Data pooled from two independent experiments with n=6-12 mice. Shown are mean + SEM. Kruskal-Wallis test followed by Dunn´s multiple comparison was used for statistical analysis. p values ≤ 0.05 are shown. Experiment was performed by Dr. Alexandra Ehrens.

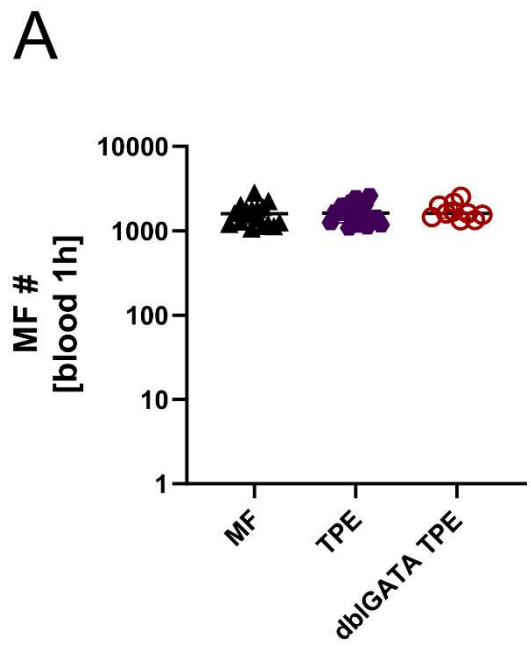

Supplement figure 2. (A) Number of microfilariae (MF) in 50 µl of peripheral blood 1 h after MF challenge injection of TPE WT and eosinophil deficient dblGATA mice as well as MF only challenged mice (MF). n=10-18 animals per group. Data is shown as median with interquartile range. Statistical analysis was performed with Kruskal-Wallis followed by Dunn´s multiple comparison test. p values ≤ 0.05 are shown.

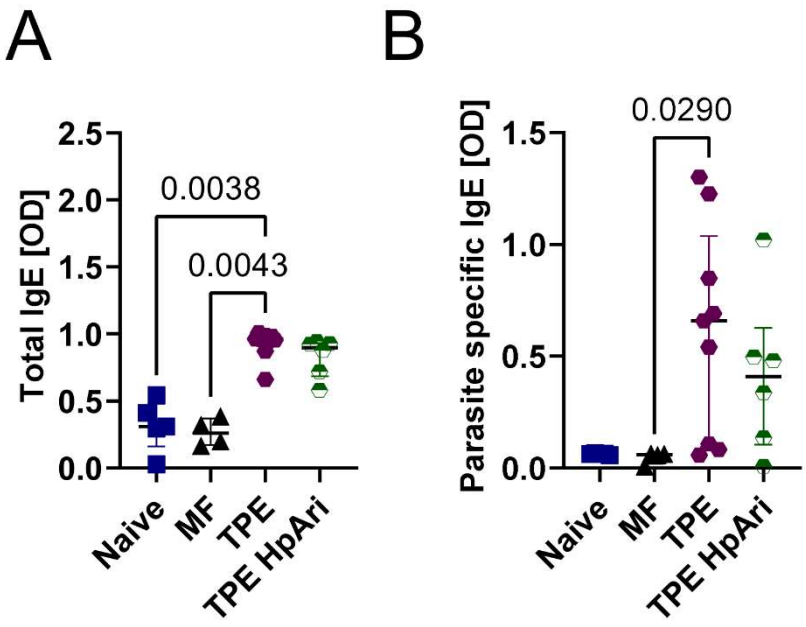

Supplement figure 3. Serum (A) IgE and (B) parasite-specific IgE of naïve, and 10 days after the final challenge of MF-challenged, TPE and dblGATA TPE mice. Data shown is from 1 experiment with n= 4-5 mice. Data is shown as median with interquartile range. Statistical analysis was performed with Kruskal-Wallis followed by Dunn´s multiple comparison test. p values ≤ 0.05 are shown.

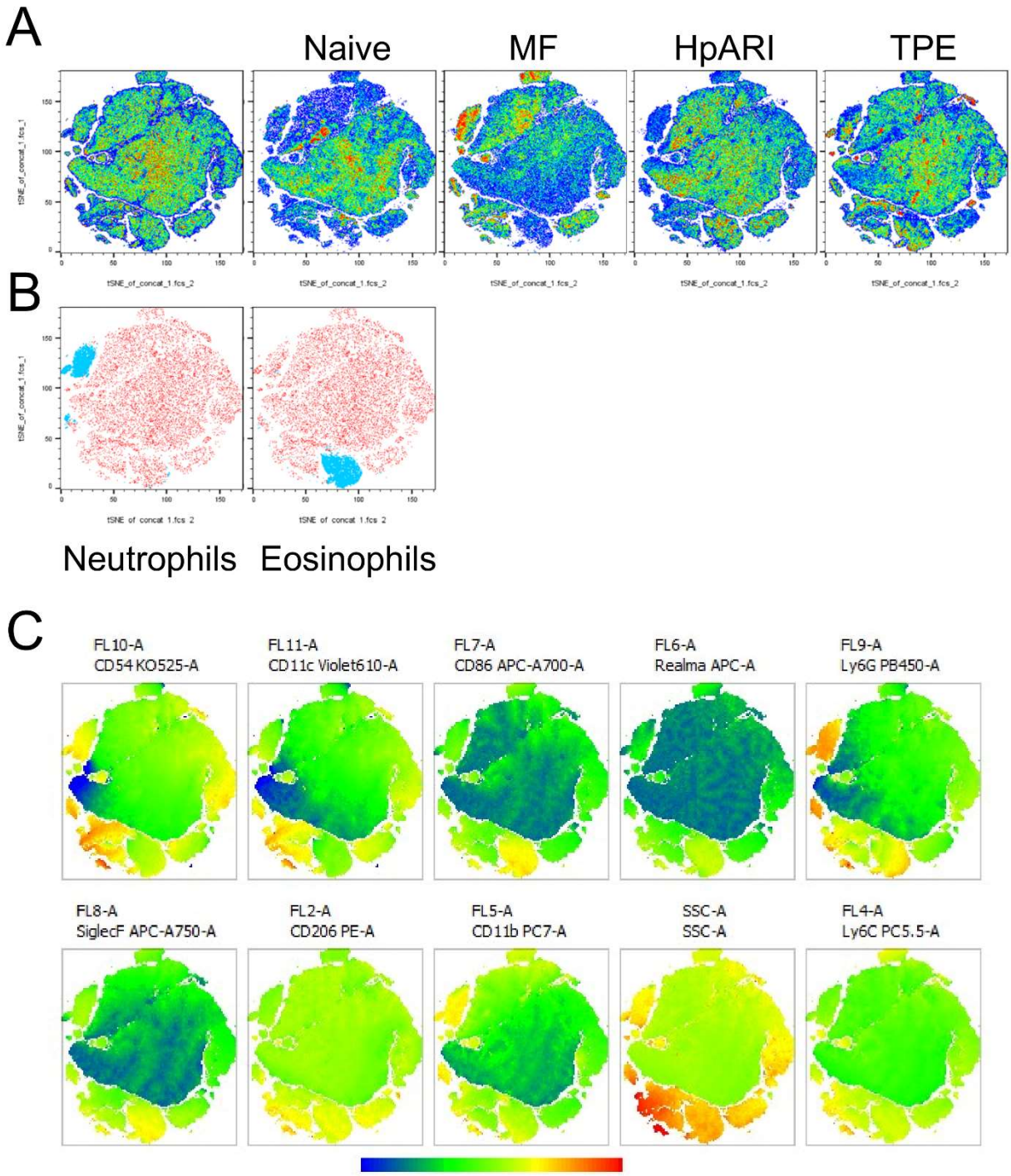

Supplement figure 4. (A) TSNE analysis of naïve, MF-challenged, HpARI treated TPE and TPE mice starting the treatment 1 hour before the challenge and afterwards every three days. Shown is one out of two representative experiments. (B) Eosinophil and neutrophils gate (shown in blue) and (C) heat maps for CD54, CD11c, CD86, RELM-α, Ly6G, Siglec-F, CD206, CD11b, SSC-A, Ly6C. Analysis was performed with FlowJo.

Supplement Table 1. FIMMIP-trial data split by sex. Data is shown as median.

	Female	**Male**

	FI	EDN	FI	EDN
Age [y]	53	49	48	48
Weight [kg}	60.5	65.4	64.7	67.3
Height [cm}	160	160	168	170
Muscle mass [%]	27.7	26.9	40.2	38.4
BMI	23.6	25.1	23.0	23.7
BP systolic [mm Hg]	70	76	76	78
BP diastolic [mm Hg]	70	77	76	78
Pulse rate [/min]	74	75	70	69
QT interval [ms]	395	389	388	385
Waist circumference [cm]	83.0	84.0	82.0	83.0
Body fat [%]	33.20	36.20	16.60	18.70
Visceral adipose tissue [%]	6.0	7.0	6.0	7.0
Liver function				
ALP [U/L]	98.00	129.5	109.00	128.00
ALT/GPT [U/L]	19.02	22.00	21.24	24.60
AST/GOT [U/L]	22.43	25.11	27.74	30.08
yGT [U/L]	20.00	22.00	28.00	30.00
CRP [mg/L]	11.17	21.73	9.79	13.03
Lipid profile				
Cholesterol [mg/dl]	145.00	143.00	127.00	132.00
LDL [mg/dl]	123.25	122.39	102.77	107,34
HDL [mg/dl]	59.21	67.08	62.61	61.13
Triglycerides [mg/dl]	38.00	33.00	36.00	37.00
HbA1c [mmol/mol Hb]	40.52	44.30	38.88	42.07
Fasting blood glucose [mg/dl]	100	100	98	98
Kidney function				
Creatinine [mg/dl]	0.56	0.66	0.67	0.78
Microalbumin [mg/L]	36.24	49.46	40.99	50.26
Urea [mg/dl]	18.70	18.40	19.50	18.70
Hemogram				
Leukocytes [10^9/L]	4.68	4.67	5.01	4.70
Neutrophils [10^6/L]	1.62	1.68	1.68	1.65
Eosinophils [10^6/L]	0.28	0.16	0.38	0.21
Basophils [10^6/L]	0.06	0.06	0.06	0.06
Platelets [10^9/L]	12.80	13.00	14.40	14.50
Hemoglobin [g/L]	237	245	228	226

Supplement Table 2. FIMMIP-trial data split by intestinal helminth infection status. Data is shown as median.

	Intestinal helminth infection	
	Negative	**Positive**
n	1409	210
Age [y]	49	50
Weight [kg]	65.3	65,1
Height [cm]	165	166
BMI	23.8	23.9
BP systolic [mm Hg]	117	119
BP diastolic [mm Hg]	76	76
Pulse rate [/min]	72	72
Muscle mass [%]	33.8	35.5
Waist circumference [cm]	83.0	82.0
Body fat [%]	24.00	21.80
QT interval [ms]	388	388
Visceral adipose tissue [%]	7.0	7.0
Liver function		
ALP [U/L]	115.00	112.00
ALT/GPT [U/L]	22.06	19.30
AST/GOT [U/L]	26.83	25.89
yGT [U/L]	25.00	25.00
CRP [mg/L]	13.65	12.28
Lipid profile		
Cholesterol [mg/dl]	138.0	131.5
LDL [mg/dl]	111.8	113.9
HDL [mg/dl]	63.4	61.0
Triglycerides [mg/dl]	63.4	61.0
HbA1c [mmol/mol Hb]	41.0	40.8
Fasting blood glucose [mg/dl]	99	99
Kidney function		
Creatinine [mg/dl]	0.69	0.51
Microalbumin [mg/L]	46.4	42.7
Urea [mg/dl]	19.0	18.0
Hemogram		
Leukocytes [10^9/L]	4.78	4.60
Neutrophils [10^6/L]	1.67	1.56
Eosinophils [10^6/L]	0.24	0.27
Basophils [10^6/L]	0.60	0.60
Platelets [10^9/L]	13.7	13.7
Hemoglobin [g/L]	235	232

Supplement Table. 3. FIMMIP-cohort split by filarial infection status and intestinal helminth infection status. Data is shown as median.

Filarial infection	**FI**		**EDN**	
STH	negative	positive	negative	positive
n	583	112	826	98
Anthropomorphic data				
Age [y]	49	53	48	48
Weight [kg]	64.2	63.4	66.7	67.7
Muscle mass [%]	36.5	37.9	31.9	33.0
BMI	23.3	22.8	24.4	24.9
Waist circumference [cm]	82.0	82.0	84.0	83.0
Body fat [%]	20.60	19.50	27.20	23.90
Visceral adipose tissue [%]	6.0	6.0	7.0	8.0
BP syst. [mm Hg]	118	117	116	120
BP dist. [mm Hg]	74	75	78	78
Pulse rate [/min]	72	71	72	74
QT interval [ms]	389	393	388	385
Circulating liver enzymes				
ALP [U/L]	104.0	108.0	129.0	120.5
ALT [U/L]	20.47	19.19	23.49	20.35
AST [U/L]	26.00	25.20	27.65	28.13
yGT [U/L]	25.00	25.00	25.69	25.00
CRP [mg/L]	10.08	11.36	16.64	14.20
Circulating marker of kidney health				
Creatinine [mg/dl]	0.64	0.47	0.73	0.59
Microalbumin [mg/L	39.89	37.85	50.26	44.62
Urea [mg/dl]	19.40	18.70	18.70	17.65
Circulating lipids and blood sugar				
Triglycerides [mg/dl]	36.00	39.00	35.00	35.50
HDL [mg/dl]	60.47	59.37	65.62	61.54
LDL [mg/dl]	110.68	108.49	112.58	123.34
HbA1c [mmol/mol Hb]	39.85	40.06	43.03	42.95
Cholesterol [mg/dl]	135	131	139	136
FB glucose [mg/dl]	99	98	99	103
Hemogram				
Leukocytes [10^9/L]	4.86	4.71	4.71	4.47
Neutrophils [10^6/L]	1.66	1.62	1.68	1.55
Eosinophils [10^6/L]	0.34	0.33	0.18	0.22
Basophils [10^6/L]	0.06	0.06	0.06	0.06
Platelets [10^9/L]	234	229	235	232
Hemoglobin [g/L]	13.80	13.80	13.60	13.60

Supplement Table 4. FIMMIP-trial data split by filarial infection and BMI status. Data is shown as median.

Infection	Endemic normal			O.v.			M.p.			Loa loa		
BMI	< 25	25-29	≥ 30	< 25	25-29	≥ 30	< 25	25-29	≥ 30	< 25	25-29	≥ 30
n	522	271	131	250	90	19	85	27	5	27	21	8
Age [y]	48	49	49	51	50	47	50	46	44	48	45	47
Weight [kg]	60.0	73.3	88.6	60.0	73.7	90.0	61.0	76.6	86.7	59.3	74.4	96.3
BMI	22.3	26.7	33.1	22.1	26.6	33.4	22.2	26.5	33.9	21.3	26.7	35.2
Waist circumference [cm]	80.0	86.0	92.0	81.6	86.0	95.0	80.0	86.0	88.0	80.0	84.0	98.0
Body fat [%]	20.50	32.40	43.80	18.3	30.9	45.6	18.2	26.1	42.8	19.3	22.7	47.2
Visceral adipose tissue [%]	5.0	9.0	11.0	5.0	9.0	11.0	5.5	9.0	10.0	5.0	9.0	11.5
Muscle mass [%]	35.7	30.0	25.1	38.0	31.2	24.2	38.3	35.1	21.2	39.1	37.1	24.1
BP dist. [mm Hg]	75	78	80	73	79	80	70	84	70	70	76	81
BP syst. [mm Hg]	111	120	120	110	120	120	114	120	98	110	116	133
Pulse rate [/min]	71	73	76	71	72	74	73	77	70	74	71	79
QT interval [ms]	389	385	383	393	394	387	393	386	398	395	383	393
Circulating Liver enzymes												
ALP [U/L]	134.0	122.0	125.0	112.0	116.0	120.5	96.0	88.0	87.0	115.0	104.0	79.5
ALT [U/L]	22.68	23.49	23.49	20.1	21.8	23.3	18.3	20.9	16.3	20.7	20.4	24.8
AST [U/L]	28.61	27.18	25.64	26.2	27.3	27.1	25.4	25.0	13.6	27.7	25.0	30.1
yGT [U/L]	25.35	25.00	27.0	25.0	26.0	25.5	26.0	26.0	19.0	27.0	27.0	16.5
CRP [mg/L]	16.73	13.07	22.09	20.0	29.1	26.8	5.51	6.56	13.7	10.9	8.44	4.13
Circulating marker of kidney health												
Creatinine [mg/dl]	0.71	0.74	0.72	0.63	0.71	0.66	0.49	0.53	0.38	0.56	0.70	0.65
Microalbumin [mg/L]	50.0	50.50	48.70	44.4	34.3	35.3	31.0	39.00	21.8	79.2	44.6	22.4
Urea [mg/dl]	18.0	19.7	19.2	19.1	19.0	22.0	20.5	18.7	20.1	17.4	20.1	17.6
Circulating lipid profile												
HbA1c [mmol/mol Hb]	43.5	42.5	43.3	40.0	42.2	39.6	40.4	41.7	41.0	40.6	41.1	40.5
HDL [mg/dl]	64.47	65.3	65.82	63,87	67,16	49,26	53,57	55,67	72,46	54,27	72,71	40,31
LDL [mg/dl]	108.1	117.5	128.6	112,0	117.6	138.6	100.5	107.2	166.5	104.9	106.7	113.9
Cholesterol [mg/dl]	135.0	139.0	149.0	139.0	140.5	143.0	124.9	132.0	184.0	121.0	140.0	112.5
Triglycerides [mg/dl]	33.0	35.0	43.0	36.0	42.0	54.5	44.0	35.0	38.0	36.0	46.0	41.0
FB glucose [mg/dl]	97	103	105	98	101	99	99	98	105	97	97	103
Hemogram												
Leukocytes [10^9/L]	4.66	4.77	4.69	5.00	5.26	4.64	4.48	4.90	5.55	4.73	4.74	5.23

Eosinophils [10^6/L]	0.19	0.16	0.19	0.55	0.66	0.17	0.40	0.36	0.24	0.27	0.24	0.21
Neutrophils [10^6/L]	1.60	1.74	1.76	1.53	1.64	1.51	1.50	1.62	1.99	1.66	1.64	1.92
Basophils [10^6/L]	0.06	0.06	0.07	0.05	0.05	0.05	0.06	0.06	0.06	0.06	0.07	0.06
Platelets [10^9/L]	234	235	236	246	222	235	229	199	304	238	227	242
Hemoglobin [g/L]	13.6	13.6	13.5	13.8	14.9	13.2	13.8	13.8	14.5	13.8	13.8	13.6

Supplement Table 5. FIMMIP-trial antibody list for flow cytometry.

Antigen	Fluorochrom	Clone	Firm	Cat.
CD20	FITC	2H7	Biolegend	302303
CD56	PE	HCD56	Biolegend	318305
CD3	PerCP-Cy5.5.	SK7	Biolegend	344807
CD16	APC	3G8	Biolegend	302011
CD4	FITC	RPTA-4	Biolegend	300505
CD197	PE	G043H7	Biolegend	353203
CD45RA	APC	HI100	Biolegend	304111
CD183	PE	G025H7	Biolegend	353705
CD161	PerCP-Cy5.5.	HP-3G10	Biolegend	339907
CD294	APC	BM16	Biolegend	350109
FOXP3	PE	259D	Biolegend	320207
CD127	PE-Cy7	A019D5	BIolegend	351319
CD25	Alexa647	M-A251	BIolegend	356109
CD279 (PD1)	PE	NAT105	Biolegend	367403
CD8	PerCP-Cy5.5.	SK1	Biolegend	344711
CD152 CTLA-4	APC	L3D10	Biolegend	349907
ICAMI	FITC	HCD54	Biolegend	322720
CD69	PerCP-Cy5.5.	FN50	Biolegend	310925
Siglec8	APC	7C9	Biolegend	347105
CD19	Alexa488	HIB19	Biolegend	302219
CD38	PE	HIT2	Biolegend	303505
CD24	PerCP-Cy5.5.	ML5	Biolegend	311115
CD1d	APC	51.1	Biolegend	350307
CD20	FITC	2H7	Biolegend	302303
CD27	PE	M-T271	Biolegend	356405
CD19	PerCP-Cy5.5.	HIB19	Biolegend	302229
CD21	APC	Bu32	Biolegend	354905
CD14	FITC	M5E2	Biolegend	301803
HLA DR	PE	L243	Biolegend	307605
CD16	PerCP-Cy5.5.	3G8	Biolegend	302027
CD45	APC	HI30	Biolegend	304011
CD40L	PerCP-Cy7.	24-31	Biolegend	310831
IFNy	PE	B27	Biolegend	506506
TNFα	APC	MAB11	Biolegend	502913
IL-2	PerCP-Cy5.5.	MQ1-17h12	Biolegend	500321
IL-13	PE	JES10-5A2	Biolegend	501903
IL-10	APC	JES3-19F1	Biolegend	506806
IL-17f	PerCP-Cy5.5.		BD	1153316
IL-22	PE	2G12A41	Biolegend	366703
IL-17a	APC	BL168	Biolegend	512333

IFNy	PerCP-Cy5.5.	B27	Biolegend	506527
IL-5	PE	JESI-39D10	Biolegend	500903
IL-4	APC	MP4-25D2	Biolegend	500811
CD8	Alexa488	HIT8a	Biolegend	300906
perforin	PerCP-Cy5.5.	B-D48	Biolegend	353313
granzyme b	APC	QA16A02	Biolegend	372203
IFNy	FITC	B27	Biolegend	506504
CD223 (LAG-3)	PE	11C3C65	Biolegend	369305

List of publications

Description of contributions to manuscripts and additional projects

Manuscripts under preparation

Lenz B, Ehrens A, Ajendra J, Risch F, Gal J, Neumann AL, Reichwald JJ, Strutz W, McSorley HJ, Martin C, Hoerauf A, Hübner MP. Repeated sensitization of mice with microfilariae of *Litomosoides sigmodontis* induces pulmonary eosinophilia in an IL-33-dependent manner. *Under review*

Data shown in this thesis is partially contained in this manuscript.

Aderhold W, **Lenz B**, Hübner MP, Schaefer HE, Gärtner FC, Heine A, Gütgemann I. Intramedullary leucocytoclastic vasculitis in POEMS syndrome. *Under review*

In the context of extracellular DNA-traps, a case report of a patient suffering from poems diseases was submitted to the British Journal of Hematology under the title “Intramedullary leukocytoclastic vasculitis in POEMS syndrome”. In this manuscript we demonstrate that leucocytoclastic vasculitis and focal NETosis was present in the bone marrow of an 80-year-old patient with POEMS syndrome (polyneuropathy, organomegaly, endocrinopathy, monoclonal plasma cell disorder, skin changes). Here most clinical and histopathologic findings could be explained by massive vascular endothelial growth factor secretion by neoplastic plasma cells. I contributed by conceptualizing and performing the fluorescence microscopy to detect neutrophils, neutrophil degranulation and neutrophil extracellular traps in the bone marrow sections of the patient.

Published manuscripts

Risch F, Scheunemann JF, Reichwald JJ, **Lenz B**, Ehrens A, Gal J, Fercoq F, Koschel M, Fendler M, Hoerauf A, Martin C, Hübner MP. The efficacy of the benzimidazoles oxfendazole and flubendazole against *Litomosoides sigmodontis*; is dependent on the adaptive and innate immune system. Front Microbiol. 2023;14 1213143. doi:10.3389/fmicb.2023.1213143. PMID: 37440891.

In this publication, Risch et al. investigated the role of the immune system in the treatment efficacy of *L. sigmodontis* infection with the benzimidazoles oxfendazole (OXF) and flubendazole (FBZ). Here, we could demonstrate that immunodeficiency in mice impairs the treatment efficacy of OXF and the addition of the cytokine IL-5, as an immune stimulus, improved treatment efficacy and allowed shorter treatment regimens. Eosinophil-deficient dblGATA, antibody-deficient µMT and B-, T-, NK-cell and ILC-deficient *Rag2/IL-2rγ*$^{-/-}$ mice infected with the rodent filaria *L. sigmodontis* were treated with an optimal and suboptimal regimen of OXF and FBZ for up to 5 days. Treatment of WT mice reduced the adult worm burden by up to 94% (OXF) and 100% (FBZ) compared to vehicle controls. In contrast, treatment efficacy was lower in all immunodeficient strains with a reduction of up to 90% (OXF) and 75% (FBZ) for *ΔdblGata1*, 50 and 92% for *IL-4r/IL-5*$^{-/-}$, 64 and 78% for µMT or 0% for *Rag2/IL-2rγ*$^{-/-}$ mice, respectively. The efficacy of a shortened 3-day treatment of OXF (33% less adult worms vs. vehicle controls) could be boosted to a 91% reduction of the worm burden via combination with IL-5, but not IL-4 or IL-33. My contribution was predominantly by assisting in the experimental procedures and animal work, i.e., performing pleura lavage, organ preparation and collecting of serum.

Lenz B*, Andrew BA*, Ritter M, Karunakaran I, Gandjui NVT, Nchang LC, Surendar J, Ebob AOB, Ehrens A, Klarmann-Schulz U, Ricchiuto A, Kuehlwein JM, Fombad FF, Ngwa AM, Katcho TD, Hoerauf A, Wanji S*, Hübner MP*. The design and development of a study protocol to investigate *Onchocerca volvulus, Loa loa* and *Mansonella perstans*-mediated modulation of the metabolic and immunological profile in lean and obese individuals in Cameroon. PLoS One. 2023;18(6) e0285689. doi:10.1371/journal.pone.0285689. PMID: 37267236; PMCID: PMC10237473. * Authors contributed equally.

This study protocol is a description of the planning and implementation of the “FIMMIP” trial. The here describe methodological approach and planned measures will be and were performed during the trial. In brief, live-style- and diet-derived metabolic inflammation and its associated cardiovascular risks, i.e., T2D, hypertension and strokes are amongst the ten leading causes of death, defined by the WHO in 2019. Prior human and animal studies indicate a potential protective effect of filarial infections against the development of T2D.

The “FIMMIP” study was designed to investigate this potential impact by recruiting lean, overweight and obese participants that are uninfected endemic controls or infected with either *M. perstans, L. loa, O. volvulus*. The anthropomorphic, immunological and metabolic profile of the participants from rural regions of Cameroon will be analyzed at baseline and 12- and 18-months after anti-filarial treatment. The trial will be conducted to obtain a comprehensive metabolic profile of the participants in rural areas of Cameroon and to investigate the relationship between filarial immunomodulation and metabolic diseases. This study will elucidate the effect of anti-filarial treatment on the metabolic and immunological parameters that partake in the development of insulin resistance, narrowing in on a potential protective effect of filarial infections on metabolic
diseases. I contributed to this manuscript by establishing the laboratory assessment of the immunological profile, training the field-team in anthropomorphic measurements, capacity building, laboratory evaluations (white blood cell analysis) and student supervision, organizing and supporting the blood biochemistry workshop, constructing the standard operating protocols (SOP) and writing the manuscript.

Scheunemann JF, Risch F, Reichwald JJ, **Lenz B**, Neumann AL, Garbe S, Frohberger SJ, Koschel M, Ajendra J, Rothe M, Latz E, Coch C, Hartmann G, Schumak B, Hoerauf A, Hübner MP. Potential of Nucleic Acid Receptor Ligands to Improve Vaccination Efficacy against the Filarial Nematode *L. sigmodontis*. Vaccines (Basel). 2023 May;11(5) 966. doi:10.3390/vaccines11050966. PMID: 37243070; PMCID: PMC10223226.

Vaccination against filarial infections is a challenging task due to the inherent immune evasive nature of filariae. Extracts and antigens produced for vaccination approaches do not induce sufficient protection. Therefore, additional approaches to formulate vaccines that bypass potential immunomodulation and elicit potent but not overshooting immune responses are necessary to develop a filarial vaccine approach. Scheunemann and Risch et al. incorporated specific nucleic acid receptor ligands into an experimental vaccination approach for *L. sigmodontis*. We demonstrate that the TLR3 receptor ligand poly:IC and the RIG-I receptor ligand 3pRNA administered together with irradiated L3 larvae reduced the adult worm burden by

73% and 57%, respectively. The vaccination approach induced a neutrophil recruitment within the skin and increased IP-10 and IFNβ levels indicating an immune response that could be beneficial for a vaccination strategy. My contributions to this project included the treatment preparation for the vaccination and treatment of the animals. Moreover, I performed *in vitro* assays with RIG-I, TLR3 and cGAS knock-out cell lines and supported the *in vivo* experiments.

Amambo GN, Innocentia N, Abong RA, Fombad FF, Njouendou AJ, Nietcho F, Ekanya R, Kien CA, Ebai R, **Lenz B**, Ritter M, Esum ME, Deribe K, Cho JF, Beng AA, Enyong PI, Li Z, Hübner MP, Pfarr K, Hoerauf A, Carlow C, Wanji S. Application of loop mediated isothermal amplification (LAMP) assays for the detection of *Onchocerca volvulus, Loa loa* and *Mansonella perstans* in humans and vectors. Front Trop Dis. 2023 Jan;3 1016176. doi:10.3389/fitd.2022.1016176. PMID: 36684508; PMCID: PMC7614089.

This manuscript investigates the option to use loop-mediated-isothermal amplification (LAMP) to detect filarial infections, i.e., *O. volvulus, M.perstans* and *L. loa*, as a diagnostic tool to support microscopy in humans and vectors. Amambo et al. demonstrated that LAMP is superior to conventional microscopy in detecting *O. volvulus* in engorged vectors and humans. LAMP showed a prevalence of 40.4% (*O. volvulus*), 17.8% (*L. loa*) and 36.6% (*M. perstans*) versus 20.6% (*O. volvulus*), 17.4% (*L. loa*) and 33.8% (*M. perstans*) with microscopy. The here demonstrated sensitivity, species specificity and rapidity of the LAMP assay established in this manuscript depicts a solid alternative or addition to microscopy for filarial diagnostics. In this project, I contributed by helping with capacity building, giving feedback and providing samples from the "FIMMIP" trial.

Reichwald JJ, Risch F, Neumann AL, Frohberger SJ, Scheunemann JF, Lenz B, Ehrens A, Strutz W, Schumak B, Hoerauf A, Hübner MP. ILC2s Control Microfilaremia During *L. sigmodontis* Infection n *Rag2*$^{-/-}$ Mice. Front Immunol. 2022;13 863663. doi:10.3389/fimmu.2022.863663. PMID: 35757689; PMCID: PMC9222899.

This publication shows that absence of type 2 innate lymphoid cell does not affect *L. sigmodontis* adult worm clearance or adult worm load, but increases the peripheral blood MF burden. Pleura ILC2s were analyzed at day 9, 30 and 70 dpi and were compared between semi-susceptible

C57BL/6 mice and susceptible BALB/c mice. Semi-susceptible C57BL/6 mice displayed increased ILC2s at day 30 post infection, which was accompanied by increased IL-5 and IL-13 levels.

Further, ILC2s were the major contributor to IL-5 production during the infection, surpassing CD4 T cells in IL-5 expression. Depletion of ILC2s using a CD90.2 depletion antibody in T and B cell deficient Rag2$^{-/-}$ mice revealed that absence of ILC2s did not impact the adult worm burden, but significantly increased MF numbers, indicating that ILC2s control MF in the *L. sigmodontis* mouse model. During this project I supported the laboratory work and measured serum and pleura IL-4. In addition, I quantified parasite-specific IgG1 and IgG2ab to further elucidate on strain differences between BALB/c and C57BL/6 mice by phenotyping the immune response.

Risch F, Koschel M, **Lenz B**, Specht S, Hoerauf A, Hübner MP, Scandale I. Comparison of the macrofilaricidal efficacy of oxfendazole and its isomers against the rodent filaria Litomosoides sigmodontis. Frontiers in Tropical Diseases 2022 volume 3, Doi:10.3389/fitd.2022.982421/ISSN=2673-7515

Pre-clinical assessment of anti-filarial chemotherapy is one of the main focuses of the group of Prof. Dr. Hübner. In this publication, it was demonstrated that the two isomers of oxfendazole, oxfendazole (+) and oxfendazole (-) have a similar efficacy when treating *L. sigmodontis* infections in the rodent model. In a five-day oral treatment, the racemate of oxfendaxole reduced the adult worm burden by 95%. Oxfendazole (+) reduced the adult worm burden by 85% and was metabolized to fenbendazole sulfate and fenbendazole to a lesser extent. Oxfendazole (-) decreased the adult worm burden by 72% and was metabolized similarly with a higher rate of fenbendazole sulfate. Taken together, both isomers displayed a pharmacokinetic profile and no single isomer is more efficacious. To this study, I contributed to the oral treatments of mice with the oxfendazole racemate and isomers.

Ehrens A, **Lenz B**, Neumann AL, Giarrizzo S, Reichwald JJ, Frohberger SJ, Stamminger W, Buerfent BC, Fercoq F, Martin C, Kulke D, Hoerauf A, Hübner MP. Microfilariae Trigger Eosinophil Extracellular DNA Traps in a Dectin-1-Dependent Manner. Cell Rep. 2021 Jan;34(2) 108621. doi:10.1016/j.celrep.2020.108621. PMID: 33440150.

The first contribution was to the manuscript “Eosinophil Extracellular DNA Traps in a Dectin-1-Dependent Manner” that demonstrated that MF from *L. sigmodontis* were entrapped by eosinophils in DNA-like structures that inhibited the motility of MF. These extracellular traps were observed using electron and fluorescence microscopy. This publication showed for the first time that MF of the rodent filarial parasite were recognized by eosinophils *in vitro* by the c-type lectin receptor dectin-1 and eosinophils respond to MF with the formation of extracellular DNA-traps. Blockage of dectin-1 abolished the recognition of MF and the DNA release *in vitro.* Moreover, we demonstrated that the mechanism was conserved, as *Dirofilaria immitis* MF*,* the dog heart worm with zoonotic potential, caused this eosinophil ETosis as well. In addition, it was shown that the injection of MF induced DNA release *in vivo* and MF coated with DNA-traps were cleared from the peripheral blood quicker than uncoated MF. Finally, we demonstrated that the DNA released by eosinophils was predominantly mitochondrial DNA. I contributed to this publication by showing that the recognition and entrapment of MF was conserved between murine and human eosinophils. For this, I established a human eosinophil isolation protocol and performed *in vitro* co-cultures with human eosinophils and MF of both *L. sigmodontis* and *Dirofilaria immitis* to assess motility and DNA release*.* Additionally, I assisted in performing the *in vivo* experiments.

Acknowledgement

First of all, I would like to thank the director of our institute, Prof. Dr. Achim Hoerauf, for giving me the opportunity to do my PhD thesis at the Institute of Medical Microbiology, Immunology and Parasitology at the University Hospital of Bonn.

Secondly, I would like to thank Prof. Dr. Marc Hübner for his patience, time and continuous efforts in supervising and supporting me during my PhD thesis after I visited and stuck around in his student courses for so long he eventually had to give me a job. Thank you very much for your leniency and giving me freedom and enabling my, at times unorthodox, way of conducting science and supporting my passion for methodology and expensive equipment. Thank you for being always available for feedback and standing up for your team at all times and your unparalleled work ethic.

Further, I would like to thank Prof. Dr. Walter Witke for agreeing to be my second supervisor despite already knowing me from my time conducting my bachelor thesis in his lab. On a more serious note, thank you for taking time out of your immensely busy schedule as dean of the science and mathematics faculty to take part in this committee.

In addition, I want to thank Prof. Dr. Thomas Bartolomaeus and PD Dr. med. Phillip Lutz for being part of the examination committee, despite their extensive responsibilities and duties. Thank you very much for taking the time out of your busy schedule.

I want to express my gratitude to Prof. Dr. Samuel Wanji´s extensive help, supervision and effort in conducting the clinical trial “FIMMIP” in Cameroon. None of the work conducted in Cameroon would have been possible without your guidance, scientific advice and leadership in the field activity, sensitization, planning and training not only the FIMMIP-team but me as well. Thank you very much Samuel for taking care of me in Cameroon and giving me insight on the extreme circumstances you work in, teaching me countless things about parasitology and what can be achieved with enough dedication.

Subsequently, I like to thank Dr. Manuel Ritter who was my travel companion and mentor in African affairs throughout my PhD thesis. First of all, thank you very much for showing me the best beer in Cameroon. Secondly, thank you for all the scientific advice on the projects and allowing me to profit from your immense knowledge on the subject matter.

A big thank you also to the Manjo-team in Cameroon. Thank you to all the parasitologists, medical doctors, nurses and students conducting the field activities. Here a special thanks to Amuam Andrew, Narciesse Gandjui, Lucy Nchang, Franck Nietcho, Gordon Nchanji, Fanny Fombad, Ambe Ngwa, Glory Amambo, Tatiana Katcho and Anita Ebob for the contributions in setting up the field activities and laboratory work during the project.

Furthermore, I want to extend a heartfelt thank you to the collaboration partners that were involved in the projects. Here I would like to thank Prof. Dr. Coralie Martin and Joséphine Gal for their contributions to the TPE project, teaching methodology and giving feedback on lung based immune responses. A special thanks also to Dr. Henry McSorley for providing the IL-33 inhibitor HpARI and giving feedback in the TPE manuscript.

Another thank you goes to the AG Klarmann-Schulz. Manny thanks to Dr. Ute Klarmann-Schulz for the tireless help with the statistical analysis plan and support with the data management. Thank you to Arcangelo Ricchiuto for managing the trial data base and digitalizing the case report file. Similarly, a big thanks to Dr. Janina Kühlwein for supporting the data base management.

Additionally, I want to thank current and past members of the AG Hübner for the support in experiments conducted in the institute. Special thanks to Frederic Risch, Dr. Alexandra Ehrens, Dr. Jesuthas Ajendra, Katharina Krings, Marianne Koschel, Wiebke Strutz, Dr. Stefan Frohberger, Dr. Anna-Lena Neumann, Dr. Surendar Jayagopi, Dr. Johanna Scheunemann, Dr. Julia Reichwald, Tilman Aden, and Dr. Indulekha Karunakaran for the support and scientific expertise.

Finally, I want to thank my parents, my brothers and my girlfriend for their continuous moral support and keeping me on my toes at all times.

Reference list

1. Dobson A, Lafferty KD, Kuris AM, Hechinger RF, Jetz W. Homage to Linnaeus: how many parasites? How many hosts? Proceedings of the National Academy of Sciences. 2008;105(supplement_1):11482-9.
2. Ebert D. Experimental Evolution of Parasites. Science. 1998;282(5393):1432-6.
3. Ebert D, Hamilton WD. Sex against virulence: the coevolution of parasitic diseases. Trends in ecology & evolution. 1996;11(2):79-82.
4. Auld SK, Tinsley MC. The evolutionary ecology of complex lifecycle parasites: linking phenomena with mechanisms. Heredity. 2015;114(2):125-32.
5. Parker GA, Chubb JC, Ball MA, Roberts GN. Evolution of complex life cycles in helminth parasites. Nature. 2003;425(6957):480-4.
6. Orlofske SA, Jadin RC, Preston DL, Johnson PT. Parasite transmission in complex communities: predators and alternative hosts alter pathogenic infections in amphibians. Ecology. 2012;93(6):1247-53.
7. Ebert D. Virulence and local adaptation of a horizontally transmitted parasite. Science. 1994;265(5175):1084-6.
8. Anderson RM, May RM. Coevolution of hosts and parasites. Parasitology. 1982;85 (Pt 2):411-26.
9. Holmes J. Modification of intermediate host behaviour by parasites. Behavioural aspects of parasite transmission. 1972.
10. Vyas A, Kim SK, Giacomini N, Boothroyd JC, Sapolsky RM. Behavioral changes induced by Toxoplasma infection of rodents are highly specific to aversion of cat odors. Proc Natl Acad Sci U S A. 2007;104(15):6442-7.
11. Ingram WM, Goodrich LM, Robey EA, Eisen MB. Mice infected with low-virulence strains of Toxoplasma gondii lose their innate aversion to cat urine, even after extensive parasite clearance. PLoS One. 2013;8(9):e75246.
12. Poirotte C, Kappeler PM, Ngoubangoye B, Bourgeois S, Moussodji M, Charpentier MJ. Morbid attraction to leopard urine in Toxoplasma-infected chimpanzees. Current biology : CB. 2016;26(3):R98-9.
13. Flegr J, Havlícek J. Changes in the personality profile of young women with latent toxoplasmosis. Folia parasitologica. 1999;46(1):22-8.
14. Flegr J, Havlícek J, Kodym P, Malý M, Smahel Z. Increased risk of traffic accidents in subjects with latent toxoplasmosis: a retrospective case-control study. BMC Infect Dis. 2002;2:11.
15. Cook TB, Brenner LA, Cloninger CR, Langenberg P, Igbide A, Giegling I, et al. "Latent" infection with Toxoplasma gondii: association with trait aggression and impulsivity in healthy adults. Journal of psychiatric research. 2015;60:87-94.
16. Johnson SK, Fitza MA, Lerner DA, Calhoun DM, Beldon MA, Chan ET, et al. Risky business: linking Toxoplasma gondii infection and entrepreneurship behaviours across individuals and countries. Proceedings Biological sciences. 2018;285(1883).
17. Gaskell EA, Smith JE, Pinney JW, Westhead DR, McConkey GA. A unique dual activity amino acid hydroxylase in Toxoplasma gondii. PLoS One. 2009;4(3):e4801.
18. Martín-Vega D, Garbout A, Ahmed F, Wicklein M, Goater CP, Colwell DD, et al. 3D virtual histology at the host/parasite interface: visualisation of the master manipulator, Dicrocoelium dendriticum, in the brain of its ant host. Sci Rep. 2018;8(1):8587.
19. Botnevik CF, Malagocka J, Jensen AB, Fredensborg BL. Relative Effects of Temperature, Light, and Humidity on Clinging Behavior of Metacercariae-Infected Ants. J Parasitol. 2016;102(5):495-500.
20. Jeandron A, Rinaldi L, Abdyldaieva G, Usubalieva J, Steinmann P, Cringoli G, et al. Human infections with Dicrocoelium dendriticum in Kyrgyzstan: the tip of the iceberg? J Parasitol. 2011;97(6):1170-2.
21. Cengiz ZT, Yilmaz H, Dulger AC, Cicek M. Human infection with Dicrocoelium dendriticum in Turkey. Annals of Saudi medicine. 2010;30(2):159-61.

22. Gottstein B, Hemphill A. Immunopathology of echinococcosis. Chemical immunology. 1997;66:177-208.
23. Gottstein B, Soboslay P, Ortona E, Wang J, Siracusano A, Vuitton D. Immunology of Alveolar and Cystic Echinococcosis (AE and CE). Adv Parasitol. 2017;96:1-54.
24. Gottstein B, Stojkovic M, Vuitton DA, Millon L, Marcinkute A, Deplazes P. Threat of alveolar echinococcosis to public health--a challenge for Europe. Trends Parasitol. 2015;31(9):407-12.
25. McManus DP, Zhang W, Li J, Bartley PB. Echinococcosis. The Lancet. 2003;362(9392):1295-304.
26. Frider B, Larrieu E, Odriozola M. Long-term outcome of asymptomatic liver hydatidosis. Journal of hepatology. 1999;30(2):228-31.
27. Wen H, Vuitton L, Tuxun T, Li J, Vuitton DA, Zhang W, et al. Echinococcosis: advances in the 21st century. Clinical microbiology reviews. 2019;32(2):e00075-18.
28. World Health O. Ending the neglect to attain the sustainable development goals: a road map for neglected tropical diseases 2021–2030: overview. Geneva: World Health Organization; 2020 2020. Report No.: 9789240018792 (electronic version)

9789240018815 (إلكترونية نسخة) Contract No.: WHO/UCN/NTD/2020.01.
29. Specht S, Brattig N, Büttner M, Büttner DW. Criteria for the differentiation between young and old Onchocerca volvulus filariae. Parasitol Res. 2009;105(6):1531-8.
30. Plaisier AP, van Oortmarssen GJ, Remme J, Habbema JD. The reproductive lifespan of Onchocerca volvulus in West African savanna. Acta Trop. 1991;48(4):271-84.
31. WHO. Progress report on the elimination of human onchocerciasis, 2016-2017. Wkly Epidemiol Rec. 2017;92(45):681-700.
32. WHO. https://www.who.int/neglected_diseases/news/NTD_disease_packs.pdf?ua=1. 2017.
33. Simonsen PE, Onapa AW, Asio SM. Mansonella perstans filariasis in Africa. Acta Tropica. 2011;120:S109-S20.
34. Hoerauf A, Mand S, Volkmann L, Buttner M, Marfo-Debrekyei Y, Taylor M, et al. Doxycycline in the treatment of human onchocerciasis: Kinetics of Wolbachia endobacteria reduction and of inhibition of embryogenesis in female Onchocerca worms. Microbes Infect. 2003;5(4):261-73.
35. Hoerauf A, Mand S, Adjei O, Fleischer B, Buttner DW. Depletion of wolbachia endobacteria in Onchocerca volvulus by doxycycline and microfilaridermia after ivermectin treatment. Lancet. 2001;357(9266):1415-6.
36. Hoerauf A, Volkmann L, Hamelmann C, Adjei O, Autenrieth IB, Fleischer B, et al. Endosymbiotic bacteria in worms as targets for a novel chemotherapy in filariasis. Lancet. 2000;355(9211):1242-3.
37. Taylor MJ, Cross HF, Ford L, Makunde WH, Prasad GB, Bilo K. Wolbachia bacteria in filarial immunity and disease. Parasite Immunol. 2001;23(7):401-9.
38. Taylor MJ, Hoerauf A, Townson S, Slatko BE, Ward SA. Anti-Wolbachia drug discovery and development: safe macrofilaricides for onchocerciasis and lymphatic filariasis. Parasitology. 2013:1-9.
39. Turner JD, Langley RS, Johnston KL, Egerton G, Wanji S, Taylor MJ. Wolbachia endosymbiotic bacteria of Brugia malayi mediate macrophage tolerance to TLR- and CD40-specific stimuli in a MyD88/TLR2-dependent manner. J Immunol. 2006;177(2):1240-9.
40. Turner JD, Langley RS, Johnston KL, Gentil K, Ford L, Wu B, et al. Wolbachia lipoprotein stimulates innate and adaptive immunity through Toll-like receptors 2 and 6 to induce disease manifestations of filariasis. J Biol Chem. 2009;284(33):22364-78.
41. Keiser PB, Coulibaly Y, Kubofcik J, Diallo AA, Klion AD, Traore SF, et al. Molecular identification of Wolbachia from the filarial nematode Mansonella perstans. Molecular and biochemical parasitology. 2008;160(2):123-8.
42. Zoure HG, Wanji S, Noma M, Amazigo UV, Diggle PJ, Tekle AH, et al. The geographic distribution of Loa loa in Africa: results of large-scale implementation of the Rapid Assessment Procedure for Loiasis (RAPLOA). PLoS Negl Trop Dis. 2011;5(6):e1210.

43. Boussinesq M, Gardon J, Kamgno J, Pion SD, Gardon-Wendel N, Chippaux JP. Relationships between the prevalence and intensity of Loa loa infection in the Central province of Cameroon. Annals of tropical medicine and parasitology. 2001;95(5):495-507.
44. Lukiana T, Mandina M, Situakibanza NH, Mbula MM, Lepira BF, Odio WT, et al. A possible case of spontaneous Loa loa encephalopathy associated with a glomerulopathy. Filaria J. 2006;5:6.
45. Ritter M, Hoerauf A, Hübner MP. Human Filariasis. 2021.
46. Fain A. [Current problems of loaiasis]. Bulletin of the World Health Organization. 1978;56(2):155-67.
47. Fain A. [Epidemiology and pathology of loaiasis]. Annales de la Societe belge de medecine tropicale. 1981;61(2):277-85.
48. Whittaker C, Walker M, Pion SD, Chesnais CB, Boussinesq M, Basáñez M-G. The population biology and transmission dynamics of Loa loa. Trends in parasitology. 2018;34(4):335-50.
49. Fischer PU, A. H, Weil GJ, M.P. H. Mansons The FIlariaisis. 2023.
50. Hemilembolo MC, Niama AC, Campillo JT, Pion SD, Missamou F, Whittaker C, et al. Excess Mortality Associated With Loiasis: Confirmation by a New Retrospective Cohort Study Conducted in the Republic of Congo. Open forum infectious diseases. 2023;10(3):ofad103.
51. WHO. Lymphatic filariasis: WHO; 2019 [updated April, 12, 2019. Available from: https://www.who.int/en/news-room/fact-sheets/detail/lymphatic-filariasis.
52. WHO. NTD-Roadmap-targets-2012-20130 2019 [Available from: https://www.who.int/neglected_diseases/news/WHO-launches-global-consultations-for-new-NTD-Roadmap/en/.
53. Ottesen EA. Immunopathology of Lymphatic Filariasis in Man. Springer Semininars Immunopathology. 2008;2:373-85.
54. Taylor MJ. A new insight into the pathogenesis of filarial disease. Curr Mol Med. 2002;2(3):299-302.
55. WHO. Progress in eliminating onchocerciasis in the WHO Region of the Americas: doxycycline treatment as an end-game strategy.; 2019.
56. Medkour H, Amona I, Laidoudi Y, Davoust B, Bitam I, Levasseur A, et al. Parasitic Infections in African Humans and Non-Human Primates. Pathogens (Basel, Switzerland). 2020;9(7).
57. Hay RJ, Mackenzie CD, Guderian R, Noble WC, Proano JR, Williams JF. Onchodermatitis--correlation between skin disease and parasitic load in an endemic focus in Ecuador. Br J Dermatol. 1989;121(2):187-98.
58. Murdoch ME. Onchodermatitis: Where Are We Now? Trop Med Infect Dis. 2018;3(3).
59. Murdoch ME, Asuzu MC, Hagan M, Makunde WH, Ngoumou P, Ogbuagu KF, et al. Onchocerciasis: the clinical and epidemiological burden of skin disease in Africa. Annals of tropical medicine and parasitology. 2002;96(3):283-96.
60. Murdoch ME, Hay RJ, Mackenzie CD, Williams JF, Ghalib HW, Cousens S, et al. A clinical classification and grading system of the cutaneous changes in onchocerciasis. Br J Dermatol. 1993;129(3):260-9.
61. Simonsen PE, Onapa AW, Asio SM. Mansonella perstans filariasis in Africa. Acta Trop. 2011;120 Suppl 1:S109-20.
62. Fux CA, Chappuis B, Holzer B, Aebi C, Bordmann G, Marti H, et al. Mansonella perstans causing symptomatic hypereosinophilia in a missionary family. Travel medicine and infectious disease. 2006;4(5):275-80.
63. Mediannikov O, Ranque S. Mansonellosis, the most neglected human filariasis. New microbes and new infections. 2018;26:S19-s22.
64. Puente S, Lago M, Subirats M, Sanz-Esteban I, Arsuaga M, Vicente B, et al. Imported Mansonella perstans infection in Spain. Infect Dis Poverty. 2020;9(1):105.

65. Bennuru S, Nutman TB. Lymphangiogenesis and lymphatic remodeling induced by filarial parasites: implications for pathogenesis. PLoS Pathog. 2009;5(12):e1000688.
66. Webb JK, Job CK, Gault EW. Tropical eosinophilia: demonstration of microfilariae in lung, liver, and lymphnodes. Lancet. 1960;1(7129):835-42.
67. Ottesen EA, Nutman TB. Tropical pulmonary eosinophilia. Annual review of medicine. 1992;43:417-24.
68. Danaraj TJ, Pacheco G, Shanmugaratnam K, Beaver PC. The etiology and pathology of eosinophilic lung (tropical eosinophilia). Am J Trop Med Hyg. 1966;15(2):183-9.
69. Mullerpattan JB, Udwadia ZF, Udwadia FE. Tropical pulmonary eosinophilia--a review. The Indian journal of medical research. 2013;138(3):295-302.
70. Frimodt-Möller C, Barton R. A pseudo-tuberculous condition associated with eosinophilia. The Indian Medical Gazette. 1940;75(10):607.
71. Weingarten R. Tropical eosinophilia. Lancet. 1943.
72. Vijayan V. Immunopathogenesis and Treatment of Eosinophilic Lung Diseases in the Tropics. Tropical Lung Disease: CRC Press; 2005. p. 227-72.
73. Jha SK, Karna B, Mahajan K. Tropical Pulmonary Eosinophilia. StatPearls [Internet]: StatPearls Publishing; 2022.
74. Tsanglao WR, Nandan D, Chandelia S, Arya NK, Sharma A. Filarial tropical pulmonary eosinophilia: a condition masquerading asthma, a series of 12 cases. Journal of Asthma. 2019;56(7):791-8.
75. Egwang TG, Kazura JW. The BALB/c mouse as a model for immunological studies of microfilariae-induced pulmonary eosinophilia. Am J Trop Med Hyg. 1990;43(1):61-6.
76. Sharma P, Sharma A, Vishwakarma AL, Agnihotri PK, Sharma S, Srivastava M. Host lung immunity is severely compromised during tropical pulmonary eosinophilia: role of lung eosinophils and macrophages. J Leukoc Biol. 2016;99(4):619-28.
77. Sharma P, Sharma A, Srivastava M. In vivo neutralization of α4 and β7 integrins inhibits eosinophil trafficking and prevents lung injury during tropical pulmonary eosinophilia in mice. European journal of immunology. 2017;47(9):1501-12.
78. Sharma P, Sharma A, Ganga L, Satoeya N, Jha R, Srivastava M. Acidic Calcium-Independent Phospholipase A2 Regulates Eosinophil-Mediated Pathology during Filarial Manifestation of Tropical Pulmonary Eosinophilia. J Immunol. 2021;206(4):722-36.
79. Mehlotra RK, Hall LR, Higgins AW, Dreshaj IA, Haxhiu MA, Kazura JW, et al. Interleukin-12 suppresses filaria-induced pulmonary eosinophilia, deposition of major basic protein and airway hyperresponsiveness. Parasite Immunol. 1998;20(10):455-62.
80. Akuthota P, Carmo LA, Bonjour K, Murphy RO, Silva TP, Gamalier JP, et al. Extracellular Microvesicle Production by Human Eosinophils Activated by "Inflammatory" Stimuli. Frontiers in cell and developmental biology. 2016;4:117.
81. Hoerauf A, Satoguina J, Saeftel M, Specht S. Immunomodulation by filarial nematodes. Parasite Immunol. 2005;27(10-11):417-29.
82. McSorley HJ, Maizels RM. Helminth infections and host immune regulation. Clinical microbiology reviews. 2012;25(4):585-608.
83. Katawa G, Layland LE, Debrah AY, von Horn C, Batsa L, Kwarteng A, et al. Hyperreactive Onchocerciasis is Characterized by a Combination of Th17-Th2 Immune Responses and Reduced Regulatory T Cells. Plos Neglect Trop D. 2015;9(1):e3414.
84. Babu S, Blauvelt CP, Kumaraswami V, Nutman TB. Regulatory networks induced by live parasites impair both Th1 and Th2 pathways in patent lymphatic filariasis: implications for parasite persistence. J Immunol. 2006;176(5):3248-56.
85. Babu S, Nutman TB. Immunology of lymphatic filariasis. Parasite immunology. 2014;36(8):338-46.
86. Babu S, Nutman TB, editors. Immunopathogenesis of lymphatic filarial disease. Seminars in immunopathology; 2012: Springer.

87. Semnani RT, Law M, Kubofcik J, Nutman TB. Filaria-induced immune evasion: suppression by the infective stage of Brugia malayi at the earliest host-parasite interface. J Immunol. 2004;172(10):6229-38.
88. Semnani RT, Mahapatra L, Moore V, Sanprasert V, Nutman TB. Functional and phenotypic characteristics of alternative activation induced in human monocytes by interleukin-4 or the parasitic nematode Brugia malayi. Infect Immun. 2011;79(10):3957-65.
89. Ritter M, Osei-Mensah J, Debrah LB, Kwarteng A, Mubarik Y, Debrah AY, et al. Wuchereria bancrofti-infected individuals harbor distinct IL-10-producing regulatory B and T cell subsets which are affected by anti-filarial treatment. Plos Neglect Trop D. 2019;13(5):e0007436.
90. Gause WC, Wynn TA, Allen JE. Type 2 immunity and wound healing: evolutionary refinement of adaptive immunity by helminths. Nat Rev Immunol. 2013;13(8):607-14.
91. Tischendorf FW, Brattig NW, Buttner DW, Pieper A, Lintzel M. Serum levels of eosinophil cationic protein, eosinophil-derived neurotoxin and myeloperoxidase in infections with filariae and schistosomes. Acta Trop. 1996;62(3):171-82.
92. McCarthy JS, Ottesen EA, Nutman TB. Onchocerciasis in endemic and nonendemic populations: differences in clinical presentation and immunologic findings. J Infect Dis. 1994;170(3):736-41.
93. Semnani RT. The interaction between filarial parasites and human monocyte/macrophage populations. Adv Exp Med Biol. 2013;785:49-56.
94. Semnani RT, Keiser PB, Coulibaly YI, Keita F, Diallo AA, Traore D, et al. Filaria-induced monocyte dysfunction and its reversal following treatment. Infect Immun. 2006;74(8):4409-17.
95. Anuradha R, George PJ, Kumaran P, Nutman TB, Babu S. Interleukin-10- and transforming growth factor β-independent regulation of $CD8^+$ T cells expressing type 1 and type 2 cytokines in human lymphatic filariasis. Clin Vaccine Immunol. 2014;21(12):1620-7.
96. Metenou S, Dembele B, Konate S, Dolo H, Coulibaly SY, Coulibaly YI, et al. At homeostasis filarial infections have expanded adaptive T regulatory but not classical Th2 cells. J Immunol. 2010;184(9):5375-82.
97. Metenou S, Nutman TB. Regulatory T cell subsets in filarial infection and their function. Front Immunol. 2013;4:305.
98. Babu S, Blauvelt CP, Kumaraswami V, Nutman TB. Diminished Expression and Function of TLR in Lymphatic Filariasis: A Novel Mechanism of Immune Dysregulation. The Journal of Immunology. 2005;175(2):1170-6.
99. Babu S, Kumaraswami V, Nutman TB. Transcriptional control of impaired Th1 responses in patent lymphatic filariasis by T-box expressed in T cells and suppressor of cytokine signaling genes. Infect Immun. 2005;73(6):3394-401.
100. Walker JA, McKenzie ANJ. TH2 cell development and function. Nat Rev Immunol. 2017.
101. Kondělková K, Vokurková D, Krejsek J, Borská L, Fiala Z, Ctirad A. Regulatory T cells (TREG) and their roles in immune system with respect to immunopathological disorders. Acta medica (Hradec Kralove). 2010;53(2):73-7.
102. Baize S, Wahl G, Soboslay PT, Egwang TG, Georges AJ. T helper responsiveness in human Loa loa infection; defective specific proliferation and cytokine production by CD4+ T cells from microfilaraemic subjects compared with amicrofilaraemics. Clinical and experimental immunology. 1997;108(2):272-8.
103. Babu S, Kumaraswami V, Nutman TB. Alternatively activated and immunoregulatory monocytes in human filarial infections. J Infect Dis. 2009;199(12):1827-37.
104. Ritter M, Ndongmo WPC, Njouendou AJ, Nghochuzie NN, Nchang LC, Tayong DB, et al. Mansonella perstans microfilaremic individuals are characterized by enhanced type 2 helper T and regulatory T and B cell subsets and dampened systemic innate and adaptive immune responses. PLoS Negl Trop Dis. 2018;12(1):e0006184.
105. Steel C, Guinea A, McCarthy JS, Ottesen EA. Long-term effect of prenatal exposure to maternal microfilaraemia on immune responsiveness to filarial parasite antigens. Lancet. 1994;343(8902):890-3.

106. Elson LH, Days A, Calvopiña M, Paredes W, Araujo E, Guderian RH, et al. In utero exposure to Onchocerca volvulus: relationship to subsequent infection intensity and cellular immune responsiveness. Infect Immun. 1996;64(12):5061-5.
107. Pit DS, Polderman AM, Schulz-Key H, Soboslay PT. Prenatal immune priming with helminth infections: parasite-specific cellular reactivity and Th1 and Th2 cytokine responses in neonates. Allergy. 2000;55(8):732-9.
108. Malhotra I, Ouma JH, Wamachi A, Kioko J, Mungai P, Njzovu M, et al. Influence of maternal filariasis on childhood infection and immunity to Wuchereria bancrofti in Kenya. Infect Immun. 2003;71(9):5231-7.
109. Arndts K, Deininger S, Specht S, Klarmann U, Mand S, Adjobimey T, et al. Elevated adaptive immune responses are associated with latent infections of Wuchereria bancrofti. PLoS Negl Trop Dis. 2012;6(4):e1611.
110. Arndts K, Specht S, Debrah AY, Tamarozzi F, Klarmann Schulz U, Mand S, et al. Immunoepidemiological profiling of onchocerciasis patients reveals associations with microfilaria loads and ivermectin intake on both individual and community levels. PLoS Negl Trop Dis. 2014;8(2):e2679.
111. Kurniawan A, Yazdanbakhsh M, van Ree R, Aalberse R, Selkirk ME, Partono F, et al. Differential expression of IgE and IgG4 specific antibody responses in asymptomatic and chronic human filariasis. J Immunol. 1993;150(9):3941-50.
112. Bouyou-Akotet MK, Moussavou Boussougou MN, Ovono-Abessolo F, Owono-Medang M, Kombila M. Influence of Mansonella perstans microfilaraemia on total IgE levels in Gabonese patients co-infected with Loa loa. Acta Trop. 2014;131:11-5.
113. Stewart GR, Boussinesq M, Coulson T, Elson L, Nutman T, Bradley JE. Onchocerciasis modulates the immune response to mycobacterial antigens. Clin Exp Immunol. 1999;117(3):517-23.
114. Cooper PJ, Espinel I, Paredes W, Guderian RH, Nutman TB. Impaired tetanus-specific cellular and humoral responses following tetanus vaccination in human onchocerciasis: a possible role for interleukin-10. J Infect Dis. 1998;178(4):1133-8.
115. Kroidl I, Saathoff E, Maganga L, Makunde WH, Hoerauf A, Geldmacher C, et al. Effect of Wuchereria bancrofti infection on HIV incidence in southwest Tanzania: a prospective cohort study. Lancet. 2016.
116. Metenou S, Dembélé B, Konate S, Dolo H, Coulibaly SY, Coulibaly YI, et al. Patent filarial infection modulates malaria-specific type 1 cytokine responses in an IL-10-dependent manner in a filaria/malaria-coinfected population. J Immunol. 2009;183(2):916-24.
117. Metenou S, Babu S, Nutman TB. Impact of filarial infections on coincident intracellular pathogens: Mycobacterium tuberculosis and Plasmodium falciparum. Current Opinion in HIV and AIDS. 2012;7(3):231.
118. Kathamuthu GR, Munisankar S, Banurekha VV, Nair D, Sridhar R, Babu S. Filarial Coinfection Is Associated With Higher Bacterial Burdens and Altered Plasma Cytokine and Chemokine Responses in Tuberculous Lymphadenitis. Frontiers in immunology. 2020;11:706.
119. Alvar J, Alves F, Bucheton B, Burrows L, Büscher P, Carrillo E, et al. Implications of asymptomatic infection for the natural history of selected parasitic tropical diseases. Semin Immunopathol. 2020;42(3):231-46.
120. Chetty A, Omondi MA, Butters C, Smith KA, Katawa G, Ritter M, et al. Impact of Helminth Infections on Female Reproductive Health and Associated Diseases. Frontiers in Immunology. 2020;11.
121. Metenou S, Dembele B, Konate S, Dolo H, Coulibaly YI, Diallo AA, et al. Filarial infection suppresses malaria-specific multifunctional Th1 and Th17 responses in malaria and filarial coinfections. J Immunol. 2011;186(8):4725-33.
122. Metenou S, Babu S, Nutman TB. Impact of filarial infections on coincident intracellular pathogens: Mycobacterium tuberculosis and Plasmodium falciparum. Curr Opin HIV AIDS. 2012;7(3):231-8.
123. Prost A, Nebout M, Rougemont A. Lepromatous leprosy and onchocerciasis. British medical journal. 1979;1(6163):589-90.

124. Chatterjee S, Kolappan C, Subramani R, Gopi PG, Chandrasekaran V, Fay MP, et al. Incidence of Active Pulmonary Tuberculosis in Patients with Coincident Filarial and/or Intestinal Helminth Infections Followed Longitudinally in South India. PLOS ONE. 2014;9(4):e94603.
125. Chatterjee S, Clark CE, Lugli E, Roederer M, Nutman TB. Filarial Infection Modulates the Immune Response to Mycobacterium tuberculosis through Expansion of CD4+ IL-4 Memory T Cells. J Immunol. 2015.
126. George PJ, Anuradha R, Kumar NP, Sridhar R, Banurekha VV, Nutman TB, et al. Helminth Infections Coincident with Active Pulmonary Tuberculosis Inhibit Mono- and Multifunctional CD4+ and CD8+ T Cell Responses in a Process Dependent on IL-10. PLOS Pathogens. 2014;10(9):e1004375.
127. Mnkai J, Ritter M, Maganga L, Maboko L, Olomi W, Clowes P, et al. Increased HIV Incidence in Wuchereria bancrofti Microfilaria Positive Individuals in Tanzania. Pathogens (Basel, Switzerland). 2023;12(3).
128. Nookala S, Srinivasan S, Kaliraj P, Narayanan RB, Nutman TB. Impairment of tetanus-specific cellular and humoral responses following tetanus vaccination in human lymphatic filariasis. Infect Immun. 2004;72(5):2598-604.
129. Aravindhan V, Mohan V, Surendar J, Muralidhara Rao M, Pavankumar N, Deepa M, et al. Decreased prevalence of lymphatic filariasis among diabetic subjects associated with a diminished pro-inflammatory cytokine response (CURES 83). PLoS Negl Trop Dis. 2010;4(6):e707.
130. Aravindhan V, Mohan V, Surendar J, Rao MM, Ranjani H, Kumaraswami V, et al. Decreased prevalence of lymphatic filariasis among subjects with type-1 diabetes. Am J Trop Med Hyg. 2010;83(6):1336-9.
131. Htun NSN, Odermatt P, Paboriboune P, Sayasone S, Vongsakid M, Phimolsarn-Nusith V, et al. Association between helminth infections and diabetes mellitus in adults from the Lao People's Democratic Republic: a cross-sectional study. Infectious Diseases of Poverty. 2018;7(1):105.
132. Chen Y, Lu J, Huang Y, Wang T, Xu Y, Xu M, et al. Association of previous schistosome infection with diabetes and metabolic syndrome: a cross-sectional study in rural China. J Clin Endocrinol Metab. 2013;98(2):E283-7.
133. Hays R, Esterman A, Giacomin P, Loukas A, McDermott R. Does Strongyloides stercoralis infection protect against type 2 diabetes in humans? Evidence from Australian Aboriginal adults. Diabetes Research and Clinical Practice. 2015;107(3):355-61.
134. Anuradha R, Munisankar S, Bhootra Y, Jagannathan J, Dolla C, Kumaran P, et al. Systemic Cytokine Profiles in Strongyloides stercoralis Infection and Alterations following Treatment. Infect Immun. 2016;84(2):425-31.
135. Anuradha R, Munisankar S, Dolla C, Kumaran P, Nutman TB, Babu S. Parasite Antigen-Specific Regulation of Th1, Th2, and Th17 Responses in Strongyloides stercoralis Infection. J Immunol. 2015;195(5):2241-50.
136. Rajamanickam A, Munisankar S, Bhootra Y, Dolla C, Nutman TB, Babu S. Microbial Translocation Associated with an Acute-Phase Response and Elevations in MMP-1, HO-1, and Proinflammatory Cytokines in Strongyloides stercoralis Infection. Infect Immun. 2017;85(1).
137. Rajamanickam A, Munisankar S, Bhootra Y, Dolla C, Thiruvengadam K, Nutman TB, et al. Metabolic Consequences of Concomitant Strongyloides stercoralis Infection in Patients With Type 2 Diabetes Mellitus. Clin Infect Dis. 2019;69(4):697-704.
138. Rajamanickam A, Munisankar S, Dolla C, Menon PA, Thiruvengadam K, Nutman TB, et al. Helminth infection modulates systemic pro-inflammatory cytokines and chemokines implicated in type 2 diabetes mellitus pathogenesis. PLoS Negl Trop Dis. 2020;14(3):e0008101.
139. Rajamanickam A, Munisankar S, Menon PA, Dolla C, Nutman TB, Babu S. Helminth Mediated Attenuation of Systemic Inflammation and Microbial Translocation in Helminth-Diabetes Comorbidity. Front Cell Infect Microbiol. 2020;10:431.

140. Rajamanickam A, Munisankar S, Menon PA, Nutman TB, Babu S. Diminished circulating levels of angiogenic factors and RAGE ligands in helminth-diabetes comorbidity and reversal following anthelmintic treatment. J Infect Dis. 2021.
141. Rajamanickam A, Munisankar S, Thiruvengadam K, Menon PA, Dolla C, Nutman TB, et al. Impact of Helminth Infection on Metabolic and Immune Homeostasis in Non-diabetic Obesity. Front Immunol. 2020;11:2195.
142. Wiria AE, Hamid F, Wammes LJ, Prasetyani MA, Dekkers OM, May L, et al. Infection with Soil-Transmitted Helminths Is Associated with Increased Insulin Sensitivity. PLOS ONE. 2015;10(6):e0127746.
143. Bain O, Wanji S, Vuong PN, Marechal P, Le Goff L, Petit G. Larval biology of six filariae of the sub-family Onchocercinae in a vertebrate host. Parasite. 1994;1(3):241-54.
144. Risch F, Ritter M, Hoerauf A, Hübner MP. Human filariasis—contributions of the Litomosoides sigmodontis and Acanthocheilonema viteae animal model. Parasitology Research. 2021.
145. Kilarski WW, Martin C, Pisano M, Bain O, Babayan SA, Swartz MA. Inherent biomechanical traits enable infective filariae to disseminate through collecting lymphatic vessels. Nat Commun. 2019;10(1):2895.
146. Taubert A, Zahner H. Cellular immune responses of filaria (Litomosoides sigmodontis) infected BALB/c mice detected on the level of cytokine transcription. Parasite Immunol. 2001;23(8):453-62.
147. Hawking F, Burroughs AM. Transmission of Litomosoides carinii to Mice and Hamsters. Nature. 1946;158(4003):98-.
148. Petit G, Diagne M, Marechal P, Owen D, Taylor D, Bain O. Maturation of the filaria Litomosoides sigmodontis in BALB/c mice; comparative susceptibility of nine other inbred strains. Annales de parasitologie humaine et comparee. 1992;67(5):144-50.
149. Marechal P, Le Goff L, Hoffman W, Rapp J, Oswald IP, Ombrouck C, et al. Immune response to the filaria Litomosoides sigmodontis in susceptible and resistant mice. Parasite Immunol. 1997;19(6):273-9.
150. Specht S, Volkmann L, Wynn T, Hoerauf A. Interleukin-10 (IL-10) counterregulates IL-4-dependent effector mechanisms in Murine Filariasis. Infect Immun. 2004;72(11):6287-93.
151. Specht S, Taylor MD, Hoeve MA, Allen JE, Lang R, Hoerauf A. Over expression of IL-10 by macrophages overcomes resistance to murine filariasis. Exp Parasitol. 2012;132(1):90-6.
152. Taylor MD, LeGoff L, Harris A, Malone E, Allen JE, Maizels RM. Removal of regulatory T cell activity reverses hyporesponsiveness and leads to filarial parasite clearance in vivo. J Immunol. 2005;174(8):4924-33.
153. Taylor MD, van der Werf N, Harris A, Graham AL, Bain O, Allen JE, et al. Early recruitment of natural CD4+ Foxp3+ Treg cells by infective larvae determines the outcome of filarial infection. European journal of immunology. 2009;39(1):192-206.
154. Volkmann L, Bain O, Saeftel M, Specht S, Fischer K, Brombacher F, et al. Murine filariasis: interleukin 4 and interleukin 5 lead to containment of different worm developmental stages. Med Microbiol Immunol (Berl). 2003;192(1):23-31.
155. Le Goff L, Lamb TJ, Graham AL, Harcus Y, Allen JE. IL-4 is required to prevent filarial nematode development in resistant but not susceptible strains of mice. Int J Parasitol. 2002;32(10):1277-84.
156. Frohberger SJ, Ajendra J, Surendar J, Stamminger W, Ehrens A, Buerfent BC, et al. Susceptibility to L. sigmodontis infection is highest in animals lacking IL-4R/IL-5 compared to single knockouts of IL-4R, IL-5 or eosinophils. Parasit Vectors. 2019;12(1):248.
157. Specht S, Saeftel M, Arndt M, Endl E, Dubben B, Lee NA, et al. Lack of eosinophil peroxidase or major basic protein impairs defense against murine filarial infection. Infect Immun. 2006;74(9):5236-43.
158. Ehrens A, Lenz B, Neumann AL, Giarrizzo S, Reichwald JJ, Frohberger SJ, et al. Microfilariae Trigger Eosinophil Extracellular DNA Traps in a Dectin-1-Dependent Manner. Cell Rep. 2021;34(2):108621.
159. Hoffmann W, Petit G, Schulz-Key H, Taylor D, Bain O, Le Goff L. Litomosoides sigmodontis in mice: reappraisal of an old model for filarial research. Parasitology today (Personal ed). 2000;16(9):387-9.

160. Allen JE, Adjei O, Bain O, Hoerauf A, Hoffmann WH, Makepeace BL, et al. Of mice, cattle, and humans: the immunology and treatment of river blindness. PLoS Negl Trop Dis. 2008;2(4):e217.
161. Finlay CM, Allen JE. The immune response of inbred laboratory mice to Litomosoides sigmodontis: A route to discovery in myeloid cell biology. Parasite Immunol. 2020;42(7):e12708.
162. Ajendra J, Berbudi A, Hoerauf A, Hübner MP. Combination of worm antigen and proinsulin prevents type 1 diabetes in NOD mice after the onset of insulitis. Clin Immunol. 2016;164:119-22.
163. Berbudi A, Ajendra J, Wardani AP, Hoerauf A, Hübner MP. Parasitic helminths and their beneficial impact on type 1 and type 2 diabetes. Diabetes Metab Res Rev. 2016;32(3):238-50.
164. Hübner MP, Stocker JT, Mitre E. Inhibition of type 1 diabetes in filaria-infected non-obese diabetic mice is associated with a T helper type 2 shift and induction of FoxP3+ regulatory T cells. Immunology. 2009;127(4):512-22.
165. Berbudi A, Surendar J, Ajendra J, Gondorf F, Schmidt D, Neumann AL, et al. Filarial Infection or Antigen Administration Improves Glucose Tolerance in Diet-Induced Obese Mice. J Innate Immun. 2016;8(6).
166. Surendar J, Frohberger SJ, Karunakaran I, Schmitt V, Stamminger W, Neumann AL, et al. Adiponectin Limits IFN-γ and IL-17 Producing CD4 T Cells in Obesity by Restraining Cell Intrinsic Glycolysis. Frontiers in immunology. 2019;10:2555.
167. Kuehn C, Tauchi M, Furtmair R, Urschel K, Raaz-Schrauder D, Neumann A-L, et al. Filarial extract of Litomosoides sigmodontis induces a type 2 immune response and attenuates plaque development in hyperlipidemic ApoE-knockout mice. The FASEB Journal. 2019;33(5):6497-513.
168. Gondorf F, Berbudi A, Buerfent BC, Ajendra J, Bloemker D, Specht S, et al. Chronic Filarial Infection Provides Protection against Bacterial Sepsis by Functionally Reprogramming Macrophages. PLoS Pathog. 2015;11(1):e1004616.
169. Breloer M, Hartmann W. Filarial infections compromise influenza vaccination efficacy: Lessons from the mouse. Immunology letters. 2023;255:62-6.
170. Urban Jr JF, Steenhard NR, Solano-Aguilar GI, Dawson HD, Iweala OI, Nagler CR, et al. Infection with parasitic nematodes confounds vaccination efficacy. Veterinary parasitology. 2007;148(1):14-20.
171. Haben I, Hartmann W, Breloer M. Nematode-induced interference with vaccination efficacy targets follicular T helper cell induction and is preserved after termination of infection. PLoS Negl Trop Dis. 2014;8(9):e3170.
172. Gluge G. Atlas der pathologischen Anatomie: oder bildliche Darstellung und Erläuterung der vorzüglichsten krankhaften Veränderungen der Organe und Gewebe des menschlichen Körpers: zum Gebrauch für Aerzte und Studierende: Mauke; 1843.
173. Vogel J. The pathological anatomy of the human body: Lea & Blanchard; 1847.
174. Jones TW. IV. The blood-corpuscle considered in its different phases of development in the animal series. Memoir I.—Vertebrata. Philosophical Transactions of the Royal Society of London. 1846(136):63-87.
175. Schultze M. Ein heizbarer Objecttisch und seine Verwendung bei Untersuchungen des Blutes. Archiv für mikroskopische Anatomie. 1865;1(1):1-42.
176. Lee JJ, Jacobsen EA, Ochkur SI, McGarry MP, Condjella RM, Doyle AD, et al. Human versus mouse eosinophils: "that which we call an eosinophil, by any other name would stain as red". J Allergy Clin Immunol. 2012;130(3):572-84.
177. Ehrlich P. Uber die spezifischen Granulationen des Blutes. Arch Anat Physiol. 1879;571.
178. Kay A. The early history of the eosinophil. Clinical & Experimental Allergy. 2015;45(3):575-82.
179. Uhm TG, Kim BS, Chung IY. Eosinophil development, regulation of eosinophil-specific genes, and role of eosinophils in the pathogenesis of asthma. Allergy, asthma & immunology research. 2012;4(2):68-79.
180. Fulkerson PC. Transcription Factors in Eosinophil Development and As Therapeutic Targets. Frontiers in medicine. 2017;4:115.

181. Kulessa H, Frampton J, Graf T. GATA-1 reprograms avian myelomonocytic cell lines into eosinophils, thromboblasts, and erythroblasts. Genes & development. 1995;9(10):1250-62.
182. Dougan M, Dranoff G, Dougan SK. GM-CSF, IL-3, and IL-5 Family of Cytokines: Regulators of Inflammation. Immunity. 2019;50(4):796-811.
183. Falanga V, Medsger TA, Jr. Frequency, levels, and significance of blood eosinophilia in systemic sclerosis, localized scleroderma, and eosinophilic fasciitis. Journal of the American Academy of Dermatology. 1987;17(4):648-56.
184. Khan GM, Zuberi FF, Zahra SBU, Ghafoor L. Frequency of Blood Eosinophilia in newly diagnosed Chronic Obstructive Pulmonary Disease patients. Pakistan journal of medical sciences. 2020;36(4):750-4.
185. Lee JJ, Jacobsen EA, McGarry MP, Schleimer RP, Lee NA. Eosinophils in health and disease: the LIAR hypothesis. Clinical and experimental allergy : journal of the British Society for Allergy and Clinical Immunology. 2010;40(4):563-75.
186. Brigger D, Riether C, van Brummelen R, Mosher KI, Shiu A, Ding Z, et al. Eosinophils regulate adipose tissue inflammation and sustain physical and immunological fitness in old age. Nature metabolism. 2020;2(8):688-702.
187. Marichal T, Mesnil C, Bureau F. Homeostatic Eosinophils: Characteristics and Functions. Frontiers in medicine. 2017;4:101.
188. Shimizu S, Kouzaki H, Ogawa T, Takezawa K, Tojima I, Shimizu T. Eosinophil-epithelial cell interactions stimulate the production of MUC5AC mucin and profibrotic cytokines involved in airway tissue remodeling. American journal of rhinology & allergy. 2014;28(2):103-9.
189. Goh YPS, Henderson NC, Heredia JE, Red Eagle A, Odegaard JI, Lehwald N, et al. Eosinophils secrete IL-4 to facilitate liver regeneration. Proceedings of the National Academy of Sciences. 2013;110(24):9914-9.
190. Heredia Jose E, Mukundan L, Chen Francis M, Mueller Alisa A, Deo Rahul C, Locksley Richard M, et al. Type 2 Innate Signals Stimulate Fibro/Adipogenic Progenitors to Facilitate Muscle Regeneration. Cell. 2013;153(2):376-88.
191. Tai Y, Woods EL, Dally J, Kong D, Steadman R, Moseley R, et al. Myofibroblasts: Function, Formation, and Scope of Molecular Therapies for Skin Fibrosis. Biomolecules. 2021;11(8).
192. Hashimoto S, Gon Y, Takeshita I, Maruoka S, Horie T. IL-4 and IL-13 induce myofibroblastic phenotype of human lung fibroblasts through c-Jun NH2-terminal kinase-dependent pathway. J Allergy Clin Immunol. 2001;107(6):1001-8.
193. Aoki A, Hirahara K, Kiuchi M, Nakayama T. Eosinophils: Cells known for over 140 years with broad and new functions. Allergology International. 2021;70(1):3-8.
194. Frangogiannis NG. Transforming growth factor–β in tissue fibrosis. Journal of Experimental Medicine. 2020;217(3).
195. Voehringer D, Reese TA, Huang X, Shinkai K, Locksley RM. Type 2 immunity is controlled by IL-4/IL-13 expression in hematopoietic non-eosinophil cells of the innate immune system. The Journal of experimental medicine. 2006;203(6):1435-46.
196. Knott ML, Matthaei KI, Giacomin PR, Wang H, Foster PS, Dent LA. Impaired resistance in early secondary Nippostrongylus brasiliensis infections in mice with defective eosinophilopoeisis. International journal for parasitology. 2007;37(12):1367-78.
197. Hewitson JP, Filbey KJ, Esser-von Bieren J, Camberis M, Schwartz C, Murray J, et al. Concerted activity of IgG1 antibodies and IL-4/IL-25-dependent effector cells trap helminth larvae in the tissues following vaccination with defined secreted antigens, providing sterile immunity to challenge infection. PLoS pathogens. 2015;11(3):e1004676.
198. Huang L, Gebreselassie NG, Gagliardo LF, Ruyechan MC, Luber KL, Lee NA, et al. Eosinophils mediate protective immunity against secondary nematode infection. J Immunol. 2015;194(1):283-90.
199. Huang L, Appleton JA. Eosinophils in Helminth Infection: Defenders and Dupes. Trends Parasitol. 2016;32(10):798-807.

200. Gebreselassie NG, Moorhead AR, Fabre V, Gagliardo LF, Lee NA, Lee JJ, et al. Eosinophils preserve parasitic nematode larvae by regulating local immunity. J Immunol. 2012;188(1):417-25.
201. Fabre V, Beiting DP, Bliss SK, Gebreselassie NG, Gagliardo LF, Lee NA, et al. Eosinophil deficiency compromises parasite survival in chronic nematode infection. J Immunol. 2009;182(3):1577-83.
202. Wildenburg G, Krömer M, Büttner D. Dependence of eosinophil granulocyte infiltration into nodules on the presence of microfilariae producing Onchocerca volvulus. Parasitology research. 1996;82:117-24.
203. Herrick JA, Metenou S, Makiya MA, Taylar-Williams CA, Law MA, Klion AD, et al. Eosinophil-associated processes underlie differences in clinical presentation of loiasis between temporary residents and those indigenous to Loa-endemic areas. Clin Infect Dis. 2015;60(1):55-63.
204. Ehrens A, Hoerauf A, Hübner MP. Eosinophils in filarial infections: Inducers of protection or pathology? Front Immunol. 2022;13:983812.
205. Gopinath R, Hanna L, Kumaraswami V, Perumal V, Kavitha V, Vijayasekaran V, et al. Perturbations in eosinophil homeostasis following treatment of lymphatic filariasis. Infection and immunity. 2000;68(1):93-9.
206. Limaye AP, Ottesen EA, Kumaraswami V, Abrams JS, Regunathan J, Vijayasekaran V, et al. Kinetics of serum and cellular interleukin-5 in posttreatment eosinophilia of patients with lymphatic filariasis. J Infect Dis. 1993;167(6):1396-400.
207. Huber HL. The Pathology of Bronchial Asthma. Archives of Internal Medicine. 1922;30(6):689.
208. Humbles AA, Lloyd CM, McMillan SJ, Friend DS, Xanthou G, McKenna EE, et al. A critical role for eosinophils in allergic airways remodeling. Science. 2004;305(5691):1776-9.
209. Green RH, Brightling CE, McKenna S, Hargadon B, Parker D, Bradding P, et al. Asthma exacerbations and sputum eosinophil counts: a randomised controlled trial. The Lancet. 2002;360(9347):1715-21.
210. Price DB, Rigazio A, Campbell JD, Bleecker ER, Corrigan CJ, Thomas M, et al. Blood eosinophil count and prospective annual asthma disease burden: a UK cohort study. The lancet Respiratory medicine. 2015;3(11):849-58.
211. Denlinger LC, Phillips BR, Ramratnam S, Ross K, Bhakta NR, Cardet JC, et al. Inflammatory and comorbid features of patients with severe asthma and frequent exacerbations. American journal of respiratory and critical care medicine. 2017;195(3):302-13.
212. Nakagome K, Nagata M. Involvement and Possible Role of Eosinophils in Asthma Exacerbation. Front Immunol. 2018;9:2220.
213. Jacoby DB, Gleich GJ, Fryer AD. Human eosinophil major basic protein is an endogenous allosteric antagonist at the inhibitory muscarinic M2 receptor. J Clin Invest. 1993;91(4):1314-8.
214. Carvalho AT, Elia CC, de Souza HS, Elias PR, Pontes EL, Lukashok HP, et al. Immunohistochemical study of intestinal eosinophils in inflammatory bowel disease. Journal of clinical gastroenterology. 2003;36(2):120-5.
215. Xu X, Rivkind A, Pikarsky A, Pappo O, Bischoff SC, Levi-Schaffer F. Mast cells and eosinophils have a potential profibrogenic role in Crohn disease. Scandinavian journal of gastroenterology. 2004;39(5):440-7.
216. Gelbmann C, Mestermann S, Gross V, Köllinger M, Schölmerich J, Falk W. Strictures in Crohn's disease are characterised by an accumulation of mast cells colocalised with laminin but not with fibronectin or vitronectin. Gut. 1999;45(2):210-7.
217. Lampinen M, Rönnblom A, Amin K, Kristjansson G, Rorsman F, Sangfelt P, et al. Eosinophil granulocytes are activated during the remission phase of ulcerative colitis. Gut. 2005;54(12):1714-20.
218. Townsend K, Tseng YH. Brown adipose tissue: Recent insights into development, metabolic function and therapeutic potential. Adipocyte. 2012;1(1):13-24.
219. Townsend MJ, Fallon PG, Matthews DJ, Jolin HE, McKenzie AN. T1/ST2-deficient mice demonstrate the importance of T1/ST2 in developing primary T helper cell type 2 responses. J Exp Med. 2000;191(6):1069-76.

220. Whittle AJ, López M, Vidal-Puig A. Using brown adipose tissue to treat obesity - the central issue. Trends in molecular medicine. 2011;17(8):405-11.
221. Qiu Y, Nguyen KD, Odegaard JI, Cui X, Tian X, Locksley RM, et al. Eosinophils and type 2 cytokine signaling in macrophages orchestrate development of functional beige fat. Cell. 2014;157(6):1292-308.
222. Misawa T, Wagner M, Koyasu S. ILC2s and Adipose Tissue Homeostasis: Progress to Date and the Road Ahead. Frontiers in Immunology. 2022;13.
223. Seiglie JA, Marcus M-E, Ebert C, Prodromidis N, Geldsetzer P, Theilmann M, et al. Diabetes Prevalence and Its Relationship With Education, Wealth, and BMI in 29 Low- and Middle-Income Countries. Diabetes Care. 2020;43(4):767.
224. Ramachandran A, Ma RC, Snehalatha C. Diabetes in Asia. Lancet. 2010;375(9712):408-18.
225. Chan JC, Malik V, Jia W, Kadowaki T, Yajnik CS, Yoon KH, et al. Diabetes in Asia: epidemiology, risk factors, and pathophysiology. Jama. 2009;301(20):2129-40.
226. Mbanya JCN, Motala AA, Sobngwi E, Assah FK, Enoru ST. Diabetes in sub-Saharan Africa. The Lancet. 2010;375(9733):2254-66.
227. Hwang CK, Han PV, Zabetian A, Ali MK, Venkat Narayan KM. Rural diabetes prevalence quintuples over twenty-five years in low- and middle-income countries: A systematic review and meta-analysis. Diabetes Research and Clinical Practice. 2012;96(3):271-85.
228. Hannon TS, Rao G, Arslanian SA. Childhood obesity and type 2 diabetes mellitus. Pediatrics. 2005;116(2):473-80.
229. Mokdad AH, Ford ES, Bowman BA, Dietz WH, Vinicor F, Bales VS, et al. Prevalence of obesity, diabetes, and obesity-related health risk factors, 2001. Jama. 2003;289(1):76-9.
230. van der Zande HJP, Zawistowska-Deniziak A, Guigas B. Immune Regulation of Metabolic Homeostasis by Helminths and Their Molecules. Trends in Parasitology. 2019;35(10):795-808.
231. Hotamisligil GS. Inflammation, metaflammation and immunometabolic disorders. Nature. 2017;542(7640):177-85.
232. Pistrosch F, Natali A, Hanefeld M. Is hyperglycemia a cardiovascular risk factor? Diabetes Care. 2011;34 Suppl 2(Suppl 2):S128-31.
233. Yanai H, Tomono Y, Ito K, Furutani N, Yoshida H, Tada N. The underlying mechanisms for development of hypertension in the metabolic syndrome. Nutrition journal. 2008;7:10.
234. Ishihara M. Acute hyperglycemia in patients with acute myocardial infarction. Circulation journal : official journal of the Japanese Circulation Society. 2012;76(3):563-71.
235. Sherwani SI, Khan HA, Ekhzaimy A, Masood A, Sakharkar MK. Significance of HbA1c Test in Diagnosis and Prognosis of Diabetic Patients. Biomarker insights. 2016;11:95-104.
236. Chatterjee S, Khunti K, Davies MJ. Type 2 diabetes. The Lancet. 2017;389(10085):2239-51.
237. Magliano DJ, Boyko EJ, committee IDFDAtes. IDF Diabetes Atlas. Idf diabetes atlas. Brussels: International Diabetes Federation© International Diabetes Federation, 2021.; 2021.

238. Kaser S, Tatarczyk T, Stadlmayr A, Ciardi C, Ress C, Tschoner A, et al. Effect of obesity and insulin sensitivity on adiponectin isoform distribution. European journal of clinical investigation. 2008;38(11):827-34.
239. De Rosa A, Monaco ML, Capasso M, Forestieri P, Pilone V, Nardelli C, et al. Adiponectin oligomers as potential indicators of adipose tissue improvement in obese subjects. European Journal of Endocrinology. 2013;169(1):37-43.
240. Drolet R, Bélanger C, Fortier M, Huot C, Mailloux J, Légaré D, et al. Fat depot-specific impact of visceral obesity on adipocyte adiponectin release in women. Obesity (Silver Spring, Md). 2009;17(3):424-30.
241. Meyer LK, Ciaraldi TP, Henry RR, Wittgrove AC, Phillips SA. Adipose tissue depot and cell size dependency of adiponectin synthesis and secretion in human obesity. Adipocyte. 2013;2(4):217-26.

242. Verboven K, Wouters K, Gaens K, Hansen D, Bijnen M, Wetzels S, et al. Abdominal subcutaneous and visceral adipocyte size, lipolysis and inflammation relate to insulin resistance in male obese humans. Scientific Reports. 2018;8(1):4677.
243. Combs TP, Marliss EB. Adiponectin signaling in the liver. Reviews in endocrine & metabolic disorders. 2014;15(2):137-47.
244. Esposito K, Nappo F, Marfella R, Giugliano G, Giugliano F, Ciotola M, et al. Inflammatory cytokine concentrations are acutely increased by hyperglycemia in humans: role of oxidative stress. Circulation. 2002;106(16):2067-72.
245. Loegering DJ, Lennartz MR. Protein kinase C and toll-like receptor signaling. Enzyme research. 2011;2011:537821.
246. Baron V, Van Obberghen E. [Mechanism of insulin action]. Comptes rendus des seances de la Societe de biologie et de ses filiales. 1995;189(1):25-41.
247. Hwang DH, Kim JA, Lee JY. Mechanisms for the activation of Toll-like receptor 2/4 by saturated fatty acids and inhibition by docosahexaenoic acid. European journal of pharmacology. 2016;785:24-35.
248. Fischer H, Ellström P, Ekström K, Gustafsson L, Gustafsson M, Svanborg C. Ceramide as a TLR4 agonist; a putative signalling intermediate between sphingolipid receptors for microbial ligands and TLR4. Cell Microbiol. 2007;9(5):1239-51.
249. Basseri S, Austin RC. Endoplasmic reticulum stress and lipid metabolism: mechanisms and therapeutic potential. Biochemistry research international. 2012;2012:841362.
250. Sproston NR, Ashworth JJ. Role of C-Reactive Protein at Sites of Inflammation and Infection. Front Immunol. 2018;9:754.
251. Li Q, Wang Q, Xu W, Ma Y, Wang Q, Eatman D, et al. C-Reactive Protein Causes Adult-Onset Obesity Through Chronic Inflammatory Mechanism. Frontiers in cell and developmental biology. 2020;8:18.
252. Kanmani S, Kwon M, Shin M-K, Kim MK. Association of C-Reactive Protein with Risk of Developing Type 2 Diabetes Mellitus, and Role of Obesity and Hypertension: A Large Population-Based Korean Cohort Study. Scientific Reports. 2019;9(1):4573.
253. Devaraj S, Singh U, Jialal I. Human C-reactive protein and the metabolic syndrome. Current opinion in lipidology. 2009;20(3):182-9.
254. Ebeling P, Koistinen HA, Koivisto VA. Insulin-independent glucose transport regulates insulin sensitivity. FEBS letters. 1998;436(3):301-3.
255. Pelleymounter MA, Cullen MJ, Baker MB, Hecht R, Winters D, Boone T, et al. Effects of the obese gene product on body weight regulation in ob/ob mice. Science. 1995;269(5223):540-3.
256. Oral EA, Simha V, Ruiz E, Andewelt A, Premkumar A, Snell P, et al. Leptin-replacement therapy for lipodystrophy. New England Journal of Medicine. 2002;346(8):570-8.
257. Muoio DM, Newgard CB. Molecular and metabolic mechanisms of insulin resistance and β-cell failure in type 2 diabetes. Nature Reviews Molecular Cell Biology. 2008;9(3):193-205.
258. Sethi JK, Vidal-Puig AJ. Thematic review series: adipocyte biology. Adipose tissue function and plasticity orchestrate nutritional adaptation. Journal of lipid research. 2007;48(6):1253-62.
259. Jamaluddin MS, Weakley SM, Yao Q, Chen C. Resistin: functional roles and therapeutic considerations for cardiovascular disease. British journal of pharmacology. 2012;165(3):622-32.
260. Steppan CM, Bailey ST, Bhat S, Brown EJ, Banerjee RR, Wright CM, et al. The hormone resistin links obesity to diabetes. Nature. 2001;409(6818):307-12.
261. Yang Q, Graham TE, Mody N, Preitner F, Peroni OD, Zabolotny JM, et al. Serum retinol binding protein 4 contributes to insulin resistance in obesity and type 2 diabetes. Nature. 2005;436(7049):356-62.
262. Das UN. GLUT-4, tumour necrosis factor, essential fatty acids and daf-genes and their role in glucose homeostasis, insulin resistance, non-insulin dependent diabetes mellitus, and longevity. The Journal of the Association of Physicians of India. 1999;47(4):431-5.
263. Sivitz WI, DeSautel SL, Kayano T, Bell GI, Pessin JE. Regulation of glucose transporter messenger RNA in insulin-deficient states. Nature. 1989;340(6228):72-4.

264. Muoio DM, Newgard CB. A is for adipokine. Nature. 2005;436(7049):337-8.
265. Chauché C, Vacca F, Chia SL, Richards J, Gregory WF, Ogunkanbi A, et al. A Truncated Form of HpARI Stabilizes IL-33, Amplifying Responses to the Cytokine. Front Immunol. 2020;11:1363.
266. Berthold MR, Cebron N, Dill F, Gabriel TR, Kötter T, Meinl T, et al., editors. KNIME: The Konstanz Information Miner. Data Analysis, Machine Learning and Applications; 2008 2008//; Berlin, Heidelberg: Springer Berlin Heidelberg.
267. Schneider CA, Rasband WS, Eliceiri KW. NIH Image to ImageJ: 25 years of image analysis. Nature Methods. 2012;9(7):671-5.
268. Poole CB, Sinha A, Ettwiller L, Apone L, McKay K, Panchapakesa V, et al. In Silico Identification of Novel Biomarkers and Development of New Rapid Diagnostic Tests for the Filarial Parasites Mansonella perstans and Mansonella ozzardi. Sci Rep. 2019;9(1):10275.
269. Abong RA, Amambo GN, Chounna Ndongmo PW, Njouendou AJ, Ritter M, Beng AA, et al. Differential susceptibility of Onchocerca volvulus microfilaria to ivermectin in two areas of contrasting history of mass drug administration in Cameroon: relevance of microscopy and molecular techniques for the monitoring of skin microfilarial repopulation within six months of direct observed treatment. BMC Infect Dis. 2020;20(1):726-.
270. Definition and diagnosis of diabetes mellitus and intermediate hyperglycemia : report of a WHO/IDF consulatition. World Health Organization; Geneva. 2006.
271. Di Pino A, Scicali R, Calanna S, Urbano F, Mantegna C, Rabuazzo AM, et al. Cardiovascular Risk Profile in Subjects With Prediabetes and New-Onset Type 2 Diabetes Identified by HbA_{1c} According to American Diabetes Association Criteria. Diabetes Care. 2014;37(5):1447.
272. Executive Summary of The Third Report of The National Cholesterol Education Program (NCEP) Expert Panel on Detection, Evaluation, And Treatment of High Blood Cholesterol In Adults (Adult Treatment Panel III). Jama. 2001;285(19):2486-97.
273. Wanji S, Tendongfor N, Esum M, Ndindeng S, Enyong P. Epidemiology of concomitant infections due to Loa loa, Mansonella perstans, and Onchocerca volvulus in rain forest villages of Cameroon. Medical Microbiology and Immunology. 2003;192(1):15-21.
274. Control CfD, Prevention. Mansonellosis treatment and diagnosis information. 2013.
275. Harris PA, Taylor R, Minor BL, Elliott V, Fernandez M, O'Neal L, et al. The REDCap consortium: Building an international community of software platform partners. Journal of biomedical informatics. 2019;95:103208.
276. Harris PA, Taylor R, Thielke R, Payne J, Gonzalez N, Conde JG. Research electronic data capture (REDCap)--a metadata-driven methodology and workflow process for providing translational research informatics support. Journal of biomedical informatics. 2009;42(2):377-81.
277. Altman DG, Machin D, Bryant TN, Gardner MJ. Statistics with confidence, Confidence intervals and statistical guidelines, 2nd edition: British Medical Journal Books; 2000.
278. Estrada E, Ferrer E, Pardo A. Statistics for Evaluating Pre-post Change: Relation Between Change in the Distribution Center and Change in the Individual Scores. Frontiers in psychology. 2018;9:2696.
279. Klauer KJ. Handbuch kognitives training. 2001.
280. Osbourn M, Soares DC, Vacca F, Cohen ES, Scott IC, Gregory WF, et al. HpARI Protein Secreted by a Helminth Parasite Suppresses Interleukin-33. Immunity. 2017;47(4):739-51.e5.
281. Hays R, Esterman A, Giacomin P, Loukas A, McDermott R. Does Strongyloides stercoralis infection protect against type 2 diabetes in humans? Evidence from Australian Aboriginal adults. Diabetes Res Clin Pract. 2015;107(3):355-61.
282. Hays R, Esterman A, McDermott R. Type 2 Diabetes Mellitus Is Associated with Strongyloides stercoralis Treatment Failure in Australian Aboriginals. PLoS Negl Trop Dis. 2015;9(8):e0003976.
283. McKinney WT, Jr., Bunney WE, Jr. Animal Model of Depression: I. Review of Evidence: Implications for Research. Archives of General Psychiatry. 1969;21(2):240-8.

284. Lommatzsch M, Speer T, Herr C, Jörres RA, Watz H, Müller A, et al. IgE is associated with exacerbations and lung function decline in COPD. Respiratory Research. 2022;23(1):1.
285. Freeman AF, Olivier KN. Hyper-IgE Syndromes and the Lung. Clinics in chest medicine. 2016;37(3):557-67.
286. Nutman TB, Vijayan V, Pinkston P, Kumaraswami V, Steel C, Crystal RG, et al. Tropical pulmonary eosinophilia: analysis of antifilarial antibody localized to the lung. Journal of Infectious Diseases. 1989;160(6):1042-50.
287. Udwadia F. Chapter III: Tropical Eosinophilia. Pulmonary Eosinophilia. 7: Karger Publishers; 1975. p. 35-155.
288. Mehlotra RK, Hall LR, Haxhiu MA, Pearlman E. Reciprocal immunomodulatory effects of gamma interferon and interleukin-4 on filaria-induced airway hyperresponsiveness. Infection and immunity. 2001;69(3):1463-8.
289. Bouchery T, Ehrhardt K, Lefoulon E, Hoffmann W, Bain O, Martin C. Differential tissular distribution of Litomosoides sigmodontis microfilariae between microfilaremic and amicrofilaremic mice following experimental infection. Parasite. 2012;19(4):351-8.
290. Fercoq F, Remion E, Vallarino-Lhermitte N, Alonso J, Raveendran L, Nixon C, et al. Microfilaria-dependent thoracic pathology associated with eosinophilic and fibrotic polyps in filaria-infected rodents. Parasit Vectors. 2020;13(1):551.
291. Karadjian G, Fercoq F, Pionnier N, Vallarino-Lhermitte N, Lefoulon E, Nieguitsila A, et al. Migratory phase of Litomosoides sigmodontis filarial infective larvae is associated with pathology and transient increase of S100A9 expressing neutrophils in the lung. PLoS neglected tropical diseases. 2017;11(5):e0005596.
292. Van De Vlekkert D, Machado E, d'Azzo A. Analysis of Generalized Fibrosis in Mouse Tissue Sections with Masson's Trichrome Staining. Bio-protocol. 2020;10(10):e3629.
293. Mei J, Riedel N, Grittner U, Endres M, Banneke S, Emmrich JV. Body temperature measurement in mice during acute illness: implantable temperature transponder versus surface infrared thermometry. Scientific Reports. 2018;8(1):3526.
294. Hoymann HG. Lung function measurements in rodents in safety pharmacology studies. Front Pharmacol. 2012;3:156.
295. Bain O, Petit G, Diagne M. [Litomosoides, parasites of rodents; taxonomic consequences]. Annales de parasitologie humaine et comparee. 1989;64(4):268-89.
296. Müller B, Lang S, Dominietto M, Rudin M, Schulz G, Deyhle H, et al. High-resolution tomographic imaging of microvessels: SPIE; 2008.
297. Ong RK, Doyle RL. Tropical pulmonary eosinophilia. Chest. 1998;113(6):1673-9.
298. Fercoq F, Remion E, Frohberger SJ, Vallarino-Lhermitte N, Hoerauf A, Le Quesne J, et al. IL-4 receptor dependent expansion of lung CD169+ macrophages in microfilaria-driven inflammation. PLoS Negl Trop Dis. 2019;13(8):e0007691.
299. Wildenburg G, Darge K, Knab J, Tischendorf FW, Bonow I, Buttner DW. Lymph nodes of onchocerciasis patients after treatment with ivermectin: reaction of eosinophil granulocytes and their cationic granule proteins. Trop Med Parasitol. 1994;45(2):87-96.
300. Maghni K, Nantel F, Lanoue C, Cloutier S, Cristol J-P, Cadieux A, et al. Role of Airway Eosinophilia and Eosinophil Activation in Sephadex-induced Inflammation. Inflammation. 2004;28(4):195-206.
301. Mesnil C, Raulier S, Paulissen G, Xiao X, Birrell MA, Pirottin D, et al. Lung-resident eosinophils represent a distinct regulatory eosinophil subset. J Clin Invest. 2016;126(9):3279-95.
302. Ganga L, Sharma P, Tiwari S, Satoeya N, Jha R, Srivastava M. Immunophenotypic and Functional Characterization of Eosinophil and Migratory Dendritic Cell Subsets during Filarial Manifestation of Tropical Pulmonary Eosinophilia. ACS infectious diseases. 2023.
303. Qi Y, Operario DJ, Oberholzer CM, Kobie JJ, Looney RJ, Georas SN, et al. Human basophils express amphiregulin in response to T cell-derived IL-3. J Allergy Clin Immunol. 2010;126(6):1260-6.e4.

304. Krishnan S, Prise IE, Wemyss K, Schenck LP, Bridgeman HM, McClure FA, et al. Amphiregulin-producing γδ T cells are vital for safeguarding oral barrier immune homeostasis. Proceedings of the National Academy of Sciences. 2018;115(42):10738-43.
305. Morimoto Y, Hirahara K, Kiuchi M, Wada T, Ichikawa T, Kanno T, et al. Amphiregulin-producing pathogenic memory T helper 2 cells instruct eosinophils to secrete osteopontin and facilitate airway fibrosis. Immunity. 2018;49(1):134-50. e6.
306. Matsumoto K, Fukuda S, Nakamura Y, Saito H. Amphiregulin production by human eosinophils. International archives of allergy and immunology. 2009;149 Suppl 1:39-44.
307. Gurtner A, Borrelli C, Gonzalez-Perez I, Bach K, Acar IE, Núñez NG, et al. Active eosinophils regulate host defence and immune responses in colitis. Nature. 2023;615(7950):151-7.
308. Schmitz J, Owyang A, Oldham E, Song Y, Murphy E, McClanahan TK, et al. IL-33, an interleukin-1-like cytokine that signals via the IL-1 receptor-related protein ST2 and induces T helper type 2-associated cytokines. Immunity. 2005;23(5):479-90.
309. Cherry WB, Yoon J, Bartemes KR, Iijima K, Kita H. A novel IL-1 family cytokine, IL-33, potently activates human eosinophils. J Allergy Clin Immunol. 2008;121(6):1484-90.
310. Suzukawa M, Koketsu R, Iikura M, Nakae S, Matsumoto K, Nagase H, et al. Interleukin-33 enhances adhesion, CD11b expression and survival in human eosinophils. Laboratory investigation; a journal of technical methods and pathology. 2008;88(11):1245-53.
311. Moussion C, Ortega N, Girard JP. The IL-1-like cytokine IL-33 is constitutively expressed in the nucleus of endothelial cells and epithelial cells in vivo: a novel 'alarmin'? PLoS ONE. 2008;3(10):e3331.
312. Furukawa S, Moriyama M, Miyake K, Nakashima H, Tanaka A, Maehara T, et al. Interleukin-33 produced by M2 macrophages and other immune cells contributes to Th2 immune reaction of IgG4-related disease. Scientific Reports. 2017;7(1):42413.
313. Wysmołek ME, Długosz E, Wiśniewski M. The Immunological Role of Vascular and Lymphatic Endothelial Cells in Filarial Infections. Animals : an open access journal from MDPI. 2022;12(4).
314. Boberg E, Johansson K, Malmhäll C, Calvén J, Weidner J, Rådinger M. Interplay Between the IL-33/ST2 Axis and Bone Marrow ILC2s in Protease Allergen-Induced IL-5-Dependent Eosinophilia. Front Immunol. 2020;11:1058.
315. Jiang M, Liu H, Li Z, Wang J, Zhang F, Cao K, et al. ILC2s Induce Adaptive Th2-Type Immunity in Acute Exacerbation of Chronic Obstructive Pulmonary Disease. Mediators Inflamm. 2019;2019:3140183.
316. Zheng H, Zhang Y, Pan J, Liu N, Qin Y, Qiu L, et al. The Role of Type 2 Innate Lymphoid Cells in Allergic Diseases. Frontiers in Immunology. 2021;12.
317. Ngo Thi Phuong N, Palmieri V, Adamczyk A, Klopfleisch R, Langhorst J, Hansen W, et al. IL-33 Drives Expansion of Type 2 Innate Lymphoid Cells and Regulatory T Cells and Protects Mice From Severe, Acute Colitis. Front Immunol. 2021;12:669787.
318. Ivanov KP, Mel'nikova NN, Potekhina IL. Structure of microvascular networks in the lungs and peculiarities of blood circulation in them. Bulletin of experimental biology and medicine. 2011;151(4):389-91.
319. Nabe T, Matsuya K, Akamizu K, Fujita M, Nakagawa T, Shioe M, et al. Roles of basophils and mast cells infiltrating the lung by multiple antigen challenges in asthmatic responses of mice. British journal of pharmacology. 2013;169(2):462-76.
320. Torrero MN, Hübner MP, Larson D, Karasuyama H, Mitre E. Basophils Amplify Type 2 Immune Responses, but Do Not Serve a Protective Role, during Chronic Infection of Mice with the Filarial Nematode Litomosoides sigmodontis. J Immunol. 2010;185(12):7426-34.
321. McLeod JJ, Baker B, Ryan JJ. Mast cell production and response to IL-4 and IL-13. Cytokine. 2015;75(1):57-61.
322. Komi DEA, Mortaz E, Amani S, Tiotiu A, Folkerts G, Adcock IM. The Role of Mast Cells in IgE-Independent Lung Diseases. Clinical Reviews in Allergy & Immunology. 2020;58(3):377-87.

323. Stone KD, Prussin C, Metcalfe DD. IgE, mast cells, basophils, and eosinophils. J Allergy Clin Immunol. 2010;125(2 Suppl 2):S73-80.
324. de Andres B, Rakasz E, Hagen M, McCormik ML, Mueller AL, Elliot D, et al. Lack of Fc-epsilon receptors on murine eosinophils: implications for the functional significance of elevated IgE and eosinophils in parasitic infections. Blood. 1997;89(10):3826-36.
325. Polverino F, Seys LJM, Bracke KR, Owen CA. B cells in chronic obstructive pulmonary disease: moving to center stage. American Journal of Physiology-Lung Cellular and Molecular Physiology. 2016;311(4):L687-L95.
326. Jung T, Schauer U, Rieger C, Wagner K, Einsle K, Neumann C, et al. Interleukin-4 and interleukin-5 are rarely co-expressed by human T cells. European journal of immunology. 1995;25(8):2413-6.
327. Kondo Y, Yoshimoto T, Yasuda K, Futatsugi-Yumikura S, Morimoto M, Hayashi N, et al. Administration of IL-33 induces airway hyperresponsiveness and goblet cell hyperplasia in the lungs in the absence of adaptive immune system. International immunology. 2008;20(6):791-800.
328. Bartemes KR, Iijima K, Kobayashi T, Kephart GM, McKenzie AN, Kita H. IL-33-responsive lineage- CD25+ CD44(hi) lymphoid cells mediate innate type 2 immunity and allergic inflammation in the lungs. J Immunol. 2012;188(3):1503-13.
329. Junker K, Buckley CM, Millar SR, Flynn S, Harrington JM, Kearney PM, et al. The prevalence and correlates of pre-diabetes in middle- to older-aged Irish adults using three diagnostic methods. PLoS One. 2021;16(6):e0253537.
330. Xia M, Liu K, Feng J, Zheng Z, Xie X. Prevalence and risk factors of type 2 diabetes and prediabetes among 53,288 middle-aged and elderly adults in China: A cross-sectional study. Diabetes, Metabolic Syndrome and Obesity. 2021:1975-85.
331. Yan Z, Cai M, Han X, Chen Q, Lu H. The Interaction Between Age and Risk Factors for Diabetes and Prediabetes: A Community-Based Cross-Sectional Study. Diabetes, metabolic syndrome and obesity : targets and therapy. 2023;16:85-93.
332. Goossens GH, Jocken JW, Blaak EE. Sexual dimorphism in cardiometabolic health: the role of adipose tissue, muscle and liver. Nature Reviews Endocrinology. 2021;17(1):47-66.
333. Kautzky-Willer A, Harreiter J, Pacini G. Sex and gender differences in risk, pathophysiology and complications of type 2 diabetes mellitus. Endocrine reviews. 2016;37(3):278-316.
334. Kautzky-Willer A, Leutner M, Harreiter J. Sex differences in type 2 diabetes. Diabetologia. 2023;66(6):986-1002.
335. Færch K, Torekov SS, Vistisen D, Johansen NB, Witte DR, Jonsson A, et al. GLP-1 response to oral glucose is reduced in prediabetes, screen-detected type 2 diabetes, and obesity and influenced by sex: the ADDITION-PRO study. Diabetes. 2015;64(7):2513-25.
336. Du T, Fernandez C, Barshop R, Guo Y, Krousel-Wood M, Chen W, et al. Sex differences in cardiovascular risk profile from childhood to midlife between individuals who did and did not develop diabetes at follow-up: the Bogalusa Heart Study. Diabetes Care. 2019;42(4):635-43.
337. Ramezankhani A, Azizi F, Hadaegh F. Sex differences in rates of change and burden of metabolic risk factors among adults who did and did not go on to develop diabetes: two decades of follow-up from the Tehran Lipid and Glucose Study. Diabetes Care. 2020;43(12):3061-9.
338. Brabin L. Sex differentials in susceptibility to lymphatic filariasis and implications for maternal child immunity. Epidemiology and infection. 1990;105(2):335-53.
339. Bundy DA. Gender-dependent patterns of infections and disease. Parasitology today (Personal ed). 1988;4(7):186-9.
340. Kifle B, Woldemichael K, Nigatu M. Prevalence of Onchocerciasis and Associated Factors among Adults Aged ≥ 15 Years in Semen Bench District, Bench Maji Zone, Southwest Ethiopia: Community Based Cross-Sectional Study. Advances in Public Health. 2019;2019:7276230.
341. Jacobsen H, Klein SL. Sex Differences in Immunity to Viral Infections. Front Immunol. 2021;12:720952.

342. Klein SL, Flanagan KL. Sex differences in immune responses. Nature Reviews Immunology. 2016;16(10):626-38.
343. Abdulmalik J, Nwefoh E, Obindo J, Dakwak S, Ayobola M, Umaru J, et al. Emotional Difficulties and Experiences of Stigma among Persons with Lymphatic Filariasis in Plateau State, Nigeria. Health and human rights. 2018;20(1):27-40.
344. Krishna Kumari A, Harichandrakumar K, Das L, Krishnamoorthy K. Physical and psychosocial burden due to lymphatic filariasis as perceived by patients and medical experts. Tropical Medicine & International Health. 2005;10(6):567-73.
345. Stoddard ST, Morrison AC, Vazquez-Prokopec GM, Paz Soldan V, Kochel TJ, Kitron U, et al. The role of human movement in the transmission of vector-borne pathogens. PLoS Negl Trop Dis. 2009;3(7):e481.
346. Mandal A, Bhattarai B, Kafle P, Khalid M, Jonnadula SK, Lamicchane J, et al. Elevated Liver Enzymes in Patients with Type 2 Diabetes Mellitus and Non-alcoholic Fatty Liver Disease. Cureus. 2018;10(11):e3626.
347. Williams CD, Stengel J, Asike MI, Torres DM, Shaw J, Contreras M, et al. Prevalence of nonalcoholic fatty liver disease and nonalcoholic steatohepatitis among a largely middle-aged population utilizing ultrasound and liver biopsy: a prospective study. Gastroenterology. 2011;140(1):124-31.
348. Tarao K, Nozaki A, Ikeda T, Sato A, Komatsu H, Komatsu T, et al. Real impact of liver cirrhosis on the development of hepatocellular carcinoma in various liver diseases-meta-analytic assessment. Cancer medicine. 2019;8(3):1054-65.
349. Belfki H, Ben Ali S, Bougatef S, Ben Ahmed D, Haddad N, Jmal A, et al. Association between C-reactive protein and type 2 diabetes in a Tunisian population. Inflammation. 2012;35(2):684-9.
350. Ngwa DN, Pathak A, Agrawal A. IL-6 regulates induction of C-reactive protein gene expression by activating STAT3 isoforms. Mol Immunol. 2022;146:50-6.
351. Chen SC-C, Tsai SP, Jhao J-Y, Jiang W-K, Tsao CK, Chang L-Y. Liver Fat, Hepatic Enzymes, Alkaline Phosphatase and the Risk of Incident Type 2 Diabetes: A Prospective Study of 132,377 Adults. Scientific Reports. 2017;7(1):4649.
352. Stettler M, Siles-Lucas M, Sarciron E, Lawton P, Gottstein B, Hemphill A. Echinococcus multilocularis alkaline phosphatase as a marker for metacestode damage induced by in vitro drug treatment with albendazole sulfoxide and albendazole sulfone. Antimicrob Agents Chemother. 2001;45(8):2256-62.
353. Elbaz T, Esmat G. Hepatic and Intestinal Schistosomiasis: Review. Journal of Advanced Research. 2013;4(5):445-52.
354. Shaker Y, Samy N, Ashour E. Hepatobiliary Schistosomiasis. Journal of clinical and translational hepatology. 2014;2(3):212-6.
355. Basu A, Kumar A, Manchanda S, Wig N. Filarial huge splenomegaly dramatically regressed by anti-filarial medication: A rare clinical scenario. Intractable & rare diseases research. 2017;6(3):215-8.
356. Pandey A, Masood S, Awasthi NP. Cystic microfilarial infestation of the liver: a rare presentation. International Journal of Infectious Diseases. 2015;31:15-7.
357. Blackwell AD, Snodgrass JJ, Madimenos FC, Sugiyama LS. Life history, immune function, and intestinal helminths: Trade-offs among immunoglobulin E, C-reactive protein, and growth in an Amazonian population. American journal of human biology : the official journal of the Human Biology Council. 2010;22(6):836-48.
358. Lal RB, Dhawan RR, Ramzy RM, Farris RM, Gad AA. C-reactive protein in patients with lymphatic filariasis: increased expression on lymphocytes in chronic lymphatic obstruction. J Clin Immunol. 1991;11(1):46-53.
359. de Gier B, Pita-Rodríguez GM, Campos-Ponce M, van de Bor M, Chamnan C, Junco-Díaz R, et al. Soil-transmitted helminth infections and intestinal and systemic inflammation in schoolchildren. Acta Tropica. 2018;182:124-7.

360. Saheb EJ, Kuba RH, Musa IS. The Role of C-Reactive Protein in the Infections Caused by Parasites. Diyala Journal of Medicine. 2020;19(2):157-64.
361. Thomas MC, Cooper ME, Zimmet P. Changing epidemiology of type 2 diabetes mellitus and associated chronic kidney disease. Nature Reviews Nephrology. 2016;12(2):73-81.
362. Guo K, Zhang L, Zhao F, Lu J, Pan P, Yu H, et al. Prevalence of chronic kidney disease and associated factors in Chinese individuals with type 2 diabetes: cross-sectional study. Journal of Diabetes and its Complications. 2016;30(5):803-10.
363. Keane WF, Eknoyan G. Proteinuria, albuminuria, risk, assessment, detection, elimination (PARADE): a position paper of the National Kidney Foundation. American Journal of Kidney Diseases. 1999;33(5):1004-10.
364. Weir MR. Microalbuminuria in type 2 diabetics: an important, overlooked cardiovascular risk factor. Journal of clinical hypertension (Greenwich, Conn). 2004;6(3):134-41; quiz 42-3.
365. Miettinen H, Haffner SM, Lehto S, Rönnemaa T, Pyörälä K, Laakso M. Proteinuria predicts stroke and other atherosclerotic vascular disease events in nondiabetic and non–insulin-dependent diabetic subjects. Stroke. 1996;27(11):2033-9.
366. Schmitz A, Vaeth M. Microalbuminuria: a major risk factor in non-insulin-dependent diabetes. A 10-year follow-up study of 503 patients. Diabetic Medicine. 1988;5(2):126-34.
367. Valmadrid CT, Klein R, Moss SE, Klein BE. The risk of cardiovascular disease mortality associated with microalbuminuria and gross proteinuria in persons with older-onset diabetes mellitus. Archives of internal medicine. 2000;160(8):1093-100.
368. Gerstein HC, Mann JF, Yi Q, Zinman B, Dinneen SF, Hoogwerf B, et al. Albuminuria and risk of cardiovascular events, death, and heart failure in diabetic and nondiabetic individuals. Jama. 2001;286(4):421-6.
369. Solomon R, Goldstein S. Real-time measurement of glomerular filtration rate. Current opinion in critical care. 2017;23(6):470-4.
370. Hosten AO. BUN and Creatinine. In: Walker HK, Hall WD, Hurst JW, editors. Clinical Methods: The History, Physical, and Laboratory Examinations. Boston: Butterworths

Copyright © 1990, Butterworth Publishers, a division of Reed Publishing.; 1990.
371. Paige NM, Nagami GT. The top 10 things nephrologists wish every primary care physician knew. Mayo Clinic proceedings. 2009;84(2):180-6.
372. Chen X, Jin H, Wang D, Liu J, Qin Y, Zhang Y, et al. Serum creatinine levels, traditional cardiovascular risk factors and 10-year cardiovascular risk in Chinese patients with hypertension. Frontiers in endocrinology. 2023;14:1140093.
373. Song DK, Hong YS, Sung Y-A, Lee H. Association of serum creatinine levels and risk of type 2 diabetes mellitus in Korea: a case control study. BMC Endocrine Disorders. 2022;22(1):4.
374. Kashima S, Inoue K, Matsumoto M, Akimoto K. Low serum creatinine is a type 2 diabetes risk factor in men and women: The Yuport Health Checkup Center cohort study. Diabetes & metabolism. 2017;43(5):460-4.
375. Nata N, Rangsin R, Supasyndh O, Satirapoj B. Impaired Glomerular Filtration Rate in Type 2 Diabetes Mellitus Subjects: A Nationwide Cross-Sectional Study in Thailand. Journal of diabetes research. 2020;2020:6353949.
376. Levey AS, Titan SM, Powe NR, Coresh J, Inker LA. Kidney Disease, Race, and GFR Estimation. Clinical journal of the American Society of Nephrology : CJASN. 2020;15(8):1203-12.
377. van Velthuysen ML, Florquin S. Glomerulopathy associated with parasitic infections. Clin Microbiol Rev. 2000;13(1):55-66, table of contents.
378. Pakasa NM, Nseka NM, Nyimi LM. Secondary collapsing glomerulopathy associated with Loa Loa filariasis. American Journal of Kidney Diseases. 1997;30(6):836-9.

379. Dreyer G, Ottesen EA, Galdino E, Andrade L, Rocha A, Medeiros Z, et al. Renal abnormalities in microfilaremic patients with Bancroftian filariasis. The American journal of tropical medicine and hygiene. 1992;46(6):745-51.
380. Rath RN, Mishra N, Sahu RN, Mohanty G, Das BK. Renal involvement in bancroftian filariasis. The National medical journal of India. 1991;4(2):65-8.
381. Langhammer J, Birk HW, Zahner H. Renal disease in lymphatic filariasis: evidence for tubular and glomerular disorders at various stages of the infection. Tropical Medicine & International Health. 1997;2(9):875-84.
382. Ngu JL, Chatelanat F, Leke R, Ndumbe P, Youmbissi J. Nephropathy in Cameroon: evidence for filarial derived immune-complex pathogenesis in some cases. Clinical nephrology. 1985;24(3):128-34.
383. Imig JD, Ryan MJ. Immune and inflammatory role in renal disease. Comprehensive Physiology. 2013;3(2):957-76.
384. Koshino A, Schechter M, Sen T, Vart P, Neuen BL, Neal B, et al. Interleukin-6 and Cardiovascular and Kidney Outcomes in Patients With Type 2 Diabetes: New Insights From CANVAS. Diabetes Care. 2022;45(11):2644-52.
385. Pecoits-Filho R, Heimbürger O, Bárány P, Suliman M, Fehrman-Ekholm I, Lindholm B, et al. Associations between circulating inflammatory markers and residual renal function in CRF patients. American Journal of Kidney Diseases. 2003;41(6):1212-8.
386. Holdsworth SR, Kitching AR, Tipping PG. Th1 and Th2T helper cell subsets affect patterns of injury and outcomes in glomerulonephritis. Kidney International. 1999;55(4):1198-216.
387. Bolton WK, Innes Jr DJ, Sturgill BC, Kaiser DL. T-cells and macrophages in rapidly progressive glomerulonephritis: clinicopathologic correlations. Kidney international. 1987;32(6):869-76.
388. Nolasco EF, Cameron JS, Hartley B, Coelho A, Hildreth G, Reuben R. Intraglomerular T cells and monocytes in nephritis: study with monoclonal antibodies. Kidney international. 1987;31(5):1160-6.
389. Stachura I, Si L, Whiteside TL. Mononuclear-cell subsets in human idiopathic crescentic glomerulonephritis (ICGN): analysis in tissue sections with monoclonal antibodies. Journal of clinical immunology. 1984;4:202-8.
390. Ottesen EA, Skvaril F, Tripathy SP, Poindexter RW, Hussain R. Prominence of IgG4 in the IgG antibody response to human filariasis. J Immunol. 1985;134(4):2707-12.
391. Korten S, Badusche M, Buttner DW, Hoerauf A, Brattig N, Fleischer B. Natural death of adult Onchocerca volvulus and filaricidal effects of doxycycline induce local FOXP3+/CD4+ regulatory T cells and granzyme expression. Microbes Infect. 2008;10(3):313-24.
392. Bianchini R, Roth-Walter F, Ohradanova-Repic A, Flicker S, Hufnagl K, Fischer MB, et al. IgG4 drives M2a macrophages to a regulatory M2b-like phenotype: potential implication in immune tolerance. Allergy. 2019;74(3):483-94.
393. Lathrop SK, Bloom SM, Rao SM, Nutsch K, Lio CW, Santacruz N, et al. Peripheral education of the immune system by colonic commensal microbiota. Nature. 2011;478(7368):250-4.
394. Johnson AMF, Costanzo A, Gareau MG, Armando AM, Quehenberger O, Jameson JM, et al. High Fat Diet Causes Depletion of Intestinal Eosinophils Associated with Intestinal Permeability. PLOS ONE. 2015;10(4):e0122195.
395. Russo S, Kwiatkowski M, Govorukhina N, Bischoff R, Melgert BN. Meta-Inflammation and Metabolic Reprogramming of Macrophages in Diabetes and Obesity: The Importance of Metabolites. Front Immunol. 2021;12:746151.
396. Jung E, Kong SY, Ro YS, Ryu HH, Shin SD. Serum Cholesterol Levels and Risk of Cardiovascular Death: A Systematic Review and a Dose-Response Meta-Analysis of Prospective Cohort Studies. International journal of environmental research and public health. 2022;19(14).
397. Bhowmik B, Siddiquee T, Mujumder A, Afsana F, Ahmed T, Mdala IA, et al. Serum Lipid Profile and Its Association with Diabetes and Prediabetes in a Rural Bangladeshi Population. International journal of environmental research and public health. 2018;15(9).

398. Yu SS, Castillo DC, Courville AB, Sumner AE. The triglyceride paradox in people of African descent. Metabolic syndrome and related disorders. 2012;10(2):77-82.
399. HbA1c as a predictor of diabetes and as an outcome in the diabetes prevention program: a randomized clinical trial. Diabetes Care. 2015;38(1):51-8.
400. Nathan DM, Turgeon H, Regan S. Relationship between glycated haemoglobin levels and mean glucose levels over time. Diabetologia. 2007;50(11):2239-44.
401. Dixit JV, Badgujar SY, Giri PA. Reduction in HbA1c through lifestyle modification in newly diagnosed type 2 diabetes mellitus patient: A great feat. Journal of family medicine and primary care. 2022;11(6):3312-7.
402. Fang HSA, Gao Q, Tan WY, Lee ML, Hsu W, Tan NC. The effect of oral diabetes medications on glycated haemoglobin (HbA1c) in Asians in primary care: a retrospective cohort real-world data study. BMC Medicine. 2022;20(1):22.
403. Bigna JJ, Nansseu JR, Katte J-C, Noubiap JJ. Prevalence of prediabetes and diabetes mellitus among adults residing in Cameroon: A systematic review and meta-analysis. Diabetes Research and Clinical Practice. 2018;137:109-18.
404. Khosla L, Bhat S, Fullington LA, Horlyck-Romanovsky MF. HbA(1c) Performance in African Descent Populations in the United States With Normal Glucose Tolerance, Prediabetes, or Diabetes: A Scoping Review. Preventing chronic disease. 2021;18:E22.
405. Team N. Diabetes, a silent killer in Africa. 2023.
406. Pilkington A-C, Paz HA, Wankhade UD. Beige Adipose Tissue Identification and Marker Specificity—Overview. Frontiers in endocrinology. 2021;12.
407. Li VL, He Y, Contrepois K, Liu H, Kim JT, Wiggenhorn AL, et al. An exercise-inducible metabolite that suppresses feeding and obesity. Nature. 2022;606(7915):785-90.
408. Nazligul Y, Sabuncu T, Ozbilge H. Is there a predisposition to intestinal parasitosis in diabetic patients? Diabetes Care. 2001;24(8):1503-4.
409. Wiria AE, Hamid F, Wammes LJ, Prasetyani MA, Dekkers OM, May L, et al. Infection with Soil-Transmitted Helminths Is Associated with Increased Insulin Sensitivity. PLoS ONE. 2015;10(6):e0127746.
410. Wiria AE, Sartono E, Supali T, Yazdanbakhsh M. Helminth infections, type-2 immune response, and metabolic syndrome. PLoS Pathog. 2014;10(7):e1004140.
411. Wiria AE, Wammes LJ, Hamid F, Dekkers OM, Prasetyani MA, May L, et al. Relationship between carotid intima media thickness and helminth infections on Flores Island, Indonesia. PLoS ONE. 2013;8(1):e54855.
412. Mendonça SC, Gonçalves-Pires Mdo R, Rodrigues RM, Ferreira A, Jr., Costa-Cruz JM. Is there an association between positive Strongyloides stercoralis serology and diabetes mellitus? Acta Trop. 2006;99(1):102-5.
413. Tahapary DL, de Ruiter K, Martin I, Brienen EAT, van Lieshout L, Cobbaert CM, et al. Effect of Anthelmintic Treatment on Insulin Resistance: A Cluster-Randomized, Placebo-Controlled Trial in Indonesia. Clin Infect Dis. 2017;65(5):764-71.
414. Tahapary DL, de Ruiter K, Martin I, van Lieshout L, Guigas B, Soewondo P, et al. Helminth infections and type 2 diabetes: a cluster-randomized placebo controlled SUGARSPIN trial in Nangapanda, Flores, Indonesia. BMC Infect Dis. 2015;15:133.
415. Rennie C, Fernandez R, Donnelly S, McGrath KC. The Impact of Helminth Infection on the Incidence of Metabolic Syndrome: A Systematic Review and Meta-Analysis. Frontiers in endocrinology. 2021;12.
416. Casulli A. New global targets for NTDs in the WHO roadmap 2021–2030. Public Library of Science San Francisco, CA USA; 2021. p. e0009373.